

# Monte Carlo Based Uncertainty and Sensitivity Analysis for Building Performance Simulation

Zur Erlangung des akademischen Grades  
Doktor-Ingenieur (Dr.-Ing.)  
der Fakultät für Architektur des Karlsruher Instituts für  
Technologie (KIT) genehmigte Dissertation von

Sebastian Burhenne, M.Eng.

Tag der mündlichen Prüfung: 13. November 2013

Referent: Prof. Dipl.-Ing. Andreas Wagner  
Korreferent: Prof. Dr. Gregor P. Henze  
Weiteres Mitglied: Prof. Dr. Petra von Both  
Vorsitzender: Prof. Dipl.-Ing. Matthias Pfeifer



## Abstract

Building performance simulation is most often used to improve the design and at times the operation of buildings. Within a building model, the thermal characteristics of the envelope and the HVAC (heating, ventilation, and air conditioning) equipment are described by parameters that often cannot be estimated with high accuracy (e.g., occupant behavior, building envelope and HVAC equipment performance). These uncertainties in simulation input have a great influence on the simulation results. An uncertainty analysis quantifies the result uncertainty given the model input uncertainty. The aim of a sensitivity analysis is to attribute the uncertainty in the model output to the uncertainty in the different model inputs. Despite the benefits which these techniques can provide, uncertainty and sensitivity analysis are not commonly applied in either design practice or scientific research.

In this thesis, a Monte Carlo based methodology for uncertainty and sensitivity analysis is introduced. A significant reduction of computational expense and an increased robustness was achieved by the application of a quasi-random sampling technique (i.e., sampling based on Sobol' sequences). Furthermore, a systematic approach for conducting the analyses is proposed. The methodology was implemented in a tool that is applicable to most simulation programs and operating systems and allows parallel computing.

Another common part of the design process of a building is a cost-benefit analysis to compare design options and different scenarios. The results are also strongly dependent on assumptions about uncertain economic parameters (e.g., future inflation rates and energy costs). An overall methodology for uncertainty and sensitivity analysis that combines building performance simulation and cost-benefit calculation is developed and demonstrated.

The methodology is applied to three case studies to illustrate possible applications. It can improve the design process or building operation and provides differentiated information on these topics for decision-making.



## Kurzdarstellung

Gebäudesimulationen werden häufig während der Planung von Gebäuden eingesetzt. Vereinzelt kommen sie auch für die Gebäudebetrieboptimierung zum Einsatz. Innerhalb von Gebäudesimulationsmodellen wird die Charakteristik der Gebäudehülle und der Anlagentechnik mittels Parametern beschrieben, die oft nicht genau bestimmbar sind (z.B. Nutzerverhalten, Spezifikation der Gebäudehülle und Anlageneffizienz). Unsichere Randbedingungen haben einen großen Einfluss auf das Ergebnis von Gebäudesimulationen. Eine Unsicherheitsanalyse quantifiziert die Ergebnisunsicherheit in Anbetracht der unsicheren Eingangsgrößen. Das Ziel einer Sensitivitätsanalyse ist die Identifikation des Anteils der Ergebnisunsicherheit, der den einzelnen Eingangsgrößen zuzuordnen ist. Trotz der Vorteile bei der Anwendung dieser Methoden werden Unsicherheits- und Sensitivitätsanalysen bisher in der Planungspraxis und auch in wissenschaftlichen Untersuchungen selten durchgeführt.

In dieser Arbeit wird eine Methodik zur Unsicherheits- und Sensitivitätsanalyse vorgestellt, die auf einem Monte Carlo Ansatz basiert. Durch ein Verfahren zum Ziehen von Stichproben, das auf Quasi-Zufallszahlen beruht (Ziehen von Stichproben auf der Basis von Sobol'-Sequenzen), kann der erforderliche Rechenaufwand signifikant verringert und die Robustheit erhöht werden. Weiterhin wird eine systematische Vorgehensweise bei der Anwendung der Analysen eingeführt. Die Methodik wurde in eine Programmumgebung implementiert, die für die meisten Simulationsprogramme und Betriebssysteme anwendbar ist und eine Parallelisierung der Berechnungen ermöglicht.

Ein weiterer üblicher Teil des Planungsprozesses von Gebäuden sind Wirtschaftlichkeitsberechnungen für den Vergleich von verschiedenen Planungsoptionen und Szenarien. Die damit erzielten Ergebnisse hängen ebenfalls stark von den Annahmen zu unsicheren wirtschaftlichen Randbedingungen ab (z. B. zukünftige Inflationsraten und Energiepreise). Eine Methodik zur Unsicherheits- und Sensitivitätsanalyse für die kombinierte Gebäudesimulation und Wirtschaftlichkeitsberechnung wurde entwickelt und angewendet.

Die Gesamtmethodik wird für drei Beispiele angewendet, um Einsatzmöglichkeiten darzustellen. Ihre Anwendung kann dazu beitragen, den Planungsprozess und den Gebäudebetrieb zu verbessern und eine Entscheidungsfindung zu erleichtern.

Für meine Eltern.

To my parents.

## Acknowledgements

Firstly, I would like to thank Prof. Andreas Wagner for accepting me as a PhD student, for his time while supervising this thesis and for the guidance he gave me.

Prof. Gregor Henze deserves my deepest gratitude for supporting me from the very first idea concerning this thesis, for his continuous support, for giving me the opportunity to work with him at the University of Colorado in Boulder and during his visits to Freiburg. This thesis benefitted greatly from his experience in conducting research.

The Fraunhofer Institute for Solar Energy Systems and my colleagues here provided me with an excellent environment for conducting this research. This includes the inspiring atmosphere, the technical infrastructure and the opportunity to present the results at various conferences. I want to thank all my colleagues at the Institute and especially within the division "Thermal Systems and Buildings". Special thanks to the head of the "Solar Building" department, Sebastian Herkel, who always supported my work on this thesis. Many thanks to Mehmet Elci and Olga Tsvetkova for writing their Bachelor/Master theses under my supervision and in the context of this thesis.

The Fraunhofer Institute for Building Physics developed the calculation routine used as the basis for the energy demand calculation of Chapter 5. The author is grateful to Marcus Fink and Florian Antretter for providing this routine for use in this thesis. The data for the analyzed building in Chapter 5 was provided by the DOMA GmbH. Many thanks to Bernd Dollt and the involved employees for this support.

I am very grateful to the Reiner Lemoine-Stiftung which supported this thesis with a scholarship. This work was also supported by the German Federal Ministry of Economics and Technology via the projects ModBen (0327410A), ModQS (0327893A) and Lüftungsmodell (0329663L).

Thanks to Dr. Helen Rose Wilson and Dr. Dirk Jacob for proof-reading the manuscript and their valuable comments.

Dr. Dirk Jacob deserves special thanks for sharing his simulation experience and the "view of a physicist" with me. Our dialogue started when he was the supervisor of my Master thesis at Fraunhofer ISE and continued as colleagues in the same office with innumerable discussions on this thesis and many other topics.

Furthermore, I want to deeply thank my family, especially my parents and grandparents. They always supported and believed in me. Danke!

Finally, Kiki, I want to express my deepest gratitude that you are always there for me, for your love and understanding.



# Contents

<b>1</b>	<b>Introduction</b>	<b>1</b>
1.1	Motivation . . . . .	1
1.2	Hypotheses . . . . .	4
1.3	Literature Review . . . . .	4
1.3.1	Model Uncertainty . . . . .	5
1.3.2	Numerical Uncertainty . . . . .	7
1.3.3	Model Input Uncertainty . . . . .	7
1.4	Purpose of Research and Objectives . . . . .	10
1.5	Structure of the Thesis . . . . .	11
<b>2</b>	<b>Statistical Fundamentals and Uncertainty Quantification for Simulation Input</b>	<b>13</b>
2.1	Background and Objectives . . . . .	13
2.1.1	Literature Review . . . . .	13
2.1.2	Objectives . . . . .	15
2.2	Methodology . . . . .	15
2.2.1	Tools . . . . .	15
2.2.2	Data Analysis . . . . .	16
2.2.3	Sources of Information . . . . .	27
2.2.4	Flowchart for the Proposed Methodology . . . . .	30
<b>3</b>	<b>Uncertainty Analysis</b>	<b>33</b>
3.1	Background and Objectives . . . . .	33
3.1.1	Literature Review . . . . .	33
3.1.2	Objectives . . . . .	36
3.2	Methodology . . . . .	37
3.2.1	Sampling . . . . .	37
3.2.2	Evaluation of the Model for each Element of the Sample . . .	44
3.2.3	Methods for Interpreting Results . . . . .	45
3.2.4	Combined Building Performance Simulation and Cost-Benefit Analysis . . . . .	48
3.2.5	Case Studies . . . . .	50
3.3	Results and Discussion . . . . .	61

3.3.1	Simple Mathematical Model . . . . .	61
3.3.2	Building Performance Simulation Model . . . . .	66
3.4	Summary . . . . .	77
<b>4</b>	<b>Sensitivity Analysis</b>	<b>81</b>
4.1	Background and Objectives . . . . .	81
4.1.1	Literature Review . . . . .	81
4.1.2	Objectives . . . . .	92
4.2	Methodology . . . . .	92
4.2.1	Scatter Plot Method . . . . .	94
4.2.2	Elementary Effects Method . . . . .	95
4.2.3	Variance-Based Method . . . . .	98
4.2.4	Monte Carlo Filtering . . . . .	99
4.2.5	Overall Sensitivity Analysis Methodology . . . . .	101
4.2.6	Case Study . . . . .	101
4.3	Results and Discussion . . . . .	108
4.3.1	Scatter Plot Method . . . . .	108
4.3.2	Elementary Effects Method . . . . .	111
4.3.3	Variance-Based Method . . . . .	114
4.3.4	Monte Carlo Filtering . . . . .	117
4.3.5	Predicted Savings and Implementation . . . . .	119
4.4	Summary . . . . .	123
<b>5</b>	<b>Application to Residential Building Design</b>	<b>125</b>
5.1	Case Study . . . . .	125
5.1.1	Quantification of Building Performance Analysis Input Uncertainty . . . . .	128
5.1.2	Quantification of Cost-Benefit Analysis Input Uncertainty . . . . .	129
5.2	Results and Discussion . . . . .	132
5.2.1	Building Performance Analysis . . . . .	132
5.2.2	Combined Building Performance and Cost-Benefit Analysis . . . . .	144
5.3	Summary . . . . .	155
5.3.1	Building Performance Analysis . . . . .	155
5.3.2	Combined Building Performance and Cost-Benefit Analysis . . . . .	156
<b>6</b>	<b>Conclusions</b>	<b>159</b>
6.1	Summary of Most Important Results . . . . .	159
6.2	Guidelines for Applying the Developed Methodology . . . . .	162
6.3	Potential of the Results and Expected Impact . . . . .	164
6.4	Outlook and Future Work . . . . .	164

<b>A Appendix</b>	<b>167</b>
A.1 Probability Distributions . . . . .	167
A.2 Data Analysis for Identifying Dependence . . . . .	173
A.3 Cost Functions . . . . .	174
A.4 Nomenclature . . . . .	175
<b>List of Figures</b>	<b>181</b>
<b>List of Tables</b>	<b>185</b>
<b>Bibliography</b>	<b>187</b>



# 1 Introduction

## 1.1 Motivation

A large share of the overall energy demand is consumed in buildings. In Germany, 45% of the overall end energy consumption can be attributed to households, trade, commerce and services (AG Energiebilanzen e.V., 2012). Moreover, the highest energy saving potential of the European Union lies in the building sector (European Commission, 2011). Reducing the energy consumption in buildings is commonly stated to be very important in the literature (e.g., Henze et al., 2004; Choi Granade et al., 2009; BMWi, 2011; Jacob, 2012). The underlying reasons for these statements are: Saving energy protects resources (Hirsch et al., 2005), helps to prevent a drastic climate change (IPCC, 2007) and possibly saves money (Tuominen et al., 2012). It seems to be obvious that methods to support the reduction of energy consumption in buildings are important in this context. Therefore, this thesis is focusing on methods and a framework that supports the design and operation of energy-efficient buildings.

Most people agree that energy-efficient buildings with advanced plant equipment commonly necessitate a complex design process. The traditional approach to design buildings and HVAC (heating, ventilation and air conditioning) equipment uses steady-state methods and worst-case scenarios. This is often not sufficient when complex systems have to be investigated (Macdonald, 2002, p. 2). This situation can be improved with building performance simulation (BPS) (Clarke, 2001, p. ix). With BPS the partial load behavior as well as the interactions between plant equipment and the building can be fully examined. Figure 1.1 provides an impression of some of these manifold interactions. An integrated analysis (e.g., analysis with BPS) is essential when net-zero-energy buildings or plus-energy buildings<sup>1</sup> are designed. Beside the application of simulation models in the design process, another interesting area is employing simulations to improve the operation of buildings and energy systems (e.g., Henze, 1995).

Although simulations are often used in building research and practice, uncertainties in their results are hardly ever quantified (Macdonald, 2002, p. 2). One reason

---

<sup>1</sup>Over the course of a year, a net-zero-energy building produces the same amount of energy from renewable energy sources as it imports from external sources. A plus-energy building produces more energy than it imports over one year (Voss and Musall, 2011, p. 12). However, different definitions exist and the interested reader is referred to Sartori et al. (2012).

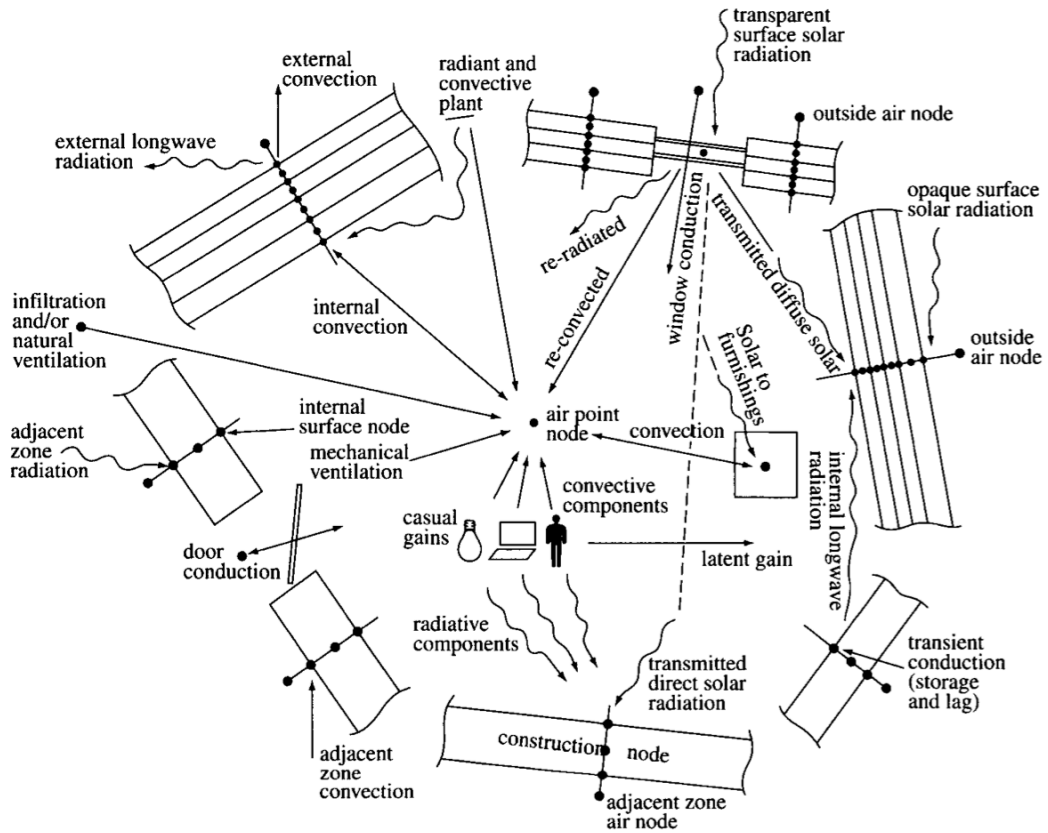


**Figure 1.1:** Energy flow paths in a building (source: Clarke, 2001, p. 6).

for this seems to be the lack of methodologies and tools which are applicable to the problem of uncertainties in buildings. A mismatch between detailed and computationally expensive simulations on the one hand and crude parameter assumptions according to some rules of thumb on the other can often be found in practice (Pfafferott and Herkel, 2008). This is misleading, as simulations sometimes introduce pseudo-accuracy, creating a false sense of validity and engineering rigor. By examining the impact of uncertainties, it is possible to increase simulation quality and thus the robustness of results. If a building simulation is considered to be a decision support instrument, it is strongly advisable to assess and communicate the problem of uncertainties properly. Otherwise decisions might be made which are based on faulty or incomplete assumptions. This can lead to disappointment after completion of the building if it does not perform as communicated during the design process.

With a classic building simulation, the answer to design questions is often either

yes or no depending on the assumptions. An example for such a design question is: *Will the renewable energy system provide 20% of the total annual energy demand?* With an uncertainty analysis (UA), it is possible to answer design questions with probabilities, e.g.: *The probability of more than 20% energy supplied by the renewable energy system is 80%.* Figure 1.2 shows a comparison of the classic simulation approach and the proposed approach. The classic approach has single numbers as input and yields single numbers (e.g., specific annual energy consumption) with unknown accuracy as output. The BPS approach with uncertainties indicates how inputs might vary and quantifies the uncertainty in the result.

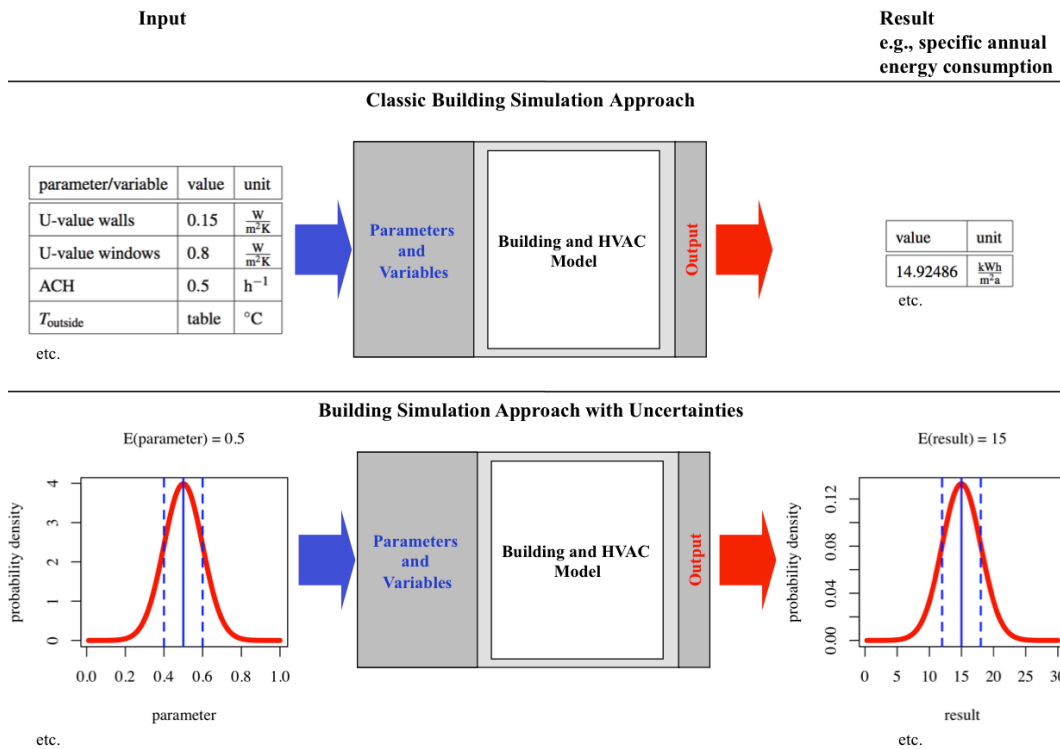


**Figure 1.2:** Classic building simulation approach versus building simulation approach with uncertainty analysis.

Furthermore, with the proposed approach it is possible to compare design options and choose the option with the highest probability of reaching a specific goal. This leads to robust design solutions that perform well within the input range that is captured in the UA.

Another interesting question is the influence of different building components, HVAC equipment and control strategies on the energy consumption or operating

cost (e.g., Clarke, 2001, pp. 285-298). A sensitivity analysis (SA) can answer this question. A UA often goes hand in hand with an SA. In this combination, the aim of an SA is to attribute the uncertainty in the model output to the uncertainty in the model input (Saltelli et al., 2008, p. 1). Sensitivity analyses can also be applied to model reduction and optimization problems (Eisenhower et al., 2012b). Typical questions that can be answered with SA are: *Which simulation input has the greatest influence on the result?; Which model input (i.e., input argument) should be varied by an optimization algorithm?; Which model variables or parameters have the least influence and hence can be neglected when simplifying the model?*

A further common task in the design process of a building is a cost-benefit analysis (CBA) to compare design options and different scenarios (Miller, 2005, p. 418). The results are also strongly dependent on assumptions about uncertain economic boundary conditions (e.g., future inflation rates and energy costs). UA and SA can also be applied to CBA. Furthermore, it is possible to perform a UA and SA for a combined BPS and CBA and use the results to support decisions.

## 1.2 Hypotheses

Monte Carlo (MC)-based techniques for UA and SA are best suited for BPS. Quasi-random sampling techniques (i.e., sampling based on Sobol' sequences) require fewer simulations until convergence of the MC simulation. Furthermore, they produce more robust results than other sampling strategies. By using parallelization, it is possible to further reduce the time required for a UA and SA. The results of a UA can be presented such that decision makers can easily interpret them. Furthermore, the results provide a significant benefit compared to simulations with single-value estimates. Performing UA and SA for combined building performance and cost-benefit analyses can provide valuable insights.

BPS has a wide range of applications. A single best method for SA does not exist. However, a combination of scatter plots, the elementary effects method, the variance-based method and Monte Carlo filtering is applicable for most cases. All methods can be applied consecutively or single methods can be selected on the basis of project requirements.

## 1.3 Literature Review

The uncertainty of simulation results can have various causes and different classifications exist (Kennedy and O'Hagan, 2001). It is important to distinguish between the different sources of uncertainty because the nature of the uncertainty determines the way it can be quantified (Hopfe and Hensen, 2011). De Wit distinguishes between specification, modeling, numerical and scenario uncertainty (de Wit, 2003, p.

29). The specification and the scenario uncertainty can be summarized as model input uncertainty. In the following, three sources of uncertainty are distinguished: model uncertainty, numerical uncertainty and model input uncertainty.

It is understandable that in (BPS) practice, the different sources of uncertainties can influence each other because of trade-off effects. An example is that many building models are very detailed to reduce the model uncertainty. At the same time, this can introduce an increased model input uncertainty because the models require information which is not always available in the desired accuracy.

### 1.3.1 Model Uncertainty

Every model is an approximation to reality and hence model uncertainty is always present (de Wit, 2003, p. 29). A BPS consists of models for different phenomena such as heat transfer through building components, infiltration and air change, and models for HVAC components and their controls. The model uncertainty depends on the complexity of the analyzed problem and how accurately the model captures reality.

Different model validation standards and procedures exist. The best validation for a simulation program or model obtained is by comparison with measured data. However, this is not the standard procedure because appropriate measurements are costly. Many existing validation standards require the comparison of results from the model that is to be validated with the results of other simulation models or programs. Examples for this can be found in VDI 6020 Part 1 (2001) and ANSI/ASHRAE Standard 140 (2011). Many validated simulation programs and models are available for BPS. Several BPS programs are validated against ANSI/ASHRAE Standard 140 (2011). When this standard is applied, the results of a simulation program or model for several test cases are compared with the results of other simulation programs. These reference programs are considered to be reliable. Examples for programs or models that were subjected to the validation procedure of ANSI/ASHRAE Standard 140 include IDA ICE (Equa Simulation AB, 2010), Modelica Buildings library (Nouidui et al., 2012), EnergyPlus (Henninger and Witte, 2012) and WUFI Plus (Antretter et al., 2011).

Different test cases are defined in the validation standards, where all the necessary input and information on boundary conditions are provided. Figure 1.3 illustrates a test case from the ANSI/ASHRAE Standard 140 (2011).

All test cases were modeled with the reference simulation programs and the results are provided. To analyze the variability of different BPS programs, the results for the annual heating energy of one test case are presented (Figure 1.4). There are differences among the results. The mean value of all results is 5.090 MWh whereas the minimum value is 4.296 MWh and the maximum value is 5.709 MWh. Figure 1.4 contains a box plot of all results. The box represents the data from the lower

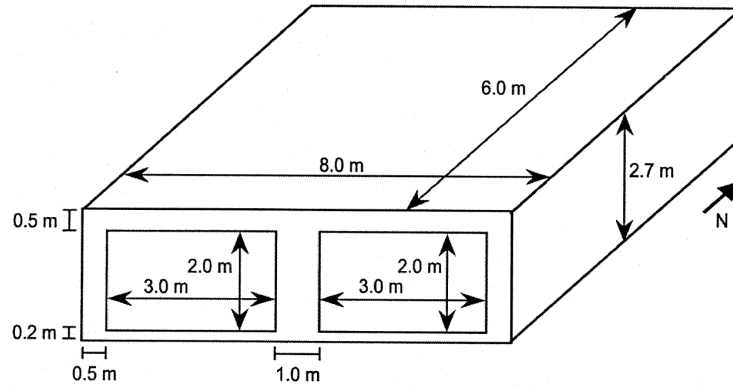


**Figure 1.3:** ANSI/ASHRAE Standard 140 reference case 600 (source: ANSI/ASHRAE Standard 140, 2011, p. 16).

quartile to the upper quartile and the median is also indicated. The height of the box is the interquartile range. The maximum length of the whiskers is 1.5 times the interquartile range<sup>2</sup>. The differences among the results in Figure 1.4 show that model uncertainty<sup>3</sup> is present when BPS programs are applied.

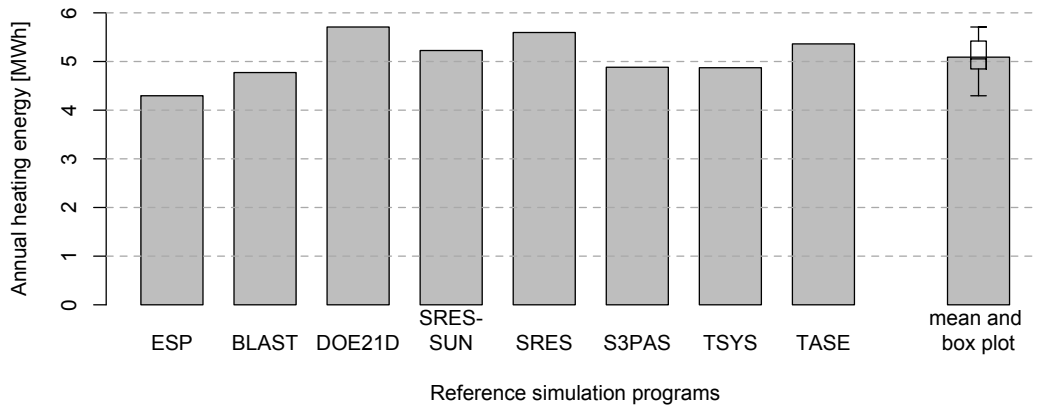


**Figure 1.4:** ANSI/ASHRAE Standard 140 reference results (data source: ANSI/ASHRAE Standard 140 (2011)).

<sup>2</sup>More details about these statistics will be presented in Section 2.2.2.1.

<sup>3</sup>It is uncertain whether all result differences are attributable to model uncertainty. Different program interfaces and different analysts might also have contributed to these differences.

### 1.3.2 Numerical Uncertainty

Numerical uncertainties are present, when (mathematical) models are solved by computers. All variables and parameters of a simulation model are stored in a computer number format, which is the representation of a value (e.g., real number). Due to limitations of memory capacity, all real numbers need to be rounded when stored on a computer and this introduces uncertainties. The floating point arithmetic used in computers is only an approximation to exact arithmetic (Jézéquel and Chesneaux, 2008). However, because of the performance of modern computers and the accuracy requirements of typical BPS, the uncertainty introduced in this way is negligible in most cases.

Another source of numerical uncertainty is the fact that computer simulations commonly apply iterative numerical methods to solve the systems of equations and to run the simulation. Every solver introduces uncertainty depending on its type and selected settings, such as tolerance or simulation step size (i.e., discretization errors).

The numerical uncertainties are specific to the program used for BPS. By analyzing the different sources of uncertainty, de Wit comes to the conclusion that the influence of numerical uncertainty can be neglected (de Wit, 2003, p. 29). His arguments stress that the chosen discretization and time steps can be selected such that this uncertainty is insignificant.

### 1.3.3 Model Input Uncertainty

Model input uncertainties comprise all uncertainties related to the determination of the parameters, variables and boundary conditions of the model. Equation 1.1 is introduced to illustrate model input uncertainties. It is the differential equation for a simple building simulation model.

$$C \frac{dT_i}{dt} = (H_{tr} + \dot{V}_{ve} c_p \rho_{air})(T_e - T_i) + \dot{Q}_{int} + \dot{Q}_{sol} + \dot{Q}_{heat} \quad (1.1)$$

with

$$\frac{dT_i}{dt} = f(T_i) ; T_i(t=0) = T_{i,0}$$

In Equation 1.1,  $C$  is the heat capacity,  $T_i$  is the internal temperature,  $t$  is the time,  $H_{tr}$  is the heat transfer coefficient,  $\dot{V}_{ve}$  is the ventilation flow rate,  $c_p$  is the specific heat capacity of the air,  $\rho_{air}$  is the density of the air,  $T_e$  is the outside air temperature,  $\dot{Q}_{int}$  is the internal heat gain,  $\dot{Q}_{sol}$  is the solar heat gain and  $\dot{Q}_{heat}$  is the heat delivered by any HVAC component. Model input uncertainties can affect almost every term of the equation. These include specifications of the building envelope ( $C$ ,  $H_{tr}$ ) and the HVAC equipment ( $\dot{Q}_{heat}$ ,  $\dot{V}_{ve}$  if an air handling unit is installed), meteorological data ( $T_e$ ,  $\dot{Q}_{sol}$ ) as well as occupancy ( $\dot{V}_{ve}$  if windows can

be opened,  $T_i$  if the set point temperature can be adjusted,  $\dot{Q}_{sol}$  if blinds can be operated).

A correct quantification of the input uncertainties is essential to obtain reliable results by performing UA and SA. Appropriate probability distributions and associated parameters are required. Depending on the project stage at which a simulation study is conducted, knowledge about the uncertainty varies and hence the approach to quantifying the input uncertainties. In the case of BPS, several types of model input uncertainties exist. Hopfe and Hensen (2011) distinguish between physical (e.g., material properties), design (e.g., geometry) and scenario (e.g., occupancy) uncertainties. Almost every BPS model has uncertain input parameters and variables<sup>4</sup>. The aim is to quantify the input uncertainty of influential parameters and variables and take the uncertainty into account when calculating and analyzing the output.

Uncertainties in a BPS context are introduced in the following case studies that address model input. Lomas and Eppel (1992) conduct a study on SA for building simulations. They compare different SA methods and analyzed over 70 uncertain inputs. Beside other methods, they also use MC techniques. An MC simulation is performed by re-running the simulation several times with different input parameters that are sampled according to a probability density function (PDF). The results of all of these simulations can be used to obtain a joint PDF for the result. In this way, it is possible to analyze the likely variation of the output given the uncertain set of inputs<sup>5</sup>. Macdonald and his co-workers compare different techniques for uncertainty quantification and implemented some methods in a simulation program (Macdonald and Strachan, 2001; Macdonald, 2002; Macdonald and Clarke, 2007). De Wit states that it is essential to communicate uncertainties to decision makers. In building simulation practice however, an explicit assessment of uncertainty is more the exception than the rule. Therefore, most of the decisions are based on single-value estimates (de Wit, 2003, p. 25). De Wit and Augenbroe (2002) analyze uncertainties in building design mainly related to thermal comfort. They identify uncertainties in ventilation rates and indoor air temperature distribution as highly influential on the simulation result. Furthermore, they propose a method for decision making in building design. Mara and Tarantola (2008) perform an SA for a test cell model and focus on the application in model development. They analyze the sensitivity of simulation input using a variance-based method. Eisenhower et al. (2011) conduct a UA and SA investigating the influence of about 1,000 parameters using quasi-random sampling and a meta-model (response surface). Hopfe and Hensen (2011) report results of an MC-based UA and SA implemented with Latin hypercube sampling

---

<sup>4</sup>A parameter has a constant value during the simulation (e.g., window area) and a variable changes over time (e.g., heating power).

<sup>5</sup>More details on MC simulations will be presented in Chapter 3.

(LHS). In their work, the physical uncertainty analysis was conducted by varying physical properties of materials, while the design uncertainty analysis was accomplished by adjusting geometry and glass surface areas. The scenario uncertainty was represented by varying the infiltration rate and internal loads. Booth et al. (2011) perform a UA of housing stock models using Bayesian techniques. Their aim is to analyze different retrofit options at an urban scale.

The literature introduced so far reveals that one commonly applied approach for UA and SA in BPS is based on MC techniques. However, it is also possible to reformulate models in a way that they can take PDFs as input and compute a PDF as output rather than producing single-value estimates of the simulation output. A study conducted by Jacob et al. (2011) shows that this method requires extensive mathematical modeling efforts and more computational resources than MC techniques for a given accuracy and building problem.

Wong et al. (2005) review research activities concerning intelligent buildings. One part of this review is the evaluation of investments and CBA is mentioned as a common technique. Wong et al. point out that the analysis of uncertainties in a CBA is important but not common practice in building design. As a reason for this they mention the lack of methods for this type of analysis. The international standard EN 15459 *Energy performance of buildings - Economic evaluation procedure for energy systems in buildings* contains specific information on calculation methods, cost types (e.g., maintenance cost) and typical life spans for HVAC equipment (DIN EN 15459, 2008). However, it does not contain information concerning UA for economic evaluations. Rysanek and Choudhary (2011) conduct an analysis where they combine building simulation and economic calculations. The economic uncertainties are explored with best-case and worst-case scenarios and different refurbishment options are analyzed by changing the technical system in the building simulation. Heo (2011) analyses different retrofit options by quantifying the uncertainty in the simple payback time (i.e., investment cost for retrofit divided by annual energy saving) of different energy saving measures.

The literature review reveals that several studies concerning UA and SA for BPS have been conducted. The approaches of previous work vary significantly depending on the analyzed application. An important aspect is the quantification of the input uncertainty because it is the prerequisite for every UA and SA. A general methodology for different applications that includes all necessary steps to conduct a UA and SA for BPS does not exist. Furthermore, quality assurance aspects such as convergence testing are often not addressed. The definition for and distinction between UA and SA varies in the BPS-related literature. Most literature is about the application concerning building design, whereas building operation aspects are hardly ever analyzed. Furthermore, a general methodology for conducting a UA and

SA for a combined BPS and CBA has not been found in the literature<sup>6</sup>.

## 1.4 Purpose of Research and Objectives

Based on the findings above, the objectives of this thesis are derived in the following.

The features and capabilities of available BPS programs are diverse and for some questions (e.g., analysis of heat and moisture transfer in the building envelope elements) only a few simulation programs can be applied. Analyzing the uncertainty in the results that is introduced by different simulation models or programs is very specific to the individual case and hence not the focus of this thesis. In the context of this thesis, it is assumed that the available BPS programs produce reliable results.

Also, the numerical uncertainty (i.e., solver tolerances and round-off errors) is not analyzed any further in the context of this thesis. However, the modeler has to ensure the applicability of the solver and the solver settings to the analyzed problem.

The main focus in this thesis is on model input uncertainties since these uncertainties have the greatest influence on the model output among the sources of uncertainty that are independent of the simulation program. Different techniques for UA and SA will be investigated. The aim is to develop a unified approach which is applicable to typical BPS and common questions in building design and operation. One important aspect is the scalability of the approach, depending on the requirements of the analysis and the questions to be answered. Because of the aim to develop a program-independent and scalable methodology, the structure of BPS models<sup>7</sup> and the findings presented in Jacob et al. (2011), the focus of this thesis is on MC-based techniques. One objective is to review the current state of the art concerning UA and SA applied to BPS. Furthermore, methods for UA and SA are taken from other disciplines, analyzed with respect to the applicability for BPS and modified where necessary. Best practices are identified and quality assurance aspects (e.g., convergence) are highlighted. A methodology to perform UA and SA with BPS models is developed. Practical limitations and ways to overcome them are discussed.

Another aspect is UA and SA for combined BPS and CBA and how this can improve decision-making processes. This is relevant because in practice many decisions are based on their monetary implications. It seems to be natural to talk about different options in the design phase in terms of money. BPS and CBA are linked because the results of a BPS influence the results of a CBA (e.g., the energy supplied by a solar thermal collector influences the cost effectiveness of the solar thermal system). Furthermore, the results of CBA are also heavily dependent on assumptions about uncertain economic parameters (e.g., future inflation rates and energy costs). It is analyzed whether and how the two analyses can be combined in a UA and SA

---

<sup>6</sup>An exception is the paper that Burhenne et al. (2013a) published in the context of this thesis.

<sup>7</sup>BPS models can be nonlinear, non-additive and they can have discontinuities.

setting and how this can aid a typical decision-making process. A further question is whether a significant benefit can be obtained when the methodology is applied to typical BPS applications. The thesis aims to provide comprehensive guidance for applying UA and SA.

Based on the aspects mentioned above, the research questions are:

- (I) What are the statistical foundations for UA and SA and how can the input uncertainty be quantified?
- (II) Which methods for UA and SA are most applicable for BPS and can they be combined to obtain a general methodology?
- (III) Is it possible to develop a methodology to perform UA and SA for a wide range of BPS applications?
- (IV) How can UA and SA be performed for a combined BPS and CBA?
- (V) Which benefit to typical BPS can be provided by UA and SA?

## 1.5 Structure of the Thesis

This thesis consists of a chapter that introduces the statistical fundamentals (Chapter 2), two main chapters on uncertainty analysis and sensitivity analysis (Chapter 3 and Chapter 4) and an application chapter (Chapter 5). Each of the Chapters 2 - 4 deals with a separate topic of the overall methodology and includes a detailed literature review in addition to the review presented in the introduction. These separate reviews do not concern only the application of the analyzed methods in the context of BPS but discuss methods and approaches applied in other disciplines. The reason for separating the different topics is to ensure clear differentiation between the analyzed aspects. Furthermore, the different steps of the methodology (UA, SA) can be applied independently of each other and are therefore presented in separate chapters. The links between the chapters are analyzed and illustrated in the application chapter.

Chapter 2 on "Statistical Fundamentals and Uncertainty Quantification for Simulation Input" introduces the statistical foundations as prerequisite for the remaining parts of the thesis. Furthermore, methods to analyze data and quantify uncertain simulation input are introduced. Parameter uncertainties are investigated as well as uncertainties in simulation variables. BPS input is the main focus. However, methods to quantify uncertain input for a CBA are also investigated.

In Chapter 3 addressing "Uncertainty Analysis", different methods for generating random numbers are analyzed with respect to their convergence and robustness properties. Furthermore, techniques to analyze the results of an MC simulation are

examined and tested. Another important aspect in this chapter is the visualization of the results. As a case study, a residential building with solar thermal collectors is investigated.

Different SA techniques are introduced in Chapter 4 on "Sensitivity Analysis". The most applicable SA methods are combined to develop an SA methodology for BPS. The case study is the application of SA in the operation phase of a large scale office building.

In Chapters 2 to 4, different parts of the overall methodology are introduced and developed. In Chapter 5, "Application to Residential Building Design", all parts are applied together to an example. A UA and an SA for a combined building performance and cost-benefit analysis are performed. In this case study, the best design options with respect to energy performance and cost efficiency are identified, taking uncertainties into account.

In Chapter 6, "Conclusions", the results of the thesis are discussed. The methodology is summarized and recommendations concerning practical application are given. Furthermore, future work and potential for enhancement are identified.

# 2 Statistical Fundamentals and Uncertainty Quantification for Simulation Input

## 2.1 Background and Objectives

This chapter introduces the statistical fundamentals and the tools used. Furthermore, model input uncertainties and their quantification are analyzed. A methodology for uncertainty quantification (UQ) for BPS and CBA input is proposed.

### 2.1.1 Literature Review

This literature review focuses on UQ for simulation input. The statistical fundamentals are introduced in Section 2.2.2. According to Saltelli and Tarantola (2002), the quantification of input uncertainty can be based on measurements, estimates, expert judgment, physical bounds, output from simulations and analogies to similar simulation input.

Macdonald applies measurement theory to distinguish between systematic and random errors and the resulting uncertainties. As an example for a systematic error, he mentions the usage of incorrect data for a given parameter or employing an inappropriate model for a physical phenomenon (Macdonald, 2002, pp. 86-88). The latter example does not correspond to the classification approach used in this thesis. Macdonald points out that one source of random errors is measurement error. As an example for a random error he uses the characterization of uncertainty in thermophysical properties and suggests to use the measurement error to quantify their random uncertainty. To express the overall uncertainty in a parameter he suggests describing the systematic and random uncertainties in a simulation parameter with a probability distribution. Furthermore, he introduces several distributions for BPS input. These are: discrete distribution, uniform distribution, normal distribution, log-normal distribution and triangular distribution (Macdonald, 2002, pp. 88-96). It is illustrated how the uncertainty can be quantified for three typical BPS inputs, thermophysical properties, internal gains and infiltration rates, by analysis of existing data and detailed modeling (Macdonald, 2002, pp. 96-116).

De Wit points out that in a first step, the uncertainty for the simulation inputs

can be quantified by using information from literature, experiments, model calculations, rules of thumb, and experience (de Wit, 2003, p. 31). He uses a two-step procedure, where a rough estimate of the input uncertainty is assigned and in the second step the UQ might be updated (de Wit, 2003, p. 31). He separates parameter and scenario uncertainties. In the case of parameter uncertainties, his quantification approach is illustrated with three parameter types (i.e., uncertainty in physical properties of materials and components, uncertainty in wind pressure coefficients and uncertainty in air temperature stratification) (de Wit, 2003, pp. 34-39). De Wit also takes dependence between parameters into account. This is done by treating a parameter as either independent or perfectly positively correlated. Uncertainty in the physical properties of materials and components is quantified on the basis of literature. The variation in wind pressure coefficients is analyzed by calculating the pressure coefficients with different tools, where the different results are used to compute lower and upper bounds. For the air temperature stratification he refines a BPS model so that it can take the temperature stratification into account and considers the vertical temperature gradient to be uncertain. Based on literature values, he varies the gradient in an MC simulation. Scenario uncertainties such as climate conditions and occupancy profiles are not investigated in his study (de Wit, 2003, pp. 34-39). Because no further information was available, de Wit assumes that all parameters are normally distributed and the ranges derived from literature and inter-tool comparison were interpreted as the 95% central confidence interval. The UQ for wind pressure coefficients is refined by an expert judgement study. This expert judgement is based on procedures described by Cooke and Goossens (2000). In his example the following steps were conducted: selection of the experts in the field of interest, training of the experts, answering of the questionnaire, elicitation meeting, analysis and combination of the experts' answers (de Wit, 2003, pp. 34-39).

As mentioned before, Hopfe and Hensen (2011) distinguish between three types of simulation input uncertainties (physical, design and scenario uncertainties). The scenario uncertainty includes internal and external boundary conditions. Hopfe assigns normal distributions to the uncertain parameters and uses literature to determine their standard deviation (Hopfe, 2009, p. 38). Furthermore, it is stated that the uncertainties in physical, design and scenario parameters are analyzed separately (Hopfe, 2009, p. 46).

Eisenhower et al. (2011) performed UA and SA for a BPS where they assumed more than 1,000 parameters to be uncertain. Because of this large number of uncertain parameters, they used a uniform distribution for all non-zero parameters and an exponential distribution for parameters with zero as the nominal value.

Assumptions concerning occupancy and the occupants' behavior are highly uncertain. According to the experience of many building operators and literature (e.g., Page et al., 2008; Brohus et al., 2009; Haldi and Robinson, 2011), the occupants

have a significant influence on building performance<sup>1</sup>.

### 2.1.2 Objectives

The objective is to develop a methodology for input UQ that meets the requirements of typical BPS applications. Criteria are the applicability with respect to available information and accuracy requirements. Hence, the methodology should be scalable depending on project requirements and constraints. Best practice will be identified by analyzing existing work in the BPS context as well as from other scientific fields.

## 2.2 Methodology

### 2.2.1 Tools

The tools used throughout this thesis are introduced in the following subsections. For applicability reasons, it is important that the developed methodology works with a variety of existing BPS programs. Many different simulation programs exist. Some of them were specifically developed for BPS (e.g., IDA ICE, ESP-r, Energy-Plus, TRNSYS, WUFI Plus) and others are more generic but also used for buildings (e.g., Dymola/Modelica, MATLAB/Simulink, IDA SE). The decision about which tool is used in a specific project is based on the questions to answer<sup>2</sup>, the experience of the modeler, license costs, and many other aspects. The majority of the programs mentioned above are not designed to perform statistical analyses, to run MC simulations and to perform simulation in parallel on computer clusters. Doing this requires some additional tools which are used together with the simulation programs. These tools belong to the simulation tool chain and are used before, parallel to and after the simulation (e.g., pre-processing and post-processing of simulation input and results). Many tools exist for performing these tasks also (e.g., MATLAB, R, Python, awk etc.).

#### 2.2.1.1 R

R is a language and a program for statistical computing and graphics. R runs on different operating systems and is available as free software under the GNU General Public License (R Core Team, 2012). In this thesis, R and several R packages are used for generating samples, performing statistical computations and arithmetic

---

<sup>1</sup>Moreover, the indoor conditions have significant influence on the occupant's performance but this is beyond the scope of this thesis.

<sup>2</sup>The application can range from building envelope and/or HVAC design, controls design, optimization of the building operation to the calculation of heat and moisture transport in building components.

calculations, managing parallel simulations on different processor cores, processing simulation input and output and result visualization. R can be used to perform a UA and SA with most BPS programs<sup>3</sup>. A further selection criterion is that it is available for different operating systems (e.g., Microsoft Windows, Mac OS X, Linux).

### 2.2.1.2 Modelica/Dymola

Modelica can be used to model differential algebraic equations (DAE). The general representation of a DAE is

$$0 = f(t, \dot{\mathbf{x}}(t), \mathbf{x}(t), \mathbf{y}(t), \mathbf{u}(t), \mathbf{p}) \quad (2.1)$$

where  $t$  is the time,  $\dot{\mathbf{x}}(t)$  is the vector of differentiated state variables,  $\mathbf{x}(t)$  is the vector of state variables,  $\mathbf{y}(t)$  is the vector of algebraic variables,  $\mathbf{u}(t)$  is the vector of input variables and  $\mathbf{p}$  is the vector of parameters and/or constants. The Modelica language is non-proprietary, equation-based and object-oriented (Modelica Association, 2012). A wide range of physical systems can be modeled with Modelica. Many Modelica libraries can be used to perform modeling tasks and contain various models that can serve as a basis for the modeling. The basis of most libraries is the Modelica Standard Library (MSL). Since Modelica is a language but not a program, an environment is required to perform the simulation. Several commercial and freely available simulation environments exist for Modelica. In the context of this thesis, the commercial program Dymola is used (Dassault Systèmes AB, 2011). Modelica was used in this thesis because it is a promising modeling approach<sup>4</sup> and well suited for models of different complexity used in an MC setting. The interested reader is referred to Burhenne et al. (2013b) for further information concerning Modelica in a BPS context.

### 2.2.2 Data Analysis

In the following sections, a methodology for quantifying the model input uncertainty is developed.

A database that provides estimates for a wide range of uncertain inputs for BPS does not exist (de Wit, 2003, pp. 25-26). Since each building and its usage is unique, such a general database for all input uncertainty types would be difficult

---

<sup>3</sup>The prerequisite is that the simulation program has text files in which the simulation input is specified and an executable file that takes these input files and performs the simulation.

<sup>4</sup>During the time this thesis was written, Modelica gained importance in the building simulation community, resulting in the approval of an Annex of the International Energy Agency (IEA), under the implementing agreement on Energy Conservation in Buildings and Community Systems (ECBCS). The Annex 60 has the title *New generation computational tools for building and community energy systems based on the Modelica and Functional Mockup Interface standards*.

to develop. Possible sources of information used in the developed methodology are physically based information on bounds and modes, literature, expert knowledge, and measurements. This is based on several other studies (Saltelli and Tarantola, 2002; Cooke and Goossens, 2000; Macdonald, 2002; de Wit, 2003) and adaptations are made.

### 2.2.2.1 Statistics

Statistics is the name of a discipline and at the same time the name of the measures applied within this discipline. In descriptive statistics, statistical methods are used to describe collected data (i.e., a sample). When these measures are used to derive inferences about the underlying population, this is called inferential statistics.

In this section, several statistics to characterize data are introduced. Most important are measures of location (e.g., arithmetic mean) and measures of spread (e.g., standard deviation or variance). If relationships between different variables are of interest, measures of linear dependence can be applied (e.g., covariance or correlation coefficient) (Box et al., 2005, pp. 24-39). Some of these measures can be used as parameters for probability distributions (see Section 2.2.2.2).

A different notation is used for statistics that describe a population and statistics for a sample of a population. The mean of a population is a population parameter and the mean of a sample (i.e., arithmetic mean of all sample elements ( $\bar{X}$ )) is an estimator of the population parameter. This is also true for the standard deviation and other statistics. In the following the notation and equations for samples are used. The arithmetic mean can be calculated by the equation

$$\bar{X} = \frac{1}{N} \sum_{i=1}^N x_i \quad (2.2)$$

where  $N$  is the sample size and  $x_i$  is an element of the sample (Saltelli et al., 2008, p. 59).

The variance of a sample ( $\mathbf{X}$ ) can be calculated by (Saltelli et al., 2008, p. 59)

$$\text{Var}(\mathbf{X}) = \frac{1}{N-1} \sum_{i=1}^N (x_i - \bar{X})^2 \quad (2.3)$$

and the standard deviation is

$$\text{StdDev}(\mathbf{X}) = \sqrt{\text{Var}(\mathbf{X})}. \quad (2.4)$$

The covariance can be used to analyze if a linear dependence between two variables exists and can be calculated according to

$$\text{Cov}(\mathbf{X}, \mathbf{Y}) = \frac{1}{N-1} \sum_{i=1}^N (x_i - \bar{X})(y_i - \bar{Y}) \quad (2.5)$$

with  $\mathbf{X}$  and  $\mathbf{Y}$  being the samples of two stochastic variables (Box et al., 2005, pp. 37-38). A value that is easier to interpret is the Pearson correlation coefficient. That is (Box et al., 2005, pp. 37-38)

$$r_{\mathbf{X}\mathbf{Y}} = \frac{\text{Cov}(\mathbf{X}, \mathbf{Y})}{\text{StdDev}(\mathbf{X}) \text{StdDev}(\mathbf{Y})}. \quad (2.6)$$

It is important to take into account that the covariance and the coefficient of correlation are only meaningful for linear dependence between two variables. A nonlinear dependence cannot usually be detected or represented by these measures<sup>5</sup>.

In addition to the introduced statistics, quantiles are commonly applied in data analysis. Quantiles are the set of  $n_{\text{sub}} - 1$  values which separate the data into  $n_{\text{sub}}$  different subsets (Montgomery and Runger, 2003, p. 698). The median (also called 2-quantile) is the value that divides the sample into two equally sized subsets (i.e., half of the values above and half below the median). If the sample size is even, the median is the arithmetic mean of the two central values (Montgomery and Runger, 2003, pp. 200-201). The median is particularly helpful when the data is not symmetrically distributed and outliers bias the mean value. Quartiles (also called 4-quantiles) implement a similar concept but divide the data into four equal parts. Approximately 25% of the values of the sample are below and 75% are above the first (also called lower) quartile. The second quartile is the median and the third (also called upper) quartile separates approximately 75% of the values of the sample below it and 25% above it (Montgomery and Runger, 2003, pp. 200-201). Several specialized quantiles exist (e.g., percentiles that are 100-quantiles). In addition to the quantiles, the minimum and the maximum values provide valuable information on the sample range.

### 2.2.2.2 Probability Distributions

Uncertainties in simulation input are commonly quantified with the help of probability distributions. Many different distributions exist and they can be separated into discrete (e.g., discrete uniform distribution) and continuous distributions (e.g., normal distribution). Evans et al. (2000) describe 40 different distributions. However, as many people may have observed, in most cases only three of them are used. These popular distributions are the uniform, the normal and the log-normal distributions. This popularity does not indicate that the selection of one of these distributions is the best choice for all cases where they are applied. However, in many cases it is done because most analysts are more familiar with these distributions than others and relatively little information is required to fit them to data. The selection of a distribution depends on the characteristics of the uncertainty and available information (e.g., measurements). In this section, some general properties on discrete

<sup>5</sup>Some exceptions exist (e.g.,  $Y = X^3$ ).

and continuous distributions are introduced briefly. Many statistical tests exist to analyze whether data can be described by a certain distribution or not and some of them will be introduced.

For a probability mass function (PMF) of a discrete random variable  $X$  with possible values  $x_1, x_2, \dots, x_N$  (Montgomery and Runger, 2003, p. 62)

$$\sum_{i=1}^N p(x_i) = 1. \quad (2.7)$$

The expected value of a discrete random variable  $X$  is (Montgomery and Runger, 2003, p. 66)

$$E(X) = \sum_x x p(x). \quad (2.8)$$

The variance of discrete random variables is (Montgomery and Runger, 2003, p. 66)

$$\text{Var}(X) = \sum_x x^2 p(x) - E(X)^2. \quad (2.9)$$

For continuous random variables

$$\int_{-\infty}^{+\infty} p(x) dx = 1 \quad (2.10)$$

where in the continuous case  $p(x)$  is the probability density function (PDF) (Montgomery and Runger, 2003, p. 99). The probability that a variate<sup>6</sup> lies in the range between  $a$  and  $b$  is the integral over the range  $a$  to  $b$  (Evans et al., 2000, p. 12). The expected value for continuous random variables is (Evans et al., 2000, p. 14)

$$E(X) = \int_{-\infty}^{+\infty} x p(x) dx. \quad (2.11)$$

The variance of continuous random variables is (Evans et al., 2000, p. 14)

$$\text{Var}(X) = \int_{-\infty}^{+\infty} (x - E(X))^2 p(x) dx. \quad (2.12)$$

## Overview of Distributions

In Table 2.1, some distributions and their possible application in a BPS context are introduced. The application examples are partly taken from Macdonald (2002). More information on these and other distributions and the corresponding references can be found in Appendix A.1.

<sup>6</sup>A variate is an outcome of a statistical experiment.

**Table 2.1:** Probability distributions and possible application in BPS context.

Distribution	Type	Parameters	Application examples
Discrete uniform distribution	Discrete	$a, b$	State or model selection, number of occupants
Uniform distribution	Continuous	$a, b$	Poorly defined parameters, random number generation
Normal distribution	Continuous	$\mu, \sigma$	Measured physical data
Log-normal distribution	Continuous	$\theta, \omega^2$	Parameters that cannot be negative (e.g., air change rate, metabolic rate of occupants)
Triangular distribution	Continuous	$a, b, c$	Data with a distribution between uniform and normal distributions

## Empirical Distributions

In the case that sufficient measurements are available, the measurements themselves may be used to compute an empirical distribution. Empirical distributions are introduced because they are useful in the context of UA and SA and often used throughout this thesis<sup>7</sup>. The PDF can be directly estimated from the sample data with kernel density estimates<sup>8</sup>. Therefore, assumptions about the algebraic form of the distribution model are not necessary (Evans et al., 2000, pp. 65-70). The advantage is that the analyst does not have to assign a probability distribution and test its applicability. However, a sufficient amount of data has to be available to obtain reasonable results. In cases where many uncertain variables have to be characterized and enough measurements are available, the application of empirical distributions is an advantage because the computation of the kernel density estimates can be automated. It is possible to use empirical cumulative distribution functions (ECDF) to draw samples in an MC sampling. This step will be further explained in Chapter 3.

Figure 2.1 shows an PDF based on empirical data<sup>9</sup> and an ECDF<sup>10</sup> coming from

---

<sup>7</sup>Empirical distributions proved to be especially useful for analyzing the results of an MC simulation (see Chapter 3).

<sup>8</sup>Kernel density estimation can be used to estimate a PDF in a non-parametric way.

<sup>9</sup>The R function `density()` is used to compute the kernel density estimates.

<sup>10</sup>The R function `ecdf()` is used to compute the empirical cumulative distribution function.

a sample that is generated with a random number generator<sup>11</sup> according to  $\mathbf{N}(0, 1)$  and with a sample size ( $N$ ) of 1,000.  $\mathbf{N}(0, 1)$  is the standard normal distribution ( $\mu = 0$  and  $\sigma = 1$ ). The normalized histogram<sup>12</sup> of the data is plotted in the same graph as the PDF.

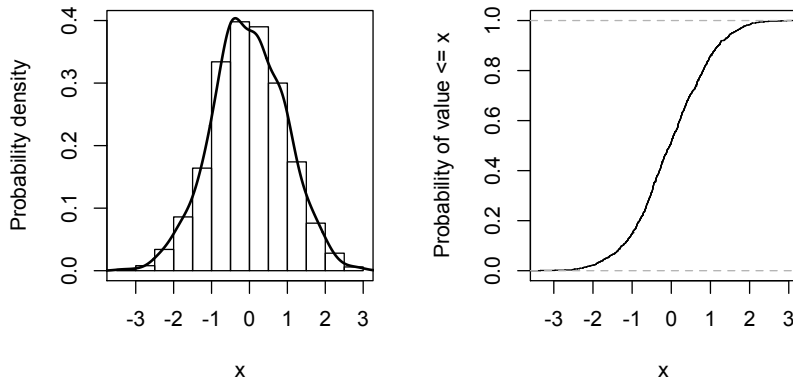


**Figure 2.1:** PDF and ECDF of a sample.

### Distribution Selection

Several distributions were introduced in the previous section. The selection of the "right" distribution for the available data is an important task. Several statistical tests exist to test whether data<sup>13</sup> can be characterized by a certain distribution. Visual inspection of the histogram of the data can be misleading and should always be complemented by other techniques. Quantile-Quantile plots (Q-Q plots) are a graphical technique to test whether data comes from a certain probability distribution. Some software packages support Q-Q plots to test data for different distributions (e.g., R Core Team, 2012). Alternatively, reference data can be generated by a pseudo-random number generator<sup>14</sup>. The quantiles of the data to be tested and the quantiles of the reference data are plotted against each other. Figure 2.2 shows an example of a Q-Q plot of data that is generated with a random number generator according to  $\mathbf{N}(0, 1)$  and with a sample size ( $N$ ) of 1,000. The plot reveals that the data is normally distributed.

<sup>11</sup>The R function `rnorm()` is used to draw the sample.

<sup>12</sup>More details on histograms can be found in Section 3.2.3.

<sup>13</sup>The tests can also be applied to analyze the results of an MC simulation.

<sup>14</sup>More details on random number generation will be presented in Chapter 3.

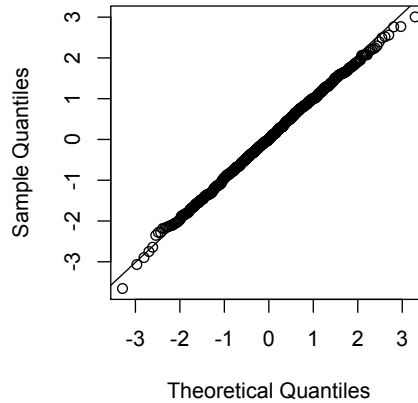


**Figure 2.2:** Q-Q plot.

The Kolmogorov-Smirnov test is a test to compute the maximum distance ( $D$ ) between CDFs (Hoel, 1966, pp. 345-349). Another result of the test is the  $p$ -value. This value is the probability that the test will take on a value for  $D$  that is at least as extreme as the observed value of the statistic when the null hypothesis<sup>15</sup> is true (Montgomery and Runger, 2003, p. 292). Commonly the null hypothesis is that data comes from the same distribution. In case the  $p$ -value is below the chosen significance level ( $\alpha$ ), the null hypothesis is rejected and the two different data sets do not come from the same distribution. A widely used significance level is 0.05. If the  $p$ -value is below this threshold, the two distributions are significantly different. Some software packages support Kolmogorov-Smirnov tests for different distributions<sup>16</sup> (e.g., R Core Team, 2012). The test result<sup>17</sup> for the sample that is used in Figure 2.2 is  $D = 0.0191$  and  $p\text{-value} = 0.8604$ . This test result indicates that the data is normally distributed.

### 2.2.2.3 Dependence between Simulation Inputs

Depending on the applied model or simulation program, the dependencies have to be treated by the modeler who performs a UA or SA or the model contains the dependencies implicitly. An example for a model that implicitly contains dependence

<sup>15</sup>A null hypothesis is a particular hypothesis that is tested with a statistical test (Montgomery and Runger, 2003, p. 697).

<sup>16</sup>Alternatively, reference data can be generated by a pseudo-random number generator.

<sup>17</sup>The R function `ks.test()` is used here.

is when internal gains (e.g., heat emitted by persons and electrical equipment) are calculated according to the number of occupants in the simulated zone.

For illustration, an example with three variables is introduced in the following. The variables are the room temperature set point ( $T_{\text{set}}$ ), the internal gains ( $\dot{Q}_{\text{int}}$ ) and the air change rate ( $ACH$ ). All of these variables influence the heating demand ( $Q_{\text{heat}}$ ).

### Statistically Independent Data

In the following, discrete random variables are used to explain independence. The concept for continuous random variables is similar. Two discrete variables  $X_1$  and  $X_2$  are statistically independent if and only if

$$p_{X_1, X_2}(x_1, x_2) = p_{X_1}(x_1) p_{X_2}(x_2) \quad \text{for all } x_1 \text{ and } x_2 \quad (2.13)$$

where  $p_{X_1, X_2}(x_1, x_2)$  is the joint probability mass function of  $X_1, X_2$  (Montgomery and Runger, 2003, p. 153).

When the model inputs are independent of each other, the input UQ can be made for each input separately. One way to visualize the dependencies in a technical system or model is a Bayesian network (also known as belief network or directed acyclic graphical model) (Dodier, 1999). These networks have nodes and edges, where nodes represent random variables and edges conditional dependencies<sup>18</sup>. Figure 2.3 shows an example of a Bayesian network where  $T_{\text{set}}$ ,  $\dot{Q}_{\text{int}}$  and  $ACH$  are inputs for a simulation model to compute  $Q_{\text{heat}}$ . In this example, there is no connection between input variables (i.e., it is assumed that they are statistically independent and Equation 2.13 holds). Thus, they can be sampled independently when an MC simulation is made. Relations between input and output are governed by physical laws (e.g., simulation model).

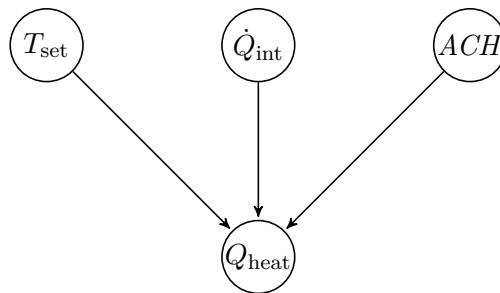


**Figure 2.3:** Example of statistically independent inputs for a simulation model represented as a Bayesian network.

<sup>18</sup>Nodes that are not connected are conditionally independent of each other.

### Statistically Dependent Data

Two random variables are statistically dependent if Equation 2.13 does not hold. In real buildings, many variables influence each other and hence many input variables are statistically dependent on each other. This demands careful handling of the relationships when setting up a (MC) BPS. In the previous example,  $T_{\text{set}}$ ,  $\dot{Q}_{\text{int}}$  and  $ACH$  were considered to be statistically independent variables. In reality, these variables are usually not statistically independent. In a window-ventilated building, the air change rate depends on the window openings, which depend on the occupants. Furthermore,  $\dot{Q}_{\text{int}}$  depends on the number of occupants in the building, their behavior and their use of electrical equipment. In the example shown in Figure 2.4, the occupancy is introduced as a variable ( $occ$ ) and each of the variables  $T_{\text{set}}$ ,  $\dot{Q}_{\text{int}}$  and  $ACH$  is considered to be statistically dependent on  $occ$  (i.e., the number of occupants in the zone and their behavior influences all other simulation input). Dependent variables make a UA and SA more complicated. Therefore it is desirable to find a model that describes the relation between variables (e.g.,  $\dot{Q}_{\text{int}} = (120 \text{ W} + \varepsilon) * occ$ ). In this case, the variables can be considered to be independent when the sampling is conducted and  $\varepsilon$  is a sampled noise term that accounts for uncertainty in the metabolic rate.

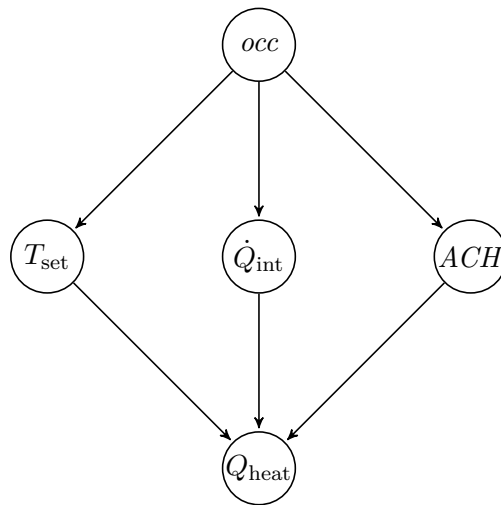


**Figure 2.4:** Example of dependent inputs for a simulation model represented as a Bayesian network.

An approach for identifying dependence is outlined in Appendix A.2.

### 2.2.2.4 Uncertainties in Time Series Data

#### Uncertainty Treatment for Variables

Analyzing an uncertain BPS parameter in an MC setting is easier than analyzing an uncertain BPS variable that changes over simulation time. A parameter can be sampled once and a single value of the parameter can be used for one simulation within the MC simulation. The situation is different for variables such as temperature set points, air change rates and the occupancy in a building. One possibility would be to sample one value for each time step of the simulation. In this case, the average value of this variable over the simulation<sup>19</sup> would be approximately the mean value of the distribution. Given a linear model, the uncertainty would not have any effect on the result because high and low values of the variables would cancel each other out. Schedules are commonly used in BPS to account for variables that change periodically. These schedules often represent a base case. In a UA or SA setting, the tabulated values can be scaled to account for uncertainties. Scaling factors or offsets can be used to implement this variation. The advantage is that such a scaling factor or offset can be kept constant over one simulation. This results in different scenarios. An example is the temperature set point in a building implemented as a schedule. In an MC simulation with different scenarios, there are cases with high temperature set points (i.e., occupants preferring high indoor air temperatures) and with low temperature set points (see Figure 2.5). Beside the variation of the set point temperature, the schedule times can also be varied to account for different scenarios.

#### Time Series Forecasting

When a UA or SA is to be applied to analyze future scenarios, it may be necessary to forecast a time series and quantify the corresponding uncertainties. When conducting a CBA, it is important to analyze future trends in economic data. Time series models such as ARIMA (auto-regressive integrated moving average) models are often applied in econometrics to predict future values based on time series data. The basics of ARIMA models are briefly introduced in the following passage. Univariate time series of economic variables can be used to fit an ARIMA model. An ARIMA model without differencing (it would be an ARMA model) can be described by

$$y_t = \varepsilon_t + \sum_{i=1}^p a_i y_{t-i} + \sum_{j=1}^q b_j \varepsilon_{t-j} \quad (2.14)$$

<sup>19</sup>This holds for cases where the number of simulation time steps equals or is greater than the sample size, where the mean of the sample converges to the mean of the underlying distribution. This is based on the central limit theorem (see Montgomery and Runger, 2003, pp. 239-241 for more information).

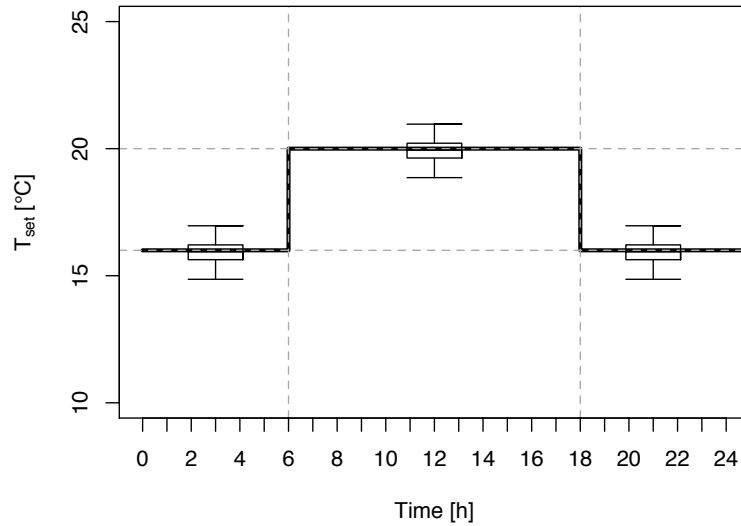


**Figure 2.5:** Variation of set point values in a schedule.

where  $\varepsilon$  is a noise term,  $a$  is the coefficient of the autoregressive (AR) part of the model,  $p$  is the order of the AR part,  $b$  is the coefficient of the moving average (MA) part of the model,  $q$  is the order of the MA part. Differencing is necessary in the case of non-stationary time series and ARMA models should be applied. The order of differencing is called  $d$ . Differencing is performed by replacing  $y_t$  with  $\Delta y_t = y_t - y_{t-1}$  (Ljung, 1987). Furthermore, it is possible to take seasonal effects into account when fitting the ARIMA model. When seasonal effects are taken into account, the model is sometimes called a SARIMA model. In the case of a model with seasonal effects, the orders of the different model components (AR, MA, I) of the seasonal part have to be set. These are  $P$  for the AR part of the seasonal model,  $Q$  for the MA part and  $D$  for the order of differencing. The interested reader is referred to Ljung (1987) for further information concerning ARIMA models. In this thesis, ARIMA models are used to predict future values of the inflation rate and the gas price as uncertain input for a CBA. The parameter identification of the coefficients for the models can be done with the help of statistical software. The orders of the different model parts have to be chosen by the analyst. An iterative process can do this (e.g., Box and Jenkins method (Box et al., 2008)) or an automated parameter variation can be applied. Another possibility is to use an optimization algorithm for this task. After such a parameter variation, the log likelihood ( $\ln(L)$ , where  $L$  is the value

of the likelihood function of the model) or the Akaike information criterion (*AIC*) can be used to choose the best order of the different model parts. Both serve as relative measures for the model fit. A model setting with higher log likelihood is preferred over a model with lower log likelihood, which is based on the maximum likelihood method (Ljung, 1987). The *AIC* includes a penalty term for the number of parameters to avoid too many parameters in the models and thus weights model performance against model complexity. This is important because a model with a large number of parameters could produce a nearly perfect fit to the data but noise would be inherent in some of the model parameters. In this case, these parameters do not contain useful information and should not be used in the model. A model setting with a lower *AIC* is preferred over a model setting with a higher value for the *AIC* (Ljung, 1987). The *AIC* is calculated with the following equation:

$$AIC = 2k - 2 \ln(L) \tag{2.15}$$

where  $k$  is the number of parameters and  $L$  is the value of the likelihood function of the model. With the help of an ARIMA model, a time series of the future values of the economic data can be predicted. The analyst should check whether the prediction looks reasonable for the analyzed case. However, the prediction is subject to uncertainties and therefore the predicted time series serves as the base case for the future trend of the economic input. The predicted time series can be varied in the MC simulation by means of scaling factors to account for different scenarios. The confidence interval or the standard error of the predicted time series can be used to determine the scaling factors. It is important to keep in mind that the approach of using historical data to predict the future has limitations, because influential events can change the future and are hard to predict. However, in many cases, historical data is the best source available to predict the future.

### 2.2.3 Sources of Information

Different sources might be used in the quantification process for simulation input uncertainties. The selection between different sources is done on the basis of available information and project scope as well as project requirements and budget. Different interpretations of uncertainties can exist. The analyst should provide the reasoning behind the UQ of the inputs. The decision makers involved in the analysis have to make the final decision concerning the uncertainties assumed in the analysis.

#### 2.2.3.1 Physical Bounds

The most obvious criteria defining the range of an uncertain input parameter are the physical bounds. An efficiency is a good example for this: by definition an efficiency can vary between 0 and 1. If no additional information is available, the

uncertainty can be described by a uniform distribution with a minimum value of 0 and a maximum value of 1 (hence  $X_i \sim \mathbf{U}(0, 1)$ ). Physical bounds do not include any information on the distribution of the variable of interest. A uniform distribution can be assumed if no other information is available. Fortunately, in most cases more information is available that can be represented by a certain type of distribution. However, analyzing the physical bounds for the variables of interest can be the first step of a UQ for simulation input.

### 2.2.3.2 Literature

As already mentioned in existing BPS literature, there is no general source (i.e., database) of information concerning simulation input uncertainty (de Wit, 2003, pp. 25-26). Distributions and their defining parameters are given for some typical simulation inputs and cases (e.g., Macdonald, 2002; de Wit, 2003; Pietrzyk and Hagentoft, 2008; Corrado and Mechri, 2009). An important aspect is that the literature sources are recent since some variables of interest have changed significantly in their magnitude in the recent past. An example is the internal gains from electric appliances. More efficient technical equipment results in lower internal gains (e.g., usage of laptop computers instead of desktop computers and energy-efficient displays) (Jenkins et al., 2008). Another problem is that most literature contains information about single-value estimates rather than the type of distribution and its parameters (e.g., normal distribution, mean and standard deviation), which describe the uncertainty. However, a literature study is an important instrument for quantifying simulation input uncertainty. Literature can contain the required statistics to set up an MC simulation or data that can be the source of computing the necessary statistics. In the latter case this would be treated like measured data (see Section 2.2.3.4).

### 2.2.3.3 Expert Knowledge

In cases where little information is available, expert knowledge is a possible source of information. The effort that is invested for the UQ by experts can vary significantly. The expert might be an experienced engineer, who conducts the simulation himself or a colleague with experience concerning the question to be answered. Under certain conditions (e.g., time/money availability and high accuracy requirements), a group of persons might act as experts. A methodology, which minimizes the bias in the UQ (e.g., overestimation or underestimation of the inherent uncertainty) is necessary. The information concerning the physical bounds and the findings of the literature search might be provided to the experts. Based on this information and their knowledge, they can quantify the uncertainty of the simulation input of interest. The experts can also be asked if they believe that variables are statistically

independent. However, the estimates concerning the uncertainty are subjective but in many cases they represent the best information that is available. Hubbard separates experts into two groups: overconfident and under-confident concerning their estimates and uses confidence intervals as a quality criterion (Hubbard, 2010, pp. 58-59). He further proposes a procedure to calibrate the experts.

The expert knowledge elicitation process can consist of the following 15 steps that can be separated into preparation for elicitation, elicitation and post-elicitation (source: Cooke and Goossens, 2000, p. 19):

- (I) Preparation for elicitation:
  - (1) Definition of case structure
  - (2) Identification of target variables
  - (3) Identification of query variables
  - (4) Identification of performance variables
  - (5) Identification of experts
  - (6) Selection of experts
  - (7) Definition of elicitation format document
  - (8) Dry run exercise
  - (9) Expert training session
- (II) Elicitation:
  - (10) Expert elicitation session
- (III) Post-elicitation:
  - (11) Combination of expert assessments
  - (12) Discrepancy and robustness analysis
  - (13) Feed back
  - (14) Post-processing analyses
  - (15) Documentation

Cooke and Goossens point out that historical and/or measured data should be preferred over quantification on the basis of expert knowledge (Cooke and Goossens, 2000, p. 20). A crucial part is the design of the elicitation format document. It provides a framework and supports the experts. Expert elicitation with the 15 steps listed above is a time-consuming and expensive task. This cannot be accomplished in most BPS cases. This results in the situation that the engineer who conducts the analysis acts as the expert and quantifies the uncertainty. This might result in a biased UQ. However, a structured guide for the elicitation and a basic elicitation document can reduce the bias.

#### 2.2.3.4 Measurements

Measurements of the variable or the parameter of interest can be an accurate source for the UQ of simulation input. Unfortunately, measurements are costly, often not available and a data analysis of the measurements can be time-consuming. However, sometimes measurements are available in the case of the simulation of an existing building (e.g., obtained from the building automation system). This is not feasible during the design stage of a building. However, data from other (similar) projects or buildings can be analyzed to obtain the required information. Such measurements can be the electricity consumption indicating internal loads, room temperatures and window openings. Statistical dependence between variables can be detected and analyzed with the help of measurements. Conversely, statistical dependence can help to obtain information on a variable that is not measured. An example is the water consumption in non-residential buildings, which is often correlated with the number of occupants in the building. A regression model can be fitted to obtain the number of persons in a building at a particular time. The number of occupants in a building at a particular time influences many other variables of interest, such as the internal loads and ventilation (see also Section 2.2.2.3). In this way, a single measurement might be used to obtain information on other variables of interest and their corresponding uncertainty. The statistics and methods introduced in Section 2.2.2.1 and 2.2.2.2 can be used to analyze the data. Once a PDF is assigned to the data, the sampling according to the distribution can be performed to generate the simulation input for the MC simulation<sup>20</sup>.

#### 2.2.4 Flowchart for the Proposed Methodology

A flow chart is constructed, drawing on the mentioned sources of information (Figure 2.6). The methodology is scalable depending on project requirements. Under certain circumstances it is also possible to shorten the process (e.g., if measurements of the variables of interest are available and easily assessable). Furthermore, conducting an expert elicitation might be an extensive task, such that the acquisition and analysis of measurements is preferable. In this case, the expert elicitation might be skipped or conducted when analysis of the measurements was not satisfactory.

---

<sup>20</sup>More details on this step will be presented in Chapter 3.

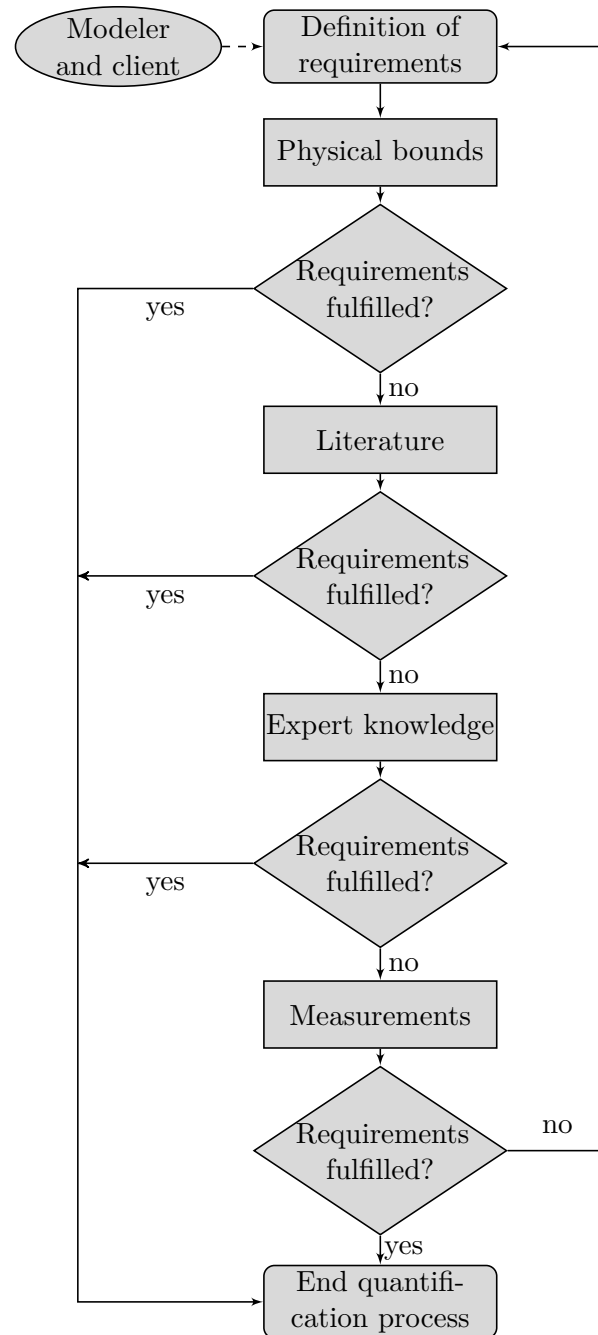


**Figure 2.6:** Flow chart of the UQ process for simulation input.



## 3 Uncertainty Analysis

### 3.1 Background and Objectives

#### 3.1.1 Literature Review

A review of methods for UA is presented in this section. Firstly, methods for performing a UA are investigated and literature from various scientific disciplines is introduced. As a second step, BPS-specific literature concerning UA is analyzed.

Cox and Baybutt (1981) distinguish five approaches to UA in probabilistic risk assessment, which are analytical techniques, Monte Carlo simulation, response surface approaches, differential sensitivity techniques, and evaluation of classic statistical confidence bounds. Analytical techniques<sup>1</sup> require the availability of an analytical solution for calculating the mean and the variance. Monte Carlo (MC) techniques have been briefly introduced in Chapter 1. The idea behind the response surface approach is to construct a meta-model that is a representation of the original model but requires less computational resources for the evaluation. The analysis itself is conducted using the response surface model. Cox and Baybutt (1981) classify differential sensitivity techniques as UA, whereas in this thesis this method is introduced in Chapter 4, as it corresponds to the definition for SA. According to Cox and Baybutt (1981), the principle behind classic statistical confidence bounds approaches is to compute the confidence interval of the result given the confidence intervals of the input. This requires sufficient statistical data for the input and well-defined models.

Finally, Cox and Baybutt point out that only the response surface and differential sensitivity approaches are applicable for a wide range of applications in probabilistic risk assessment. They state that MC methods have the disadvantage that they cannot be applied for computationally expensive models. However, Cox and Baybutt conducted their analysis in 1981 and computational power has increased greatly since then. As an example of this increase, the computers that are used for the simulations in this thesis are compared. Three computers were bought during the period from 2010 to 2012 and each of them costs  $\approx 5,000$  EUR. All of them are mounted in a rack and act as server. The key performance indicators are listed in Table 3.1. Furthermore, the sample size ( $N$ ) of an MC simulation that can be simulated within 24 hours on the computer is listed. The underlying model is the example that will

---

<sup>1</sup>In the course of this chapter, an analytical technique will be applied to calculate the mean and variance for a simple mathematical model.

be used in this chapter and a one-year simulation is conducted. Hence,  $N$  equals the number of one-year simulations. This example is also chosen to introduce the hardware that is used for the simulations in this thesis. The table reveals that the applicability of MC methods can be improved by powerful computers. However, the high computational cost of MC methods can be a problem. Methods that require low sample sizes for convergence are very important to improve the feasibility of MC simulation in BPS practice.

**Table 3.1:** Comparison of computers.

Computer	Year	CPU cores	CPU GHz	Memory	N/24 h
Computer 1	2010	12	2.6 GHz	32 GB	6,360
Computer 2	2011	24	1.7 GHz	64 GB	7,795
Computer 3	2012	32	2.4 GHz	128 GB	17,953

UA is applied in different disciplines such as ecological modeling (e.g., Reckhow, 1994), public health (e.g., Thompson et al., 1992), atmospheric sciences (e.g., Webster et al., 2003), the energy sector (e.g., Maurice et al., 2000), and risk analysis (e.g., Nilsen and Aven, 2003). Many publications on risk analysis deal with UA since it is an important tool to assess risk. Furthermore, risk analyses are multi-disciplinary and hence conducted for many different scientific fields. MC techniques are mentioned as an approach to UA in all of the publications mentioned above.

In an MC analysis, a large number of evaluations of the model is performed with randomly sampled model inputs (Campiono et al., 2000, pp. 20-24). It consists of the following main steps:

- (I) Selection of PDFs for each uncertain input ( $X_i$ ).
- (II) Generation of a sample from the PDFs.
- (III) Evaluation of the model for each element of the sample.
- (IV) Result analysis.

Figure 3.1 is an overview of the MC simulation, where the uncertain parameters are listed in an input matrix, the number of analyzed parameters is  $k$  and the sample size is  $N$ . One simulation is conducted for each row of this matrix (illustrated as red arrows). The output can be a vector or a matrix with the results of interest.

In the following, UA in BPS-specific applications is analyzed. Lomas and Eppel (1992) describe the application of MC techniques for BPS. They conduct an MC simulation with three different simulation tools (i.e., ESP, HTB-2 and SERI-RES) and show the results for stochastic output (i.e., daily energy use, peak power, and maximum air temperature). Furthermore, uncertainties in time series output (e.g., peak

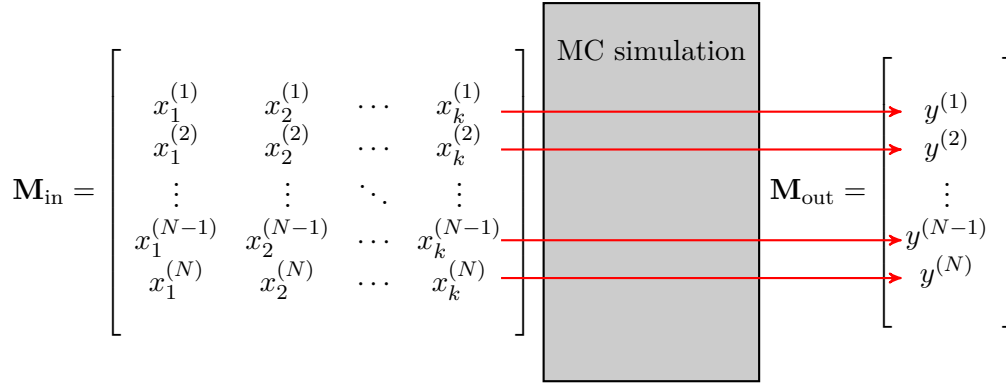


**Figure 3.1:** Input and output of an MC simulation.

power, and maximum air temperature) are investigated. Lomas and Eppel (1992) use the frequency of occurrences to visualize stochastic output and plot different time series obtained by the MC simulation. Furthermore, they analyze convergence for the standard deviation of the daily energy use and conclude that 60-80 simulations are sufficient to estimate the standard deviation<sup>2</sup>. The standard deviation is used as a statistic for the result analysis and 2.33 standard deviations<sup>3</sup> are used to analyze the upper and lower bounds of the MC simulation.

Macdonald (2002) analyses different UA techniques and distinguishes between internal and external approaches. Internal approaches require modification of the BPS model or program. He investigates interval, fuzzy and affine arithmetic in this context. External approaches treat the BPS model as a black box and input parameters are perturbed to analyze the effects on the results. Macdonald investigates a differential, a factorial and an MC method for the external approach. The differential and factorial methods are SA techniques and are further analyzed in Chapter 4 of this thesis. Macdonald (2002) states that an MC simulation usually requires 60-80 simulations and bases this statement partly on the findings of Lomas and Eppel (1992). He further points out that the advantage of applying MC techniques is that they fully account for interactions among the analyzed parameters and states that the result of an MC simulation is normally distributed. Macdonald mentions that the normality of the result is based on the central limit theorem. He implemented all three external approaches and one internal approach for the BPS program ESP-r.

De Wit and Augenbroe (2002) conduct an MC-based UA for analyzing thermal

<sup>2</sup>Special attention will be given to convergence in the course of this chapter.

<sup>3</sup> $\pm 2.33\sigma$  corresponds to a confidence level of 98%.

comfort. They apply Latin hypercube sampling (LHS) for their MC simulation. Firstly, they perform a crude UA that is followed by an SA to identify the most influential parameters. As a result of the SA, a refined UA with the most influential inputs is performed. Unlike Macdonald (2002), they do not comment on the normality assumption and do not test normality. However, the histogram of the MC results of the analyzed thermal comfort performance indicator does not appear to be normally distributed.

Hopfe and Hensen (2011) report results of an MC-based UA implemented with LHS as the sampling technique. In their work, physical, design and scenario uncertainty are distinguished. The physical uncertainty analysis is conducted by varying properties of materials, while the design uncertainty analysis is accomplished by adjusting the geometry and glass surface areas. The scenario uncertainty is implemented by varying the infiltration rate and internal loads.

Eisenhower et al. (2011) perform a UA where they analyze the uncertainties of about 1,000 parameters. They vary all parameters by  $\pm 10\%$  and  $\pm 20\%$  of their nominal value and use a sample size of 5,000. Eisenhower et al. employ EnergyPlus as the BPS program and quantify the uncertainties for cooling and heating peak power and annual energy demand. They use a quasi-random sampling method that shows a better convergence rate than conventional sampling methods. Eisenhower et al. present findings that contradict the generality of the convergence statements of Lomas and Eppel (1992) and Macdonald (2002).

Heo (2011) investigates decision-making under uncertainty for energy retrofit projects. She uses Bayesian calibration where measurements from the building are required for the BPS. Heo introduces a systematic procedure for retrofit analysis and employs the calibrated model to compute probabilistic outcomes for energy saving measures. She analyses the probabilistic simulation results (i.e., simple payback time of the required investment) with three decision-making measures (i.e., expected value, 95-quantile and the expected value divided by the standard deviation).

#### 3.1.2 Objectives

In order to make MC simulations feasible in practice it is important to decrease the number of MC runs required (i.e., computational cost). In this chapter, different sampling strategies are investigated in order to achieve this reduction. Furthermore, different methods for analyzing the results of an MC simulation are compared. The aim is to find appropriate ways of visualizing the results and to find informative statistics for different applications. The developed methodology is intended to guide analysts through the UA and to provide quality assurance (e.g., convergence testing, correct interpretation of figures and statistics).

## 3.2 Methodology

### 3.2.1 Sampling

A key element of MC techniques is the sampling of input parameters for the simulation, where the goal is to explore the entire input space with a reasonable sample size ( $N$ ). The sample size determines the computational cost of the analysis since  $N$  is equal to the required number of simulation runs. The input parameter space has  $k$  dimensions where  $k$  is the number of analyzed parameters. Exploring the input parameter space with a sufficient sample density becomes numerically expensive when  $k$  is large, as the number of partial volumes increases dramatically with  $k$ . This phenomenon is known as the curse of dimensionality (Saltelli and Annoni, 2010). In this section, different sampling techniques are analyzed with respect to the convergence of the estimators of the mean and the variance of the result. Another measure of the performance of the sampling strategy is its robustness. It can be investigated using multiple MC simulations and analyzing their results. One way to visualize the robustness is to compare the empirical cumulative density functions (CDFs) of several repetitions of the MC simulation (Helton and Davies, 2003). A further way to analyze the robustness is to use the Kolmogorov-Smirnov test which was introduced in Section 2.2.2.2. This test can be used to supplement visual inspection of the ECDFs. The test result is the longest distance ( $D$ ) between two cumulative distribution functions. The maximum  $D$  of all combinations can serve as a measure of robustness. The higher the maximum  $D$  of all combinations of the ECDFs, the greater is the possible difference between two MC experiments due to the sampling technique. Hence, a low maximum  $D$  for all combinations indicates a robust sampling technique.

Sampling can be done randomly, where the random numbers are independent realizations of a random variable (Sobol' and Levitan, 1999). A random number is a mathematical definition and "real" random numbers cannot be generated in a computer experiment because computers use algorithms for sampling. Therefore, random number generators are often and more correctly called pseudo-random number generators (Sobol' and Levitan, 1999). Beside pseudo-random numbers quasi-random numbers can be used. Quasi-random numbers are generated using an algorithm or a sequence of numbers that fulfill requirements as if they were true random numbers. The difference is that successive sampled points take the position of previously sampled points into account (Saltelli et al., 2010). The properties of the samples can be analyzed by means of statistical tests (Sobol' and Levitan, 1999). Many software packages include sampling algorithms for the most common distributions (e.g., uniform, normal and log-normal distributions). Another way is to use sampling algorithms to produce random numbers which are uniformly distributed over the interval from 0 to 1 (i.e.,  $X_i \sim \mathbf{U}(0, 1)$ ) and to convert these numbers with

the quantile function (i.e., inverse cumulative distribution function) of a distribution into a certain range (Campolongo et al., 2011). Sometimes it is difficult to find an appropriate PDF to describe data (see Chapter 2). In these cases, the data might be used to compute the empirical inverse cumulative distribution function.

### 3.2.1.1 Random Sampling

A random sample can be generated by a pseudo-random number generator which is available in many software packages. A sample is randomly distributed in a defined interval according to some distribution (e.g., uniform distribution over the interval  $[0,1]$ , hence  $X_i \sim \mathbf{U}(0,1)$  with  $i = 1, 2, \dots, N$ ). For small sample sizes ( $N$ ), the samples can contain clusters and gaps as shown in Figure 3.2 on line a. Regions with gaps are not taken into account in the statistical analyses for any UA or SA and function values in the regions with clusters are overemphasized in the calculations (Saltelli et al., 2008, p. 83). The sample on line b is drawn using the same pseudo-random number<sup>4</sup> generator but shows a better coverage of the interval.

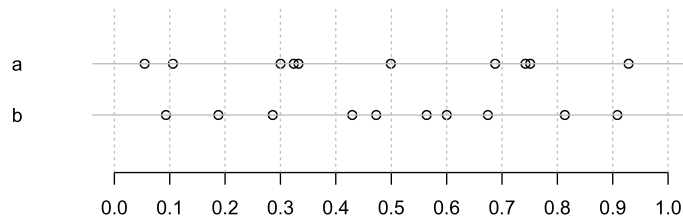


**Figure 3.2:** Two examples of sampling with a pseudo-random number generator.

The unbiased mean and variance of the model output can be calculated by Equations 2.2 and 2.3 that were introduced in Section 2.2.2.1. The mean and the variance resulting from the sample and calculated with these two equations are uncertain. Based on the central limit theorem, the uncertainty in the estimate of the mean can be quantified with the standard error (Saltelli et al., 2008, p. 59)

$$\text{SE}(\bar{Y}) = \sqrt{\frac{\text{Var}(\mathbf{Y})}{N}}. \quad (3.1)$$

This equation shows that the uncertainty decreases slowly when  $N$  increases since it depends on the square root of  $N$ .

In the following example, a three-dimensional parameter space is used to illustrate the properties of the sampling methods. However, the reader should keep in

<sup>4</sup>The R function `runif()` is used to draw the sample.

mind that exploring the parameter space becomes harder as the number of analyzed parameters ( $k$ ) increases. The sampling is performed according to a uniform distribution in the interval  $[0,1]$ . Figure 3.3 shows a three-dimensional plot of the parameter space  $X_1$ ,  $X_2$  and  $X_3$  with  $N = 128$ . This number was chosen because of the properties of the sampling based on Sobol' sequences which will be explained later. For pseudo-random sampling, any  $N$  can be chosen but  $N = 128$  is used for the sake of comparability.

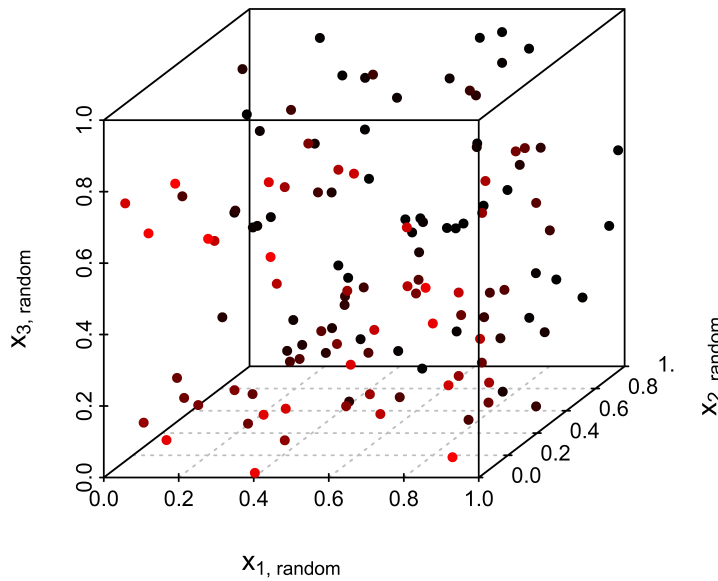
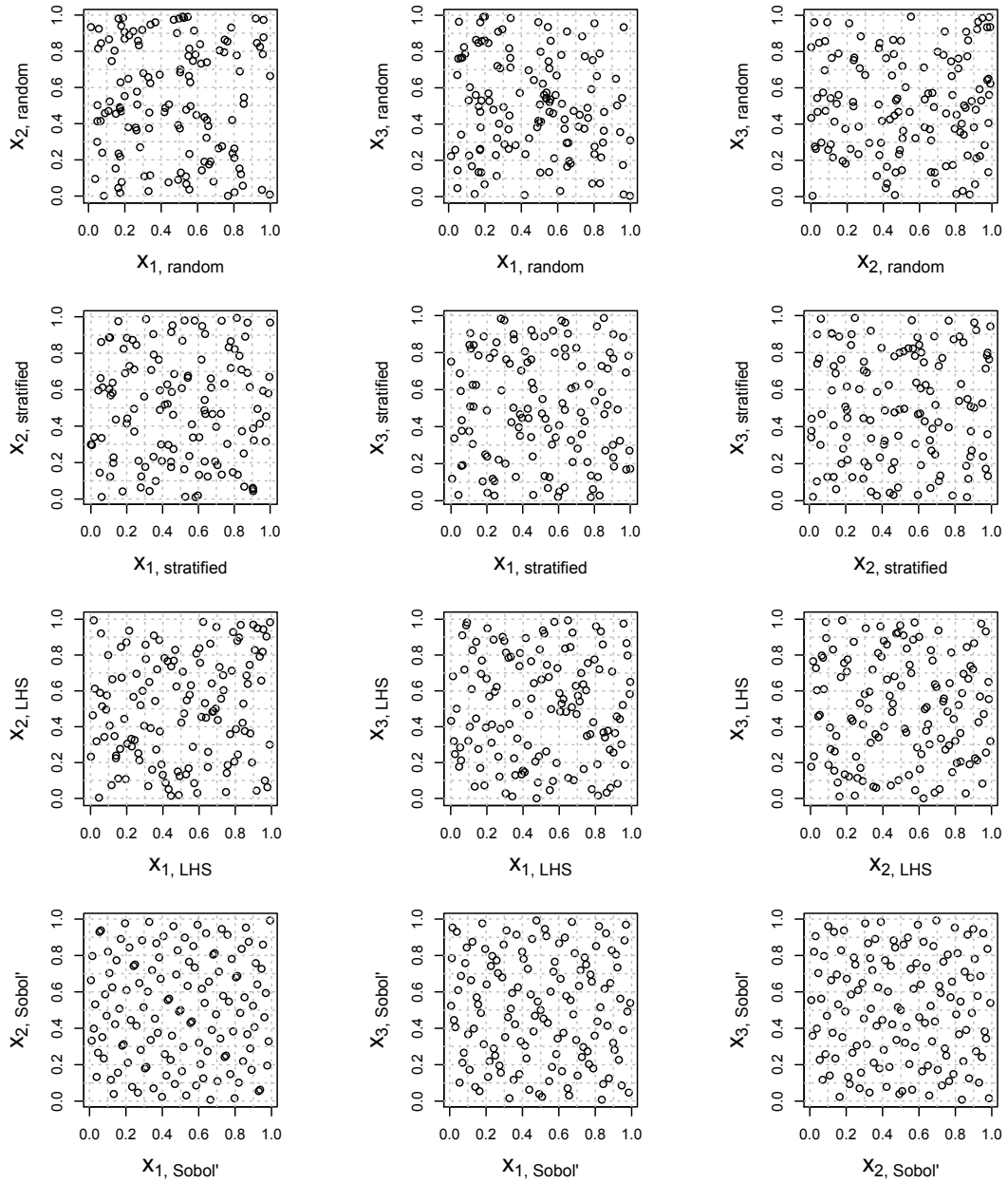


**Figure 3.3:** Three-dimensional plot of the pseudo-randomly sampled points in the parameter space  $X_1$ ,  $X_2$  and  $X_3$ . The color of the points varies from red to black depending on the value of  $X_2$  to allow easier interpretation of the plot.

With a three-dimensional plot, it is a difficult task to check whether the parameter space is explored appropriately. For this reason, Figure 3.4 shows the variables  $X_1$ ,  $X_2$  and  $X_3$  plotted against each other in two-dimensional plots. The plots for random sampling show clusters and gaps.

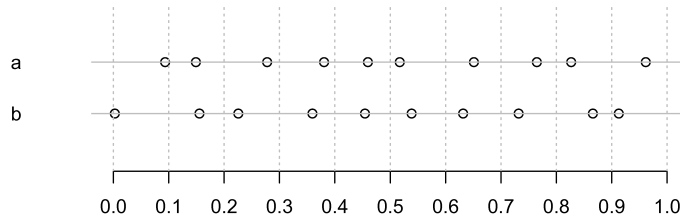
### 3.2.1.2 Stratified Sampling

Figure 3.2 showed that a random sample may contain clusters and gaps. Using a stratified sampling technique can solve that problem. In a scheme which applies stratified sampling, the domain of  $X_i$  is divided into subintervals. Each of the subintervals contains the same number of sample points. These points are sampled



**Figure 3.4:** Three sampled parameters plotted against each other in pairs, for sample sets obtained by different sampling techniques. Left to right:  $X_1$  vs.  $X_2$ ,  $X_1$  vs.  $X_3$ , and  $X_2$  vs.  $X_3$ . Top to bottom: Pseudo-random, stratified sampling, Latin hypercube sampling and sampling based on Sobol' sequences.

randomly within each subinterval using a pseudo-random number generator. If one compares Figure 3.2 with Figure 3.5, it is obvious that the stratified sampling technique ensures the avoidance of clusters and gaps at a certain resolution. The mean and variance are calculated in the same way as for pseudo-random sampling (see Equations 2.2 and 2.3).



**Figure 3.5:** Two examples of stratified sampling. The position of the points within each subinterval is chosen randomly.

The same technique is applied in multivariate stratified sampling. Figure 3.6 shows a two-dimensional parameter space obtained by stratified sampling with 10 strata for each parameter. This results in 100 cells with one point in each cell. For a given resolution, stratified sampling results in less uncertain mean and variance estimates than pseudo-random sampling (Saltelli et al., 2008, p. 80). Note that the required sample size for this approach is

$$N = s^k. \quad (3.2)$$

Hence, for stratified sampling with 10 strata ( $s$ ) and 5 parameters ( $k$ ), a sample size ( $N$ ) of  $10^5 = 100,000$  is required.

In Figure 3.4, the stratified sampling set shows gaps and clusters like the random sampling. The reason is that a sample size of 125 (128 as for the other techniques could not be used because of the property described by Equation 3.2) results in 5 strata, which is not sufficient to avoid visible clusters and gaps.

### 3.2.1.3 Latin Hypercube Sampling

Latin hypercube sampling (LHS) is a particular kind of stratified sampling. One feature is that each parameter is stratified over  $s > 2$  intervals (levels), where the same number of points is located in each interval (Saltelli et al., 2008, p. 76). An example of LHS with two parameters, 10 intervals and a sample size ( $N$ ) of 10 is shown in Figure 3.7. The unique property of the sampled points of an LHS is visible: each sampled point is associated with one of the 10 rows and one of the 10 columns.

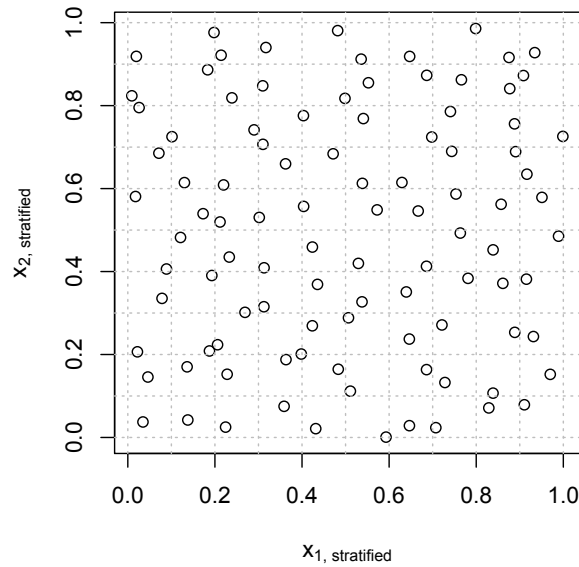


**Figure 3.6:** Scatter plot of a two-dimensional sample set obtained by stratified sampling. The position of the points within each cell is chosen randomly.

In Figure 3.4, the Latin hypercube sampling<sup>5</sup> results in gaps and clusters like the random sampling because the sample size is too small to generate a sample with the same density across the parameter space. The mean and variance are calculated in the same way as for pseudo-random sampling (see Equations 2.2 and 2.3).

#### 3.2.1.4 Sampling Based on Sobol' Sequences

The investigated method is based on Sobol' sequences. Sobol' sequences belong to the family of quasi-random sequences, which are designed to generate samples of multiple parameters as uniformly as possible over the multi-dimensional parameter space (Saltelli et al., 2010). Quasi-random numbers can be applied similarly to pseudo-random numbers. The greatest difference to pseudo-random numbers is that the sample values are chosen under consideration of the previously sampled points, thus avoiding the occurrence of clusters and gaps. One criterion for assessing the performance of a sampling method is the discrepancy in the exploration of the multi-dimensional parameter space. The discrepancy metric was defined by Ilya M. Sobol' and is the maximum deviation between the theoretical density  $d_t = 1/N$  and the point density  $d_i$  in an arbitrary hyper-parallelepiped within the parameter space (hypercube) (Saltelli et al., 2010). The sampling based on Sobol' sequences is

<sup>5</sup>The LHS was implemented using the R package *lhs* (Carnell, 2007).

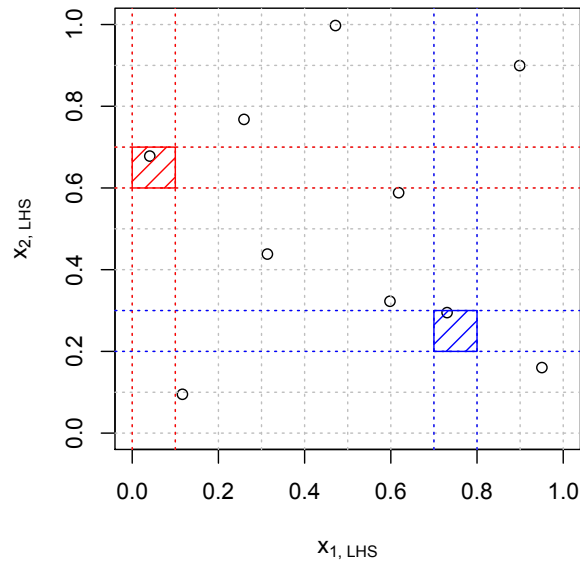


**Figure 3.7:** Scatter plot of an LHS:  $X_1$  vs.  $X_2$ . The colored dotted lines indicate the intervals to which the sampled point belongs. For reasons of clarity, this is plotted for two points only. However, each point can be similarly characterized.

designed to generate samples with a low discrepancy value.

Figure 3.4 shows that the points produced by sampling based on Sobol' sequences<sup>6</sup> are more evenly distributed than the points produced by the other sampling techniques. As a result, the discrepancy in the exploration of the multi-dimensional parameter space is lower than for the other sampling techniques. The mean and variance are calculated in the same way as for the other sampling techniques (see Equation 2.2 and 2.3).

One result of the low discrepancy value is that the estimated mean of a function

<sup>6</sup>Sampling based on Sobol' sequences is implemented using the R package *randtoolbox*. For the repetitions needed to test the robustness of the MC simulation, the sampling was done using the Owen type of scrambling with a random seed (Dutang, 2009).

$Y(X_1, X_2, \dots, X_k)$  evaluated at the points of a sampled input matrix

$$\mathbf{M}_{\text{in}} = \begin{bmatrix} x_1^{(1)} & x_2^{(1)} & \cdots & x_k^{(1)} \\ x_1^{(2)} & x_2^{(2)} & \cdots & x_k^{(2)} \\ \vdots & \vdots & \ddots & \vdots \\ x_1^{(N-1)} & x_2^{(N-1)} & \cdots & x_k^{(N-1)} \\ x_1^{(N)} & x_2^{(N)} & \cdots & x_k^{(N)} \end{bmatrix}$$

will converge more quickly to the true mean than in the case of pseudo-random sampling (Saltelli et al., 2008, p. 83). How quickly depends on the model structure and will be analyzed later. The properties of the Sobol' sequences require a sample size of

$$N = 2^j \tag{3.3}$$

where  $j \in \mathbb{N}^+$  (Saltelli et al., 2010).

### 3.2.2 Evaluation of the Model for each Element of the Sample

The most time-consuming part of an MC simulation for BPS is the evaluation of the model for each row of the input matrix. This process requires a software tool that can be used to change simulation input files, to execute the simulation and to save the results. MC simulations are well suited for parallelization because the simulations for each row of the input matrix are independent of each other. This is especially important for BPS, where models are fairly complex and full-year simulations are common practice. The applicability in practice has improved due to the availability of multi-core processors, which became standard in recent years (see also Table 3.1). Given sufficient memory and hard drive performance, the number of processor cores equals the possible number of parallel simulations. In the context of this thesis, R is used to manage the parallelization and to call the executable generated by Dymola<sup>7</sup>. Three scripts are employed to conduct the parallel MC simulation<sup>8</sup>. One is the main script (`MainScript.R`) that generates the samples, generates the same number of folders as parallel computations to be conducted and sets the required symbolic links for the file system or copies files as required. The second script (`Simulation.R`) is copied into each of the subfolders and called from the main script. This simulation script changes input files<sup>9</sup>, calls the simulation and processes

---

<sup>7</sup>The R function `system()` is used to call the executable.

<sup>8</sup>The scripts were partly developed in cooperation with Dirk Jacob (Jacob, 2012) and Olga Tsvetkova (Tsvetkova, 2011).

<sup>9</sup>A template file with tokens representing the values of the uncertain input is used to generate the input files.

the results. The third script (`CollectResults.R`) is used to collect and process the results from the different subfolders. Figure 3.8 shows an overview of the MC simulation on the server computers. The folders with gray and files with light gray filling are generated during the MC simulation. This approach can be used to employ several processor cores on one computer or distribute the simulations to different computers in a network.

In the course of this chapter, the convergence of MC simulations is analyzed. A practical issue concerning MC simulations is that the required sample size for which the simulation converges<sup>10</sup> is not known *a priori*. Hence, different sample sizes have to be tested. A termination criterion might be that the analyzed estimator does not change by more than a certain amount (absolute or relative) from one to another sample size. However, this can happen by chance. A more reliable termination rule would be that the estimator does not change significantly for the last 3 sample sizes. The significance level can be chosen depending on accuracy requirements. If more than one estimator is analyzed, this must hold for each estimator separately (e.g., mean and variance). Beside the mean and variance, the sensitivity indices could be used as estimators<sup>11</sup>.

### 3.2.3 Methods for Interpreting Results

An MC simulation generates a large amount of data. Statistics and visualization techniques are required to interpret the results. Several statistics were introduced in Section 2.2.2. Their applicability for MC simulation results is tested in the following.

#### 3.2.3.1 Stochastic Output

Stochastic output refers to a result of an MC simulation (e.g., annual energy consumption, CO<sub>2</sub> emissions, net present value of an investment<sup>12</sup>). Most commonly, these results are simulation variables integrated over a time interval (usually the entire simulation period).

#### Visualization

A widely used form of presenting results from MC simulations is a histogram. The x-axis of a histogram is divided into intervals and the number of observations of the MC result that occur in one interval ( $n_i$ ) is counted. A rectangle with the width of the interval and a height corresponding to the counted number (frequency) of

<sup>10</sup>Different definitions of convergence exist and some definitions will be introduced in the course of this chapter.

<sup>11</sup>This will be investigated in Chapter 4.

<sup>12</sup>More details on the calculation of net present values will be presented in the course of this chapter (Equation 3.6).

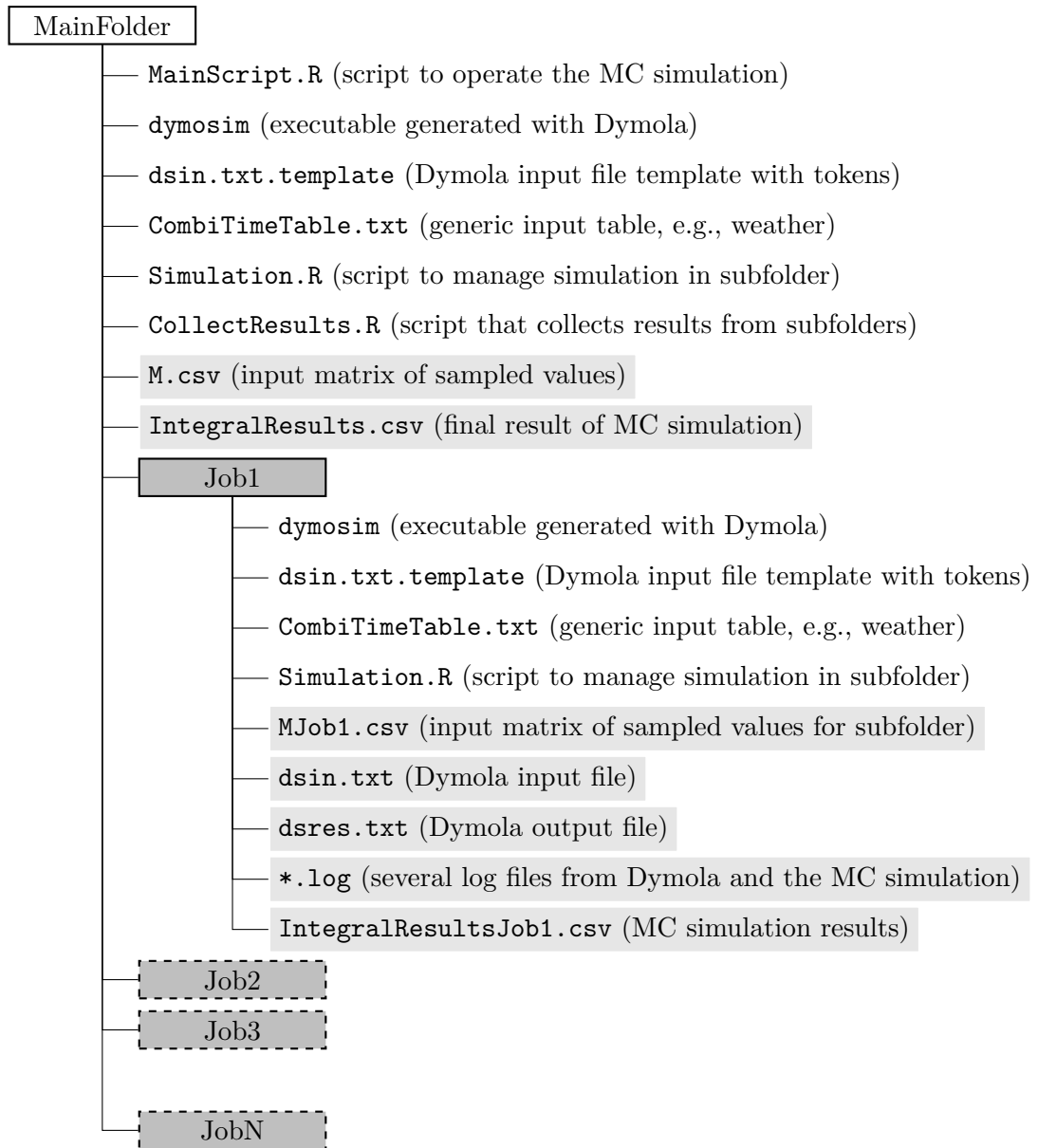


**Figure 3.8:** File system tree for the parallelization of an MC simulation.

observations is constructed (Box et al., 2005, p. 19). A histogram provides an impression of the location, spread, minimum and maximum value of the MC result. From a histogram, it is also possible to infer which distribution is suitable to describe

the data. However, as already mentioned in Chapter 2, a histogram might not be sufficient to decide which distribution is most suitable. A further visualization step is to normalize the histogram. This can be done by making the area of the  $i$ th rectangle equal to the relative frequency  $n_i/N$ , where  $N$  is the sample size. After normalization, the area under the histogram is equal to unity (Box et al., 2005, p. 20). Furthermore, Section 2.2.2.2 contains tests to find the most suitable distribution to describe the uncertainty of the results.

### Statistics

Various statistics were introduced in Section 2.2.2. They can be calculated to allow quantitative result interpretation. Depending on the purpose of the analysis, different statistics can be calculated. The median and the mean specify the location of the result. The variance and the standard deviation serve as quantitative measures of spread. Minimal and maximal values might be analyzed to account for best-case and worst-case scenarios.

#### 3.2.3.2 Stochastic Time Series Output

The time series output can be analyzed to characterize the dynamic behavior of the simulated system. Visualization techniques are one way to interpret results. The uncertainty of time series can vary between the different points in time. This makes the calculation of statistics more complicated because it can be necessary to compute the statistics for each timestamp. This can result in many statistics. However, it is a way to analyze the uncertainties for time series.

### Visualization

Box plots can be used to indicate result uncertainties for time series. In this approach, a box plot indicates the variation of the results for one point in time or for a time interval. Jacob (2012) uses this kind of visualization for a time series for 24 hours with one box plot per 15 minutes. However, some simulations require higher result resolution (e.g., analysis of controls under dynamic conditions) or visualization for a longer period. This might require too many box plots in one figure for straightforward interpretation. An alternative is visualization as a contour plot with colors indicating the probability density at different timestamps or for different time intervals.

### Statistics

The statistics for stochastic time series are similar to the statistics for stochastic output but they are calculated for each timestamp or timestamps with comparable

conditions (e.g., mean and variance for the heating power of a weekday at 9:00 am). Another possibility is to aggregate the results and to compute statistics for these aggregated values.

#### 3.2.4 Combined Building Performance Simulation and Cost-Benefit Analysis

In practice, many decisions are based on monetary criteria. It seems to be natural to talk about different options in terms of money. Particularly for people without an engineering background, it is appealing to make a decision on the basis of a monetary value. CBA is a common approach for making economic decisions. The main idea underlying CBA is that total expected costs are compared with the total expected benefits of a project in order to choose the most profitable of the compared options. Benefits and costs are usually expressed in terms of money (Nas, 1996). The length of the analyzed time interval plays an important role. Usually the cash flows of costs and benefits occur at different times and the analyzed time frame for buildings varies from 5 to 50 years. The longer the time frame, the greater the difference in monetary value becomes. Due to this fact, costs and benefits need to be adjusted for the time value of money. All cost and benefit flows in the course of the project are expressed in a common term, their present discounted value (*PDV*) (Pindyck and Rubinfeld, 2005, p. 718).

In this thesis, a method for combining BPS and CBA and for performing a UA and SA for this combination is proposed. The analysis is conducted using a 2-step procedure. The first part is an MC simulation of the performance of the building and its HVAC equipment. The output of the BPS (e.g., the gas consumption) is used as input for the MC CBA. Figure 3.9 shows an overview of the simulation process. All CBA inputs which are considered uncertain are sampled except for one input of the CBA that is the result of the BPS. The histograms represent the inputs that are considered to be uncertain and the uncertain output, respectively. Besides the uncertain inputs, there are many parameters and variables that can be considered as known. Hence, single-value estimates are used for these inputs. The decision on whether a parameter or variable is considered to be known or uncertain can be based on several criteria (see Chapter 2 and 4).

As already mentioned, expected costs are compared in a CBA with the expected benefits of a project. The different times at which cash flows take place require an analysis that takes interest and compound interest as well as inflation rates and energy price escalation into account. This is done by calculating the present discounted value (*PDV*) of every cost and benefit over the analyzed time span (Pindyck and

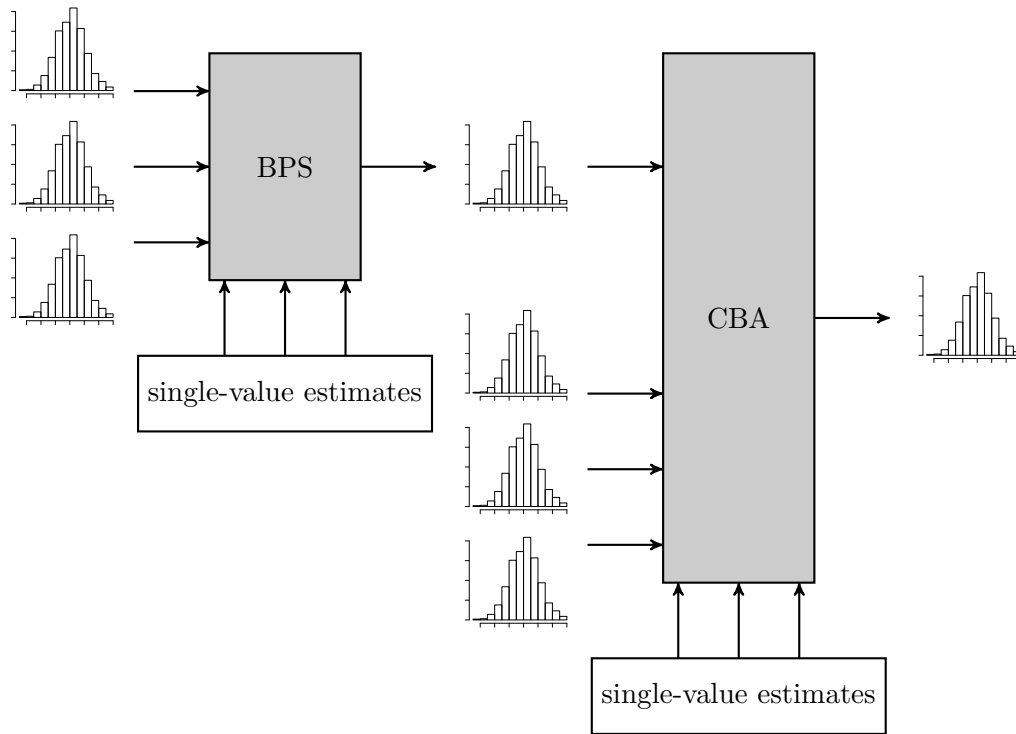


**Figure 3.9:** Overview of the MC simulation with consecutively conducted BPS and CBA.

Rubinfeld, 2005, p. 718). The *PDV* can be calculated according to

$$PDV = \sum_{t=1}^n \frac{CF_t}{\left(\frac{1+IR}{1+Infl_t}\right)^t} \quad (3.4)$$

where  $CF_t$  is a future cash flow at time  $t$ ,  $t$  is the year in which the cash flow takes place,  $IR$  is the nominal interest rate,  $\overline{Infl}_t$  is the average inflation rate from year 1 until year  $t$  and  $n$  is the number of years taken into account in the analysis.  $\overline{Infl}_t$  can be calculated according to

$$\overline{Infl}_t = \left( \prod_{z=1}^t (1 + Infl_z) \right)^{\frac{1}{t}} - 1 \quad (3.5)$$

where  $Infl_z$  is the inflation rate for year  $z$  in the period from year 1 till year  $t$ .

The final decision criterion used for the CBA in this thesis is the net present value (*NPV*) over the life cycle ( $n$ ) of the analyzed technical system. The *NPV* is defined as the difference between the *PDV* of the benefits and the *PDV* of the costs (Pindyck and Rubinfeld, 2005, p. 726) (see Equation 3.6).

$$NPV = PDV_{\text{benefits}} - PDV_{\text{costs}} \quad (3.6)$$

A positive *NPV* indicates that the analyzed option is beneficial for the given set of assumptions. When different design options are compared, the one with the highest *NPV* is the most beneficial option<sup>13</sup>.

### 3.2.5 Case Studies

In the following two examples are introduced. The results of the UA for both examples will be presented in Section 3.3.

#### 3.2.5.1 Simple Mathematical Model

The first model used to analyze the performance of the different sampling techniques is a simple mathematical model. It has the advantage that analytical solutions are available, which results in straightforward analysis and provides a test case for the analyzed methods. The model was introduced by Tarantola (2010) and Figure 3.10 shows a contour plot of the model.

The 2-dimensional model equation is

$$f(x_1, x_2) = 4x_1^2 + 3x_2 \quad (3.7)$$

with the input distributions

$$x_1, x_2 \sim \mathbf{U} \left( -\frac{1}{2}, \frac{1}{2} \right).$$

The expected value is

$$\begin{aligned} E(f(x_1, x_2)) &= \int_{-0.5}^{0.5} \int_{-0.5}^{0.5} (4x_1^2 + 3x_2) dx_1 dx_2 \\ &= \frac{1}{3} \end{aligned} \quad (3.8)$$

---

<sup>13</sup>For more information on CBA for HVAC equipment, the interested reader is referred to the international standard EN 15459 *Energy performance of buildings - Economic evaluation procedure for energy systems in buildings* (DIN EN 15459, 2008).

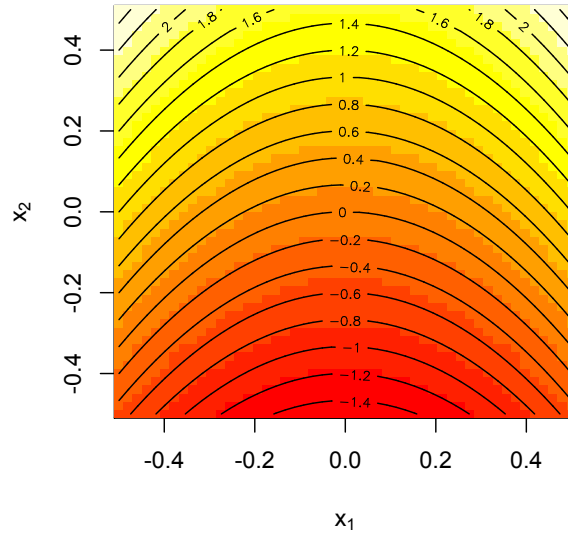


**Figure 3.10:** Contour plot of the simple mathematical model for  $f(x_1, x_2)$  according to Equation 3.7.

and the variance is

$$\begin{aligned} \text{Var}(f(x_1, x_2)) &= \int_{-0.5}^{0.5} \int_{-0.5}^{0.5} (4x_1^2 + 3x_2)^2 dx_1 dx_2 - (\mathbb{E}(f(x_1, x_2)))^2 \\ &= 0.838. \end{aligned} \quad (3.9)$$

The availability of the analytical solution makes it convenient to check the convergence of the MC simulation.

### 3.2.5.2 Building Performance Simulation Model

The building simulated is a typical German building with a net floor area of 436 m<sup>2</sup>. The model was introduced in Burhenne and Jacob (2008) and Burhenne et al. (2010b). There is no air-conditioning equipment in the building and the heat for space heating is emitted by radiators. The building<sup>14</sup> is equipped with sensors (e.g., outside temperature, heating consumption, room temperatures) to allow for a validation of the simulation. The main building parameters are shown in Table 3.2 and Figure 3.11 is a 3D-view of the building.

MC simulations require many simulation runs and are therefore computationally expensive. Especially the tests with repetitions of the analysis require many simulations but are necessary to evaluate the performance of the different sampling

<sup>14</sup>The building served as a demonstration building in the project ModBen (Neumann et al., 2011).

**Table 3.2:** Building parameters.

Parameter	Value	Unit
$\frac{A}{V}$ (envelope area to volume ratio)	0.81	$\frac{\text{m}^2}{\text{m}^3}$
$\bar{U}$ value (mean U-value)	0.53	$\frac{\text{W}}{\text{m}^2\text{K}}$
$A_{\text{win}}$ (total window area)	106	$\text{m}^2$
$A_{\text{NFA}}$ (net floor area)	436	$\text{m}^2$

**Figure 3.11:** 3D-view of the building.

techniques. For this chapter, more than 100,000 one-year simulations were executed to perform the analysis (100 repetitions for four techniques with a sample size of 256 for each MC simulation). The simulations are performed in parallel on a Linux-based computer. However, in order to reduce the computing time, it is desirable to use an appropriate simple model for the BPS. The simple hourly method (SHM) according to the ISO 13790 (2008) standard is used as a zone model. This zone model is based on five resistances and one capacity. The model was calibrated for this building; it showed a good agreement with the measured room temperatures and the heating demand of the building (Burhenne and Jacob, 2008).

In actuality, the building is an office building heated by a gas boiler. For this analysis, however, it is assumed that it is a residential building with 12 occupants<sup>15</sup>. A solar thermal collector with 25 m<sup>2</sup> area and a 2,000 liter storage tank are modeled. The collector model is implemented in Modelica using a model described by Isakson and Eriksson (1994). The collector flow rate is controlled by an on/off controller; the storage tank is modeled as a simple one-resistor/one-capacitor (R1-C1) network. The radiation processor is implemented on the basis of an equation-based model

---

<sup>15</sup>The reason for this assumption is that this case is more interesting with respect to the analyzed HVAC equipment.

(written in the modeling language Neutral Model Format; (Sahlin, 1996)) from the simulation software IDA ICE (Sahlin et al., 2004). The solar thermal system is designed for domestic hot water (DHW) and space heating. When the heat from this solar thermal system is not sufficient, a gas boiler meets the remainder of the load. Further details on the model can be found in Burhenne et al. (2010b). The primary result is the annual solar fraction which is defined as

$$SolFrac = \frac{Q_{collector}}{Q_{total}} \quad (3.10)$$

where  $Q_{collector}$  is the annual energy supplied by the solar collector and  $Q_{total}$  is the annual energy demand for space heating and DHW.

Furthermore, the case study is intended to illustrate the capabilities of the UA methodology for a combined BPS and CBA. The central question is the cost effectiveness of different building design options. In order to answer this question, two scenarios are analyzed. The base case scenario is a conventional gas boiler that supplies the building with heat and domestic hot water. The second scenario is a solar thermal collector system in conjunction with a gas boiler as was described above. It is analyzed whether the additional investment for the solar thermal collector, the storage tank and the additional necessary equipment is cost-effective or not<sup>16</sup>. This requires only one set of MC simulations with the renewable plant equipment. This is possible because the total energy consumption of both design options is assumed to be the same<sup>17</sup>. The economic efficiency is assessed on the basis of the necessary additional investment for the solar thermal system (costs) and the savings based on the reduced gas consumption when a renewable system supplies a fraction of the total energy demand (benefits). The analyzed period in the CBA is 25 years. This period has to be chosen depending on the durability of the analyzed system and other project boundaries. It is assumed that the performance of the building and its energy demand is similar each year. Given the time frame of 25 years, climate change and other variations for the BPS might play a role and could be analyzed within the proposed framework. However, this is not taken into account here for the sake of simplicity.

### Uncertain BPS Input

It is assumed that the mass flow rate of the domestic hot water ( $\dot{m}_{DHW}$ ) and the air change rate ( $ACH$ ) are uncertain. Furthermore, the number of people ( $occ$ ) present

<sup>16</sup>Design parameters (e.g., collector area, tank volume) could be varied as well. However, in this case, only scenario parameters were varied to account for uncertain boundary conditions.

<sup>17</sup>For the sake of simplicity, it is assumed that the storage losses are the same. This is a simplification but can be the case because solar thermal storage tanks are commonly better insulated than conventional DHW tanks (base case scenario).

at a particular time and the set point for the room temperature ( $T_{\text{set}}$ ) cannot be determined exactly. These four values ( $\dot{m}_{\text{DHW}}$ ,  $ACH$ ,  $occ$ ,  $T_{\text{set}}$ ) are all dependent on occupant behavior and were selected here because such variables have been identified as influential parameters in several studies (e.g., Page et al., 2008; Brohus et al., 2009; Haldi and Robinson, 2011). The schedule for the domestic hot water flow rates is generated with a program, which was developed in the Solar Heating and Cooling Program of the International Energy Agency (IEA-SHC), Task 26: Solar Combisystems (Jordan and Vajen, 2003). The air change rates, the number of occupants and the room temperature set point are also implemented using a schedule. The variation of the schedule values is implemented by multiplying a sampled scaling factor or adding an offset value. The scaling parameters are listed in Table 3.3. The distributions and the standard deviation were chosen on the basis of experience and literature. Pietrzyk and Hagentoft (2008) also use normal distributions for characterizing air change rates and the mean and standard deviation of  $ACH$  implemented in the simulations is comparable with cases illustrated in their study. In the case of  $\dot{m}$ , a standard deviation of 10% of the schedule values and a normal distribution seems appropriate to account for different consumption scenarios. Occupancy is very specific to the case analyzed and the normal distribution around the assumed schedule is intended to explore some possible scenarios. Note that the values for the offset for the number of occupants and the set point are rounded (integers for the occupancy and values with one decimal place for the set point). Figure 3.12 illustrates the use of the scaling factors for  $ACH$  and the offsets for  $occ$ . The red line represents the base case schedule and the box plots indicate the different values for  $ACH$  and  $occ$  used in the MC Simulation. As mentioned in Section 2.2.2, there might be dependence between some of the uncertain input variables (e.g., the number of occupants present influences the air change rate and the domestic hot water consumption). However, these relationships are neglected in this study for the sake of simplicity and to allow easier interpretation of the example.

**Table 3.3:** Parameters selected for variation and their distributions for the BPS ( $\mu$  is the mean and  $\sigma$  is the standard deviation).

Parameter	Distribution	$\mu$	$\sigma$	Unit
$\dot{m}_{\text{DHW}}$ (scaling factor)	normal	1	0.1	–
$ACH$ (scaling factor)	normal	1	0.2	–
$occ$ (offset)	normal	0	2	–
$T_{\text{set}}$ (offset)	normal	0	1	K

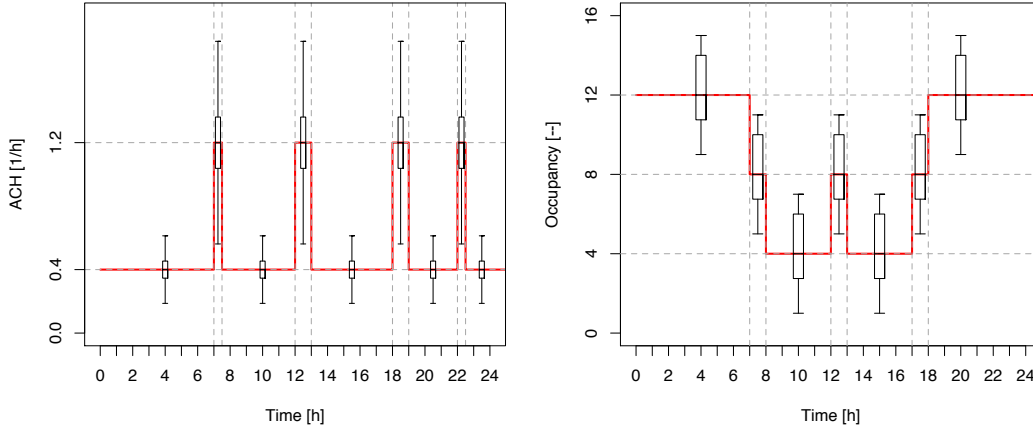


**Figure 3.12:** Variation of schedule values for air change rate ( $ACH$ ) and occupancy using scaling factors and offsets.

### Uncertain CBA Input

For the CBA, it is assumed that the gas price ( $GP$ ), the inflation rate ( $Infl$ ), the interest rate ( $IR$ ), the investment cost ( $IC$ ) and  $Q_{\text{collector}}$  are uncertain. The uncertainty in  $Q_{\text{collector}}$  is an input coming from the BPS.

Some aspects of the UQ for the economic inputs and the UA for the combined BPS and CBA have been published by Burhenne et al. (2013a).

As input for a potential CBA, the inflation rate and the gas price for Germany are predicted using ARIMA models. Literature data is used to fit the ARIMA model and to predict the base case scenario for the development of the gas price and the inflation rate. This base case scenario is varied during the MC simulation to account for uncertainties.

### Inflation Rate

The inflation rate is the rate at which prices in an economy increase. The inflation rates for Germany in the period of 1997-2011 are used as the basis for the analysis (European Commission Eurostat, 2012). The data from this period are used to fit an ARIMA model with seasonal components<sup>18</sup>. The order of the model parts ( $p$ ,  $q$ ,

<sup>18</sup>The R function `arima()` is used for the ARIMA model parameter identification.

d, P, Q, D) is chosen on the basis of a parametric run<sup>19</sup> of all possible combinations with p, q, P and Q varied from 0 to 3 and the order of differencing varied from 0 to 2. This results in 2,304 different combinations. The Akaike information criterion (*AIC*) value of the different model configurations is used as the selection criterion (see Equation 2.15). Not all possible combinations produce reasonable predictions and some result in errors or warning messages for the ARIMA fit function in R. The reason for this might be limitations introduced by the time series data since the analyzed period is relatively short and only annual values are used<sup>20</sup>. However, the configurations with a low *AIC* were analyzed by visual inspection. The chosen configuration is among the best (i.e., low *AIC*) 11% of all possible model configurations. Figure 3.13 shows the historical data, the prediction of the chosen model configuration and the confidence interval of the predicted time series<sup>21</sup>. The prediction is performed for 25 years (2012-2036). The inflation rate has a periodic characteristic over time. The parameters of the model are listed in Table 3.4.

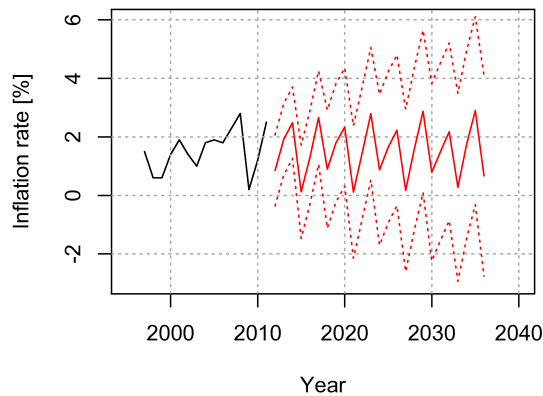


**Figure 3.13:** Time series for the inflation rate in Germany. The values from 1997-2011 are historical data. The values starting in 2012 are predicted using an ARIMA model that is fitted with the historical data. The dashed lines represent the confidence interval.

To vary the base case prediction during the MC simulation, the standard error of the predicted time series is used in the sampling procedure. The variation is assumed to be normally distributed. This results in different scenarios within the MC simulation (different complete time series of inflation are used to conserve the periodicity). However, the standard error of the prediction is very high and could

<sup>19</sup>The procedure for this exhaustive search in R was introduced by Zoonekynd (2007). This procedure has been modified and used in this thesis.

<sup>20</sup>In the presented case, the cyclic component has a longer period than one year.

<sup>21</sup>The R function `predict()` is used for the prediction and corresponding statistics.

**Table 3.4:** ARIMA model parameters for the inflation rate.

Parameter	Value	SE
Order of AR (p)	2	–
Order of MA (q)	2	–
Order of differencing (d)	0	–
Order of seasonal AR (P)	0	–
Order of seasonal MA (Q)	0	–
Order of seasonal differencing (D)	1	–
Coefficient AR ( $a_1$ )	0.8749	0.1278
Coefficient AR ( $a_2$ )	-0.9899	0.0377
Coefficient MA ( $b_1$ )	-0.7435	0.3058
Coefficient MA ( $b_2$ )	1.0000	0.3829
Result	Value	SE
log likelihood	-12.43	–
Akaike information criterion ( <i>AIC</i> )	34.86	–
Variance ( $\sigma^2$ ) estimate	0.332	–

result in an overestimation of uncertainty. Based on historical data and the fact that political measures aim to keep the inflation rate within a certain range, it was arbitrarily assumed that the standard deviation in the sampling procedure is 60% of the standard error of the ARIMA prediction. Figure 3.14 shows box plots of the sampled values as well as the ARIMA prediction and its confidence interval. The circles represent outliers. This is data that lies outside the whisker range<sup>22</sup>. Predictions until 2036 are highly uncertain. A single "correct" assumption does not exist. As already mentioned above, the decision makers involved in the analysis would have to make the final decision as to the uncertainty which should be assumed. The analyst should provide guidance in this process.

### Gas Price

Historical data from 1991 to 2011 (BMW<sub>i</sub>, 2012) is used to fit an ARIMA model. The ARIMA model parameter identification is conducted similarly to that for the inflation rate. Figure 3.15 shows the historical data, the prediction and the confidence intervals of the predicted time series. Unlike the inflation rate, the consumer gas price has an increasing trend rather than a periodic one. The configurations with the lowest *AIC* were analyzed by visual inspection. As for the ARIMA fit for the inflation rate, not all possible combinations produce reasonable predictions and

<sup>22</sup>As mentioned in Chapter 1 the maximum length of the whiskers is 1.5 times the interquartile range. The interquartile range equals the length of the box.

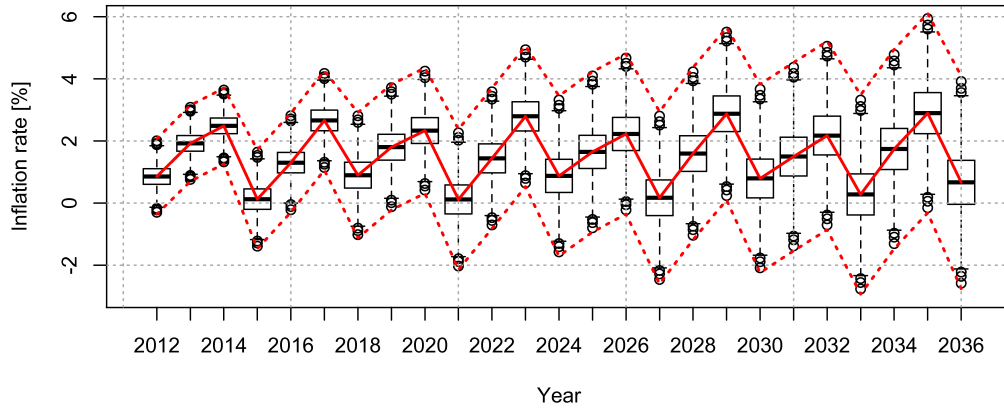


**Figure 3.14:** Box plot of the sampled values for the inflation rate used in the MC simulation. For illustration, the ARIMA prediction (red line) and the corresponding confidence interval (dotted red lines) are also plotted.

some result in error or warning messages for the ARIMA function in R. The chosen model configuration is among the best (i.e., low  $AIC$ ) 34% of all combinations. The confidence interval indicates that the model outcome becomes highly uncertain when the future values are far away from the time when the investment is made. The parameters of the model are listed in Table 3.5.

It is not likely that the gas price will become negative, although the confidence interval in Figure 3.15 indicates it. At the same time, very high energy price scenarios can occur, even though they do not have a high probability. For these reasons, the uncertainty of the gas price time series is considered to be log-normally distributed. This results in different gas price scenarios. Similar to the assumptions for the uncertainty of the predicted inflation rates, the standard deviation in the sampling procedure is assumed to be 60% of the standard error of the ARIMA prediction. Figure 3.16 shows box plots of the sampled values as well as the ARIMA prediction.

### Interest Rate

Depending on the specific project boundary conditions, different assumptions for the  $IR$  used in the CBA can be chosen. The most significant difference is probably whether the money for any additional investment has to be borrowed from a bank or not<sup>23</sup>. In this example, a fixed  $IR$  over the analyzed period is assumed. To

<sup>23</sup>If the money comes from a loan with a fixed loan period and contract,  $IR$  might not be subject to any uncertainty.

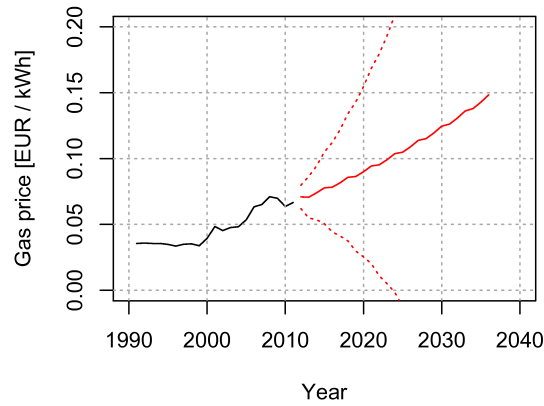


**Figure 3.15:** Time series for the consumer gas price in Germany. The values from 1991 to 2011 are historical data. The values starting in 2012 are predicted using an ARIMA model that is fitted with the historical data. The dashed lines represent the confidence interval.

**Table 3.5:** ARIMA model parameters for the gas price.

Parameter	Value	SE
Order of AR (p)	1	–
Order of MA (q)	2	–
Order of differencing (d)	2	–
Order of seasonal AR (P)	0	–
Order of seasonal MA (Q)	1	–
Order of seasonal differencing (D)	1	–
Coefficient AR ( $a_1$ )	-0.6190	0.3238
Coefficient AR ( $a_2$ )	0.0649	0.6773
Coefficient MA ( $b_1$ )	-0.8518	0.5917
Coefficient MA ( $b_2$ )	-0.7051	0.5028
Result	Value	SE
log likelihood	-12.07	–
Akaike information criterion (AIC)	34.15	–
Variance ( $\sigma^2$ ) estimate	0.1966	–

account for different scenarios,  $IR$  is varied in the MC simulation.  $IR$  is sampled according to a uniform distribution in the interval  $[2, 10]$ , hence  $IR \sim \mathbf{U}(2, 10)$  with  $i = 1, 2, \dots, N$ . Interest rates in this range seem reasonable for investments in renewable energy systems.

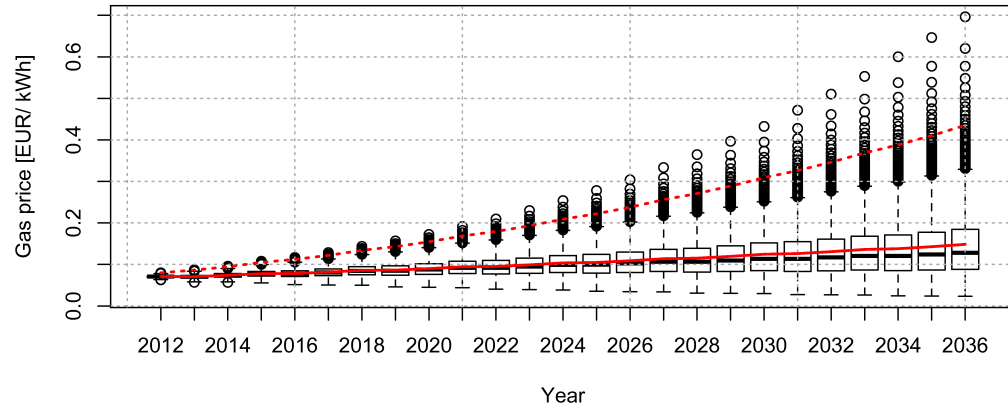


**Figure 3.16:** Box plot of the sampled values for the gas price used in the MC simulation. For illustration, the ARIMA prediction (red line) and the corresponding confidence interval (dotted red line) is also plotted.

### Investment Cost

During the design process, prices for the investment are assumed. Depending on the market, the final  $IC$  might be different to the costs assumed in the design stage. To take this into account,  $IC$  is assumed to be uncertain. Only the additional cost for the solar thermal system is taken into account. The specific investment cost for one square meter collector area including all other costs (e.g., storage tank, pumps, pipes) is sampled according to a normal distribution with  $\mu = 700 \text{ EUR/m}^2$  and  $\sigma = 50 \text{ EUR/m}^2$ , hence  $IC \sim \mathbf{N}(700, 50)$  with  $i = 1, 2, \dots, N$ . Not only the investment cost but also running costs, periodic replacement cost and maintenance costs are included in many CBA (specific information can be obtained from DIN EN 15459 (2008)). However, they are not considered in this example for reasons of simplicity. It is assumed that in the case of the analyzed solar thermal system, these costs are relatively low compared to the other considered cash flows (e.g., the maintenance cost is orders of magnitude lower than the investment costs). Furthermore, the cash flow for replacement costs occurs 10-15 years after the investment is made and its influence on the  $NPV$  is reduced because of the compound interest effect.

The UQ for the CBA input is summarized in Table 3.6.

**Table 3.6:** Parameters selected for variation and their distributions for the CBA.

Parameter	Distribution	$\mu$	$\sigma$	Unit
<i>IC</i>	normal	700	50	$\frac{\text{EUR}}{\text{m}^2}$
Parameter	Distribution	min.	max.	Unit
<i>IR</i>	uniform	2	10	%
Variable	UQ			Unit
<i>Infl</i>	ARIMA prediction			%
<i>GP</i>	ARIMA prediction			$\frac{\text{EUR}}{\text{kWh}}$
Parameter	UQ			Unit
$Q_{\text{collector}}$	BPS result			kWh

### 3.3 Results and Discussion

#### 3.3.1 Simple Mathematical Model

##### 3.3.1.1 Sampling

Some of the results concerning the comparison of different sampling strategies were published by Burhenne et al. (2011). However, the work is extended in this thesis.

Figure 3.17 shows a comparison of the different sampling techniques used to compute the mean and the variance of the function with different sample sizes. Different quantitative criteria to analyze the convergence exist and have to be selected with respect to the accuracy requirements of the analysis. For this example, convergence is defined to be reached when the value of the estimate is in the range of the analytical value  $\pm 5\%$  (see Table 3.7). The analytical value for the mean is  $0.\bar{3}$  and the analytical value for the variance is  $0.83\bar{8}$  (see also Section 3.2.5). The random sampling shows the worst convergence to the analytical mean of the function. Latin hypercube sampling shows the fastest convergence to the analytical mean (sample size 16). The mean estimates derived with stratified sampling and sampling based on Sobol' sequences both converge for a sample size of 64. The variance estimate for the sampling based on Sobol' sequences results in the fastest convergence ( $N = 8: 0.846, +0.8\%$ )<sup>24</sup> whereas random and stratified sampling converge at a sample size of 256. Although, LHS showed the fastest convergence with respect to the mean estimate, it required a sample size of 512 until the variance estimate converged.

<sup>24</sup>Note that this result is not shown in Table 3.7.

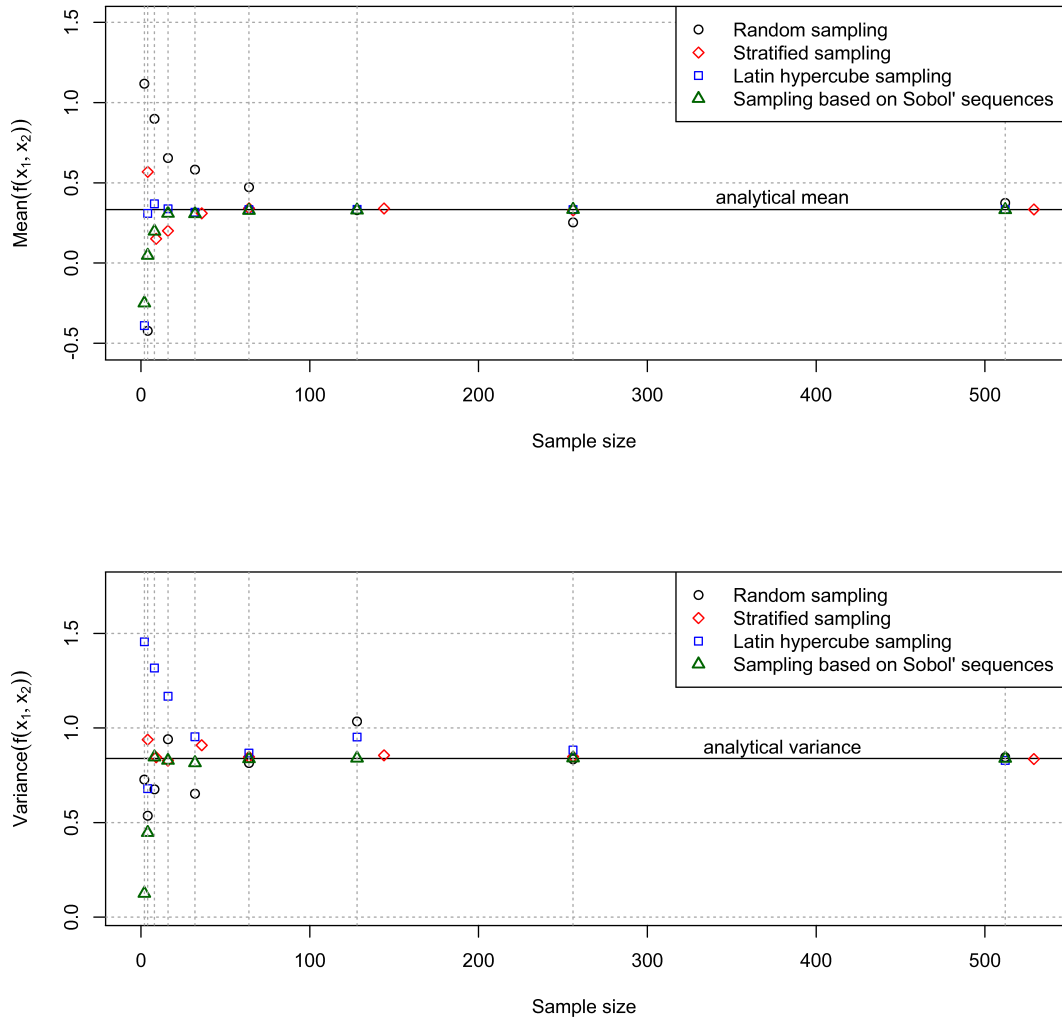


**Figure 3.17:** Comparison of the mean and variance estimates, obtained by different sampling techniques applied to the evaluation of the simple mathematical model.

**Table 3.7:** Convergence of mean and variance estimates for the simple mathematical model to the analytically determined values. Gray cells indicate estimates that have converged to the analytical value  $\pm 5\%$ . The red cells indicate that the estimate falls within the target range but that convergence has not been reached. The percentages in the cells indicate the deviation from the analytical value. The sample size in brackets is for stratified sampling. The different sample sizes are due to the properties of stratified sampling as explained in Section 3.2.1.

Sample size	16	32	64	128 (144)	256	512 (529)
	<b>Mean estimate</b>					
<b>Random</b>	0.655 +96.4%	0.582 +74.6%	0.473 +41.8%	0.329 -1.2%	0.253 -24.1%	0.375 +12.4%
<b>Stratified</b>	0.201 -39.8%	0.310 -7.1%	0.341 +2.2%	0.340 +2.0%	0.328 -1.5%	0.334 +0.2%
<b>LHS</b>	0.338 +1.3%	0.317 -4.9%	0.333 -0.2%	0.335 +0.4%	0.333 0.0%	0.333 0.0%
<b>Sobol'</b>	0.309 -7.3%	0.306 -8.1%	0.327 -1.8%	0.329 -1.3%	0.333 0.0%	0.332 -0.4%
	<b>Variance estimate</b>					
<b>Random</b>	0.941 +12.1%	0.653 -22.2%	0.815 -2.9%	1.034 +23.3%	0.834 -0.6%	0.846 +0.8%
<b>Stratified</b>	0.827 -1.4%	0.909 +8.3%	0.847 +1.0%	0.855 +1.9%	0.848 +1.1%	0.836 -0.4%
<b>LHS</b>	1.167 +39.2%	0.954 +13.7%	0.867 +3.3%	0.952 +13.5%	0.883 +5.3%	0.828 -1.2%
<b>Sobol'</b>	0.828 -1.3%	0.815 -2.8%	0.836 -0.3%	0.840 +0.1%	0.841 +0.3%	0.839 0.0%

Empirical CDFs (ECDFs) are used to visualize the robustness (i.e., stability) of results obtained by different sampling strategies. The sampling and model evaluation was repeated 100 times for each sampling technique and the chosen sample size of 256. Figure 3.18 shows a comparison of the ECDFs for the simple mathematical model. One can see that in this case, the robustness of stratified sampling and sampling based on Sobol' sequences is the best (i.e., ECDFs show least variability) followed by Latin hypercube sampling. The ECDFs constructed for random sampling show the most variability.

To further analyze the robustness, one Kolmogorov-Smirnov test is performed for all possible combinations of the different ECDFs. All combinations of 100 different

ECDFs result in  $n_{\text{ECDF}}! / ((n_{\text{ECDF}} - k)! k!) = 100! / ((100 - 2)! * 2!) = 4,950$  Kolmogorov-Smirnov tests. Table 3.8 contains the results, which confirm the findings of the visual inspection. This quantitative measure reveals that the sampling based on Sobol' sequences is slightly more robust than stratified sampling<sup>25</sup>.

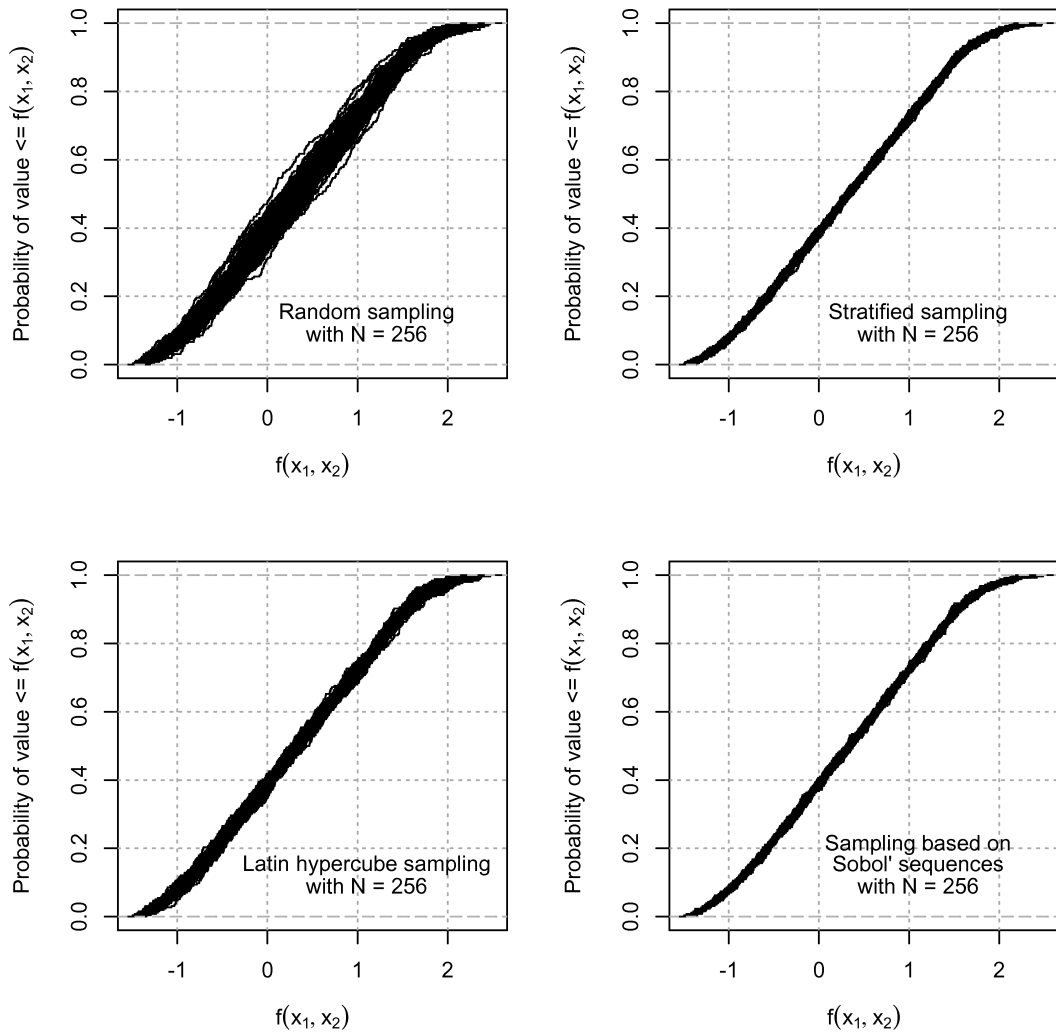


**Figure 3.18:** Comparison of ECDFs for the simple mathematical model with 100 repetitions, for four different sampling techniques.

<sup>25</sup>The lower the maximum  $D$  for all ECDF combinations, the more robust is the sampling technique.

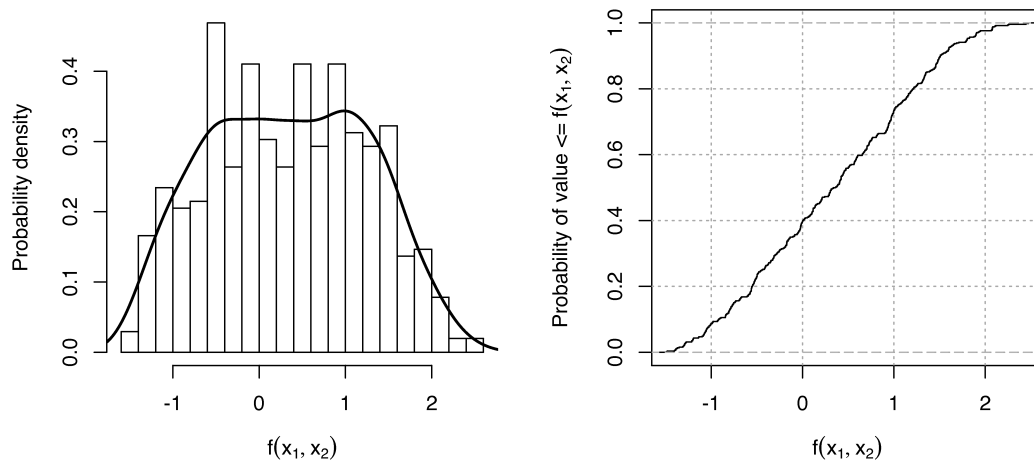
**Table 3.8:** Kolmogorov-Smirnov test results for the simple mathematical model.

Sampling technique	Max. D for all ECDF combinations
Random	0.1953
Stratified	0.0547
LHS	0.0820
Sobol'	0.0508

Sampling based on Sobol' sequences showed the fastest convergence. For the investigated example, a sample size of 64 was enough to obtain good results for both estimates. Moreover, the sampling based on Sobol' sequences was the most robust sampling technique in this example. The second best sampling technique with respect to convergence and robustness was stratified sampling.

### 3.3.1.2 Stochastic Output

Figure 3.19 shows the normalized histogram of the result vector (sampling based on Sobol' sequences with  $N = 512$ ) together with a PDF calculated with kernel density estimates and an ECDF. The statistics for this result are summarized in Table 3.9. No further analysis of the uncertainty is conducted for the simple mathematical model. A more detailed analysis will be presented for the BPS model in the next section.

**Figure 3.19:** PDF and ECDF for the simple mathematical model ( $N = 512$ ).

**Table 3.9:** Statistical summary of the result for the simple mathematical model ( $N = 512$ ).

Statistic	Value
Mean	0.3319
Variance	0.8391
Standard deviation	0.9160
Minimum	-1.4940
Lower (first) quartile	-0.4393
Median	0.3508
Upper (third) quartile	1.0450
Maximum	2.4730

### 3.3.2 Building Performance Simulation Model

#### 3.3.2.1 Sampling

Figure 3.20 compares the convergence to the mean and the variance of the solar fraction for the different sampling strategies for the BPS model. The black horizontal lines show the mean and variance values after an MC simulation with random sampling and a sample size of 25,600. Due to this large sample size, this value can be taken as a reference. For this example, convergence is defined to be reached when the value of the estimate is within the range of the reference value  $\pm 5\%$ . The reference value for the mean is 0.197 and the reference value for the variance is  $5.26e-4$ . The mean estimate obtained with sampling based on Sobol' sequences converges at a sample size of 4 (0.194, -1.5%) and the mean estimate for LHS also converges at  $N = 4$  (0.196, -0.7%)<sup>26</sup>. However, the mean estimates of the other sampling techniques also converge for a sample size of 16. The variance estimates converge much more slowly than the mean estimates. The variance estimate obtained with sampling based on Sobol' sequences converges at a sample size of 128. Stratified sampling and LHS converge at a sample size of 256. This sample size is not sufficient to obtain an accurate variance estimate with random sampling. The variance estimate for random sampling converges at a sample size of 1,024 ( $5.48e-4$ , +4.2%)<sup>27</sup>.

Figure 3.21 shows the comparison of the estimated CDFs for the BPS model. The model evaluation was repeated 100 times for each sampling technique. The sampling based on Sobol' sequences has the least variation, followed by stratified sampling and LHS. The CDFs constructed for the random sampling show the most variability.

As for the simple mathematical model, the Kolmogorov-Smirnov tests are performed for all combinations of the 100 different ECDFs (4,950). In this example,

---

<sup>26</sup>Note that these results are not shown in Table 3.10.

<sup>27</sup>Note that this result is not shown in Figure 3.20 and Table 3.10.

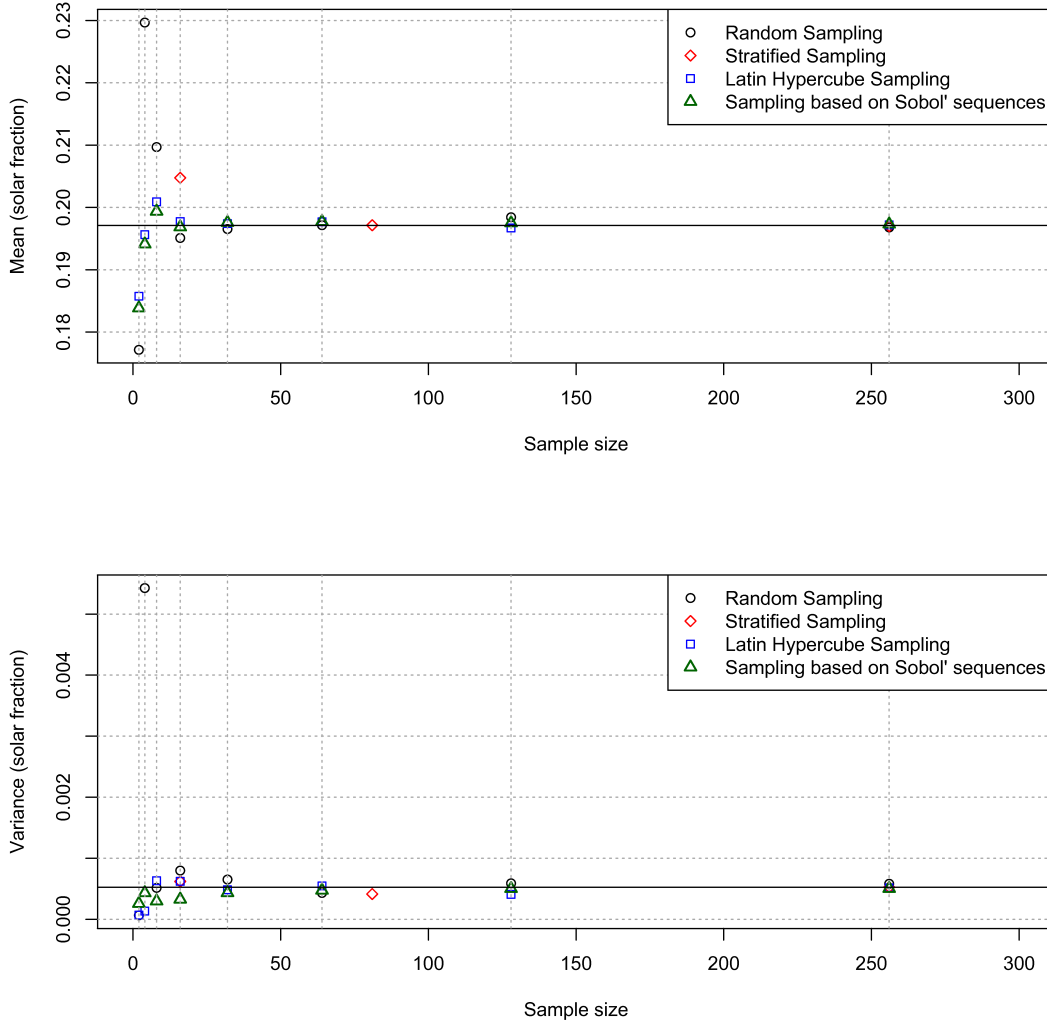


**Figure 3.20:** Comparison of the mean and variance estimates of the solar fraction, obtained by different sampling techniques applied to the evaluation of the BPS model.

**Table 3.10:** Convergence of mean and variance estimates for the BPS model. Gray cells indicate estimates that have converged to the reference value  $\pm 5\%$ . The red cells indicate that the estimate falls within the target range but that convergence has not been reached. The sample size in brackets is for stratified sampling. The different sample sizes (i.e., 64 and 81) are due to the properties of stratified sampling as explained in Section 3.2.1.

Sample size	8	16	32	64 (81)	128	256
	<b>Mean estimate</b>					
<b>Random</b>	0.210 +6.4%	0.195 -1.0%	0.197 -0.3%	0.197 0.0%	0.198 +0.7%	0.197 -0.2%
<b>Stratified</b>	–	0.205 +3.9%	–	0.197 0.0%	–	0.197 -0.1%
<b>LHS</b>	0.201 +1.9%	0.198 +0.3%	0.197 +0.2%	0.198 +0.3%	0.197 -0.2%	0.197 +0.1%
<b>Sobol'</b>	0.199 +1.2%	0.197 -0.1%	0.198 +0.2%	0.198 +0.3%	0.198 +0.2%	0.197 +0.1%
	<b>Variance estimate</b>					
<b>Random</b>	5.15e-4 -2.1%	7.98e-4 +51.7%	6.51e-4 +23.8%	4.31e-4 -18.0%	5.89e-4 +12.0%	5.81e-4 +10.6%
<b>Stratified</b>	–	6.20e-4 +17.9%	–	4.14e-4 -21.3%	–	5.27e-4 +0.1%
<b>LHS</b>	6.31e-4 +20.1%	6.21e-4 +18.0%	4.82e-4 -8.3%	5.47e-4 +4.0%	4.07e-4 -22.6%	5.17e-4 -1.7%
<b>Sobol'</b>	2.98e-4 -43.4%	3.27e-4 -37.8%	4.34e-4 -17.4%	4.74e-4 -9.8%	5.01e-4 -4.7%	5.02e-4 -4.5%

this is particularly useful because the spread of the ECDFs for stratified, LHS and sampling based on Sobol' sequences is similar. Table 3.11 documents the results, which reveal that the sampling based on Sobol' sequences is the most robust.

**Table 3.11:** Kolmogorov-Smirnov test results for the BPS model.

Sampling technique	Max. D for all ECDF combinations
Random	0.2031
Stratified	0.0938
LHS	0.1211
Sobol'	0.0820

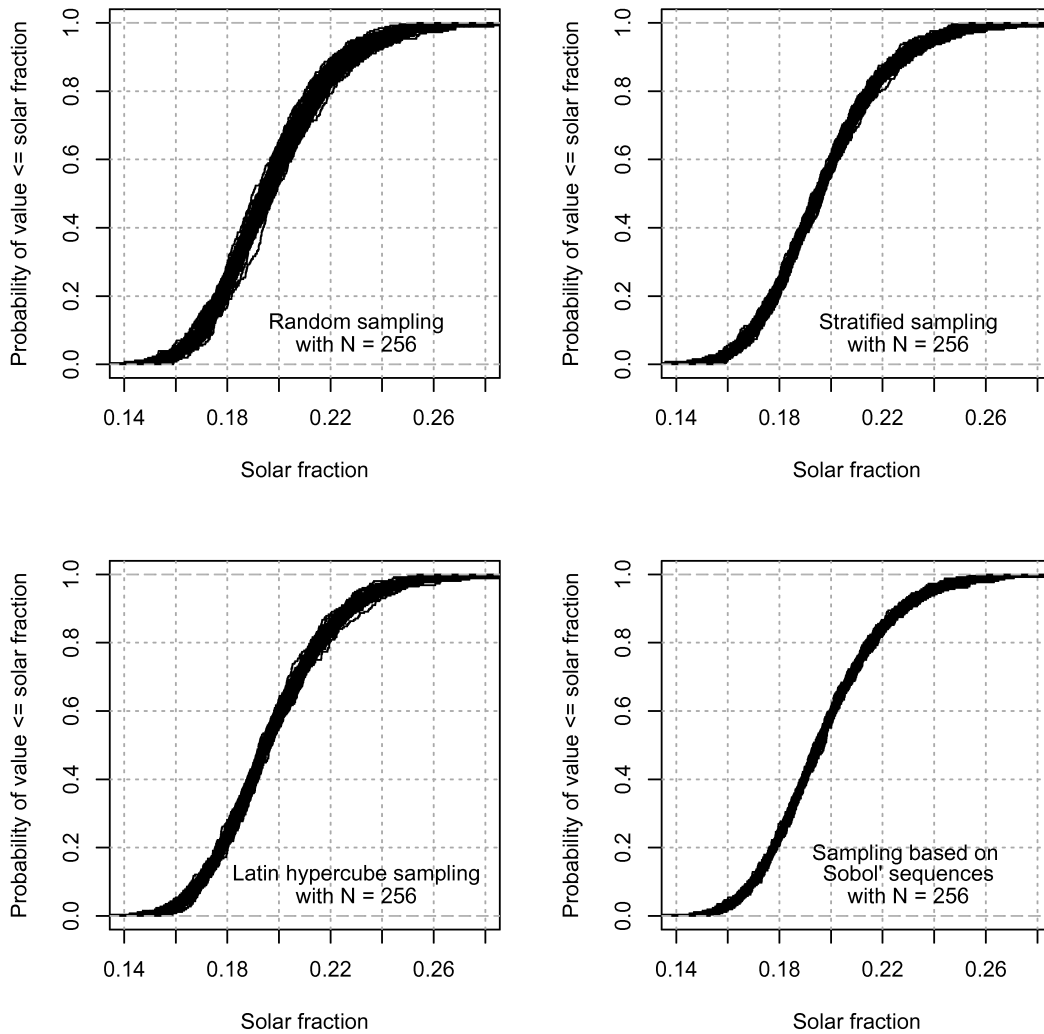


**Figure 3.21:** Comparison of ECDFs for the four sampling techniques for the BPS model with 100 repetitions, for four different sampling techniques.

Sampling based on Sobol' sequences showed the fastest convergence for both investigated estimates (required sample size until both estimates converge: 128). However, at a sample size of 256, all sampling strategies except random sampling converged and produced comparable results for the mean and variance estimates. Sampling based on Sobol' sequences was the most robust sampling technique for the investigated BPS model. The second-best sampling techniques with respect

to convergence and robustness were stratified sampling and LHS. The sample size restrictions of stratified sampling led to limitations concerning possible sample sizes.

### 3.3.2.2 Stochastic Output

For each simulation, one solar fraction is obtained. Figure 3.22 shows the normalized histogram of the result vector together with a PDF calculated with kernel density estimates and an ECDF for a sample produced with sampling based on Sobol' sequences with a sample size of 256. The figure gives an indication of how the result varies given the uncertainties in the inputs. A practical design question might be:

- *What is the probability to reach a solar fraction of  $> 20\%$ ?*

The gray area under the PDF represents the probability that the solar fraction is  $> 20\%$  and the number in the ECDF plot indicates the probability that the solar fraction is  $\leq 20\%$ . This probability (i.e., relative frequency) is computed by dividing the number of simulation results for which the solar fraction is  $\leq 20\%$  ( $n_{SolFrac \leq 20\%}$ ) by the total number of simulations ( $N$ ) according to

$$P(SolFrac \leq 20\%) = \frac{n_{SolFrac \leq 20\%}}{N}. \quad (3.11)$$

Hence the probability for a solar fraction  $> 20\%$  is  $(1 - 0.5898) \approx 0.41$ . 41% probability for reaching the design goal might be too low. The decision makers can decide whether the design of the plant equipment should be changed or not. A larger collector area and an increased tank volume would increase the solar fraction but also require a higher investment. The results of the CBA for this design will be presented in the course of this chapter.

In Figure 3.22, the PDF was computed using kernel density estimates. It is now tested whether the data can be described by a normal distribution. A normality test is conducted to find an appropriate distribution. Figure 3.23 shows the quantile-quantile plot (Q-Q plot) of the MC simulation result. The result of the Kolmogorov-Smirnov test<sup>28</sup> for the MC result is  $D = 0.047$  and  $p$ -value = 0.6248. This test result indicates that the data is normally distributed. Hence, the PDF can be described with

$$p(x) = \frac{1}{\sigma\sqrt{2\pi}} \exp\left(-\frac{1}{2}\left(\frac{x-\mu}{\sigma}\right)^2\right). \quad (3.12)$$

The parameters for the normal distribution can be found in Table 3.12.

---

<sup>28</sup>The R function `ks.test()` is used here. More details on the test can be found in Section 2.2.2.2.

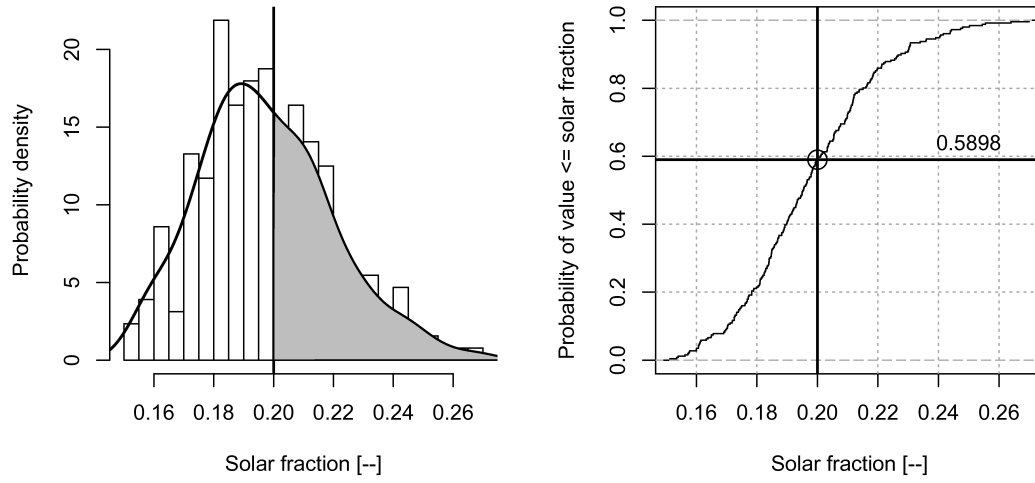


**Figure 3.22:** PDF and ECDF for the solar fraction ( $N = 256$ ).

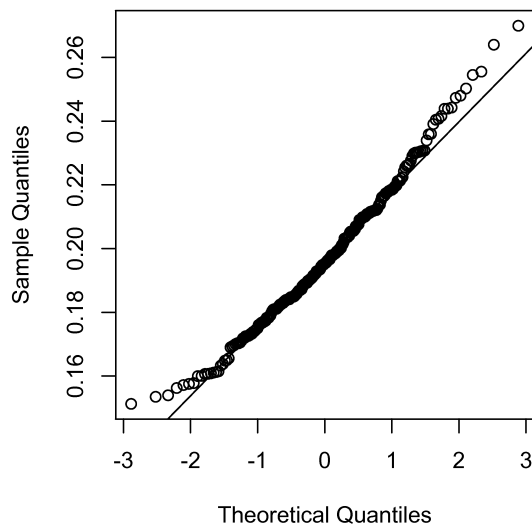


**Figure 3.23:** Q-Q plot for the MC simulation result.

**Table 3.12:** Distribution parameters for the MC simulation result.

Result	Distribution	$\mu$	$\sigma$
<i>SolFrac</i>	normal	0.1973	0.02241

With the function introduced in Equation 3.12, it is possible to calculate the answer to the defined design question with

$$\begin{aligned} P(\text{SolFrac} \geq 20\%) &= \int_{0.2}^{+\infty} p(\text{SolFrac}) \, d\text{SolFrac} & (3.13) \\ &\approx 0.4523 \cong \underline{45.2\%}. \end{aligned}$$

In principle, both approaches (counting the simulation results above/below a threshold or testing the applicability of a distribution and computing the probability based on the PDF) are applicable to compute a probability. However, there is a risk that the distribution test yields an incorrect result and testing data for different distributions is a time-consuming task. Therefore, in the following, only PDFs computed with kernel density estimates and ECDFs are used to analyze MC simulation results. Table 3.13 documents the statistics for the result. This is supplementary information to the visualization.

**Table 3.13:** Statistical summary of the BPS result ( $N = 256$ ).

Statistic	Value
Mean	0.1973
Variance	0.0005024
Standard deviation	0.02241
Minimum	0.1513
Lower (first) quartile	0.1823
Median	0.1953
Upper (third) quartile	0.2113
Maximum	0.2699

### 3.3.2.3 Results for the Combined BPS and CBA

In the following, the results for a combined BPS and CBA are presented. The basis is the input that was presented in Section 3.2.5.2. An analysis of the convergence should be part of every UA. This can be simplified compared to the previous investigations on convergence. Based on the findings above, only sampling based on Sobol' sequences is used. Figure 3.24 shows the convergence of the estimates for

the mean and the variance of the *NPV*. The horizontal lines represent the results for the largest sample size (i.e., 1,024). These results are used as the reference (i.e., -6,948 EUR for the mean and  $2.228e+7$  EUR<sup>2</sup> for the variance). For this example, convergence is defined to be reached when the values of the estimates are within the range of the reference results  $\pm 5\%$ . Based on this criterion, the mean estimate converges at a sample size of 4 (-6,753 EUR, -2.8%)<sup>29</sup> whereas the variance estimate converges at a sample size of 128.

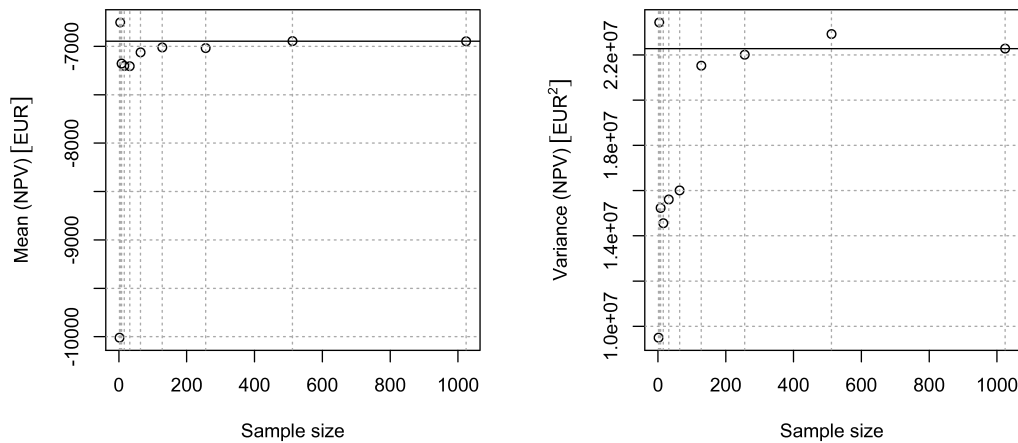


**Figure 3.24:** Convergence plot for the mean and variance estimates of the *NPV* (Note that the y-axes do not start at 0).

**Table 3.14:** Convergence of mean and variance estimates for combined BPS and CBA. Gray cells indicate estimates that have converged to the reference value  $\pm 5\%$ .

Sample size	32	64	128	256	512	1,024
Mean estimate in EUR	-7,206 +3.7%	-7,062 +1.7%	-7,012 +0.9%	-7,018 +1.0%	-6,946 0.0%	-6,948 0.0%
Variance estimate in EUR <sup>2</sup>	1.561e+7 -30.0%	1.60e+7 -28.2%	2.15e+7 -3.4%	2.20e+7 -1.2%	2.29e+7 +2.9%	2.23e+7 0.0%

Figure 3.25 shows the PDF computed with kernel density estimates and the ECDF

<sup>29</sup>Note that this result is not shown Table 3.14.

for the *NPV*. The underlying sample size is 1,024 and the *NPV* of the additional investment varies significantly. This massive variation is due to the significant influence of some analyzed parameters. The ECDF reveals that the probability that the investment has a positive *NPV* is approximately 9%  $((1 - 0.911) * 100\%)$  under the chosen assumptions. This probability will not be satisfactory in cases where the decisions are made on the basis of monetary values rather than for environmental reasons. With a conventional BPS and CBA, the result would have been a single value. Depending on the assumptions, it could be a positive or negative *NPV* without information on probabilities of the result. Table 3.15 provides the statistics for the result of the analysis.

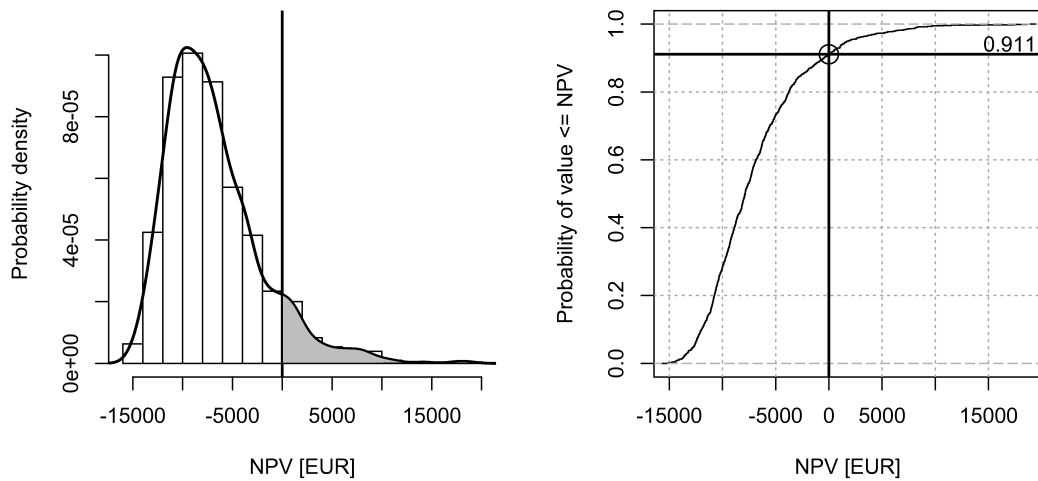


**Figure 3.25:** PDF and ECDF for the *NPV* ( $N = 1,024$ ).

### 3.3.2.4 Stochastic Time Series Output

In the previous section, the solar fraction over one year was analyzed. To illustrate a UA for time series, the heating power supplied to the building is analyzed over time. The time step for the simulation is 60 seconds. Figure 3.26 shows the different time series of the heating power for one day in January (January 13). The figure contains 128 time series coming from an MC simulation with  $N = 128$ . It reveals that the uncertainty in the heating power varies over time due to the uncertain boundary conditions. It is evident that *ACH* is a dominant parameter because the pattern of the *ACH* schedule that was presented in Figure 3.12 is visible in the time series. However, the interpretation of the different time series is difficult.

**Table 3.15:** Statistical summary of the result for the combined BPS and CBA ( $N = 1,024$ ).

Statistic	Value
Mean	-6,948
Variance	2.228e+7
Standard deviation	4,721
Sample minimum	-15,090
Lower (first) quartile	-10,330
Median	-7,868
Upper (third) quartile	-4,662
Sample maximum	18,630

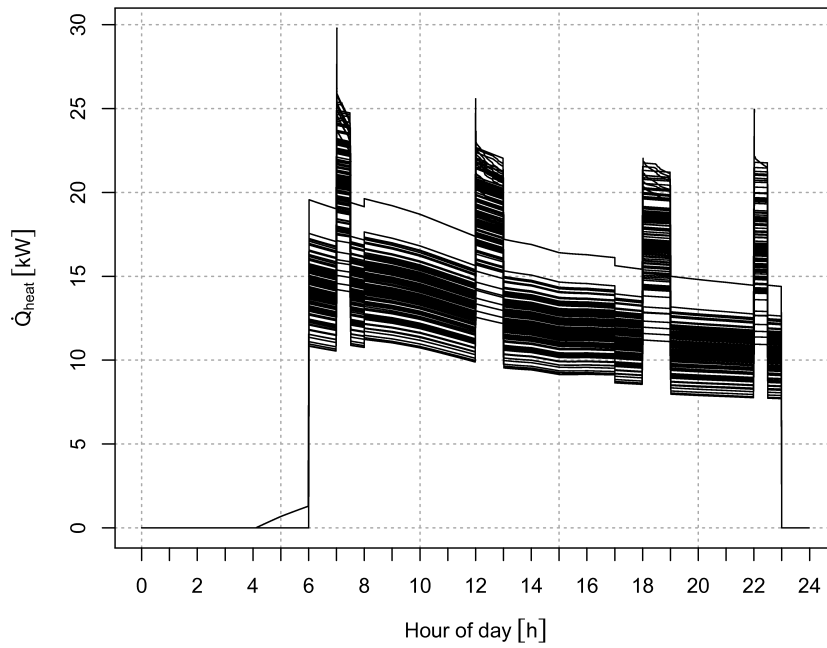
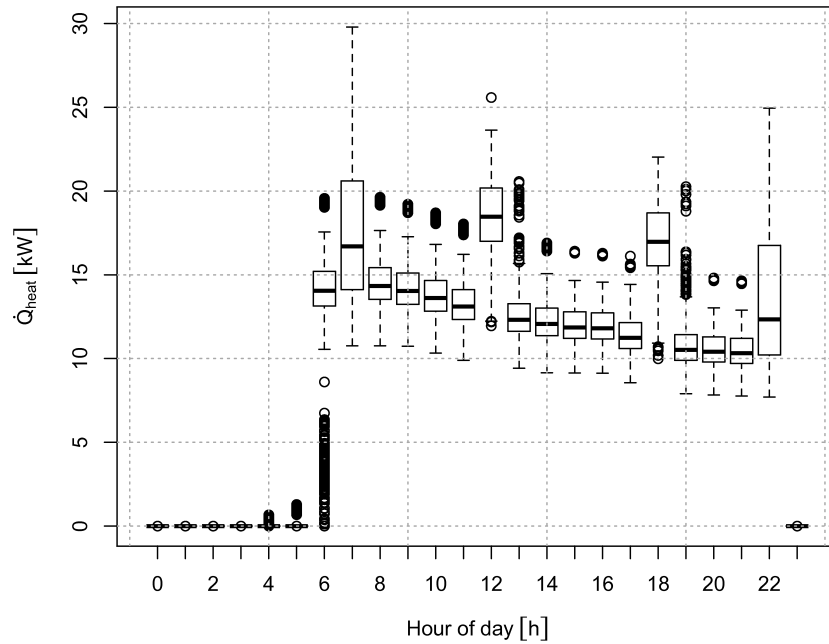
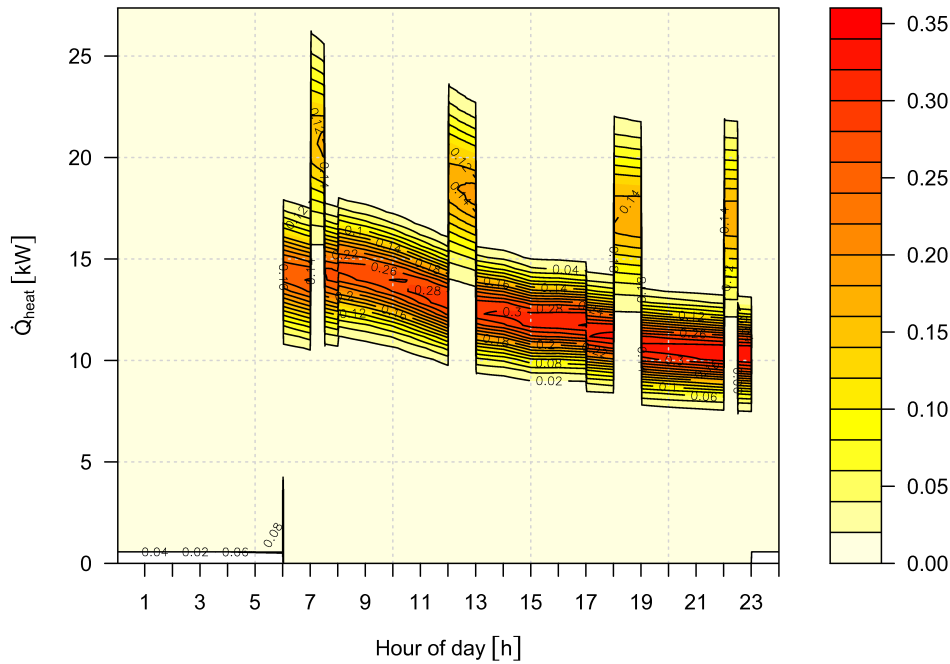
**Figure 3.26:** Time series for the heating power demand on January 13.

Figure 3.27 is a box plot representation of the time series data, where the values from one hour are aggregated. This allows better interpretation of the distribution of the time series data. However, the analyzed output changes quickly over time, resulting in misleading ranges for the data corresponding to the hours 6, 13, 19 and 22. A smaller time interval might be used when constructing the boxes to overcome this problem (e.g., 15 minutes).



**Figure 3.27:** Box plot for the heating power demand on January 13.

Figure 3.28 is a contour plot that indicates the probability density. In this way, the probability that the heating power exceeds a certain value can be analyzed. A typical application of this information is critical plant sizing. For this application, the day with the highest peak power is analyzed. Based on the underlying data of Figure 3.28, the probability that the peak power exceeds 23 kW between 7:00 and 7:30 a.m. can be computed.



**Figure 3.28:** Contour plot indicating the probability density for the heating power demand on January 13.

### 3.4 Summary

Different sampling strategies were analyzed with respect to the convergence of the mean and variance estimates and their robustness. The performance of the techniques depends on the number of input parameters ( $k$ ) and the properties of the analyzed model (e.g., nonlinearity). Overall, the sampling based on Sobol' sequences showed the best performance with respect to convergence of the mean and variance estimates. Latin hypercube sampling and stratified sampling resulted also in good convergence. The stratified sampling has restrictions with respect to possible sample sizes, which becomes a limiting aspect when the number of analyzed parameters is high. Comparison of the ECDFs showed that the sampling based on Sobol' sequences has the least variations in the ECDFs. Having the least variation proves that this sampling technique produces the most robust results. It is surmised that the larger the number of analyzed input parameters, the better the sampling based on Sobol' sequences performs in comparison to the other sampling strategies. It is recommended to use sampling based on Sobol' sequences when MC techniques are applied to BPS and the sample size is limited because of computationally expensive

models. Sampling based on Sobol' sequences will be used for all remaining examples in this thesis.

Different ways of conducting a UA were investigated and methods for interpreting the results were introduced. Visualization techniques and statistics can be used to communicate the results of a UA to decision makers. Different methods were applied for stochastic output and for stochastic time series output. These can provide beneficial information for many common BPS problems. A BPS program-independent approach for the parallelization of an MC analysis was developed. The methodology was tested with different examples (simple mathematical model, BPS and a combined BPS and CBA) that are intended to guide people who want to conduct a similar UA. Instead of answering design questions with *yes* or *no*, they can answer using probabilities. This increases the transparency in the design process and avoids a false sense of validity and engineering rigor.

The different steps of a UA that were introduced require a toolchain<sup>30</sup> to conduct the analysis. This toolchain consists of several R scripts and has been developed as part of the work for this thesis. For the applicability of the proposed methodology in practice, it is a prerequisite that a UA can be set up in a reasonable time for a variety of BPS problems. Furthermore, a methodology for UA for combined BPS and CPA was introduced. To summarize, the main findings are:

- (I) Sampling based on Sobol' sequences results in rapid convergence and robust results. The sample size for which convergence is reached can not be computed *a priori*. Hence, a convergence test should be part of every MC simulation.
- (II) Parallelization of the MC simulation and advances in computer technology improve the applicability of the proposed approach.
- (III) The introduced framework with tools and methods allows for UA that can be set up quickly. Given the additional insights provided by a UA, this additional effort compared to a classic BPS is reasonable.
- (IV) Methods for result analysis and interpretation have to be selected in accordance with the project requirements. In this context, it is also important to take the knowledge of the audience of the result presentation into account and to guide people without or with limited experience in statistics.
- (V) UA provides insights on the likely variation of the simulation results and common design questions can be answered with probabilities, taking uncertain boundary conditions into account.
- (VI) Stochastic time series output can be used for realistic plant dimensioning despite uncertainty in the inputs.

---

<sup>30</sup>Toolchain refers to a series of scripts that are used to implement the methodology.

- (VII) A way of combining BPS and CBA was presented. A UA for both provides insight into the probabilities concerning a cost-effective design and supports decision-making.



# 4 Sensitivity Analysis

## 4.1 Background and Objectives

### 4.1.1 Literature Review

Sensitivity analysis (SA) can help to validate and calibrate models, identify critical regions in the input parameter space, uncover research requirements and support model simplifications (Saltelli et al., 2008, p. 11). Generally SA methods can be classified as local or global methods. Global methods can be further subdivided into qualitative or quantitative methods. The result of a qualitative SA can be a ranking according to the influence of the investigated parameters on the simulation result or a plot that provides insight on the influence of the analyzed parameters. A quantitative SA provides the percentage of the total uncertainty that can be attributed to the different model parameters as a result. Quantitative methods are commonly computationally more expensive than qualitative methods.

In the following Section, different methods for performing SA are introduced and analyzed with respect to their applicability to BPS<sup>1</sup>. The literature review is divided according to the classification mentioned above. The different methods are briefly explained and BPS-related studies that employ a specific method are introduced.

#### 4.1.1.1 Local Methods

Local methods investigate a local range around a base point in the parameter space and the corresponding change in the output. The methods are widely used for SA (Saltelli et al., 2008, p. 11). This is also true for building research and practice (Mara and Tarantola, 2008). In cases where the model input is uncertain, analysis around a base point is a strong limitation, because this base point and hence the parameter space region of interest might not be known.

#### Derivative-Based Methods

In a mathematical sense, the local sensitivity of an output  $Y_i$  versus an input  $X_i$  is the partial derivative  $\partial Y_i / \partial X_i$  (Saltelli et al., 2008, p. 11). Computing these

---

<sup>1</sup>Note that many more methods exist. However, the author believes that the introduced methods include those which are most relevant to BPS.

derivatives algebraically requires that the model is an explicit algebraic equation. This might not be the case for typical BPS problems (Wetter, 2008, p. 8; Jacob, 2012, p. 101).

A partial derivative for a model is commonly expressed in units which depend on the choice of units for the output and the input of the model (e.g., kWh/K when the influence of a temperature set point on the annual energy consumption is analyzed.). This leads to the problem that the results of the analysis are difficult to compare when units for different quantities are involved. A ranking according to the influence requires normalization of the SA measures.

Rao and Haghghat (1993) perform a derivative-based SA for a multi-zone airflow model. They point out that their approach has advantages with respect to the computational expense when compared to other SA techniques. However, they illustrate the problems of this approach when applied to nonlinear models.

### One-at-a-time methods

In the literature, one-at-a-time (OAT) methods for SA can often be found (Saltelli and Annoni, 2010). The traditional OAT method has similar capabilities to the derivative-based method<sup>2</sup> but does not require analytical computation of the derivative. Instead, the analyzed parameters are varied from their nominal value (i.e., base point) to another value. If this variation is small, OAT is a local method<sup>3</sup>. This is done consecutively while all other parameters are set to their nominal value (Saltelli and Annoni, 2010). The estimator for the partial derivatives is  $\Delta Y_i / \Delta X_i$ .

The OAT design is illustrated by the following matrices

$$\mathbf{M}_{\text{in}} = \begin{bmatrix} x_1^{(0)} & x_2^{(0)} & \cdots & x_{k-1}^{(0)} & x_k^{(0)} \\ x_1^{(1)} & x_2^{(0)} & \cdots & x_{k-1}^{(0)} & x_k^{(0)} \\ x_1^{(0)} & x_2^{(1)} & \cdots & x_{k-1}^{(0)} & x_k^{(0)} \\ \vdots & \vdots & \ddots & \vdots & \vdots \\ x_1^{(0)} & x_2^{(0)} & \cdots & x_{k-1}^{(1)} & x_k^{(0)} \\ x_1^{(0)} & x_2^{(0)} & \cdots & x_{k-1}^{(0)} & x_k^{(1)} \end{bmatrix} = \begin{bmatrix} 0 & 0 & \cdots & 0 & 0 \\ 1 & 0 & \cdots & 0 & 0 \\ 0 & 1 & \cdots & 0 & 0 \\ \vdots & \vdots & \ddots & \vdots & \vdots \\ 0 & 0 & \cdots & 1 & 0 \\ 0 & 0 & \cdots & 0 & 1 \end{bmatrix}$$

---

<sup>2</sup>The result of an OAT method is an approximation to the partial derivative  $\partial Y_i / \partial X_i$ .

<sup>3</sup>In cases where the variation is larger, it is not a local method anymore.

$$\mathbf{M}_{\text{out}} = \begin{bmatrix} y^{(0)} \\ y^{(X_1)} \\ y^{(X_2)} \\ \vdots \\ y^{(X_{k-1})} \\ y^{(X_k)} \end{bmatrix}$$

where a 0 in the input matrix ( $\mathbf{M}_{\text{in}}$ ) indicates that the parameter has its nominal value and a 1 indicates that it is perturbed. The output matrix ( $\mathbf{M}_{\text{out}}$ ) contains the corresponding results. The sensitivity of a parameter  $X_i$  is (Spitler et al., 1989)

$$\frac{\Delta Y_i}{\Delta X_i} = \frac{y^{(0)} - y^{(X_i)}}{x_i^{(0)} - x_i^{(1)}}. \quad (4.1)$$

This ratio is often called the influence coefficient. It can be normalized to allow comparability between different analyzed parameters (e.g., % output change/% input change) (Spitler et al., 1989). OAT methods do not capture the interactions between the input parameters and are not suitable for global investigations of nonlinear models (Saltelli and Annoni, 2010). Figure 4.1 shows a three-dimensional parameter space and the points for which a model is evaluated in an OAT SA.

Spitler et al. (1989) present an OAT SA for residential buildings. They approximate the partial derivatives with an OAT design and call the results for the investigated parameters influence coefficients. They use the BPS program BLAST and introduce methods to normalize the influence coefficients. Furthermore, Spitler et al. (1989) point out limitations when this method is used for nonlinear models but for their case study they state that the introduced error is acceptable.

Lam and Hui (1996) perform an SA for office buildings in Hong Kong and follow Spitler et al. (1989) in the use of influence coefficients. They employ DOE-2 as the BPS program and use influence coefficients with units and normalized influence coefficients. They analyze the influence of about 60 different parameters on the annual electricity consumption and peak electricity demand. The most influential parameters are the occupancy density, lighting load, summer thermostat set point, supply fan efficiency, fan static pressure, coefficient of performance (COP) of the chillers, chilled water supply temperature, chilled water design temperature difference and chilled water pump efficiency. Lam and Hui (1996) point out that the estimated error of the result is obtained by multiplying the estimated error in the input by the influence coefficient.

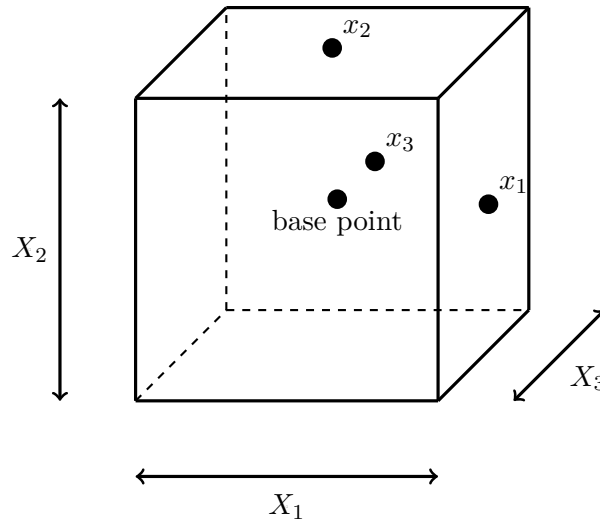


**Figure 4.1:** OAT design in a three-dimensional parameter space. This design would require 4 model runs (indicated by the filled circles).

It is obvious that the implementation of an OAT method is straightforward and can be performed with any BPS program without employing additional software. That might be one reason why OAT is popular among practitioners despite the mentioned shortcomings. Another reason might be the lack of simple tools and methodologies which are applicable to a wide range of different BPS problems.

### Factorial Design

Full factorial design is a suitable method for SA when the number of parameters is small. The required sample size is

$$N = l^k \quad (4.2)$$

where  $l$  is the number of levels each parameter can take and  $k$  is the number of investigated parameters (Saltelli et al., 2008, pp. 71-72). In most cases, two levels are used for full factorial designs when  $k$  is high because higher-level designs<sup>4</sup> are too computationally expensive (Saltelli et al., 2008, p. 72). According to Equation 4.2, a two-level design for 10 parameters results in  $2^{10} = 1,024$  simulation runs and 20 parameters require  $2^{20} = 1,048,576$  simulation runs. Figure 4.2 shows a full factorial design in a three-dimensional parameter space.

The main effect ( $ME_i$ ) of a factorial design can be calculated by subtracting the average result of all simulation runs for which  $X_i$  was at its low level ( $\bar{Y}^-$ ) from the

<sup>4</sup>When more than two levels are used for factorial design it is not a local method anymore.

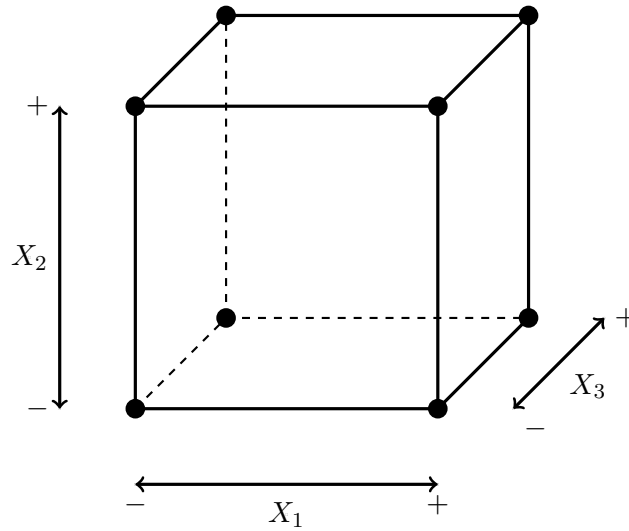


**Figure 4.2:** Full factorial design in a three-dimensional parameter space. This design would require 8 model runs (indicated by the filled circles).

average result of all simulation runs for which  $X_i$  was at its high level ( $\bar{Y}^+$ ) (see Equation 4.3; Box et al., 2005, pp. 178-181).

$$ME_i = \bar{Y}^+ - \bar{Y}^- \quad (4.3)$$

It is also possible to compute higher-order interactions (i.e., interactions between input parameters) (Box et al., 2005, pp. 181-183). This is an advantage of factorial designs compared to OAT methods.

The disadvantage of the high number of required simulations can be reduced by using fractional factorial design. The basis is full factorial design but omitting evaluation at some points. Different fractional factorial designs exist. The reduction of required simulation runs comes at the cost that the analysis loses its power for investigating higher-order effects (i.e., depending on the specific design, some effects are confounded). The interested reader is referred to Box et al., 2005, pp. 235-279 for more details.

Fürbringer and Roulet (1995) compare factorial analysis with an MC method and use a 3-storey building as an example. They focus on air-flow modeling and analyze the influence of 23 parameters with respect to the air exchange in four zones. Fürbringer and Roulet conclude that factorial analysis is superior to the MC method that they used with respect to the computational cost and the inferences that can be drawn from the results.

Langner et al. (2011) performed an SA with a two-level fractional factorial analysis to quantify the influence of building parameters on the energy demand in three commercial high-rise buildings. They perform an SA for four different climate zones (hot and dry, warm and humid, warm and dry, cool and humid) using typical meteorological year (TMY) data. In their study, Langner et al. analyze the influence of 16 parameters with respect to the first-order influence and the second-order influence (i.e., two-factor interactions) on the electricity consumption and demand. They identify the equipment and lighting power density, the chiller efficiency, the window U-values, the mass of the furnishings in the zone and the static pressure of the supply fan as the most influential parameters. The conclusion derived from this study is that these influential parameters should be of special interest during building audits and the calibration process of BPS simulation models.

### 4.1.1.2 Global Methods

In most cases, global methods represent the best choice for conducting an SA for a BPS model because they do not rely on linear models. Instead, the parameter space is analyzed with respect to the corresponding model output. Several different global SA methods exist and are introduced in the following.

#### Scatter Plot Method

On the basis of the results of an MC simulation as described in Chapter 3, a simple SA can be conducted by using graphical methods such as scatter plots. Scatter plots belong to the qualitative category of SA methods. Each sample value and its corresponding result (e.g.  $x_1^{(1)}, y^{(1)}; \dots; x_1^{(N)}, y^{(N)}$ ) is plotted in a scatter plot. Important parameters can be identified by analyzing the pattern in the scatter plots. A uniform cloud of points is an indicator of a non-influential parameter whereas a non-uniform distribution of points indicates an influential parameter (Saltelli et al., 2008, pp. 21-23). Scatter plots can also reveal information about the linearity or nonlinearity of a model. They are only applicable for a limited number of investigated parameters, because each plot has to be visually inspected. Another prerequisite is that a few very important parameters exist that are dominant enough to generate a visible pattern.

#### Elementary Effects Method

The elementary effects (*EE*) method<sup>5</sup> is well suited to screening applications with a moderate computational cost compared to other global methods. Screening aims to identify non-influential model inputs and can result in ranking of the analyzed

---

<sup>5</sup>This method is sometimes also called the Morris method.

parameters. The method was introduced by Morris (1991). In this first version, the input parameters are moved OAT<sup>6</sup> with a step of  $\Delta_i$ . The  $EE$  is calculated according to

$$EE_i(\mathbf{X}) = \frac{Y(x_1, \dots, x_{i-1}, x_i + \Delta_i, x_{i+1}, \dots, x_k) - Y(x_1, \dots, x_k)}{\Delta_i} \quad (4.4)$$

where  $Y(\cdot)$  is the result of the evaluated function at the coordinates indicated within the parentheses and  $\Delta_i$  is the step size in the domain of the input parameter (Campolongo et al., 2011). To explore different regions of the parameter space,  $r$  trajectories are evaluated. The average of the effects ( $\mu_i$ ) is (Campolongo et al., 2011)<sup>7</sup>

$$\mu_i = \frac{\sum_{j=1}^r EE_i(\mathbf{X}^{(j)})}{r}. \quad (4.5)$$

Figure 4.3 illustrates a trajectory for a three-dimensional parameter space.  $k$  is the number of analyzed parameters and each trajectory has  $k + 1$  points that are moved OAT in the analysis (the roman numerals in brackets ( $\mathbf{X}(\text{roman numeral})$ ) indicate the steps of the analysis). In Figure 4.3, the  $EE$  for parameter  $X_1$  is

$$EE_1 = \frac{Y(\mathbf{X}(\text{II})) - Y(\mathbf{X}(\text{I}))}{\Delta_1}.$$

A second measure serves as indicator of parameter interactions and nonlinearity (Campolongo et al., 2011):

$$\sigma_i = \frac{\sum_{j=1}^r (EE_i(\mathbf{X}^{(j)}) - \mu_i)^2}{r} \quad (4.6)$$

The  $EE$  method requires  $r(k + 1)$  simulation runs.

The method is widely applied in BSP research. De Wit and Augenbroe (2002) use the  $EE$  method to screen 89 parameters. They analyze the thermal comfort performance and derive a table with the most influential parameters in decreasing order of their importance. They perform a more detailed UA for these most influential parameters.

Brohus et al. (2009) use the  $EE$  method to screen parameters for a BPS of a residential building. They analyze eleven parameters with the  $EE$  method and conduct a further analysis for the seven most influential ones. One result of the study is that the most influential parameters are related to occupant behavior.

<sup>6</sup>The  $EE$  method is repeated OAT. The repetition resolves the shortcomings of traditional OAT methods.

<sup>7</sup>Note that the notation used by Campolongo et al. (2011) has been slightly modified to make it nonambiguous.

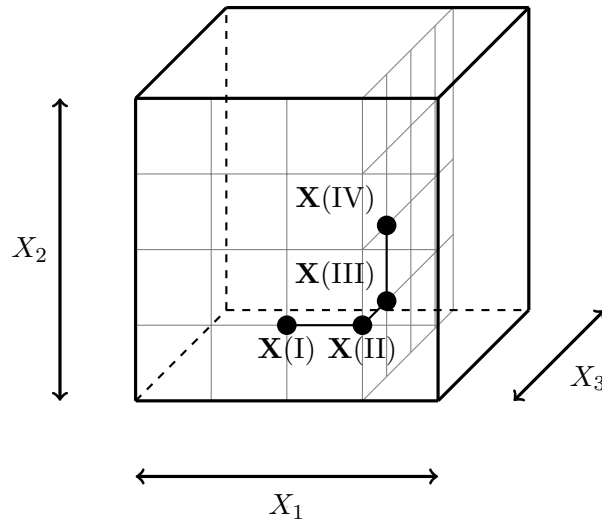


**Figure 4.3:** Example of a trajectory in a three-dimensional parameter space. The filled circles indicate model runs (source: adapted figure based on Campolongo et al. (2011)).

Corrado and Mechri (2009) analyze the influence of 129 input parameters on the result of an energy rating by means of the *EE* method. They use the monthly method of the ISO 13790 standard as their model (ISO 13790, 2008). The parameters with the greatest influence in the study of Corrado and Mechri are the indoor temperature, the air change rate, the number of occupants, the metabolism rate and the equipment heat gains.

### Variance-Based Methods

Employing variance-based (VB) methods allows the exploration of uncertain input parameters over the range of interest<sup>8</sup>. Interactions between uncertain parameters are fully accounted for (Campolongo et al., 2011). The method is independent of the model under consideration<sup>9</sup>. It is based on the idea of analyzing the variance of the result and attributing the variance to the different input parameters (variance decomposition). The result of a complete analysis of variance (ANOVA) can be  $2^k$  sensitivity indices (first order and all higher orders) (Saltelli et al., 2010). These indices are defined as the ratio of the variance of interest to the total variance, where the variance of interest can be the first-order or any higher-order variance. For most

<sup>8</sup>This range is described by the PDFs of the input parameters.

<sup>9</sup>The computational cost of a model is a constraint. However, this can be targeted with efficient sampling techniques and parallel computing (see Chapter 3).

applications, two sensitivity indices per input parameter are sufficient. These are the first-order sensitivity index and the total sensitivity index.

The first-order sensitivity index is defined as

$$S_i = \frac{\text{Var}_{X_i}(\mathbf{E}_{\mathbf{X}_{\sim i}}(Y|X_i))}{\text{Var}(Y)} \quad (4.7)$$

where  $\text{Var}_{X_i}(\cdot)$  is the variance of argument  $(\cdot)$  taken over the parameter  $X_i$ ,  $\mathbf{E}_{\mathbf{X}_{\sim i}}(\cdot)$  is the mean of argument  $(\cdot)$  taken over all parameters except  $X_i$ , and  $Y$  is the model output (Saltelli et al., 2010).  $S_i$  is a normalized measure and can vary between 0 and 1. It expresses the percentage of variance in the result that can be attributed to the variance of parameter  $X_i$ . Hence,  $\text{Var}_{X_i}(\mathbf{E}_{\mathbf{X}_{\sim i}}(Y|X_i))$  is the expected reduction of the variance if  $X_i$  were treated as a single-value estimate (Saltelli et al., 2010). When all  $S_i$  are computed, conclusions on the model properties can be drawn. In general,  $\sum S_i \leq 1$  and if  $\sum S_i = 1$  then the model is additive (i.e., no interactions between input parameters). Furthermore,  $1 - \sum S_i$  can be understood as an indicator of interactions between the input parameters (Mara and Tarantola, 2008).

The total sensitivity index measures the total influence of the analyzed parameter on the result. This includes the first-order and all higher-order effects<sup>10</sup>. It is defined as

$$S_{Ti} = \frac{\mathbf{E}_{\mathbf{X}_{\sim i}}(\text{Var}_{X_i}(Y|\mathbf{X}_{\sim i}))}{\text{Var}(Y)} \quad (4.8)$$

where  $\mathbf{X}_{\sim i}$  is the matrix of all parameters except  $X_i$  (Saltelli et al., 2010). The term  $\mathbf{E}_{\mathbf{X}_{\sim i}}(\text{Var}_{X_i}(Y|\mathbf{X}_{\sim i}))$  is the expected variance that would remain if all parameters apart from  $X_i$  were treated as single-value estimates (Saltelli et al., 2010). Note that,  $\sum S_{Ti} \geq 1$  because the interaction effects are counted for each parameter (Homma and Saltelli, 1996).

Different ways of calculating the sensitivity indices exist. They can be calculated analytically or with the help of estimators within an MC setting. The latter is the relevant approach for typical BPS. With the estimators employed in this thesis, the computational cost<sup>11</sup> is  $N(k + 2)$ . The VB method can be applied to the most influential parameters derived from an SA screening method (e.g., the *EE* method) in cases where VB SA for all parameters costs too much computational power.

Eisenhower et al. (2011) and Mara and Tarantola (2008) use a VB method in combination with a meta-model. Both studies will be described below in Section 4.1.1.4.

<sup>10</sup>The higher-order effects are due to interactions with other model parameters.

<sup>11</sup>More details will be given in the course of this chapter.

### Monte Carlo Filtering

MC filtering (MCF) isolates those inputs of the model realizations of an MC simulation that produce the desired result (Saltelli et al., 2008, pp. 183-185). Hence, the method is used to determine the particular subset of the model parameter space that drives the model output into specific regions. Figure 4.4 illustrates MCF.

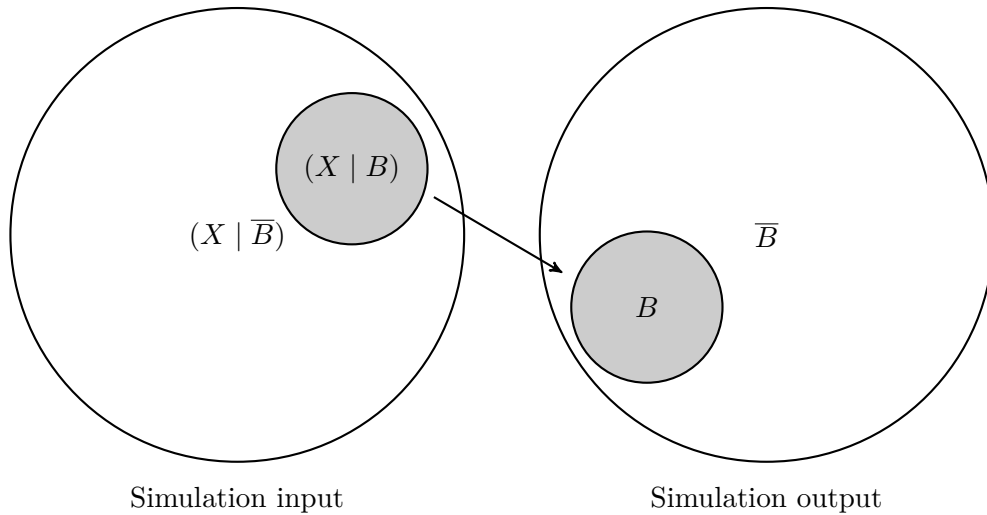


**Figure 4.4:** Mapping of input and output subsets.  $B$  is the desired region of the simulation output and  $(X|B)$  is the subset of the simulation inputs that results in  $B$ . In this example  $(X|B)$  is compact, which might not always be the case, depending on the analyzed simulation (source: own figure based on Saltelli et al., 2008, p. 40).

One ECDF for the full set of simulations, one for the behavioral subset  $(X | B)$  and one for the non-behavioral subset  $(X | \bar{B})$  are plotted for each input parameter. The differences between the ECDFs provide insight on the influence of a parameter in driving the simulation output into a certain region. This application is called regionalized SA (Saltelli et al., 2008, p. 184). The larger the difference between the ECDFs of  $(X | B)$  and  $(X | \bar{B})$ , the greater the influence of the parameter for which the ECDF is constructed. In addition to visual inspection, a Kolmogorov-Smirnov test can provide a quantitative measure of the maximum distance between the ECDFs (see Section 2.2.2.2).

With MCF, it is possible to infer the necessary design and settings of the technical systems that lead to the desired outcome (e.g., annual energy demand less than a certain threshold). This might lead to design improvements as well as to more insights into the building and HVAC characteristics. The computational cost of

MCF depends on the convergence of the MC simulation (see Chapter 3). Although MCF appears to be of high value to supplement the typical building design process, no literature has been found on its application in the BPS context<sup>12</sup>.

#### 4.1.1.3 Group Sampling

In the previous sections, different techniques were introduced, some of which are computationally expensive. The computational expense depends on the number of analyzed parameters ( $k$ ). In cases where ( $k$ ) is too high for a given model and its computational cost, a group sampling technique can be applied. When applying group sampling, all parameters are randomly subdivided into different groups. The input parameters of one group are all treated as one input and perturbed correspondingly. If one group does not have much influence, the analyst can conclude that no parameter within this group is influential. The parameters in the non-influential groups are not analyzed further. All other parameters are randomly assigned to new groups and a new analysis of these groups is conducted. Depending on the number of parameters and the number of groups, the analysis is repeated until the influential parameters have been identified (Saltelli et al., 2008, pp. 89-96). Group sampling works for different SA methods. It can be applied as the first step of an SA if the number of analyzed parameters exceeds the capabilities of an SA method.

Rahni et al. (1997) use group screening to identify 23 influential parameters out of 390 parameters involved in the analysis. They employ the BPS program CLIM 2000 for the simulation of a test-cell building and use a regression model for the SA. The analyzed model output is the indoor air temperature.

#### 4.1.1.4 Meta-Models

As mentioned above, many BPS models are computationally expensive. Therefore it is appealing to construct a meta-model for the original model. This meta-model aims to be computationally cheaper. Once a reliable meta-model has been identified, the analysis can be performed with this less computationally demanding meta-model. The prerequisite for fitting a meta-model is data. This data can be obtained from measurements or from an MC simulation. Different ways to construct meta-models exist. Local approximation methods (e.g., Taylor series) aim to fit a function that matches for data points at a base point and in the nearby region. Interpolation methods are used to find a function (i.e., polynomial and its coefficients) that represents all data points and the region between data points for the entire domain of the data. Regression and smoothing methods are used to fit models for many

---

<sup>12</sup>An exception is a paper that was published in the framework of this thesis (Burhenne et al., 2013a).

data points (Saltelli et al., 2008, p. 212). However, a meta-model is an approximation of another model. This introduces an error and hence uncertainty into the meta-model predictions. When MC simulations are used to produce the data for which the meta-model is constructed, the convergence of the MC simulation is very important to avoid incorrect analysis. In principle, all SA methods can be applied for a meta-model-based analysis.

Mara and Tarantola (2008) perform an SA using a meta-model-based technique. They use LHS to generate the samples and fit a polynomial to the MC result. Mara and Tarantola (2008) use this polynomial to compute the first-order sensitivity indices.

Eisenhower et al. (2011) conducted a meta-model-based SA for a non-residential building modeled with EnergyPlus. They use a response surface as a meta-model that is constructed by support vector regression using Gaussian kernels. Eisenhower et al. analyzed 1,009 parameters in their study and use the total sensitivity based on the derivatives of the meta-model. They state that in their experience, BPS models are primarily additive<sup>13</sup> (i.e., no interactions between parameters).

A disadvantage of using the meta-model technique is that it requires a new model in addition to an existing model. In most cases, analysts are familiar with BPS models and know the underlying concepts and physical equations. A meta-model might employ concepts with which the analyst is not familiar. This can lead to misinterpretation of the model and its results. Furthermore, separate validation of the meta-model might become necessary.

### 4.1.2 Objectives

The most general and most applicable methods for BPS will be selected from the introduced methods. The criteria are the applicability for typical BPS problems with respect to computational costs, the effort required to set up the analysis and additional inferences compared to a classical BPS. The developed methodology will be demonstrated by means of a case study to analyze its performance and guide practitioners.

## 4.2 Methodology

Different SA methods were introduced in Section 4.1. In general, different SA applications can be distinguished (Saltelli et al., 2008, pp. 156-157):

- (I) **Factor<sup>14</sup> prioritization (FP)** is the identification of the most influential factors and often results in ranking according to the influence of the parame-

---

<sup>13</sup>This will be analyzed in the course of this thesis.

<sup>14</sup>Saltelli et al. (2008) use "factor" when they refer to a model input parameter.

ters on the result. This can be used to identify research needs, decide which parameters have to be handled with care because of their influence and which input parameter uncertainty needs to be reduced to reduce the uncertainty in the results.

- (II) **Factor fixing (FF)** is the opposite of FP. The aim is to identify non-influential parameters. The result of FF can be the identification of parameters that are not further analyzed in a subsequent SA. Furthermore, this SA application is helpful when models are to be simplified without losing accuracy.
- (III) **Variance cutting (VC)** aims to reduce the variance of the result. Hence, the amount of variance that is caused by an input needs to be quantified. This SA application can be valuable in risk analysis to identify the required boundary conditions for a system to be operated without errors or failure.
- (IV) **Factor mapping (FM)** identifies the regions of model parameter space that produce the desired result. The desired result is often defined by a threshold.

A single method that is applicable for all SA applications does not exist. However, each of the SA applications can be interesting in a BPS context. Furthermore, the computational expense of a model might introduce restrictions affecting the method selection. Therefore, the methodology developed in the course of this chapter involves different methods. Some methods are suitable for only one SA application and others are useful for more applications. Given common BPS problems and their structure, only global methods are the focus of this thesis. Table 4.1 summarizes the findings concerning global SA methods from the literature review and illustrates the capabilities of the introduced methods. Furthermore, it is specified for which SA applications the methods can be used.

**Table 4.1:** Overview SA methods (source: partly based on Saltelli et al., 2008, p. 273).

Method	SA application	Computational cost	Higher order effects	Non-linearity
Scatter plots	FM	low	yes	yes
Elementary effects	FF	low	yes	yes
Variance-based	FP, FF, VC	high	yes	yes
MC filtering	FM	low	yes	yes

The most appropriate SA methods for BPS are further analyzed and combined into an overall methodology in the following. The scatter plot method is part of the methodology because it can provide a first impression concerning model structure and sensitivities. Furthermore, its implementation is a straightforward procedure on the basis of the MC results obtained in a UA. The variance-based method is selected because of its general applicability for different SA applications. The *EE* method is used for screening purposes (i.e., FF application) when the use of the VB method is not possible because of a large number of analyzed parameters and computationally expensive models. The MCF method is selected to be part of the methodology because it provides valuable FM insights. Group sampling and meta-models can potentially be used in combination with all SA methods. However, given the structure and the capabilities of the proposed methodology, their usage may not be necessary. Therefore these techniques are not further analyzed in this thesis.

#### 4.2.1 Scatter Plot Method

The scatter plot method as introduced in Section 4.1 can be extended to allow easier interpretation. Saltelli et al. describe a method called *Conditional Variances – Second Path* to supplement scatter plot results (Saltelli et al., 2008, pp. 21-23). Its implementation is a straightforward process and it requires only one MC simulation as used for the UA in Chapter 3. To illustrate the method, the following generic model is introduced:

$$Y = f(X_1, X_2, \dots, X_k) \quad (4.9)$$

As already mentioned, an influential model input is identified in a scatter plot by the existence of a shape or pattern in the points.

The following steps have to be conducted for each parameter  $X_i$ :

- (I) The range of  $X_i$  is divided into several slices (each slice has an equal number of points)<sup>15</sup>.
- (II) The mean value of  $Y(X_i)$  is determined in each slice (see Equation 2.2). The mean value for each slice is plotted in the scatter plot with a different color to aid the visual inspection.
- (III) The variance of the mean values of  $Y(X_i)$  over all slices is calculated (see Equation 2.3).

The mean values of  $Y(X_i)$  allow easier identification of a pattern. The calculated variance is used as a sensitivity measure of parameter importance. The higher the

---

<sup>15</sup>The number of slices is on the order of ten. It should be selected depending on  $N$  to ensure an equal number of points in each slice.

variance, the more influential is the parameter investigated. This information can be used to obtain an initial ranking of the analyzed parameters. This approach applies the same underlying concept as the variance-based method (Saltelli et al., 2008, pp. 160-161). However, parameter rankings based on the VB method should be preferred because they are more accurate.

#### 4.2.2 Elementary Effects Method

The basics of the *EE* method have been presented in Section 4.1. The original *EE* method has been extended and improved by several researchers. In the context of this thesis, an improved design is used that is proposed by Campolongo et al. (2011). Campolongo et al. (2011) showed by numerical experiments with five different test functions that this design is superior to other designs for the *EE* method. It is based on so-called radial sampling instead of the trajectory-based design of the original *EE* method. Figure 4.5 illustrates a radial design.

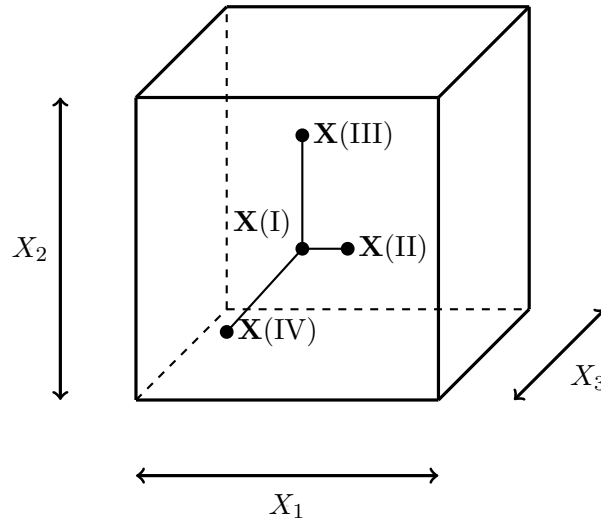


**Figure 4.5:** Example of a radial sample in a three-dimensional parameter space. The filled circles indicate model runs and the roman numerals in brackets ( $\mathbf{X}(\text{roman numeral})$ ) are the row numbers of the block as shown in Figure 4.6 (source: adapted figure based on Campolongo et al. (2011)).

The basis of the design are two sampled matrices  $\mathbf{A}$  and  $\mathbf{B}$  (Figure 4.6 ①) with  $a_{ji}$  and  $b_{ji}$  ( $j$  indicates the row number and  $i$  the column number) as elements. The values of these matrices are used to construct the radial design for the *EE* method. Each block ( $r$ ) contains the coordinates of one radial in the parameter space (Figure 4.6 ②). The number of rows in each block (i.e., number of points in the parameter

space that are evaluated) is  $k + 1$ . Typically  $r$  is in the range of 4-8 (Campolongo et al., 2011). The required number of simulations for this version of the  $EE$  method is  $r(k + 1)$  as for the original version.

One result is obtained for each row of the blocks (Figure 4.6 ③). The  $EE_i$  are calculated on the basis of the parameter values of the blocks and these results.

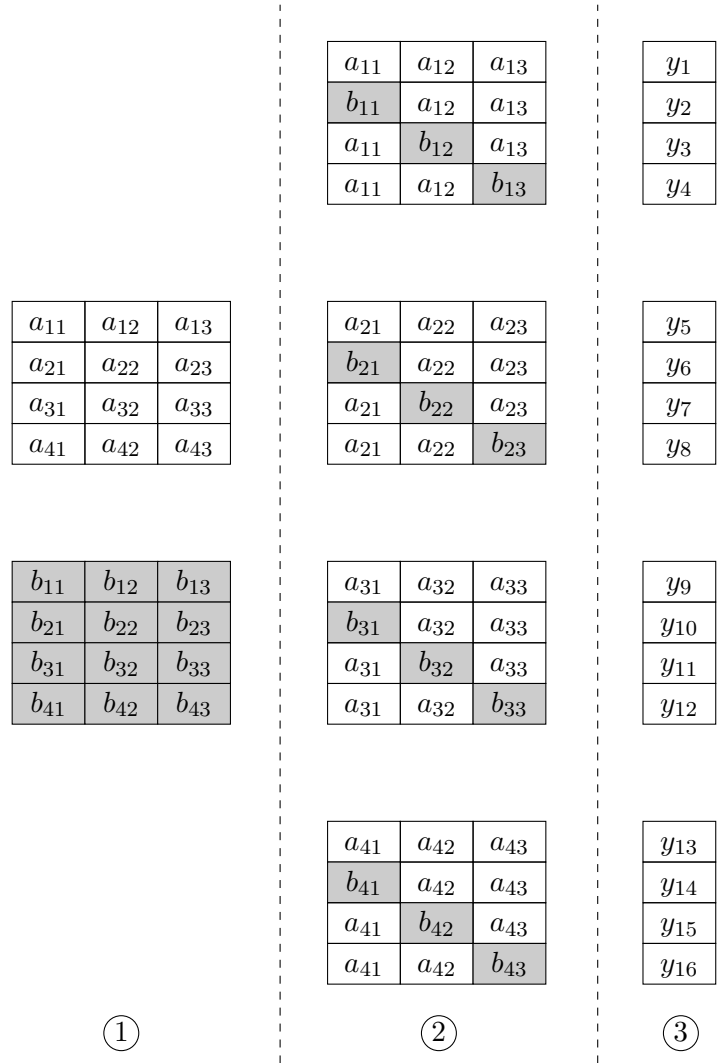


**Figure 4.6:** Radial design for the elementary effects method.

Campolongo et al. (2011) change the calculation of  $\mu_i$  slightly by using the absolute

value of  $EE_i$  and call the statistic  $\mu_i^*$  (see Equation 4.10)<sup>16</sup>. This adjustment allows application of the  $EE$  method to non-monotonic models.

$$\mu_i^* = \frac{\sum_{j=1}^r |EE_i(\mathbf{X}^{(j)})|}{r} \quad (4.10)$$

In Figure 4.5 it can be seen that the distance between the points varies. This is different to the original  $EE$  method, where  $\Delta_i$  is constant. Therefore, the  $EE_i$  have to be calculated differently than for the original design (Campolongo et al., 2011). As an example, the  $EE_i$  of the parameter in the first column (e.g., for parameter  $X_1$ ) in Figure 4.6 are calculated (the superscript in brackets  $EE_i(\mathbf{X}^{(\text{superscript})})$  is the block number):

$$\begin{aligned} |EE_1(\mathbf{X}^{(1)})| &= \left| \frac{y_2 - y_1}{b_{11} - a_{11}} \right| \\ |EE_1(\mathbf{X}^{(2)})| &= \left| \frac{y_6 - y_5}{b_{21} - a_{21}} \right| \\ |EE_1(\mathbf{X}^{(3)})| &= \left| \frac{y_{10} - y_9}{b_{31} - a_{31}} \right| \\ |EE_1(\mathbf{X}^{(4)})| &= \left| \frac{y_{14} - y_{13}}{b_{41} - a_{41}} \right| \end{aligned}$$

As explained in Section 3.2.1, the samples can be drawn by using sampled numbers in the interval  $[0,1]$  and transforming them with an inverse cumulative distribution function into any desired range. If this is the case, the basis of the values for all  $x$  needs to be the values before the transformation (i.e., the values in the interval  $[0,1]$ ).

For the calculation of  $\sigma_i$ ,  $\mu_i$  is replaced by  $\mu_i^*$  (Equation 4.11).

$$\sigma_i = \frac{\sum_{j=1}^r (EE_i(\mathbf{X}^{(j)}) - \mu_i^*)^2}{r} \quad (4.11)$$

The results can be presented graphically by plotting  $\mu_i$  against  $\sigma_i$ . In this plot, a line can be drawn that is defined as

$$\mu_i^* = \pm 2 \frac{\sigma_i}{\sqrt{r}}. \quad (4.12)$$

Points above this line indicate that the analyzed parameter is involved in interactions with other parameters or the model contains nonlinear effects (de Wit and Augenbroe, 2002).

---

<sup>16</sup>Note that the notation used by Campolongo et al. (2011) has been slightly modified to make it nonambiguous.

### 4.2.3 Variance-Based Method

The principles of the VB method were introduced in Section 4.1. It is the most general SA method and can be applied for three SA applications (i.e., FP, FF and VC). FP is linked to the first-order sensitivity indices ( $S_i$ ) and FF and VC are linked to the total sensitivity indices ( $S_{Ti}$ ) (Saltelli et al., 2008, pp. 42-45). In the following, the details of the variance decomposition are briefly introduced<sup>17</sup>. The basis is the functional decomposition of a square-integrable function

$$Y = f(X_1, X_2, \dots, X_k) \quad (4.13)$$

over the  $k$ -dimensional unit hypercube ( $\Omega$ ) (Saltelli et al., 2010). Furthermore, all  $X_i$  are uniformly distributed over the interval  $[0,1]$ . The decomposition of this function into a sum of functions is

$$f = f_0 + \sum_i f_i + \sum_i \sum_{j>i} f_{ij} + \dots + f_{12\dots k} \quad (4.14)$$

where  $f_i = f_i(X_i)$ ,  $f_{ij} = f_{ij}(X_i, X_j)$  etc. for all  $2^k$  terms including  $f_0$  (Saltelli et al., 2010). The functions are

$$\begin{aligned} f_0 &= E(Y) \\ f_i &= E_{\mathbf{X}_{\sim i}}(Y|X_i) - E(Y) \\ f_{ij} &= E_{\mathbf{X}_{\sim ij}}(Y|X_i, X_j) - f_i - f_j - E(Y) \end{aligned} \quad (4.15)$$

etc. for higher orders (Saltelli et al., 2010). The relations between these functions and the partial variances are

$$\begin{aligned} \text{Var}_i &= \text{Var}(f_i(X_i)) = \text{Var}_{X_i}(E_{\mathbf{X}_{\sim i}}(Y|X_i)) \\ \text{Var}_{ij} &= \text{Var}(f_{ij}(X_i, X_j)) \\ &= \text{Var}_{X_i X_j}(E_{\mathbf{X}_{\sim ij}}(Y|X_i, X_j)) - \text{Var}_{X_i}(E_{\mathbf{X}_{\sim i}}(Y|X_i)) - \text{Var}_{X_j}(E_{\mathbf{X}_{\sim j}}(Y|X_j)) \end{aligned} \quad (4.16)$$

etc. for higher order terms (Saltelli et al., 2010). All terms are linked by (Saltelli et al., 2010)

$$\text{Var}(Y) = \sum_i \text{Var}_i + \sum_i \sum_{j>i} \text{Var}_{ij} + \dots + \text{Var}_{12\dots k}. \quad (4.17)$$

By dividing both sides of Equation 4.17 by  $\text{Var}(Y)$  one obtains (Saltelli et al., 2010)

$$1 = \sum_i S_i + \sum_i \sum_{j>i} S_{ij} + \dots + S_{12\dots k}. \quad (4.18)$$

---

<sup>17</sup>For more details, the interested reader is referred to Saltelli et al. (2010).

The relations for the higher-order terms in Equations 4.14-4.18 only hold if the parameters are independent (Saltelli et al., 2010). As mentioned in Section 4.1, the first-order ( $S_i$ ) and total ( $S_{T_i}$ ) sensitivity indices are sufficient for most common analyses. Therefore this thesis focuses on these two sensitivity indices. Several estimators and different experimental set-ups for these two estimators exist. A performance comparison of different designs can be found in Saltelli et al. (2010). For brevity, only the design and the estimators with the best performance are introduced in the following. Figure 4.7 provides an overview of the experimental set-up. Similarly to the *EE* method, two sampled matrices  $\mathbf{A}$  and  $\mathbf{B}$  are used as the basis for the experimental design (Figure 4.7 ①). The elements of these matrices are used to construct other matrices that contain the simulation inputs. These matrices are called  $\mathbf{A}_B^{(i)}$ . In the  $\mathbf{A}_B^{(i)}$  matrices, all columns are from matrix  $\mathbf{A}$  except the column  $i$  that is from matrix  $\mathbf{B}$  (Figure 4.7 ②).

The equations for  $S_i$  and  $S_{T_i}$  were introduced in Section 4.1 (Equations 4.7 and 4.8). Estimators for  $\text{Var}_{X_i}(\text{E}_{\mathbf{X}_{\sim i}}(Y|X_i))$  and  $\text{E}_{\mathbf{X}_{\sim i}}(\text{Var}_{X_i}(Y|\mathbf{X}_{\sim i}))$  are required to compute the sensitivity indices. These are (Saltelli et al., 2010)

$$\text{Var}_{X_i}(\text{E}_{\mathbf{X}_{\sim i}}(Y|X_i)) = \frac{1}{N} \sum_{j=1}^N f(\mathbf{B})_j \left( f(\mathbf{A}_B^{(i)})_j - f(\mathbf{A})_j \right) \quad (4.19)$$

and

$$\text{E}_{\mathbf{X}_{\sim i}}(\text{Var}_{X_i}(Y|\mathbf{X}_{\sim i})) = \frac{1}{2N} \sum_{j=1}^N \left( f(\mathbf{A})_j - f(\mathbf{A}_B^{(i)})_j \right)^2. \quad (4.20)$$

The variance-based method requires  $N(k+2)$  simulations, with  $N$  being the MC sample size and  $k$  the number of analyzed parameters.

#### 4.2.4 Monte Carlo Filtering

MCF was introduced in Section 4.1. In the following, more information on the details is provided. Performing MCF consists of the following steps (Saltelli et al., 2008, pp. 39-40):

- (I) Separating the MC simulation output and the corresponding simulation inputs into two subsets. One is the behavioral subset (i.e., where the desired design goal is reached;  $B$ ) and the remaining is the non-behavioral subset (i.e., where the desired design goal is not reached;  $\bar{B}$ ).
- (II) Plotting the ECDFs for each input parameter for the full set of simulations, the behavioral subset and the non-behavioral subset.
- (III) Comparing the plots and performing a visual inspection of the difference in the ECDFs.

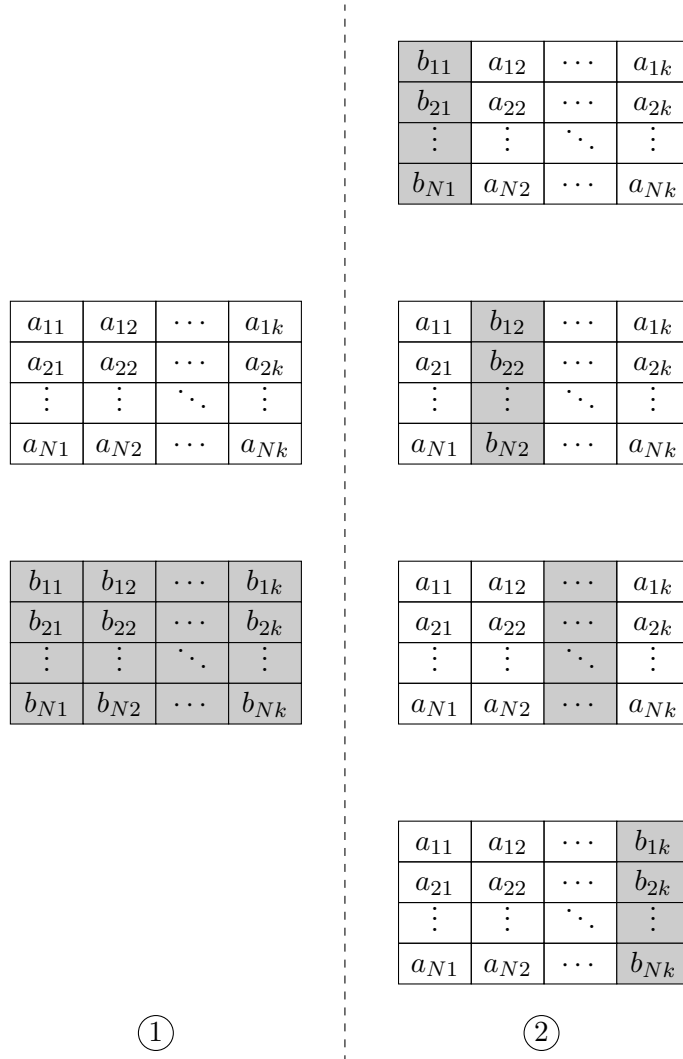


**Figure 4.7:** Experimental design for the variance-based method.

- (IV) Performing a Kolmogorov-Smirnov test (two-sided) to compare the two subsets for each analyzed parameter.

If the ECDFs are visually different and the maximum difference between the two cumulative distributions computed by the Kolmogorov-Smirnov test is large, the analyzed simulation parameter is influential in driving the simulation output into certain regions. This maximum difference is

$$D_{X_i} = \max \left| F(X_i | B) - F(X_i | \overline{B}) \right| \quad (4.21)$$

where  $F(X | B)$  is the ECDF of the behavioral subset and  $F(X | \overline{B})$  is the ECDF of the non-behavioral subset (Saltelli et al., 2008, pp. 184-189). Furthermore, the EDCFs provide insight on the maximal and the minimal values of the results for the complete set, the behavioral subset and the non-behavioral subset.

#### 4.2.5 Overall Sensitivity Analysis Methodology

All SA methods are implemented in R. The implementation is based on the R scripts described in Section 3.2.2. The scripts are extended<sup>18</sup> to allow the generation of the matrices that are required for the *EE* method and the *VB* method (see Figure 4.6 and Figure 4.7). Furthermore, the script that collects the results from the subfolders (`CollectResults.R`) is extended and computes the estimators as described in the previous sections.

Figure 4.8 is a flow chart for conducting an SA for a BPS according to the proposed methodology. The start of an SA is the definition of the outcome and the requirements of the analysis. This can be based on an agreement between the modeler and the client. Based on these requirements the relevant SA applications (i.e., FP, FF, VC and FM) can be identified. Depending on the relevant SA applications some steps of the analysis might be skipped. Sometimes the required applications cannot be selected *a priori*. In these cases the SA can be terminated once the requirements are fulfilled.

#### 4.2.6 Case Study

The case study presented in Chapter 3 focused on building design. The analysis in the following example demonstrates how SA can support the energy-efficient operation of buildings. In this case study, an approach to implement energy-saving measures using the proposed SA methodology with a BPS model and data analysis of measured data from the building is proposed. The building that is analyzed is a large non-residential building<sup>19</sup> for which detailed measurements are available. The SA methodology that was introduced in the previous sections is used to determine those parameters and variables that influence the building's heating energy consumption most. This information is employed to improve building operation. Furthermore, the MC simulations of the building are used to calculate potential energy savings for operational improvements and the corresponding uncertainty. One energy-saving measure is implemented in the real building and the result of the implementation is analyzed using measured data.

<sup>18</sup>The scripts were partly developed in cooperation with Olga Tsvetkova (Tsvetkova, 2011).

<sup>19</sup>The building served as a demonstration building in the Building EQ project (Neumann and Jacob, 2010).

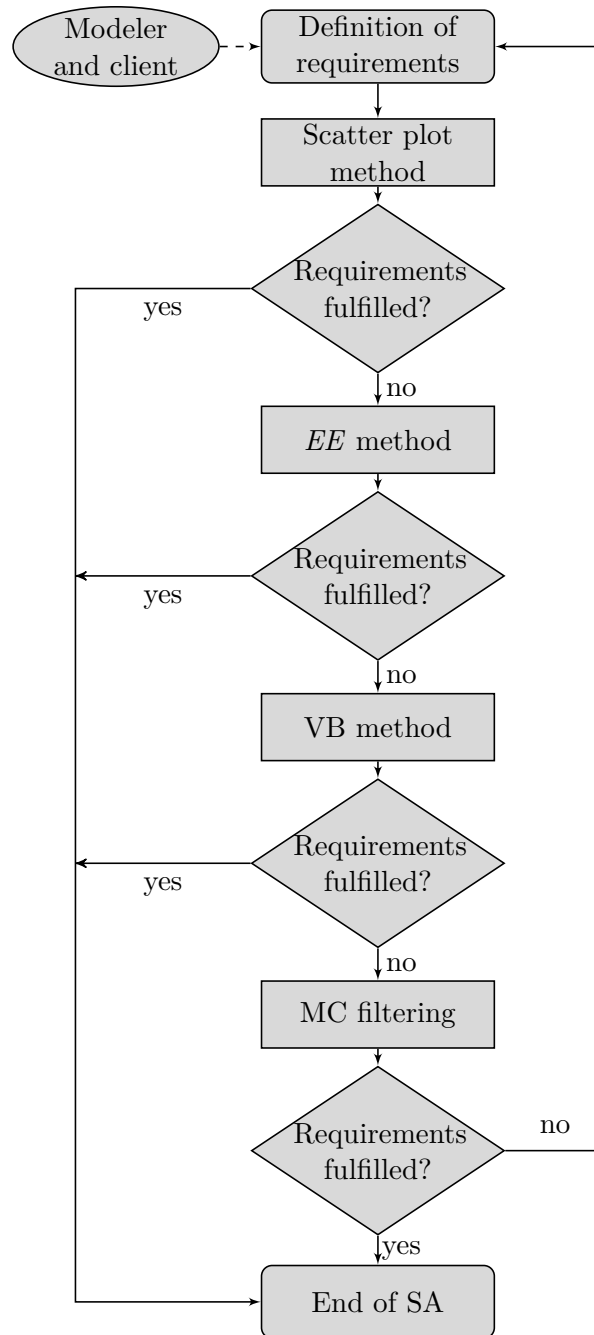


**Figure 4.8:** Flow chart of the SA methodology.

In Figure 4.9, the structure of the proposed application of the SA methodology to improve building operation is illustrated. Influential parameters are identified with the SA methodology and based on this information, building operation strategies are developed. The decision about which operational changes should be implemented can depend on the budget, building-specific requirements, realizable savings<sup>20</sup> etc. A UA is conducted to analyze the saving potential due to the improved control strategy, and the corresponding uncertainty. Therefore, two additional MC simulations are made (i.e., one MC simulation with the improved control strategy and one with the old strategy). On the basis of these MC simulations, the potential energy savings and the corresponding uncertainty are analyzed. Depending on the results, the improved control strategy can be implemented in the building. The final step is to analyze the measurements to verify the heating energy savings.

The building simulated is a typical German office building of the 1980's. About 90% of the rooms are used as offices, mostly single-occupant offices. The building is equipped with sensors (e.g., outdoor temperature, heating energy consumption, room temperatures, control signals, solar irradiance) to allow validation of the simulation. The main building parameters are shown in Table 4.2 and Figure 4.10 is a floor plan of the building. The heat is emitted by radiators equipped with thermostatic valves. Some rooms are cooled by split units and one simulation zone has an air handling unit (AHU) with heat recovery and a heating coil. The heating energy is provided by a district heating system.

**Table 4.2:** Building parameters.

Parameter	Value	Unit
$\frac{A}{V}$ (envelope area to volume ratio)	0.28	$\frac{\text{m}^2}{\text{m}^3}$
$\bar{U}$ -value (mean U-value)	0.74	$\frac{\text{W}}{\text{m}^2\text{K}}$
$A_{\text{win}}$ (total window area)	3,102	$\text{m}^2$
$A_{\text{NFA}}$ (net floor area)	21,117	$\text{m}^2$

For SA, appropriate but simple models for BPS are often better suited than very detailed and hence computationally expensive models. For this case study, a resistance-capacity network is used to model the building. The model was developed within the framework of a Bachelor thesis (Elci, 2010). In this model, a wall is modeled with three thermal resistances and two thermal capacitances. Heat gains (e.g., gains from appliances, occupants, HVAC equipment etc.) are distributed to the different temperature nodes (e.g., air temperature and surface temperature nodes) of the model. The building envelope model is a simplified version of the

<sup>20</sup>The methodology for combined BPS and CBA could be also applied in this context.

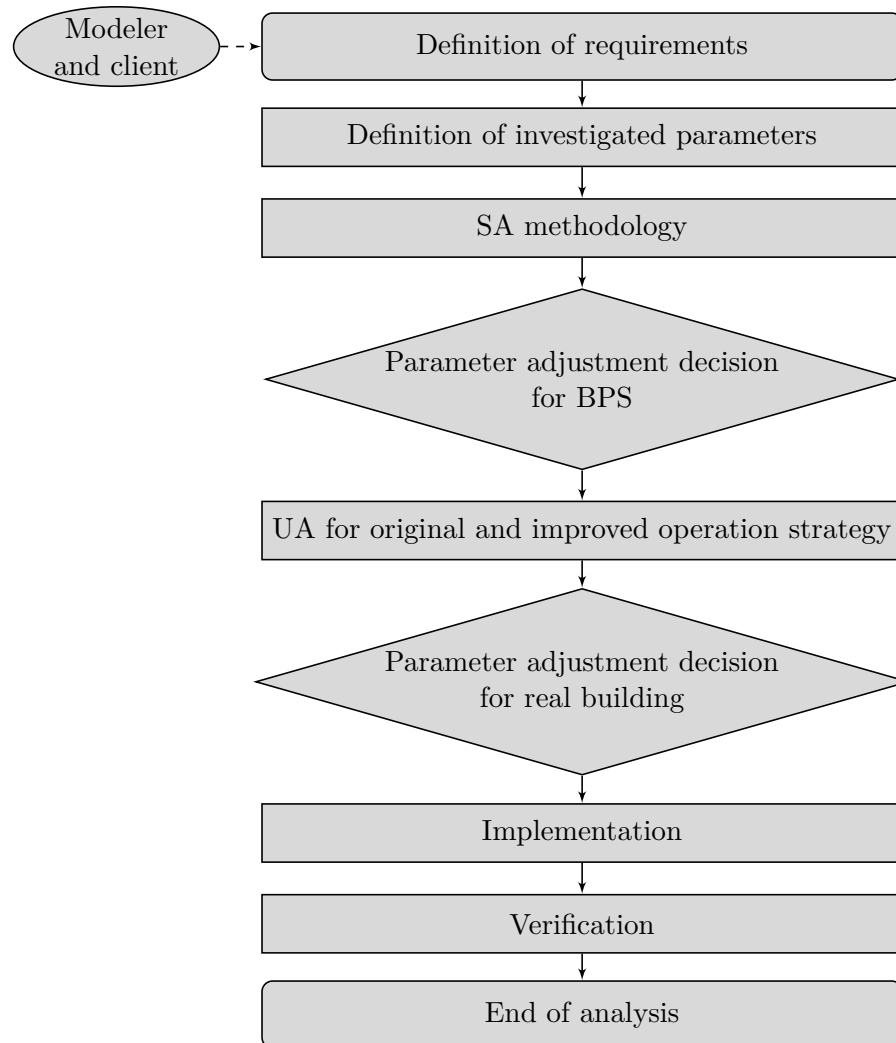


**Figure 4.9:** SA methodology employed to improve building operation.

model introduced in VDI 6007 Part 1 (2007). Simplifications include the treatment of long-wave radiation exchange and inter-zonal air exchange. Components from the Modelica Standard Library (MSL) are used as the basis for modeling whenever possible. The same radiation processor as for the case study in Chapter 3 is used. More details of the modeling can be found in Elci (2010) and in Burhenne et al. (2010a).

The building is modeled in 5 different zones which are connected by internal walls. The usage of the zones, their net floor areas ( $A_{\text{NFA}}$ ) and their plant equipment can

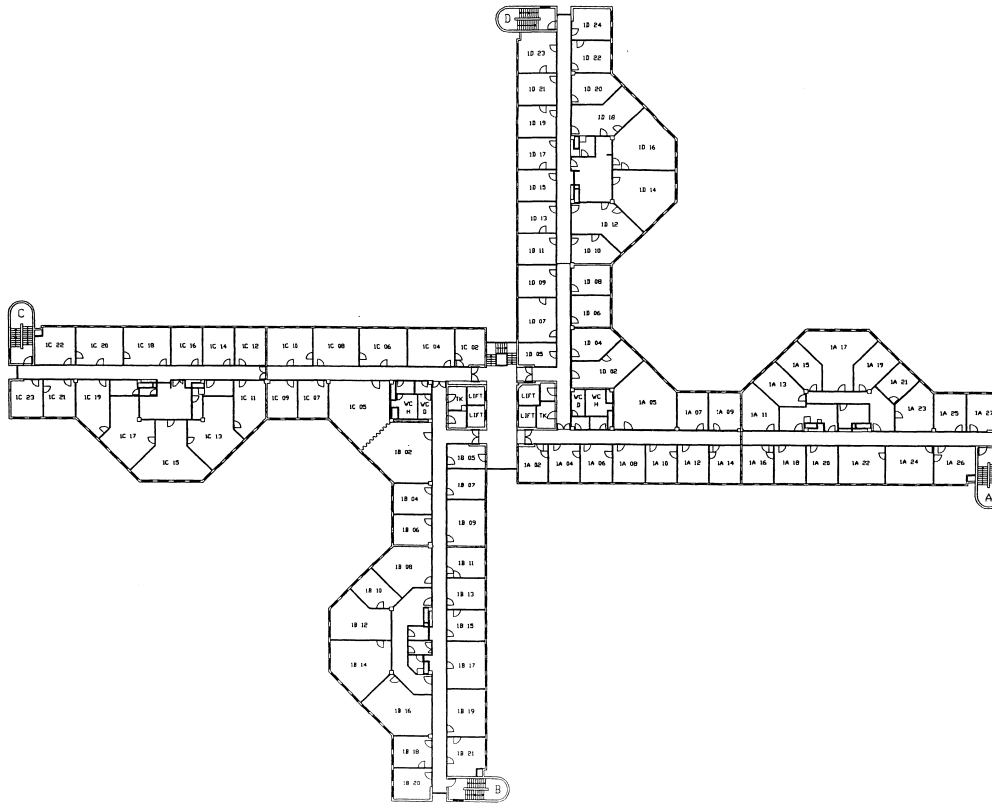


**Figure 4.10:** Floor plan of the building.

be found in Table 4.3.

**Table 4.3:** Building zones and their HVAC equipment.

Zone	Usage	$A_{NFA}$ in $m^2$	AHU	Cooling
1	Corridors, restrooms, small kitchens	6,908	partly	no
2	Offices	2,252	no	no
3	Offices	8,813	no	yes
4	Offices	2,015	yes	no
5	Central kitchen and canteen	1,129	yes	no

Which parameters are considered to be uncertain depends on the project (e.g., available data and documentation). Also, control settings might be considered to be uncertain even though they are usually known. They are explicitly considered in

this SA application in order to identify energy-efficient control strategies.

Several occupant-dependent parameters and variables are selected to be analyzed in the SA because, as mentioned in Chapter 3, they are known to be highly influential on BPS results (e.g., Page et al., 2008; Brohus et al., 2009; Haldi and Robinson, 2011). As in the BPS case study in Section 3.2.5, the air change rates are defined by a schedule and the value is varied by a sampled factor indicated by the box plots (Figure 4.11). The factors are  $ACH_{\text{nat}}$  (natural ventilation including infiltration) for Zones 1, 2, 3 and 5,  $ACH_{\text{inf}}$  (infiltration) for Zone 4 and  $ACH_{\text{AHU}}$  (volume flow rate through the AHU) for Zone 4. The efficiency of the heat exchanger of the AHU ( $\eta_{\text{HX}}$ ) in zone 5 is also considered to be uncertain.

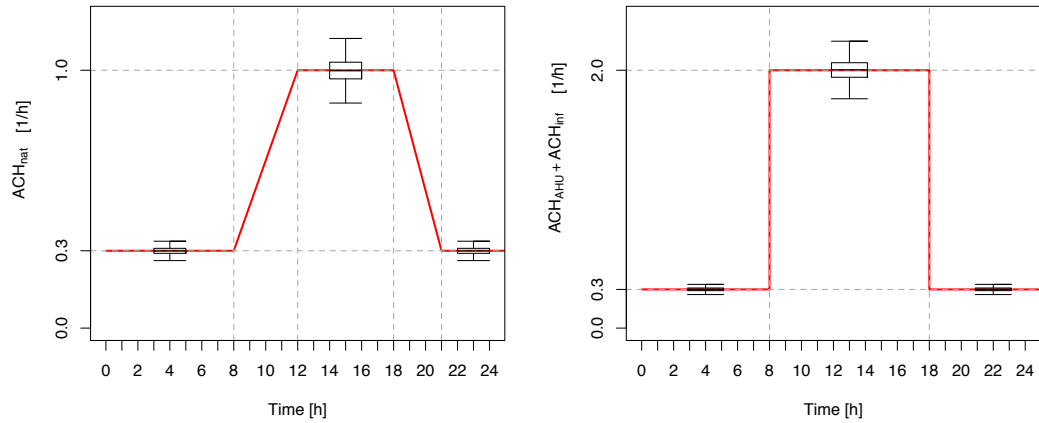


**Figure 4.11:** Schedules for the air change rates. The box plots indicate the variation of the schedule values in the MC simulation.

The room temperature set point ( $T_{\text{set}}$ ), the irradiance threshold for shading control ( $I_{\text{shad}}$ ) and the operating schedule for the pumps of the heating circuits (daily pump operation time  $\Delta k_{\text{pump}}$ ) are also varied during the MC simulation and are applied for all zones.  $T_{\text{set}}$  is considered to be uncertain because it is mainly set by the occupants in the offices. The shading elements are controlled by the occupants and the irradiance on the façade is assumed to be the trigger that leads to adjustments by the occupants. This behavior is implemented via  $I_{\text{shad}}$ . The variance for the parameters is smaller than for the case study in Chapter 3. This is because the large number of occupants in the building is assumed to result in less variation (i.e., extreme behavior of single occupants does not dominate the overall effect). The pump operation times ( $\Delta k_{\text{pump}}$ ) are usually set in the building automation system. In the real building, the pumps were operated 24 hours per day and there was no temperature setback for the supply temperature of the heating circuits during

unoccupied hours. However, it is varied in the SA to analyze the influence of this control strategy setting on the heating energy demand of the building.  $\Delta k_{\text{pump}}$  is implemented as a schedule that is generated by an R script. This implementation is the reason that the maximum value is 23.99 instead of 24. 12:00 is the basis for the schedule generation. The pump operation starts at  $12:00 - \Delta k_{\text{pump}}/2$  and ends at  $12:00 + \Delta k_{\text{pump}}/2$ . Many more variables and parameters could be analyzed. These seven simulation inputs were selected in order to implement each step of the methodology with the same number of parameters, to allow comparability of the results<sup>21</sup>. Brevity is another reason for this selection. The parameters for the distributions which are used for the sampling can be found in Table 4.4.

**Table 4.4:** Parameters selected for variation and their distributions.

Parameter	Distribution	$\mu$	$\sigma$	Unit
$ACH_{\text{nat}}$ (scaling factor)	normal	1	0.05	–
$ACH_{\text{inf}}$ (scaling factor)	normal	1	0.05	–
$ACH_{\text{AHU}}$ (scaling factor)	normal	1	0.05	–
$\Delta T_{\text{set}}$ (offset)	normal	0	0.15	K
$\eta_{\text{HX}}$ (efficiency heat recovery AHU)	normal	0.6	0.05	–
$I_{\text{shad}}$ (irradiance threshold for control)	normal	200	20	$\frac{\text{W}}{\text{m}^2}$
Parameter	Distribution	min.	max.	Unit
$\Delta k_{\text{pump}}$ (pump operation time)	uniform	12	23.99	h

The simulated period is from September 1, 2008 to November 30, 2008 because heating energy consumption is the main focus of the case study<sup>22</sup>. The model was validated with the measured data from this period (Elci, 2010; Burhenne et al., 2010a). The outdoor air temperature and irradiance were also taken from on-site measurements.

<sup>21</sup>Some methods that are used in the SA methodology can only cope with a limited number of inputs (e.g., the scatter plot and the VB method).

<sup>22</sup>This is not the full heating period. However, the selection of this period is based on the availability of measurements.

## 4.3 Results and Discussion

### 4.3.1 Scatter Plot Method

Scatter plots are used to obtain the first impression concerning model structure and parameter significance. As in Chapter 3, convergence is analyzed with the mean and variance estimates as convergence criteria. The heating energy ( $Q_{\text{heat}}$ ) of the building from September 1, 2008 to November 30, 2008 is the primary model result in this example. Figure 4.12 shows the convergence plot for the mean and the variance estimates. The horizontal line represents the results for the highest sample size (i.e., 1024). These results are used as the reference (i.e., 343.94 MWh for the mean and 227.43 MWh<sup>2</sup> for the variance). As for the examples shown in Section 3.2.5, it is assumed that convergence is reached when the values of the estimates are within the range of the reference results  $\pm 5\%$ . Table 4.5 shows the results and their deviation from the reference values. The mean estimate converges already at a sample size of 2 (354.80 MWh; +3.2%)<sup>23</sup> whereas the variance estimate converges at a sample size of 128.

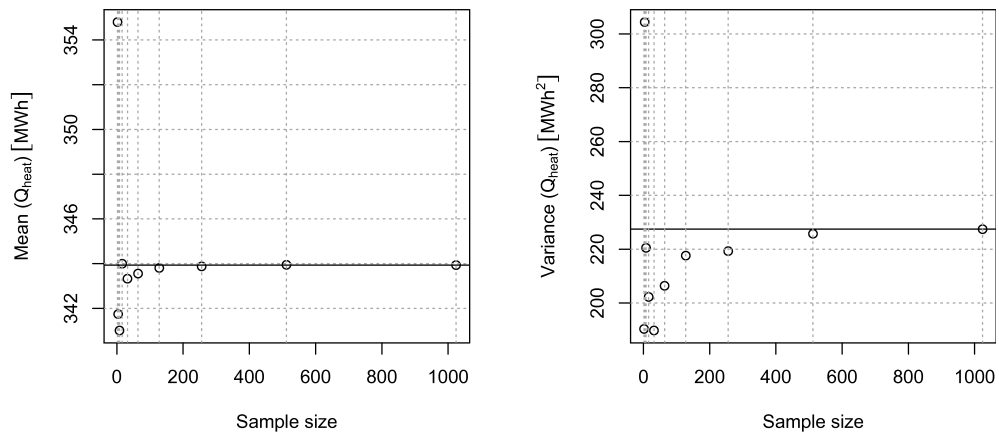


**Figure 4.12:** Convergence plot for the mean and variance estimates of the heating energy demand (Note that the y-axes do not start at 0).

<sup>23</sup>Note that this result is not shown Table 4.5. Results coming from very low sample sizes are likely to occur by chance.

**Table 4.5:** Convergence of mean and variance estimates for the SA MC simulation. Gray cells indicate estimates that have converged to the reference value  $\pm 5\%$ .

Sample size	32	64	128	256	512	1,024
Mean estimate in MWh	343.33 -0.2%	343.56 -0.1%	343.81 0.0%	343.88 0.0%	343.95 0.0%	343.94 0.0%
Variance estimate in MWh <sup>2</sup>	189.78 -16.6%	206.39 -9.2%	217.60 -4.3%	219.27 -3.6%	225.73 -0.7%	227.43 0.0%

Figure 4.13 shows scatter plots of the sampled parameters and  $Q_{\text{heat}}$  for the analyzed period. The sample size of the underlying MC simulation for this plot is 128. It is evident that the heat consumption of the building ( $Q_{\text{heat}}$ ) is very sensitive to the natural ventilation ( $ACH_{\text{nat}}$ ) for Zones 1, 2, 3 and 5 as well as to the room temperature set point ( $\Delta T_{\text{set}}$ ). The red points indicate the mean value within each slice. The distribution pattern of the points and the slope of an imaginary line through the red points indicate that the higher  $ACH_{\text{nat}}$  and  $\Delta T_{\text{set}}$  are, the higher is  $Q_{\text{heat}}$ .  $\Delta T_{\text{set}}$  is very influential although the variation of the offset and hence the variation of the set point temperatures is small. The scatter plot for the pump operating hours ( $\Delta k_{\text{pump}}$ ) does not show such a clear pattern. However, the red points indicate that  $Q_{\text{heat}}$  increases as  $\Delta k_{\text{pump}}$  for the heating circuit pumps increases.  $I_{\text{shad}}$  has a minor influence. A weak trend of the red points is visible, with higher values for  $I_{\text{shad}}$  leading to a slightly smaller  $Q_{\text{heat}}$ . The remaining parameters ( $ACH_{\text{inf}}$ ,  $ACH_{\text{AHU}}$  and  $\eta_{\text{HX}}$ ) do not show a strong influence on  $Q_{\text{heat}}$ . This is most likely to be due to the fact that all of them are only applied to one zone (i.e., zone 4). Furthermore, they influence each other (e.g., the influence of a higher  $ACH_{\text{AHU}}$  on  $Q_{\text{heat}}$  can be compensated by a lower  $ACH_{\text{inf}}$  and/or a higher  $\eta_{\text{HX}}$ ), resulting in a weaker influence of a single parameter. The scatter plots allow initial insights concerning the driving model inputs. However, such a qualitative measure is sometimes hard to interpret (e.g., the question *What is more influential,  $ACH_{\text{AHU}}$  or  $ACH_{\text{inf}}$ ?* would be difficult to answer.). Hence, it is worthwhile to apply another sensitivity analysis method to further examine the influence of the parameters and variables of the model and possible interactions.

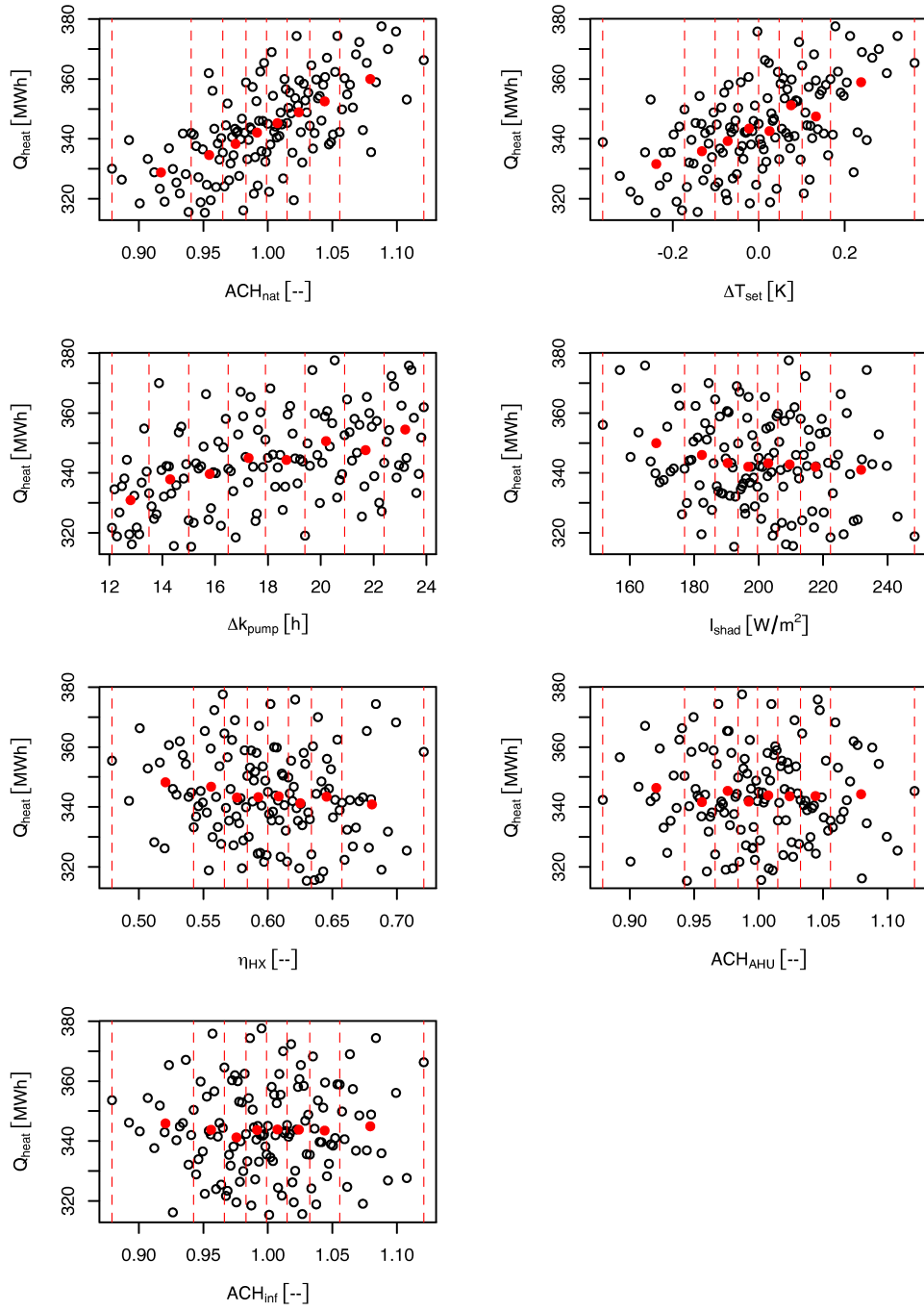


**Figure 4.13:** Scatter plots of heating energy demand of the building versus the analyzed parameters. The dashed vertical lines divide the scatter plots into 8 slices with 16 dots in each slice. The red points represent the mean value of  $Q_{\text{heat}}(X_i)$  in each slice.

The ranking of the inputs according to their sensitivity is shown in Table 4.6. It is performed by calculating the variance of the mean values of  $Q_{\text{heat}}(X_i)$  over all 8 slices and ordering the parameters according to it (decreasing order).

**Table 4.6:** Ranking of the parameters and variables according to their influence on the BPS result based on the scatter plot method ( $N = 128$ ).

Ranking	Parameter	Variance of mean values over slices in MWh <sup>2</sup>
1	$ACH_{\text{nat}}$ (scaling factor)	101.3
2	$\Delta T_{\text{set}}$ (offset)	75.9
3	$\Delta k_{\text{pump}}$ (hours of pump operation)	56.5
4	$I_{\text{shad}}$ (irradiance threshold for control)	8.2
5	$\eta_{\text{HX}}$ (efficiency heat recovery AHU)	6.4
6	$ACH_{\text{AHU}}$ (scaling factor)	2.6
7	$ACH_{\text{inf}}$ (scaling factor)	1.8

### 4.3.2 Elementary Effects Method

Given the small number of analyzed parameters ( $k$ ) in the case study, the next step could be a variance-based SA. However, the *EE* method is applied for illustration purposes. As mentioned earlier,  $r$  is commonly in the range of 2 to 8. However, the number of blocks is increased successively to analyze the convergence of the *EE* measures  $\mu^*$  and  $\sigma$  (Figure 4.14). The aim of the *EE* method is to identify a subset of non-influential parameters and variables (i.e., factor-fixing application). Hence, the relation of the values for  $\mu^*$  to each other is more important than their absolute value. The method fails when an important parameter or variable remains unrecognized. Table 4.7 reveals that ranking the parameters according to  $\mu^*$  would result in the same order for any analyzed  $r$ . The reference results<sup>24</sup> come from an MC simulation with  $r = 512$ . The results show that the estimator for  $\mu^*$  converges faster than the estimator for  $\sigma$ . However,  $\mu^*$  is the primary result of the *EE* method.

Table 4.8 contains the results for  $r = 8$  that are further analyzed. In Figure 4.15  $\mu^*$  and  $\sigma$  estimates are plotted against each other for  $r = 8$ . The figure reveals that there are no significant interactions between the analyzed parameters or nonlinearities in the model (i.e., no points above the line that satisfies the condition  $\mu^* = \pm 2 \frac{\sigma_i}{\sqrt{r}}$ ).

<sup>24</sup>Note that these results are not shown in the table.

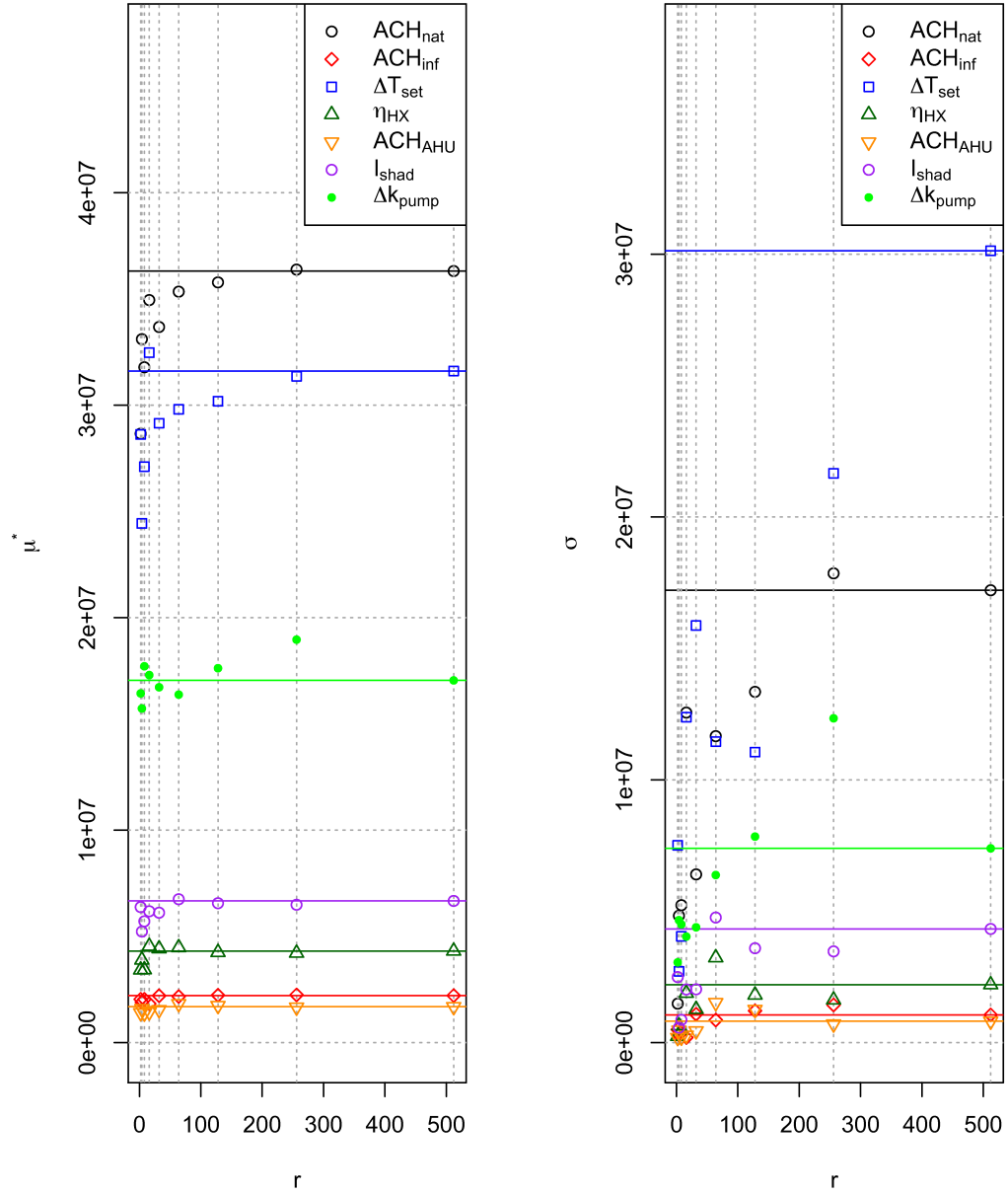


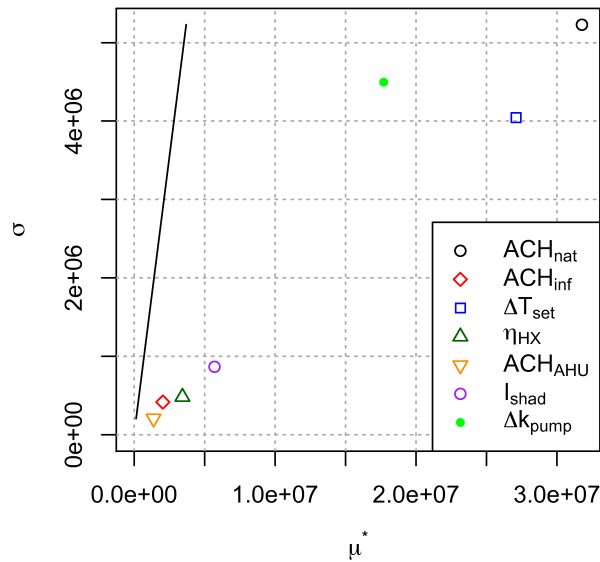
Figure 4.14: Convergence plot for the  $\mu^*$  and  $\sigma$  estimates.

**Table 4.7:** Convergence of  $\mu^*$  and  $\sigma$  estimates. Gray cells indicate estimates that have converged to the reference value  $\pm 5\%$ . The red cells indicate that the estimate falls within the target range but that convergence has not been reached.

<b>r</b>	<b>2</b>	<b>4</b>	<b>8</b>	<b>16</b>	<b>32</b>	<b>64</b>
	$\mu^*$					
$ACH_{\text{nat}}$	2.87e+7 -21.1%	3.31e+7 -8.8%	3.18e+7 -12.5%	3.49e+7 -3.8%	3.37e+7 -7.3%	3.53e+7 -2.7%
$\Delta T_{\text{set}}$	2.86e+7 -9.4%	2.44e+7 -22.7%	2.71e+7 -14.2%	3.25e+7 +2.8%	2.91e+7 -7.8%	2.98e+7 -5.7%
$\Delta k_{\text{pump}}$	1.64e+7 -3.6%	1.57e+7 -7.8%	1.77e+7 +3.9%	1.73e+7 +1.5%	1.67e+7 -1.9%	1.64e+7 -3.9%
$I_{\text{shad}}$	6.38e+6 -4.3%	5.23e+6 -21.6%	5.71e+6 -14.4%	6.18e+6 -7.3%	6.11e+6 -8.3%	6.75e+6 +1.2%
$\eta_{\text{HX}}$	3.42e+6 -20.6%	3.89e+6 -9.7%	3.43e+6 -20.4%	4.54e+6 +5.3%	4.42e+6 +2.5%	4.47e+6 +3.8%
$ACH_{\text{inf}}$	2.04e+6 -7.8%	1.90e+6 -14.0%	2.04e+6 -7.8%	1.83e+6 -17.2%	2.21e+6 -0.4%	2.17e+6 -2.0%
$ACH_{\text{AHU}}$	1.41e+6 -16.7%	1.60e+6 -5.0%	1.38e+6 -18.0%	1.44e+6 -14.8%	1.55e+6 -8.2%	1.83e+6 +8.5%
	$\sigma$					
$ACH_{\text{nat}}$	1.48e+6 -91.4%	4.83e+6 -71.9%	5.23e+6 -69.6%	1.26e+7 -27.0%	6.4e+6 -62.8%	1.17e+7 -32.3%
$\Delta T_{\text{set}}$	7.51e+6 -75.1%	2.71e+6 -91.0%	4.04e+6 -86.6%	1.24e+7 -58.9%	1.59e+07 -47.3%	1.15e+7 -62.0%
$\Delta k_{\text{pump}}$	3.05e+6 -58.7%	4.66e+6 -36.9%	4.50e+6 -39.2%	4.04e+6 -45.4%	4.39e+6 -40.6%	6.38e+6 -13.7%
$I_{\text{shad}}$	2.49e+6 -42.3%	5.69e+5 -86.8%	8.66e+5 -80.0%	2.02e+6 +53.2%	2.03e+6 -53.1%	4.76e+6 +10.0%
$\eta_{\text{HX}}$	2.43e+5 -89.0%	6.43e+5 -70.8%	4.81e+5 -78.1%	1.88e+6 -14.6%	1.27e+6 -42.2%	3.23e+6 +46.8%
$ACH_{\text{inf}}$	4.99e+5 -52.7%	2.97e+5 -71.9%	4.16e+5 -60.6%	1.96e+5 -81.4%	1.08e+6 +2.5%	8.59e+5 -18.5%
$ACH_{\text{AHU}}$	1.90e+5 -76.7%	4.71e+5 -42.3%	2.06e+5 -74.7%	2.82e+5 -65.5%	4.45e+5 -45.5%	1.52e+6 +86.2%

**Table 4.8:** Ranking of the parameters and variables according to their influence on the BPS result based on the *EE* method ( $r = 8$ ).

Ranking	Parameter	$\mu^*$	$\sigma$
1	$ACH_{\text{nat}}$ (scaling factor)	3.18e+7	5.23e+6
2	$\Delta T_{\text{set}}$ (offset)	2.71e+7	4.04e+6
3	$\Delta k_{\text{pump}}$ (hours of pump operation)	1.77e+7	4.50e+6
4	$I_{\text{shad}}$ (irradiance threshold for control)	5.71e+6	8.66e+5
5	$\eta_{\text{HX}}$ (efficiency heat recovery AHU)	3.43e+6	4.81e+5
6	$ACH_{\text{inf}}$ (scaling factor)	2.04e+6	4.16e+5
7	$ACH_{\text{AHU}}$ (scaling factor)	1.38e+6	2.06e+5

**Figure 4.15:**  $\mu^*$  and  $\sigma$  estimates plotted against each other ( $r = 8$ ).

### 4.3.3 Variance-Based Method

The VB method can be applied for a selection (i.e., most influential parameters) of initially analyzed parameters. Given the number of parameters in this example, it is possible to analyze all parameters and variables with the VB method. The sample size ( $N$ ) of the underlying MC simulation is increased successively to analyze the convergence (Figure 4.16 and Table 4.9). The reference results come from an MC simulation with  $N = 8,192$ .

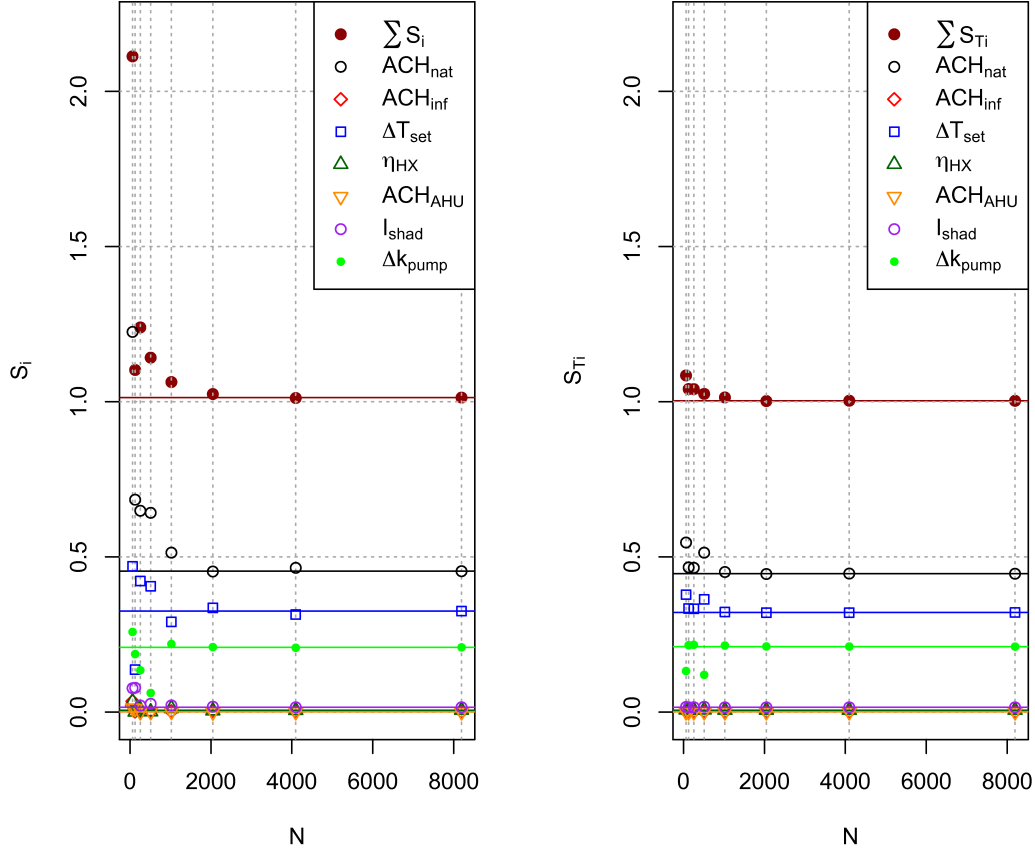


**Figure 4.16:** Convergence plot for the first-order ( $S_i$ ) and total ( $S_{Ti}$ ) sensitivity index estimates.

It is evident that the estimator for  $S_{Ti}$  converges more quickly than the estimator for  $S_i$ . Especially the non-influential parameters ( $S_i$  and  $S_{Ti} \leq 0.05 \cong 5\%$ ) require large sample sizes for convergence to be reached. This is due to the small influence on the result. Even when the convergence criterion is not reached, the results provide insights on the importance. In cases where the *EE* method is used for factor fixing (FF), these parameters are not analyzed with the variance-based approach. Instead of analyzing the convergence of all estimators, the convergence of only  $\sum S_i$  and  $\sum S_{Ti}$  can be analyzed for simplicity reasons. The estimator for  $\sum S_i$  converges at  $N = 1,024$  and  $\sum S_{Ti}$  converges at  $N = 128$ .

**Table 4.9:** Convergence of  $S_i$  and  $S_{T_i}$  estimates. Gray cells indicate estimates that have converged to the reference value  $\pm 5\%$ . The red cells indicate that the estimate falls within the target range but that convergence has not been reached.

$N$	<b>64</b>	<b>128</b>	<b>256</b>	<b>512</b>	<b>1,024</b>	<b>2,048</b>
	$S_i$					
$ACH_{\text{nat}}$	1.225 +169.8%	0.684 +50.7%	0.649 +42.9%	0.642 +41.4%	0.514 +13.2%	0.453 -0.2%
$\Delta T_{\text{set}}$	0.470 +44.2%	0.137 -57.9%	0.422 +29.7%	0.406 +24.6%	0.291 -10.6%	0.336 +3.2%
$\Delta k_{\text{pump}}$	0.259 +23.8%	0.187 -10.4%	0.135 -35.4%	0.062 -70.4%	0.220 +5.2%	0.210 +0.5%
$I_{\text{shad}}$	0.077 +385.7%	0.079 +394.2%	0.021 +35.0%	0.027 +70.4%	0.022 +37.3%	0.018 +11.0%
$\eta_{\text{HX}}$	0.034 +429.4%	0.001 -88.1%	0.008 +26.6%	0.001 -81.5%	0.012 +87.6%	0.005 -25.9%
$ACH_{\text{inf}}$	0.035 +2302.0%	0.003 +75.5%	0.003 +80.5%	0.003 +76.2%	0.003 +83.3%	0.003 +90.0%
$ACH_{\text{AHU}}$	0.013 +1262.3%	0.012 +1083.4%	0.001 -14.1%	0.001 +36.5%	0.002 +110.0%	0.000 -54.1%
$\sum S_i$	2.112 +108.5%	1.102 +8.8%	1.239 +22.3%	1.142 +12.7%	1.063 +4.9%	1.025 +1.1%
	$S_{T_i}$					
$ACH_{\text{nat}}$	0.547 +22.6%	0.466 +4.6%	0.465 +4.3%	0.514 +15.2%	0.451 +1.3%	0.445 -0.2%
$\Delta T_{\text{set}}$	0.379 +17.8%	0.334 +3.8%	0.333 +3.7%	0.364 +13.2%	0.323 +0.5%	0.321 -0.1%
$\Delta k_{\text{pump}}$	0.133 -37.2%	0.216 +2.2%	0.217 +2.8%	0.120 -43.0%	0.215 +1.7%	0.212 +0.3%
$I_{\text{shad}}$	0.017 +7.9%	0.016 +1.1%	0.016 +3.3%	0.017 +12.1%	0.016 +0.2%	0.016 -0.1%
$\eta_{\text{HX}}$	0.007 +12.2%	0.007 +4.7%	0.007 +6.1%	0.007 +12.6%	0.006 +0.5%	0.006 +0.2%
$ACH_{\text{inf}}$	0.002 +20.7%	0.002 +0.6%	0.002 +1.2%	0.002 +14.8%	0.002 +1.0%	0.002 +0.2%
$ACH_{\text{AHU}}$	0.001 +0.1%	0.001 +2.6%	0.001 +4.4%	0.001 +11.6%	0.001 -0.9%	0.001 -0.1%
$\sum S_{T_i}$	1.085 +8.1%	1.041 +3.8%	1.041 +3.8%	1.025 +2.2%	1.014 +1.1%	1.002 -0.1%

Table 4.10 contains the reference results for  $N = 8,192$ . The total number of simulations required is  $N(k + 2) = 8,192 * (7 + 2) = 73,728$ . The results reveal that the model is primarily additive (i.e., no interactions between the parameters). Approximately 45% of the result variance can be explained by the variance of  $ACH_{\text{nat}}$ . Approx. 32% of the variance in the results can be explained by  $\Delta T_{\text{set}}$ . The pump operation hours cause approx. 21% of the result variance. All remaining parameters have a negligible influence on the results. 1.6% can be attributed to  $I_{\text{shad}}$  and less than 1% is caused by  $ACH_{\text{inf}}$ ,  $ACH_{\text{AHU}}$  and  $\eta_{\text{HX}}$ .

**Table 4.10:** Results of the variance-based method ( $N = 8,192$ ).

Ranking	Parameter	$S_i$	$S_{Ti}$
1	$ACH_{\text{nat}}$ (scaling factor)	0.454	0.446
2	$\Delta T_{\text{set}}$ (offset)	0.326	0.321
3	$\Delta k_{\text{pump}}$ (hours of pump operation)	0.209	0.211
4	$I_{\text{shad}}$ (irradiance threshold for control)	0.016	0.016
5	$\eta_{\text{HX}}$ (efficiency heat recovery AHU)	0.006	0.006
6	$ACH_{\text{inf}}$ (scaling factor)	0.001	0.002
7	$ACH_{\text{AHU}}$ (scaling factor)	0.001	0.001
	$\Sigma$	1.013	1.003

#### 4.3.4 Monte Carlo Filtering

MC filtering is performed on the basis of the MC simulation results that were used for the VB method. For the separation into the behavioral and non-behavioral bins, a threshold of 350 MWh for the heating energy ( $Q_{\text{heat}}$ ) is used. This number is arbitrarily chosen. In practice, it could be based on an agreement between the building owner and a company that aims to improve the building's energy efficiency (e.g., performance contracting). The underlying MC sample size is 8,192 and the MC results used for the VB method are used. The behavioral subset contains 5,319 results and the non-behavioral subset contains 2,873 results. The larger the differences between the ECDFs for the behavioral and non-behavioral result subsets, the greater is the influence of the analyzed parameter in driving the simulation output into a specific region. Figure 4.17 reveals that  $ACH_{\text{nat}}$  has a significant influence on whether  $Q_{\text{heat}}$  is below or equal to 350 MWh or not. Other interesting pieces of information that can be obtained by analyzing the ECDFs are the minimal and maximal values of a variable in the subsets. The lowest value for  $ACH_{\text{nat}}$  in the behavioral subset is approx. 0.82 whereas the lowest scaling factor in the non-behavioral subset is approx. 0.90. If minimal values of the behavioral and the non-behavioral subset are significantly different, this indicates a very influential parameter. The same is

true for the maximal values for both subsets. For the offset for the temperature set point ( $\Delta T_{\text{set}}$ ), the minimal values of both subsets are also different. For all other analyzed parameters, the minimal and maximal values of the behavioral and the non-behavioral subsets are approximately equal. The lower  $\Delta T_{\text{set}}$  is, the higher is the probability that  $Q_{\text{heat}}$  is less than or equal to 350 MWh. The same is true for  $\Delta k_{\text{pump}}$ . The probability of  $\Delta k_{\text{pump}}$  being less than 18 h in the behavioral subset is approx. 60%, whereas the probability for the same criterion in the non-behavioral subset is approx. 30%. These probabilities indicate that shorter pump operating duration contribute to the defined goal being reached (i.e.,  $Q_{\text{heat}} \leq 350$  MWh). The ECDFs also reveal that the remaining parameters and variables are less influential on  $Q_{\text{heat}}$ . It can be seen that the ECDFs for the two subsets of  $\eta_{\text{HX}}$  and  $I_{\text{shad}}$  have larger distances between each other than those for  $ACH_{\text{inf}}$  and  $ACH_{\text{AHU}}$ .

In addition to the visual inspection of the ECDFs, a Kolmogorov-Smirnov test is conducted to compute the maximum distance between the behavioral and the non-behavioral ECDFs. Table 4.11 shows the results of the Kolmogorov-Smirnov test. The test confirms the findings based on visual inspection of Figure 4.17. Another interesting result of the test is the  $p$ -value. In the analyzed case, the null hypothesis is that the results for the behavioral and the non-behavioral subsets come from the same distribution. If the  $p$ -value is below the chosen significance level, the null hypothesis is rejected and the two different subsets do not come from the same distribution. In this example, a significance level of 0.05 is chosen. The  $p$ -values for  $ACH_{\text{nat}}$ ,  $\Delta T_{\text{set}}$ ,  $\Delta k_{\text{pump}}$ ,  $I_{\text{shad}}$  and  $\eta_{\text{HX}}$  are below this threshold, which means that the two distributions are significantly different and the analyzed simulation input has significant influence on the result. The  $p$ -values for the remaining parameters are above the threshold (i.e., the null hypothesis that both subsets come from the same distribution cannot be rejected), which indicates that the ECDFs for the subsets are not significantly different.

**Table 4.11:** Results of the Kolmogorov-Smirnov test ( $N = 8,192$ ).

Ranking	Parameter	$D$	$p$ -value
1	$ACH_{\text{nat}}$ (scaling factor)	0.4651	$< 2.2\text{e-}16$
2	$\Delta T_{\text{set}}$ (offset)	0.4042	$< 2.2\text{e-}16$
3	$\Delta k_{\text{pump}}$ (hours of pump operation)	0.3194	$< 2.2\text{e-}16$
4	$I_{\text{shad}}$ (irradiance threshold for control)	0.1046	$< 2.2\text{e-}16$
5	$\eta_{\text{HX}}$ (efficiency heat recovery AHU)	0.0573	9.599e-6
6	$ACH_{\text{inf}}$ (scaling factor)	0.0258	0.1669
7	$ACH_{\text{AHU}}$ (scaling factor)	0.0225	0.3025

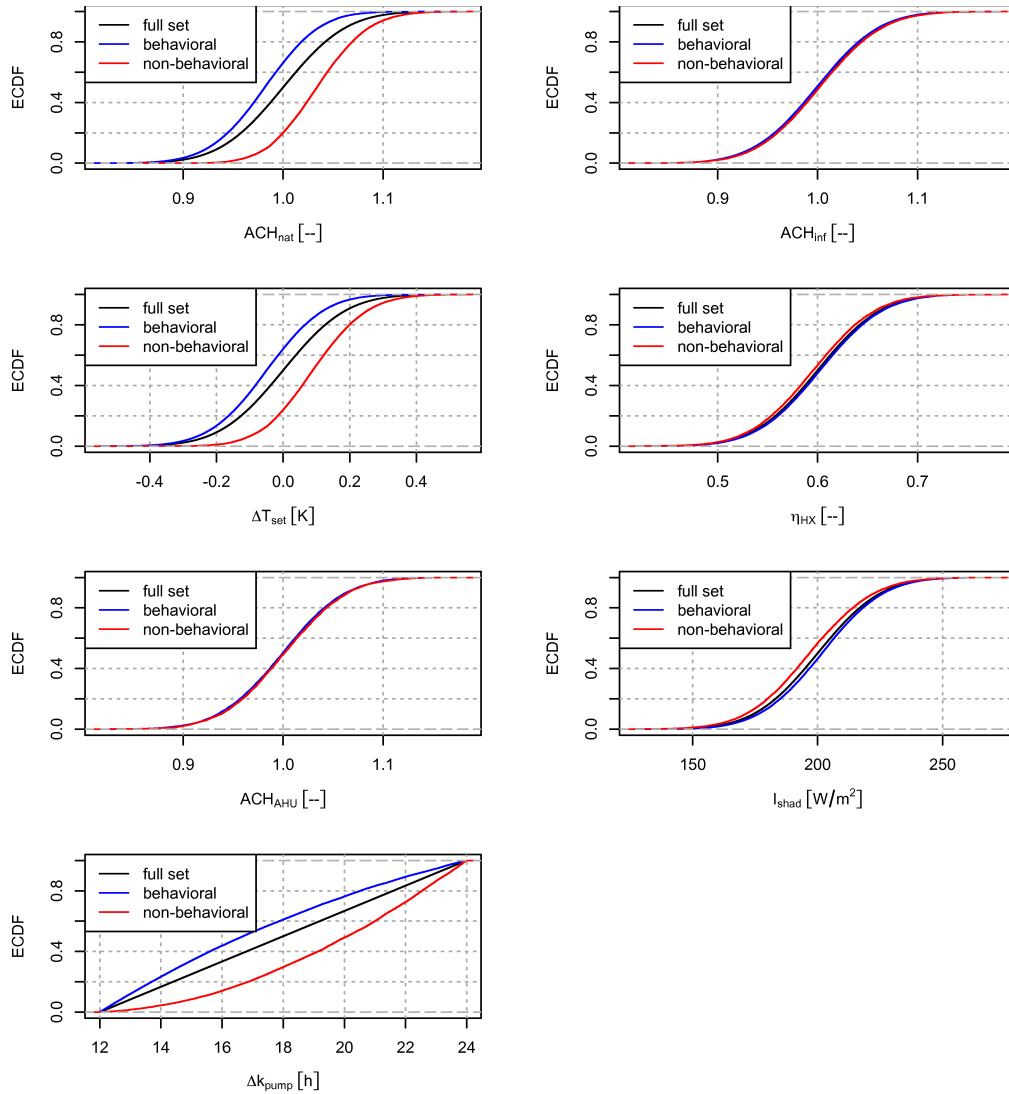


**Figure 4.17:** Monte Carlo filtering plot for the heating energy demand ( $N = 8,192$ ).

### 4.3.5 Predicted Savings and Implementation

As mentioned in Section 4.2.6, the aim is to leverage the SA methodology to improve building operation. Based on the SA results, the analyst can decide which changes should be implemented in the real building. The SA showed that the pump operation schedule ( $\Delta k_{\text{pump}}$ ) is the third most influential input. The most influential inputs ( $ACH_{\text{nat}}$ ,  $\Delta T_{\text{set}}$ ) cannot be fixed to a certain value because they are dependent on

occupants' behavior. However, user feedback could inform the occupants and lead to energy savings. The pump schedule can be changed in the building automation system. The influence of  $ACH_{inf}$ ,  $ACH_{AHU}$  and  $\eta_{HX}$  is small because they are applied only to the simulation zone with the AHU equipped with heat recovery unit.

To allow calculation of the potential energy savings, a new pump schedule is introduced in the simulation. This schedule is based on the SA results and requirements concerning the building's occupancy. According to this schedule, the pumps are operated from 6:00 till 20:00 on weekdays and from 6:00 till 16:00 on Saturdays. All other parameters that were analyzed in the SA (i.e.,  $ACH_{nat}$ ,  $\Delta T_{set}$ ,  $I_{shad}$ ,  $\eta_{HX}$ ,  $ACH_{AHU}$  and  $ACH_{inf}$ ) are considered to be uncertain. Two sets of MC simulations were conducted, each for the period from December 1, 2008 till November 30, 2009. In the first set, the pump is operated 24 hours per day and in the second set, the new schedule is implemented. The values sampled for both simulations are the same<sup>25</sup> and Figure 4.18 shows the PDFs of the results.

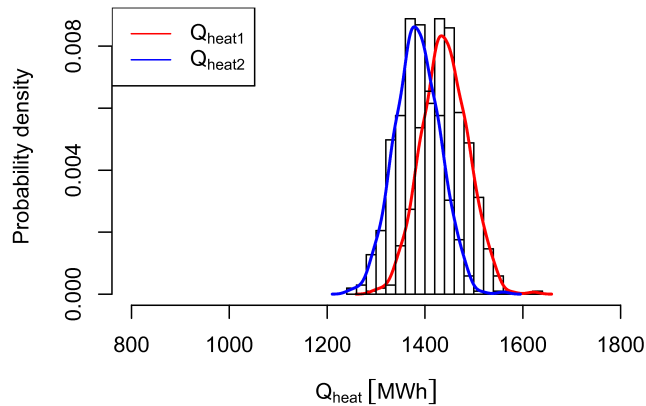


**Figure 4.18:** PDFs of  $Q_{heat}$  for two operation strategies ( $N = 512$ ). The red curve is with 24 h/d pump operation and the blue one is with the new pump schedule.

The potential savings are calculated according to Equation 4.22.

---

<sup>25</sup>This is important for the comparability of the two MC simulations.

$$\mathbf{M}_{\text{out}} = \begin{bmatrix} Q_{\text{heat}_1}^{(1)} \\ Q_{\text{heat}_1}^{(2)} \\ \vdots \\ Q_{\text{heat}_1}^{(N-1)} \\ Q_{\text{heat}_1}^{(N)} \end{bmatrix} - \begin{bmatrix} Q_{\text{heat}_2}^{(1)} \\ Q_{\text{heat}_2}^{(2)} \\ \vdots \\ Q_{\text{heat}_2}^{(N-1)} \\ Q_{\text{heat}_2}^{(N)} \end{bmatrix} \quad (4.22)$$

Figure 4.19 shows the probability density function for the potential energy saving. The mean value of the potential energy saving is 55.6 MWh.

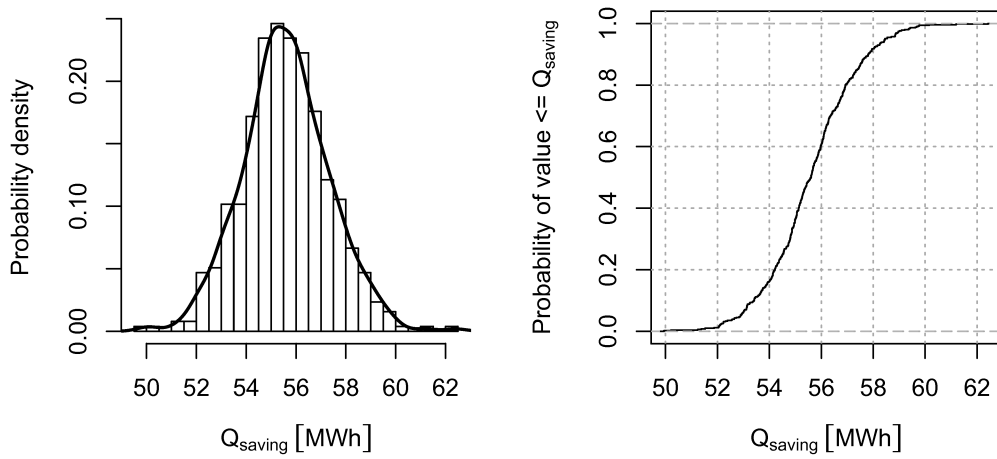


**Figure 4.19:** PDF and ECDF for the heating energy saving ( $N = 512$ ).

Following the decision that the pump schedules should be changed, the process of implementing it in the building automation system starts. Figure 4.20 shows a carpet plot of the measured data before and after the change of operation. According to the control signal, the pump ran constantly from October till December 2008 ( $Ctrl_{\text{pump}}$ ; ①). In December 2008, the pump schedule was implemented in the building ( $Ctrl_{\text{pump}}$ ; ②). After that, the temperature difference ( $\Delta T$ ) between the supply and the return pipe is high during the night ( $\Delta T$ ; ③). Furthermore, the supply temperature is high ( $T_{\text{sup}}$ ; ③). After further investigation, it turned out that the 3-way valve of the heating circuit was in a partly open position during the night. The main distribution pump pressed the hot water through this valve, which led to a high supply temperature (approx.  $90^\circ\text{C}$ ). The valve was adjusted in April 2009 ( $\Delta T$  and  $T_{\text{sup}}$ ; ④). The measured heat consumption from December 1,

2008 till November 30, 2009 is 1,191 MWh. The measured energy consumption is less than the simulated demand, which is likely to be due to other optimizations of the building operation. Furthermore, changed occupants' behavior could also be a reason.

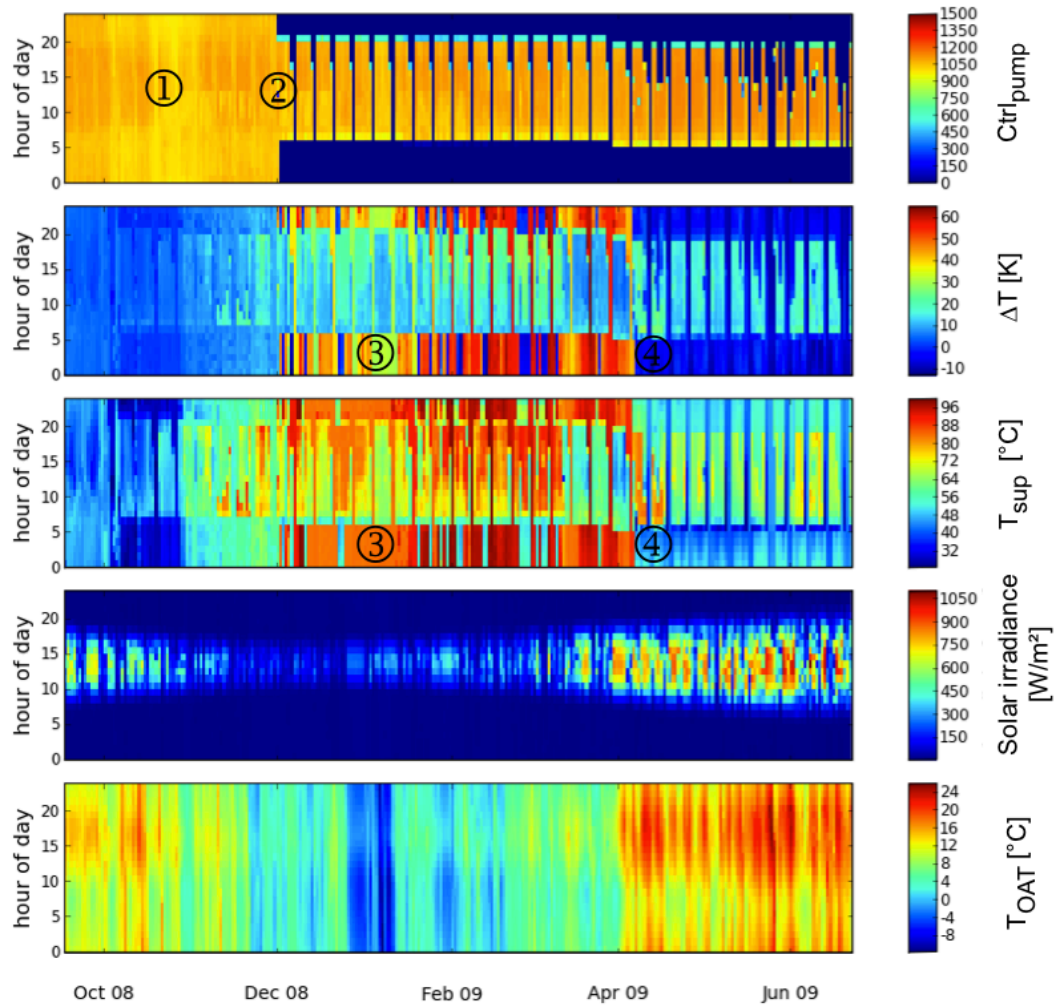


**Figure 4.20:** Carpet plot of the measured data in the building. The time of each day is shown on the y-axis from 0:00 to 24:00 and the days are plotted next to each other along the x-axis. The measurement value itself is represented by different colors according to its value.

## 4.4 Summary

An SA methodology for BPS was proposed. The methodology is scalable depending on project requirements and able to answer questions commonly raised in building design and operation as well as in BPS model development. The SA methods were taken from literature and combined to define the proposed methodology. The individual SA methods can be considered to be best practice. All methods were implemented in R because a program that fulfilled the requirements (i.e., applicability for BPS, ability to parallelize the MC simulation) did not previously exist.

The case study revealed that the ranking for  $ACH_{inf}$  and  $ACH_{AHU}$  that was produced by the *EE* method, the VB method and MC filtering is different to that obtained with the scatter plot method. The results coming from the VB method are considered to be the reference. However, the ranking varied only for the parameters that have minor influence. This minor influence was also detected by the scatter plot method. The analyzed model is primarily additive (i.e., no interactions between the analyzed parameters) which was revealed by the  $\mu^*$ - $\sigma$  plot and the similar results for  $S_i$  and  $S_{Ti}$ .

The main findings are:

- (I) SA provides insights into the model structure (e.g., additivity of the models).
- (II) There is no single SA methodology that fulfills all potential requirements for an SA with BPS models. Therefore different methods have been combined to a scalable SA methodology. Recommendations concerning typical applications have been given.
- (III) The variance-based method provides most insights. It can be used for factor prioritization ( $S_i$ ), factor fixing ( $S_{Ti}$ ) and variance cutting ( $S_{Ti}$ ). However, it is computationally expensive. In combination with the other proposed methods, this disadvantage can be overcome.
- (IV) All investigated MC-based SA methods are well suited for parallelization and the developed R tool chain is capable of distributing the simulations among different processor cores.
- (V) Similar to the UA, an SA provides valuable additional insights compared to a classic BPS. UA and SA can be easily combined.
- (VI) A methodology for applying SA (and UA) to improve building operation has been developed and demonstrated.



# 5 Application to Residential Building Design

The different parts of the overall methodology have been introduced in Chapters 2, 3 and 4. Two case studies illustrated aspects of the proposed approach to UA and SA. In this Chapter, all steps of the methodology will be applied to a single example.

## 5.1 Case Study

The analyzed building<sup>1</sup> is a residential building and serves as an example. In the standard configuration, the building fulfills the requirements of the German *Energieeinsparverordnung* (EnEV) from 2009 that is mandatory for newly built buildings (EnEV, 2009). In this example, this standard configuration is compared with a design that meets the *Passivhaus* standard (Feist et al., 2007) with respect to the energy performance and the cost-effectiveness. This information is commonly demanded in almost every design phase of a (residential) building. Figure 5.1 shows the analyzed building and Table 5.1 contains an overview of selected building parameters. A gas boiler supplies the building with heat. For this case study, Freiburg in Germany is assumed to be the location of the building.

**Table 5.1:** Building parameters.

Parameter	Value	Unit
$\frac{A}{V}$ (envelope area to volume ratio)	0.72	$\frac{\text{m}^2}{\text{m}^3}$
$V_e$ (gross volume)	675.7	$\text{m}^3$
$A_{\text{win}}$ (total window area)	35.9	$\text{m}^2$
$A_{\text{NFA}}$ (net floor area)	216.2	$\text{m}^2$

<sup>1</sup>The building has been designed and built several times in the area of Karlsruhe, Germany by DOMA GmbH. The company provided all necessary data to perform this analysis. The cost data are based on calculations of the company and are therefore case-specific. However, residential buildings of similar size and type represent a large share of the building stock in Germany.

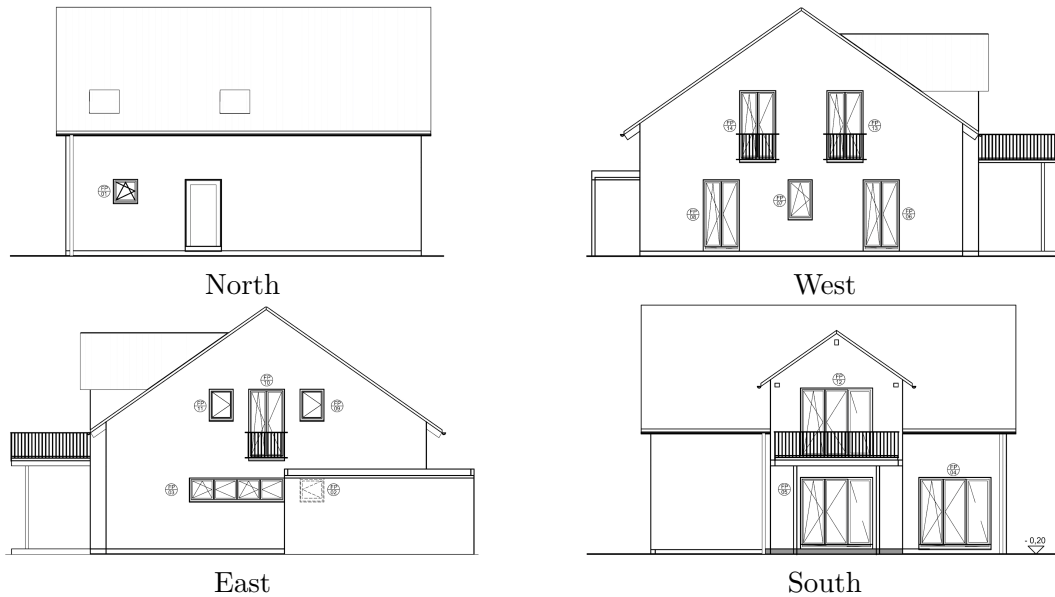


**Figure 5.1:** Analyzed residential building.

In Table 5.2, the key requirements of both standards are compared for the building analyzed in this case study.

The software PHPP (*Passivhaus Projektierungspaket*) is commonly used to design and certify passive houses (Feist et al., 2007). In this thesis, the software is used to model the standard configuration and the *Passivhaus* configuration. An R implementation of PHPP is used for the MC simulation<sup>2</sup>. This implementation has been validated against the original PHPP by comparing the results for the standard configuration and the *Passivhaus* configuration. The underlying calculations concerning the energy demand of the buildings are based on a monthly method (Feist et al., 2007). The advantage of the monthly method is that it produces reliable results for the annual heating energy demand and is computationally cheap.

The central question of the presented case study concerns the consequences of different building design options on building performance (i.e., the annual heating energy demand per square meter floor area) and the corresponding cost-effectiveness (i.e., the net present value).

In the combined building performance and cost-benefit analysis it is analyzed whether and/or under what conditions the additional investment for improving the

<sup>2</sup>This implementation has been developed by the Fraunhofer Institute for Building Physics (IBP). The R scripts are adapted in order to fulfill the MC simulation requirements.

**Table 5.2:** Key requirements for the *Energieeinsparverordnung* from 2009 and the *Passivhaus* standard. The requirements of the *Passivhaus* standard are fixed requirements. The requirements of the *Energieeinsparverordnung* are dependent on the investigated building and are based on the compliance calculation for the *Energieeinsparverordnung* that was provided by the company. The EnEV and the *Passivhaus* standard use different definitions of floor area. For the table the definition of the the *Passivhaus* standard is used.

Criterion	EnEV 2009	<i>Passivhaus</i> standard	Unit
Specific annual heating demand ( $q_{\text{heat}}$ )	–	15	$\frac{\text{kWh}}{\text{m}^2\text{a}}$
Specific max. heating power ( $\dot{q}_{\text{heat}}$ )	–	10	$\frac{\text{W}}{\text{m}^2}$
Specific heat transfer coefficient ( $H'_T$ )	0.40	–	$\frac{\text{W}}{\text{m}^2\text{K}}$
Max. infiltration at 50 Pa ( $ACH_{50}$ )	3.0	0.6	$\frac{1}{\text{h}}$
Max. specific annual primary energy demand ( $q_{\text{prim}}$ ) without household electricity demand	122		$\frac{\text{kWh}}{\text{m}^2\text{a}}$
Max. specific annual primary energy demand ( $q_{\text{prim}}$ ) including household electricity demand		120	$\frac{\text{kWh}}{\text{m}^2\text{a}}$

standard configuration is cost-effective or not. Hence, the base case scenario is the standard configuration. One model evaluation was conducted with all parameters at the value for the standard configuration. The result coming from this model evaluation ( $q_{\text{heat,standard}} = 62.4 \text{ kWh/m}^2\text{a}$ ) is used to compute the energy saving. The approach described in Section 3.2.4 is used for the combined building performance and cost-benefit analysis. The economic efficiency is assessed on the basis of the necessary additional investment for the building that makes it better than the standard configuration (costs) and the savings based on the reduced energy consumption compared to the standard configuration (benefits). The period under consideration for the CBA is 25 years. This period has to be chosen depending on the expected lifetime and other project boundary conditions. It is assumed that the performance of the building and its energy demand is similar each year.

## 5.1.1 Quantification of Building Performance Analysis Input Uncertainty

### 5.1.1.1 Specification of the Building

In this case study, the building specification parameters are analyzed by means of an MC simulation. The characteristics of the building components are continuously varied between the values for the standard configuration and the values for the *Passivhaus* configuration. The continuous variation allows for the analysis of configurations that are intermediate between the standard configuration and the *Passivhaus* configuration. The U-values for the outside walls, the ground floor, the wooden ceiling, the roof, the windows, the outside door, the thermal bridge design, the measures for improving the air tightness and the HVAC equipment are varied in the MC simulation. The aim of this is to determine how the different building characteristics influence the energy performance and whether the improvements are cost-effective.

For the certification of passive houses, an air tightness test<sup>3</sup> needs to be conducted because the air tightness is a *Passivhaus* criterion (see Table 5.2). A ventilator is used to generate a pressure difference between the inside and the outside of the building of 50 Pa and the volume flow rate into the building is measured. The test result is the air change per hour under these test conditions ( $ACH_{50}$ ) and is an indicator of the air tightness. However, this test represents the air tightness at the moment the test is conducted and has measurement uncertainties. Over the analyzed period, the air tightness might decrease (e.g., damaged foil).

A ventilation system with a heat recovery unit is known to be essential for passive houses. The efficiency for the heat recovery unit ( $\eta_{HX}$ ) is also continuously varied from 0 (i.e., no heat recovery unit) to 0.92. Values of  $\eta_{HX}$  from 0 to 0.5 are not common for heat recovery units used in residential buildings. However, in this example it is assumed that parts of the building might be equipped with decentralized air handling units with heat recovery systems. In cases where not all spaces are equipped with these units, overall  $\eta_{HX}$  for the whole building can be in the range from 0 to 0.92.

The parameters for the distributions which are used for the sampling can be found in Table 5.3. Uniform distributions are used because all design specifications are assumed to have an equal probability. In the table  $\Delta U_{TB}$  is a U-value correction to account for thermal bridges.  $U_{ceiling}$  is the U-value for the ceiling that separates the living space and the attic.

---

<sup>3</sup>The air tightness test is often called Blower Door test after the company that invented the test.

**Table 5.3:** Specification of the building components selected for variation and their distributions.

Parameter	Distribution	min.	max.	Unit
$U_{\text{wall}}$	uniform	0.115	0.203	$\frac{\text{W}}{\text{m}^2\text{K}}$
$U_{\text{roof}}$	uniform	0.084	0.203	$\frac{\text{W}}{\text{m}^2\text{K}}$
$U_{\text{ceiling}}$	uniform	0.114	0.219	$\frac{\text{W}}{\text{m}^2\text{K}}$
$U_{\text{floor}}$	uniform	0.144	0.427	$\frac{\text{W}}{\text{m}^2\text{K}}$
$U_{\text{door}}$	uniform	0.690	1.000	$\frac{\text{W}}{\text{m}^2\text{K}}$
$U_{\text{window}}$	uniform	0.744	1.335	$\frac{\text{W}}{\text{m}^2\text{K}}$
$ACH_{50}$	uniform	0.6	3.0	$\frac{1}{\text{h}}$
$\Delta U_{\text{TB}}$	uniform	0.01	0.05	$\frac{\text{W}}{\text{m}^2\text{K}}$
$\eta_{\text{HX}}$	uniform	0.00	0.92	–

### 5.1.1.2 Boundary Conditions

To account for different scenarios, the boundary conditions are varied in addition to the specification of the building.

In the previous examples, the uncertainty in air change rates ( $ACH_{\text{vent}}$ ) had a great influence on the results. Therefore, they are also considered as uncertain in this case study. The variation is assumed to be similar to the case study of Chapter 3 because a residential building is analyzed in both case studies. The number of occupants ( $occ$ ) in the building is also varied. The number of occupants is directly linked to the internal gains. Five occupants is the default value in PHPP for the floor area of the building. This number is varied on the basis of a normal distribution with a standard deviation of 1. In PHPP, the standard value for the room temperature set point ( $T_{\text{set}}$ ) is 20°C. In this example, this parameter is assumed to be uniformly distributed within the interval [20, 22]°C because temperature set points in this range can often be found in residential buildings. Table 5.4 documents the distributions for the uncertain boundary conditions and their parameters.

### 5.1.2 Quantification of Cost-Benefit Analysis Input Uncertainty

In the CBA,  $q_{\text{heat}}$  is an uncertain input coming from the BPA with the PHPP implementation in R.  $q_{\text{heat}}$  is the effective energy in the zone and is transformed to final energy by a constant factor that comes from the EnEV compliance calculation.

**Table 5.4:** Uncertain boundary conditions selected for variation and their distributions.

Parameter	Distribution	$\mu$	$\sigma$	Unit
$ACH_{\text{vent}}$ (scaling factor)	normal	1	0.2	–
$occ$	normal	5	1	–
Parameter	Distribution	min.	max.	Unit
$T_{\text{set}}$	uniform	20	22	°C

In the following, the other CBA-related uncertainties are quantified.

The costs are implemented with cost functions that are based on data provided by the company that builds the house. Separate cost functions for the outside wall, the ground floor, the wooden ceiling, the roof, the windows, the outside door, the thermal bridge design, the measures for improving the air tightness and the plant equipment are used. The total cost for the additional investment is calculated with the cost functions and is based on the sampled values for the building specification. Hence, the cost functions are used to assign costs to the improved building characteristics. The sum of the costs is varied by means of a scaling factor to account for cost-related uncertainties. This scaling factor can be considered to be market-dependent uncertainty (i.e., prices can vary depending on the business cycle of the building industry). Furthermore, this variation captures cases where the specified design (e.g., U-value) is not implemented. Figure 5.2 shows the cost functions. The cost functions represent the cost differences compared to the standard configuration. Specific costs (i.e., EUR/m<sup>2</sup> component area) are used for  $U_{\text{roof}}$ ,  $U_{\text{ceiling}}$ ,  $U_{\text{floor}}$  and  $U_{\text{wall}}$ . All other cost functions represent the total additional cost. The cost functions for  $U_{\text{roof}}$ ,  $U_{\text{ceiling}}$  and  $U_{\text{floor}}$  have a step when the U-value is better than the one for the standard configuration. This step is implemented because of minimal insulation thicknesses. The cost functions for  $U_{\text{roof}}$ ,  $U_{\text{ceiling}}$ ,  $U_{\text{floor}}$  and  $U_{\text{wall}}$  are based on the additional insulation thickness required to achieve a lower U-value. The cost functions based on the additional insulation thickness can be found in Appendix A.3.

The additional investment cost is

$$IC = [c(U_{\text{wall}})A_{\text{wall}} + c(U_{\text{roof}})A_{\text{roof}} + c(U_{\text{ceiling}})A_{\text{ceiling}} + c(U_{\text{floor}})A_{\text{floor}} + c(U_{\text{door}}) + c(U_{\text{window}}) + c(ACH_{50}) + c(\Delta U_{\text{TB}}) + c(\eta_{\text{HX}})] IC_{\text{scale}} \quad (5.1)$$

where  $c(U)$  are the cost functions,  $A$  represent the surface areas and  $IC_{\text{scale}}$  is the scaling factor for the investment cost.  $IC_{\text{scale}}$  is assumed to be normally distributed with  $\mu = 1$  and  $\sigma = 0.1$ , hence  $IC_{\text{scale}} \sim \mathbf{N}(1, 0.1)$ . Similarly to the case study presented in Section 3.2.5.2 and for the same reasons, running costs, periodic replacement costs and maintenance costs are not considered in this example. Furthermore,

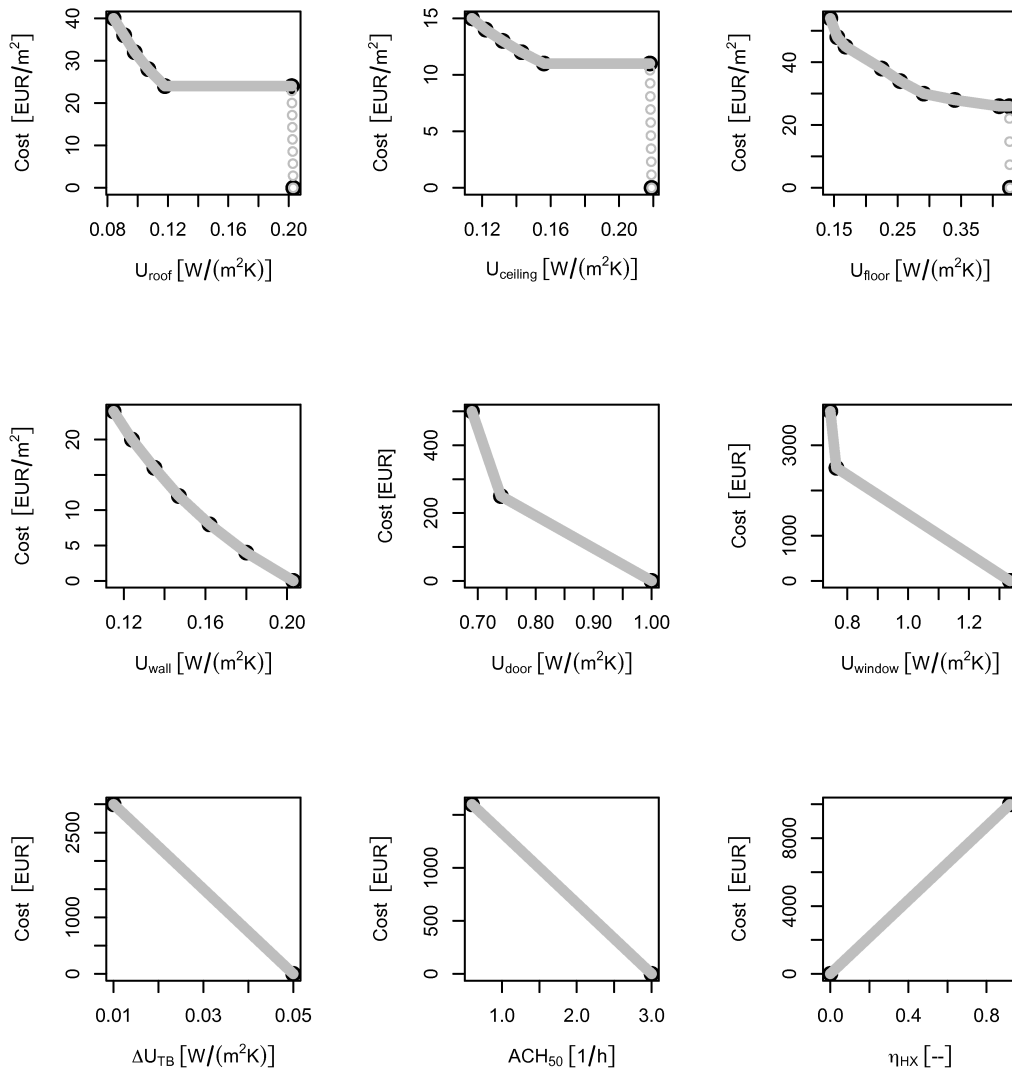


**Figure 5.2:** Cost functions dependent on the U-value of the building envelope elements and other building characteristics.

a potential investment cost reduction for the heating system due to the peak load reduction is not considered. It is assumed that this cost reduction is marginal as the peak power of a boiler in small residential buildings is usually determined by the domestic hot water demand. Hence, a cost reduction would be solely due to smaller radiators.

In this example, both UA and SA are considered to be equally important. UA

provides an impression of the variation that can be expected given the input variations. SA is a tool to identify the important parameters that can be changed in order to improve the design in a cost-effective way.

For the CBA, uncertain future boundary conditions are taken into account. It is assumed that the gas price (*GP*), the inflation rate (*Infl*) and the interest rate (*IR*) are uncertain. These uncertainties were quantified in Section 3.2.5.2 and are used similarly for this example.

## 5.2 Results and Discussion

### 5.2.1 Building Performance Analysis

#### 5.2.1.1 Uncertainty Analysis

In the UA, all parameters ( $k = 12$ ) are varied as described above. Given the variation of design specification (e.g., U-values), this is likely to result in large output uncertainties.

As in Chapters 3 and 4, convergence is analyzed with the mean and variance estimates as convergence criteria. The annual heating energy per floor area ( $q_{\text{heat}}$ ) is the primary model result for the building performance analysis (BPA). Figure 5.3 shows the convergence plot for the mean and the variance estimates. The horizontal line represents the results for the largest sample size (i.e., 1,024). These results are used as a reference (i.e., 40.7 kWh/(m<sup>2</sup>a) for the mean and 73.0 (kWh/(m<sup>2</sup>a))<sup>2</sup> for the variance). As for the previous examples the convergence criterion is the reference result  $\pm 5\%$ . Table 5.5 shows the results and their deviation from the reference values. The mean estimate converges already at a sample size of 8 (40.8 kWh/(m<sup>2</sup>a);  $+0.5\%$ )<sup>4</sup>. The variance estimate converges at a sample size of 64.

Figure 5.4 shows the normalized histogram of the result vector together with a PDF calculated with kernel density estimates and an ECDF for a sample size of 256. This sample size is chosen to be larger than the sample sizes for convergence of the mean and variance to obtain a reasonable histogram. The figure indicates how the result varies given the uncertainties in the inputs. It is evident that the criterion for reaching the *Passivhaus* standard is not reached in the MC simulation. This is due to the fact that the probability of all parameters simultaneously being close to their *Passivhaus* value is extremely small (i.e., high-dimensional parameter space). This high dimensionality is the reason that no simulation run exists where all design parameters are at their *Passivhaus* value. However, reaching the *Passivhaus* standard is not the main focus of this example, as the aim is to compare different design options.

---

<sup>4</sup>Note that this result is not shown in Table 5.5.

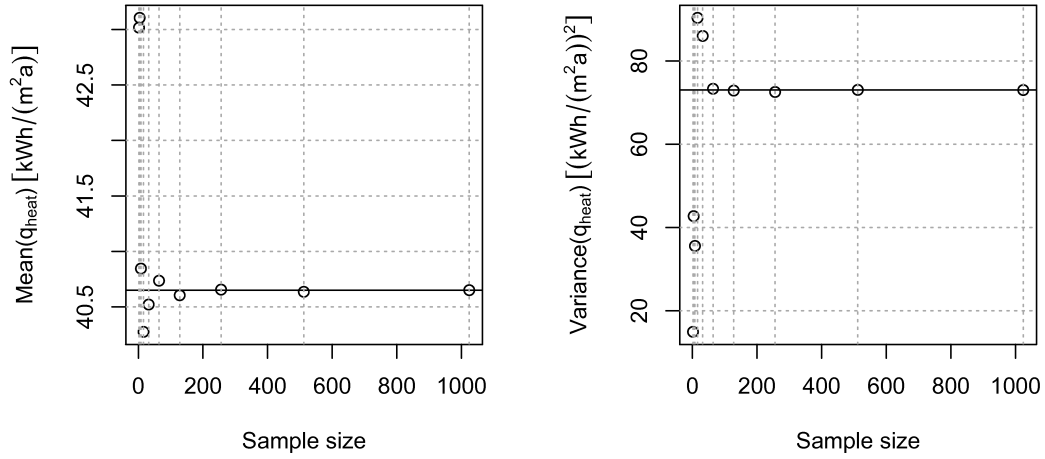


**Figure 5.3:** Convergence plot for the mean and variance estimates of  $q_{\text{heat}}$  (Note that the y-axes do not start at 0).

**Table 5.5:** Convergence of mean and variance estimates for  $q_{\text{heat}}$ . Gray cells indicate estimates that have converged to the reference value  $\pm 5\%$ .

Sample size	16	32	64	128	256	512	1,024
Mean estimate in kWh/(m²a)	40.3 -0.9%	40.5 -0.3%	40.7 +0.2%	40.6 -0.1%	40.7 0.0%	40.6 0.0%	40.7 0.0%
Variance estimate in (kWh/(m²a))²	90.3 +23.8%	86.0 +17.7%	73.3 +0.4%	72.9 -0.2%	72.5 -0.6%	73.0 +0.1%	73.0 0.0%

However, a design question might be:

- What is the probability to reach an annual heating energy demand per square meter of  $\leq 35$  kWh/(m²a)?

This heating energy demand approximately<sup>5</sup> corresponds to the value that would be required for a *KfW-Effizienzhaus 55* design. Buildings that comply with this design are eligible for special loans and financial support in Germany (KfW, 2013). As in the example presented in Chapter 3, the gray area under the PDF represents the probability  $q_{\text{heat}} \leq 35 \text{ kWh}/(\text{m}^2\text{a})$  and it is also indicated in the ECDF plot. Hence, the answer of the design question is approximately 27% probability for reaching the design goal.

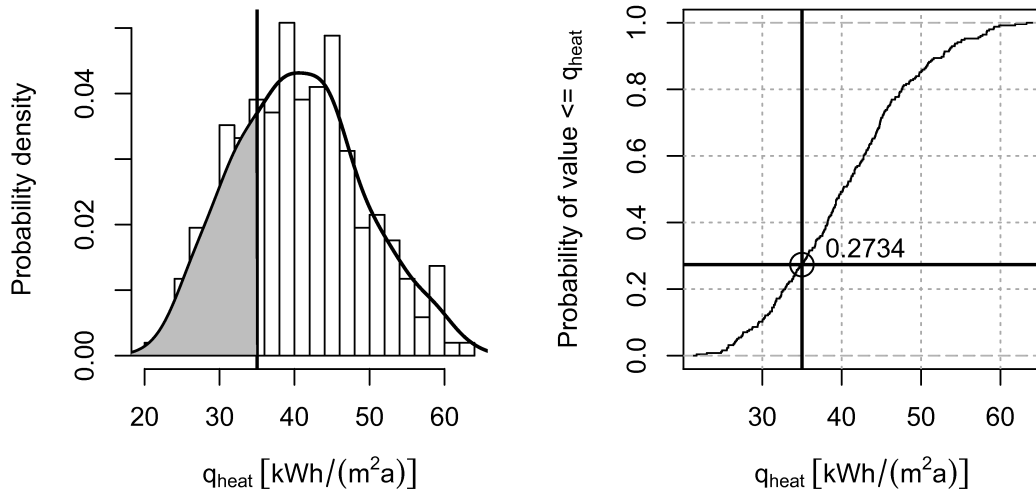


**Figure 5.4:** PDF and ECDF for the annual heating energy demand per square meter ( $N = 256$ ).

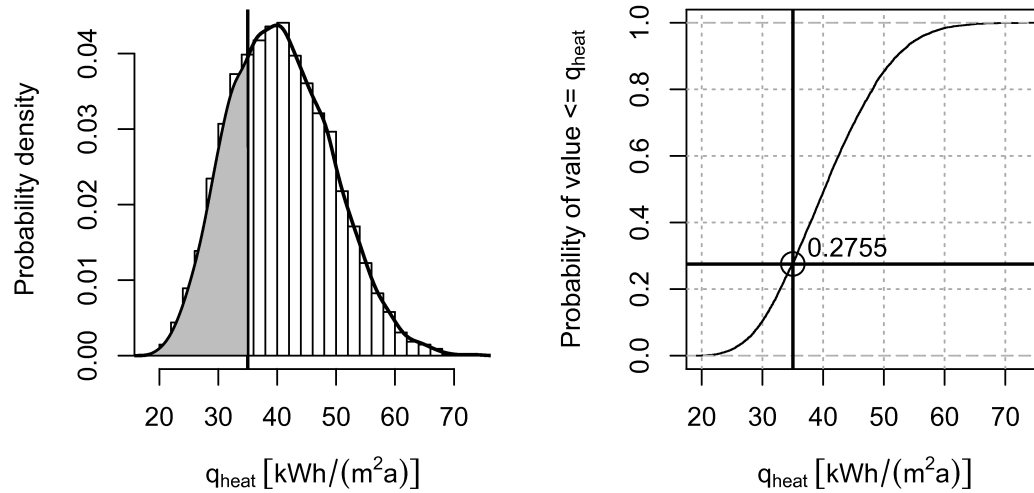
Table 5.6 presents the statistical summary for the result. To illustrate the advantage of larger sample sizes, statistics are also computed for  $N = 1,024$  and  $N = 8,192$ . This reveals that the minimum value and the maximum value changes when the sample size is increased whereas the other statistics are comparable.

Figure 5.5 shows the PDF and CDF of the results from the MC simulation with  $N = 8,192$ . It reveals that the histogram is smoother for large sample sizes. The accuracy requirements are case-dependent and determine the required sample size.

<sup>5</sup>The criteria are the annual primary energy demand per square meter and the specific heat transfer coefficient. For the analyzed building these criteria would be reached if  $q_{\text{heat}} < 35 \text{ kWh}/(\text{m}^2\text{a})$ .

**Table 5.6:** Statistical summary of the BPA result.

Statistic	Value for N=256	Value for N=1,024	Value for N=8,192
Mean	40.7	40.7	40.7
Variance	72.5	73.0	73.6
Standard deviation	8.52	8.54	8.58
Minimum	21.7	20.5	19.6
Lower (first) quartile	34.3	34.3	34.3
Median	40.2	40.1	40.2
Upper (third) quartile	45.9	46.3	46.6
Maximum	63.3	69.5	74.0

**Figure 5.5:** PDF and ECDF for the annual heating energy demand per square meter ( $N = 8,192$ ).

### 5.2.1.2 Sensitivity Analysis

The SA methodology is applied as described in Chapter 4.

#### Scatter Plot Method

Twelve input parameters are analyzed for the BPA. For the first impression, the scatter plot method is employed for all of them. The underlying sample size is 256

and the MC simulation results are the same as for the UA presented above. Figure 5.6 shows that the analyzed input parameters have a linear influence on the result (i.e., the red points fall on straight lines). As expected, a higher efficiency of the heat recovery unit leads to a lower heating energy demand and higher U-values result in a higher heating energy demand. The uncertain boundary conditions have a noticeable influence on the results. The higher  $T_{\text{set}}$  and  $ACH_{\text{vent}}$  are, the higher is  $q_{\text{heat}}$ . By contrast, an increase in  $occ$  causes  $q_{\text{heat}}$  to decrease, because the number of occupants determines the internal gains.

The ranking of the inputs according to their sensitivity (i.e., variance of the mean values of  $q_{\text{heat}}(X_i)$  over all slices) is shown in Table 5.7.  $\eta_{\text{HX}}$  is the most influential parameter in the analysis. The influence of  $U_{\text{door}}$  is likely to be overestimated because of a too small sample size<sup>6</sup>.  $U_{\text{ceiling}}$  and  $U_{\text{roof}}$  have minor influence on the result. This is likely to be due to the smaller proportion of the overall envelope area compared to the other building components. Furthermore, the U-values of these components are already relatively low in the standard configuration.

**Table 5.7:** Ranking of the parameters and variables according to their influence on the BPA result based on the scatter plot method ( $N = 256$ ).

Ranking	Parameter	Variance of mean values over slices in $\left(\frac{\text{kWh}}{\text{m}^2\text{a}}\right)^2$
1	$\eta_{\text{HX}}$	50.98
2	$T_{\text{set}}$	7.70
3	$U_{\text{door}}$	7.07
4	$U_{\text{wall}}$	6.18
5	$ACH_{\text{vent}}$	4.72
6	$\Delta U_{\text{TB}}$	4.23
7	$occ$	2.07
8	$U_{\text{floor}}$	2.05
9	$U_{\text{window}}$	2.00
10	$ACH_{50}$	1.19
11	$U_{\text{ceiling}}$	0.84
12	$U_{\text{roof}}$	0.65

---

<sup>6</sup>This can be due to artifacts in the sample set (zig-zag-pattern in the red points). However, the ranking will be compared with the ranking produced with the *EE* method.

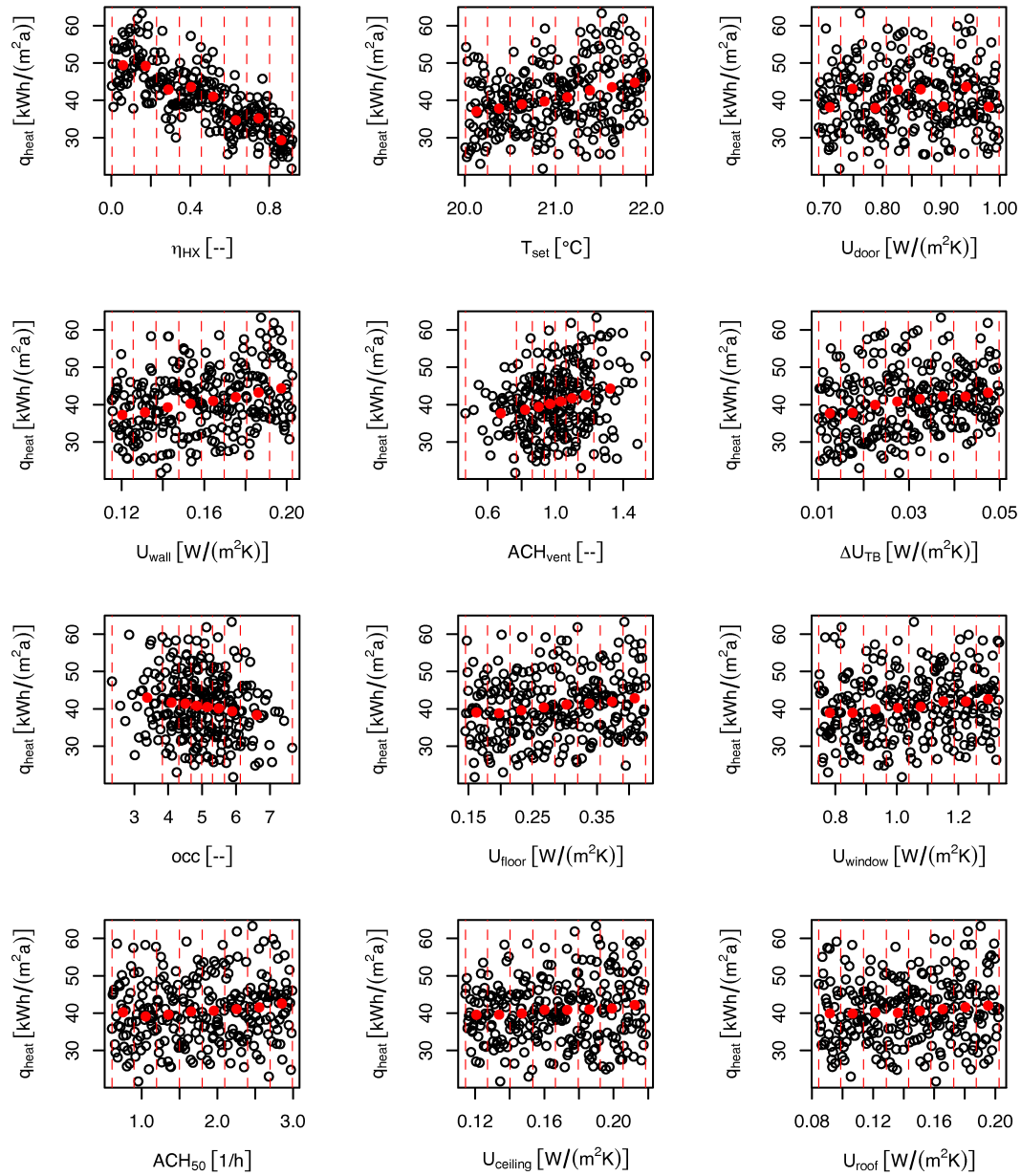


**Figure 5.6:** Scatter plots of the specific annual heating energy demand of the building versus the analyzed parameters. The dashed vertical lines divide the scatter plots into eight slices with 32 dots in each slice. The red points represent the mean value of  $q_{\text{heat}}(X_i)$  in each slice.

### Elementary Effects Method

In order to reduce the number of investigated parameters, the *EE* method is applied for screening. Table 5.8 contains the results for  $r = 8$ . Similar to the case study in Chapter 4, the  $\mu^*$  and  $\sigma$  estimates are plotted against each other in Figure 5.7. The figure reveals that most parameters do not have any significant interactions or nonlinearities in the PHPP implementation (i.e., no points above the line that indicates  $\mu^* = \pm 2 \frac{\sigma_i}{\sqrt{r}}$ ). However,  $\sigma$  for  $ACH_{\text{vent}}$  and  $\eta_{\text{HX}}$  is relatively high, which indicates the obvious interaction between these two parameters (i.e., a low  $ACH_{\text{vent}}$  reduces the influence of  $\eta_{\text{HX}}$  and vice versa). The six most influential parameters and variables can be identified (i.e.,  $\eta_{\text{HX}}$ ,  $T_{\text{set}}$ ,  $ACH_{\text{vent}}$ ,  $U_{\text{wall}}$ ,  $\Delta U_{\text{TB}}$  and  $U_{\text{floor}}$ ). As revealed by the scatter plot,  $\eta_{\text{HX}}$  has a dominant influence on the result. The ranking obtained by the *EE* method is not similar to that determined by the scatter plot method. As assumed before, the influence of  $U_{\text{door}}$  is overestimated in the ranking based on the scatter plot method. The required number of simulations for the *EE* method is  $r(k + 1) = 8 * (12 + 1) = 104$ .

**Table 5.8:** Ranking of the parameters and variables according to their influence on the BPA result based on the *EE* method ( $r = 8$ ).

Ranking	Parameter	$\mu^*$	$\sigma$
1	$\eta_{\text{HX}}$	21.57	4.0220
2	$T_{\text{set}}$	9.43	1.1572
3	$ACH_{\text{vent}}$	9.26	8.0555
4	$U_{\text{wall}}$	8.34	0.3090
5	$\Delta U_{\text{TB}}$	6.67	0.2362
6	$U_{\text{floor}}$	5.07	0.4790
7	$U_{\text{window}}$	4.75	0.4177
8	$occ$	3.87	0.6865
9	$ACH_{50}$	3.63	2.1840
10	$U_{\text{ceiling}}$	2.94	0.1166
11	$U_{\text{roof}}$	2.89	0.1118
12	$U_{\text{door}}$	0.35	0.0139

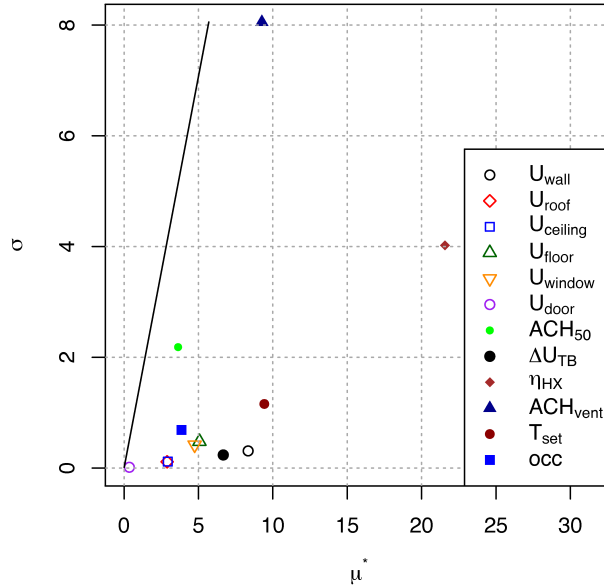


**Figure 5.7:**  $\mu^*$  and  $\sigma$  estimates plotted against each other (analyzed result:  $q_{\text{heat}}$ ;  $r = 8$ ).

### Variance-Based Method

The VB method is applied for the six most influential parameters that were identified from the initially analyzed parameters with the *EE* method. The non-influential design parameters are fixed to the value for the standard configuration and the boundary conditions are fixed to their expected value. The sample size ( $N$ ) of the underlying MC simulation is successively increased to analyze the convergence (Figure 5.8 and Table 5.9). The reference results come from the MC simulation with  $N = 2,048$ .

As in the case study in Chapter 4, the estimators for  $S_{T_i}$  converge faster than the estimators for  $S_i$ . However, the estimators for  $\sum S_i$  and  $\sum S_{T_i}$  both converge at  $N = 256$ . The total number of model evaluations required for  $N = 2,048$  is  $N(k + 2) = 2,048 * (6 + 2) = 16,384$ . The results reveal that the model is non-additive. However, only limited interactions between the parameters exist (i.e.,  $1 - \sum S_i$  is small).

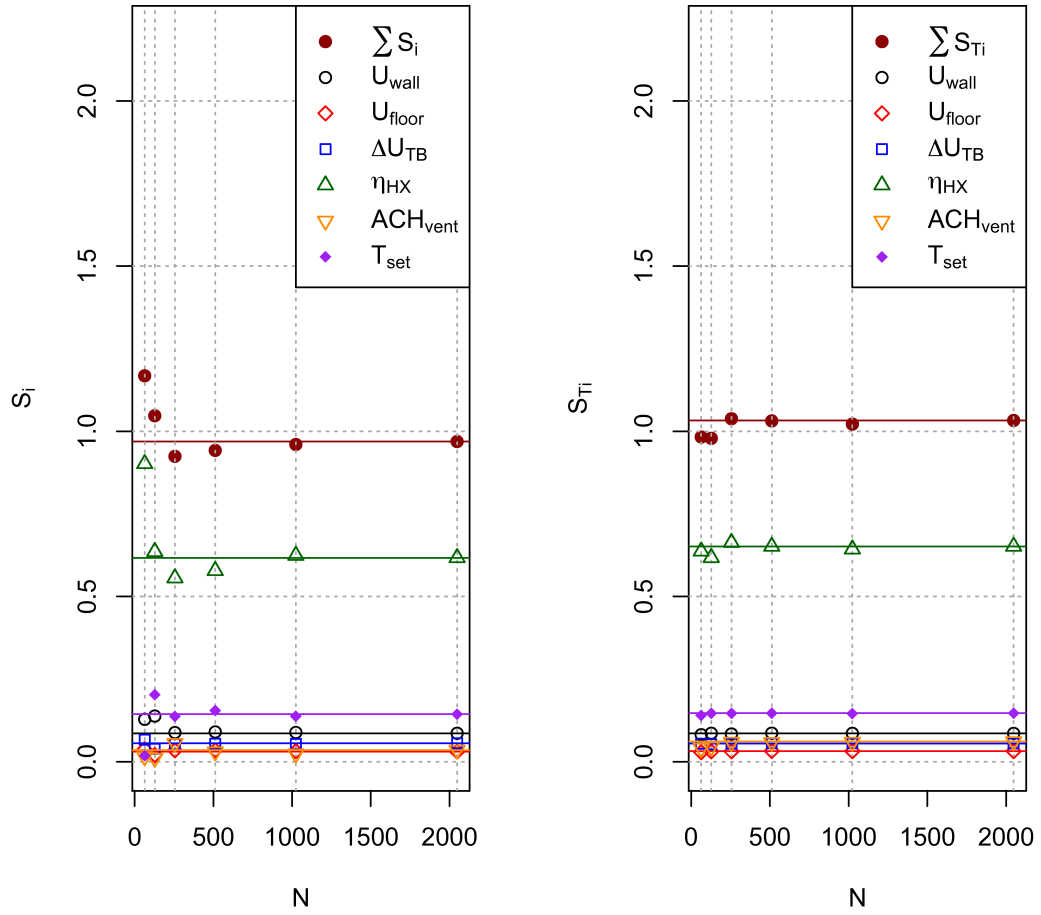


**Figure 5.8:** Convergence plot for the first-order ( $S_i$ ) and total ( $S_{Ti}$ ) sensitivity index estimates for the BPA.

**Table 5.9:** Convergence of  $S_i$  and  $S_{Ti}$  estimates for the BPA. Gray cells indicate estimates that have converged to the reference value  $\pm 5\%$ . The red cells indicate that the estimate falls within the target range but that convergence has not been reached.

$N$	64	128	256	512	1,024	2,048
	$S_i$					
$\eta_{HX}$	0.902 +46.1%	0.636 +3.0%	0.556 -9.9%	0.578 -6.3%	0.624 +1.1%	0.617 0.0%
$T_{set}$	0.018 -87.2%	0.203 +41.0%	0.138 -4.4%	0.155 +7.4%	0.138 -4.4%	0.144 0.0%
$U_{wall}$	0.128 +49.1%	0.138 +60.5%	0.088 +2.6%	0.090 +4.7%	0.089 +2.9%	0.086 0.0%
$\Delta U_{TB}$	0.066 +18.6%	0.039 -30.4%	0.053 -5.9%	0.054 -3.5%	0.054 -3.6%	0.056 0.0%
$ACH_{vent}$	0.016 -56.0%	0.011 -68.8%	0.055 +56.4%	0.031 -13.6%	0.024 -32.8%	0.035 0.0%
$U_{floor}$	0.038 +23.3%	0.020 -33.9%	0.034 +12.5%	0.035 +13.5%	0.032 +4.4%	0.031 0.0%
$\sum S_i$	1.168 20.5%	1.047 +8.1%	0.924 -4.6%	0.942 -2.8%	0.960 -0.9%	0.969 0.0%
	$S_{Ti}$					
$\eta_{HX}$	0.637 -2.3%	0.618 -5.2%	0.663 +1.7%	0.651 0.0%	0.643 -1.3%	0.652 0.0%
$T_{set}$	0.140 -4.5%	0.146 -0.5%	0.146 -0.3%	0.147 -0.1%	0.146 -0.9%	0.147 0.0%
$U_{wall}$	0.082 -4.6%	0.086 +0.4%	0.084 -2.1%	0.087 +0.8%	0.086 +0.2%	0.086 0.0%
$ACH_{vent}$	0.041 -33.4%	0.045 -26.8%	0.059 -3.2%	0.059 -3.4%	0.059 -2.8%	0.061 0.0%
$\Delta U_{TB}$	0.054 -2.0%	0.053 -4.5%	0.054 -2.1%	0.055 +0.3%	0.055 +0.3%	0.055 0.0%
$U_{floor}$	0.029 -9.9%	0.031 -2.5%	0.031 -2.0%	0.032 +0.9%	0.032 +0.3%	0.032 0.0%
$\sum S_{Ti}$	0.983 -4.8%	0.979 -5.2%	1.038 +0.5%	1.032 -0.1%	1.022 -1.1%	1.033 0.0%

Table 5.10 presents the ranking obtained by the VB method. The interactions between the investigated parameters lead to different rankings for  $S_i$  and  $S_{T_i}$  (only the ranking of  $\Delta U_{\text{TB}}$  and  $ACH_{\text{vent}}$  differs). Approximately 65% of the result variance can be explained by the variance of  $\eta_{\text{HX}}$  and corresponding interactions with other parameters.

**Table 5.10:** Ranking of the six most influential parameters and variables according to their influence on  $q_{\text{heat}}$  based on the VB method ( $N = 2,048$ ).

Ranking	Parameter	$S_i$	Parameter	$S_{T_i}$
1	$\eta_{\text{HX}}$	0.617	$\eta_{\text{HX}}$	0.652
2	$T_{\text{set}}$	0.144	$T_{\text{set}}$	0.147
3	$U_{\text{wall}}$	0.086	$U_{\text{wall}}$	0.086
4	$\Delta U_{\text{TB}}$	0.056	$ACH_{\text{vent}}$	0.061
5	$ACH_{\text{vent}}$	0.035	$\Delta U_{\text{TB}}$	0.055
6	$U_{\text{floor}}$	0.031	$U_{\text{floor}}$	0.032
	$\Sigma$	0.969	$\Sigma$	1.033

### Monte Carlo Filtering

For MCF, a threshold value has to be defined. As for the design question in the UA, a value of 35 kWh/(m<sup>2</sup>a) is chosen as the threshold. The threshold has to be determined such that a sufficient number of results fall in the behavioral subset and the non-behavioral subset to guarantee the required statistical reliability. The underlying MC sample size is 2,048 and the MC simulation results that were generated for the VB method are used. The behavioral subset contains 88 results and the non-behavioral subset contains 1,960 results. Figure 5.9 shows the MCF plot and reveals that  $\eta_{\text{HX}}$  has a significant influence on whether  $q_{\text{heat}}$  is less than or equal to 35 kWh/(m<sup>2</sup>a) or not. The lowest value for  $\eta_{\text{HX}}$  in the behavioral subset is approx. 0.5, which indicates that in the MC simulation,  $\eta_{\text{HX}}$  has to be higher than 0.5 to reach a  $q_{\text{heat}} \leq 35$  kWh/(m<sup>2</sup>a). For all other analyzed parameters, the minimal and maximal values of the behavioral and the non-behavioral subsets are closer together. As expected, it is visible that lower U-values lead to  $q_{\text{heat}} \leq 35$  kWh/(m<sup>2</sup>a). This is also true for low values for  $T_{\text{set}}$ .

Furthermore, a Kolmogorov-Smirnov test is conducted to compute the maximum distance between the behavioral and the non-behavioral ECDFs. Table 5.11 shows the results of the test and confirms the findings based on visual inspection of Figure 5.9. The  $p$ -values reveal that, given a significance level of 0.05, the null hypothesis (i.e., the results for the behavioral and the non-behavioral subset come from the same distribution) can be rejected for all parameters except  $ACH_{\text{vent}}$  (i.e., all  $p$ -

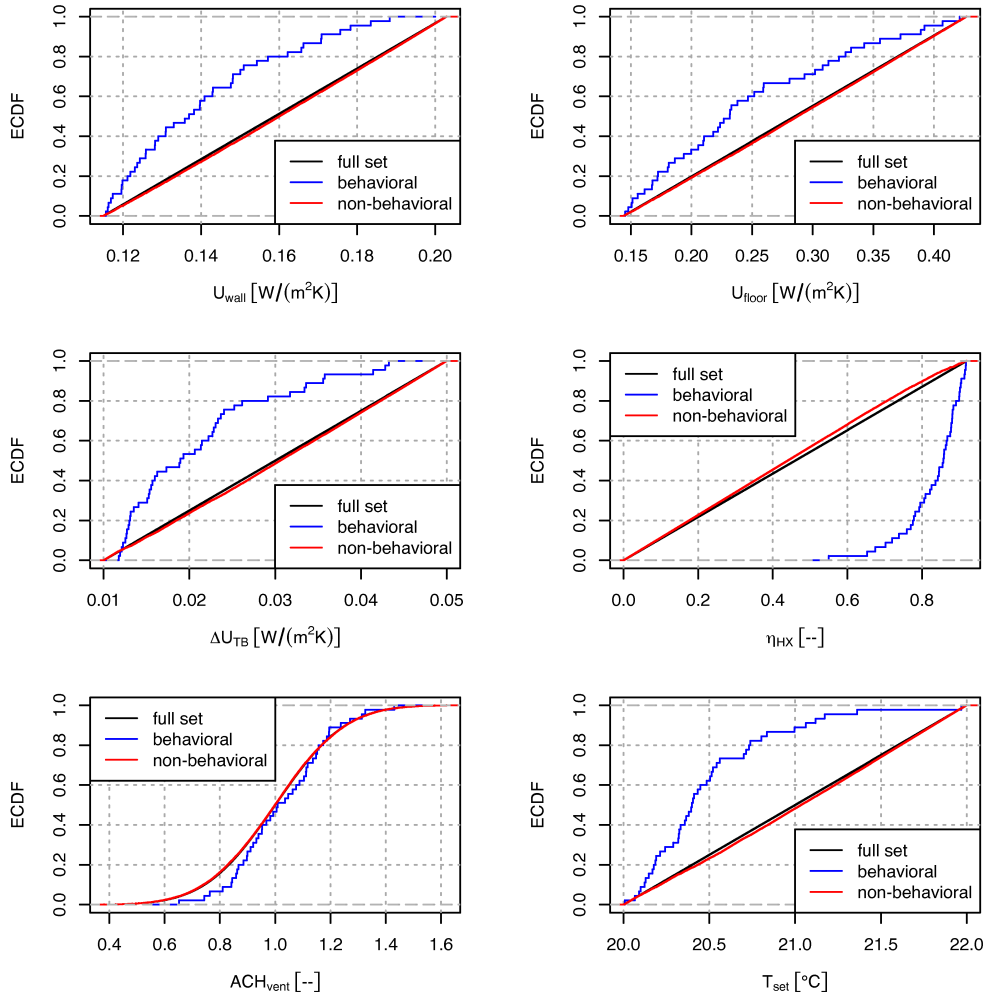


**Figure 5.9:** Monte Carlo filtering plot for the BPA ( $N = 2,048$ ).

values are below this threshold, which means that two distributions are significantly different and the analyzed simulation input has significant influence on the result). The ranking produced with the Kolmogorov-Smirnov test is different to the ranking based on the VB method. This can be due to the fact that the ranking is based on the influence of the parameters on values for  $q_{\text{heat}} \leq 35 \text{ kWh}/(\text{m}^2\text{a})$  and not on the overall influence on  $q_{\text{heat}}$ .

**Table 5.11:** Results of the Kolmogorov-Smirnov test for the BPA ( $N = 2,048$ ).

Ranking	Parameter	$D$	$p$ -value
1	$\eta_{\text{HX}}$	0.7342	$< 2.2\text{e-}16$
2	$U_{\text{wall}}$	0.4160	$4.381\text{e-}13$
3	$T_{\text{set}}$	0.4103	$9.756\text{e-}13$
4	$\Delta U_{\text{TB}}$	0.3811	$4.737\text{e-}11$
5	$U_{\text{floor}}$	0.2448	$8.262\text{e-}5$
6	$ACH_{\text{vent}}$	0.0770	0.7010

## 5.2.2 Combined Building Performance and Cost-Benefit Analysis

### 5.2.2.1 Uncertainty Analysis

For the combined building performance and cost-benefit analysis, 16 input parameters and variables are investigated.

Convergence is analyzed with the mean and variance estimates as convergence criteria. The net present value ( $NPV$ ) is the primary model result for the combined BPA and CBA. Figure 5.10 shows the convergence plot for the mean and the variance estimates. The horizontal line represents the results for the largest sample size (i.e., 4,096). These results are used as the reference (i.e., -9,510 EUR for the mean and  $1.830\text{e}+7$  EUR<sup>2</sup> for the variance). Again, the convergence criterion is the reference result  $\pm 5\%$ . Table 5.12 shows the results and their deviation from the reference values. The mean estimate converges at a sample size of 8 (-9,308 EUR; -2.1%)<sup>7</sup>. The variance estimate converges at a sample size of 1,024.

**Table 5.12:** Convergence of mean and variance estimates for  $NPV$ . Gray cells indicate estimates that have converged to the reference value  $\pm 5\%$ . The red cell indicates that the estimate falls within the target range but that convergence has not been reached.

Sample size	64	128	256	512	1,024	2,048
Mean estimate in EUR	-9,504 -0.1%	-9,592 +0.9%	-9,544 +0.4%	-9,565 +0.6%	-9,521 +0.1%	-9,526 +0.2%
Variance estimate in EUR <sup>2</sup>	$1.693\text{e}+7$ -7.5%	$1.769\text{e}+7$ -3.3%	$1.636\text{e}+7$ -10.6%	$1.687\text{e}+7$ -7.8%	$1.825\text{e}+7$ -0.3%	$1.803\text{e}+7$ -1.5%

<sup>7</sup>Note that this result is not shown in Table 5.12.

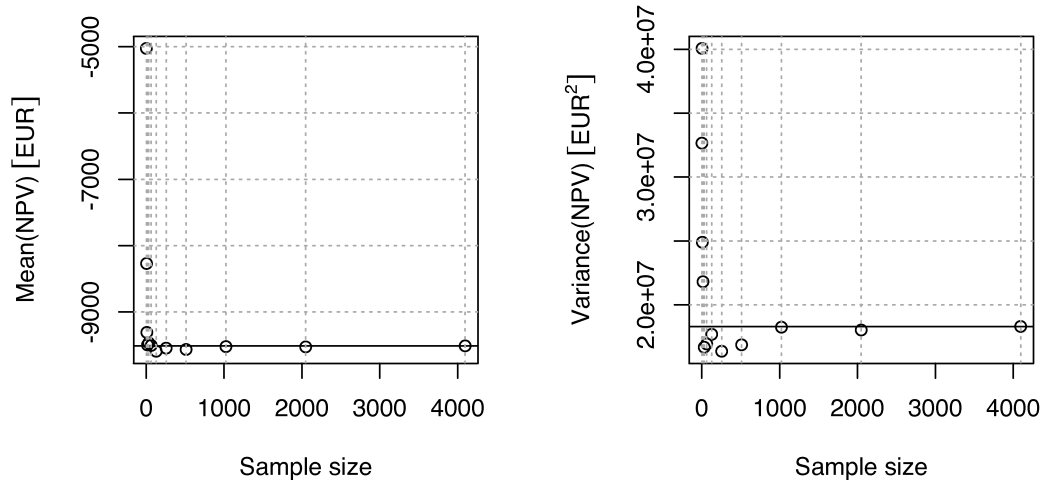


**Figure 5.10:** Convergence plot for the mean and variance estimates of the *NPV* (Note that the y-axes do not start at 0).

In this example the design question is:

- *What is the probability to reach a net present value of  $> 0$  EUR?*

A positive *NPV* indicates a profitable design compared to the standard design.

Figure 5.11 shows the normalized histogram of the result vector together with a PDF calculated with kernel density estimates and an ECDF for a sample size of 1,024. The answer to the design question is  $(1 - 0.9717) \approx 3\%$ .

Table 5.13 presents the statistical summary for the result for  $N = 1,024$  and  $N = 8,192$ . As for the separate BPA, this reveals that the minimum and the maximum values change when the sample size is increased whereas the other statistics remain comparable.

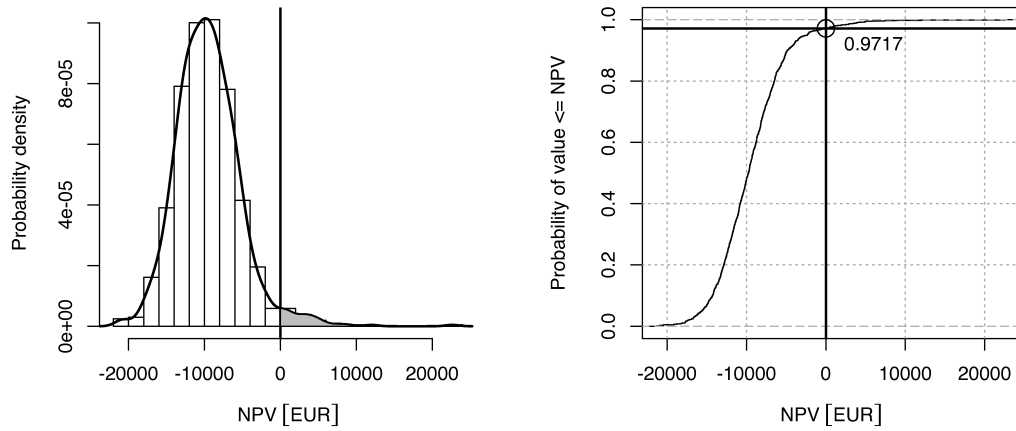


**Figure 5.11:** PDF and ECDF for the net present value ( $N = 1,024$ ).

**Table 5.13:** Statistical summary for the combined BPA and CBA result.

Statistic	Value for N=1,024	Value for N=8,192
Mean	-9,509	-9,502
Variance	1.825e+7	1.828e+7
Standard deviation	4,272	4,276
Minimum	-21,370	-23,540
Lower (first) quartile	-12,320	-12,190
Median	-9,755	-9,807
Upper (third) quartile	-7,117	-7,261
Maximum	22,640	23,210

### 5.2.2.2 Sensitivity Analysis

#### Scatter Plot Method

Similar to the UA, 16 input parameters are investigated for the SA of the combined BPA and CBA. Firstly, a scatter plot is used to gain a first impression of the analyzed parameters and their effects on the  $NPV$ . The underlying results are the same as for the UA ( $N = 1,024$ ). Figure 5.12 shows that most of the analyzed input parameters have a linear influence on the result (i.e., the red points fall approximately on straight lines). However, some nonlinearities seem to exist (e.g.,  $GP_{scale}$  and  $IR$ ). In Figure 5.12,  $GP_{scale}$  and  $Infl_{scale}$  are represented by the sampled values obtained by sampling from a uniform distribution in the interval  $[0,1]$ . These values were

the basis for calculating the values for the gas price and the inflation rate which are different in each year of the analyzed period (see Section 3.2.5.2 for details). Hence, the numbers for  $GP_{\text{scale}}$  and  $Infl_{\text{scale}}$  shown in the figure can be interpreted similarly to scaling factors (e.g.,  $GP_{\text{scale}} = 1$  is a scenario with high gas prices and  $GP_{\text{scale}} = 0$  is a scenario with low gas prices). As one would expect, the lower  $T_{\text{set}}$  and  $ACH_{\text{vent}}$  are, the higher is the  $NPV$  as these parameters decrease the heating energy consumption without associated cost. For the design parameters, better (i.e., lower) U-values lead to a lower  $NPV$ . Hence, the associated cost for an improved design does not seem to be cost-effective in the case study. It is also visible that the uncertain economic boundary conditions (i.e.,  $GP_{\text{scale}}$ ,  $IR$  and  $IC_{\text{scale}}$ ) have a dominant influence on the  $NPV$ .

The ranking of the inputs according to their sensitivity (i.e., variance of the mean values of  $NPV(X_i)$  over all slices) is shown in Table 5.14. It confirms the findings of the visual inspection.

**Table 5.14:** Ranking of the parameters and variables according to their influence on the combined BPA and CBA result based on the scatter plot method ( $N = 1,024$ ).

Ranking	Parameter	Variance of mean values over slices in EUR <sup>2</sup>
1	$GP_{\text{scale}}$	5,259,860
2	$IR$	4,527,628
3	$IC_{\text{scale}}$	3,000,237
4	$T_{\text{set}}$	887,729
5	$ACH_{\text{vent}}$	727,895
6	$U_{\text{floor}}$	645,369
7	$\eta_{\text{HX}}$	543,800
8	$U_{\text{wall}}$	393,246
9	$Infl_{\text{scale}}$	386,533
10	$occ$	217,264
11	$U_{\text{window}}$	138,721
12	$U_{\text{ceiling}}$	117,350
13	$\Delta U_{\text{TB}}$	65,294
14	$U_{\text{roof}}$	47,380
15	$ACH_{50}$	27,143
16	$U_{\text{door}}$	24,069

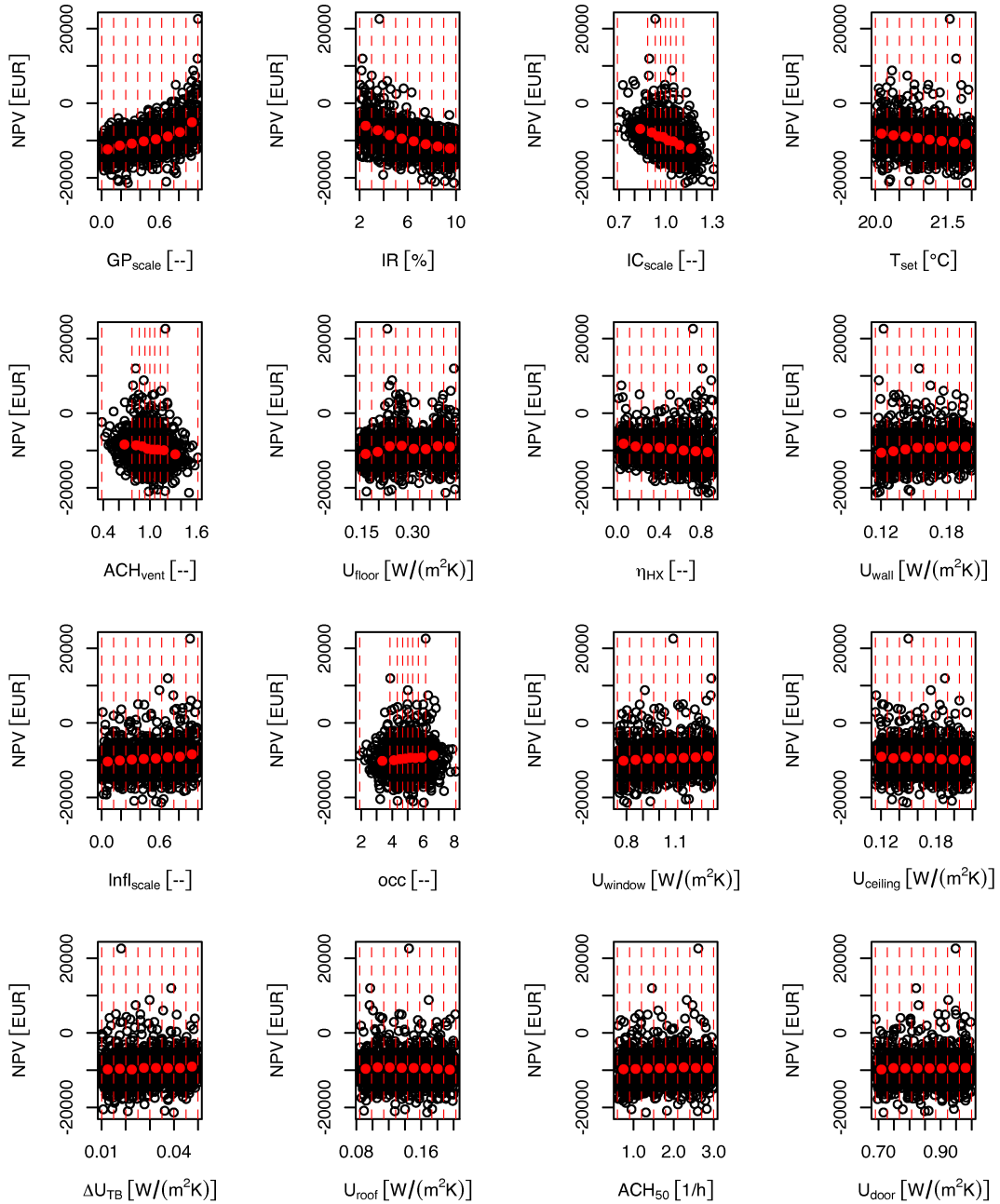


**Figure 5.12:** Scatter plots of the net present value versus the analyzed parameters. The dashed vertical lines divide the scatter plots into eight slices with 128 dots in each slice. The red points represent the mean value of the *NPV* in each slice.

### Elementary Effects Method

As a second step, the *EE* method is applied for screening. Table 5.15 contains the results for  $r = 8$  and in Figure 5.13 the  $\mu^*$  and  $\sigma$  estimates are plotted against each other. The table and the figure reveal that some parameters have interactions or nonlinearities in the combined BPA and CBA (e.g., the influential parameters  $GP_{\text{scale}}$ ,  $IR$ ,  $IC_{\text{scale}}$ ,  $\eta_{\text{HX}}$  and  $ACH_{\text{vent}}$ ). However, no points fall above the line that indicates  $\mu^* = \pm 2 \frac{\sigma_i}{\sqrt{r}}$ . As revealed by the scatter plot  $GP_{\text{scale}}$ ,  $IR$  and  $IC_{\text{scale}}$  have a dominant influence on the result. Unlike the other economic boundary conditions, the inflation rates have a lower influence. One reason for this is the periodic characteristic of the inflation rate that leads to high and low values in the course of the analyzed 25 years, meaning that the influence compensates itself. The ranking obtained by the *EE* method is not similar to that from the scatter plot method. However, the ranking produced by the *EE* method is considered to be more reliable for the factor-fixing application. The required number of simulations for the *EE* method is  $r(k + 1) = 8 * (16 + 1) = 136$ .

**Table 5.15:** Ranking of the parameters and variables according to their influence on the *NPV* based on the *EE* method ( $r = 8$ ).

Ranking	Parameter	$\mu^*$	$\sigma$
1	$GP_{\text{scale}}$	6,951	3,787
2	$IR$	6,584	2,984
3	$IC_{\text{scale}}$	5,915	2,074
4	$\eta_{\text{HX}}$	3,415	2,295
5	$T_{\text{set}}$	3,264	1,335
6	$ACH_{\text{vent}}$	2,939	1,799
7	$U_{\text{wall}}$	2,447	1,219
8	$Infl_{\text{scale}}$	1,483	519
9	$U_{\text{floor}}$	1,340	994
10	$occ$	1,262	374
11	$U_{\text{window}}$	969	587
12	$U_{\text{roof}}$	939	593
13	$\Delta U_{\text{TB}}$	877	636
14	$U_{\text{ceiling}}$	810	471
15	$ACH_{50}$	779	316
16	$U_{\text{door}}$	340	308

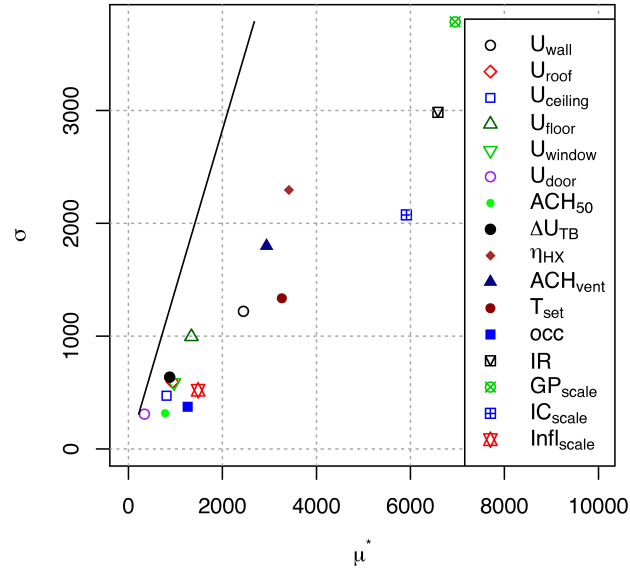


**Figure 5.13:**  $\mu^*$  and  $\sigma$  estimates plotted against each other (analyzed result: *NPV*;  $r = 8$ ).

### Variance-Based Method

The VB method is applied for the seven most influential parameters of the initially analyzed parameters that were identified with the *EE* method. Seven parameters were selected to include different types of parameters in the analysis. There are three uncertain economic boundary conditions (i.e.,  $GP_{scale}$ ,  $IR$  and  $IC_{scale}$ ), two uncertain building analysis parameters (i.e.,  $T_{set}$  and  $ACH_{vent}$ ) and two design parameters (i.e.,  $\eta_{HX}$  and  $U_{wall}$ ). The non-influential design parameters are fixed to the value for the standard configuration and the non-influential boundary conditions of the building analysis are fixed to their expected value. Furthermore, the ARIMA prediction for  $Infl_{scale}$  is assumed to be without uncertainties. The convergence of the estimators is analyzed (Figure 5.14 and Table 5.16). The reference results come from the MC simulation with  $N = 16,384$ . The total number of model evaluations required for  $N = 16,384$  is  $N(k + 2) = 16,384 * (7 + 2) = 147,456$ . This number is hard to afford for computationally expensive models. However, for this example, one model evaluation takes less than one second and therefore this large sample size was feasible. Compared to the previous examples, a larger sample size is required for convergence. It is surmised that this is caused by the nonlinearities and the fact that the model is non-additive.

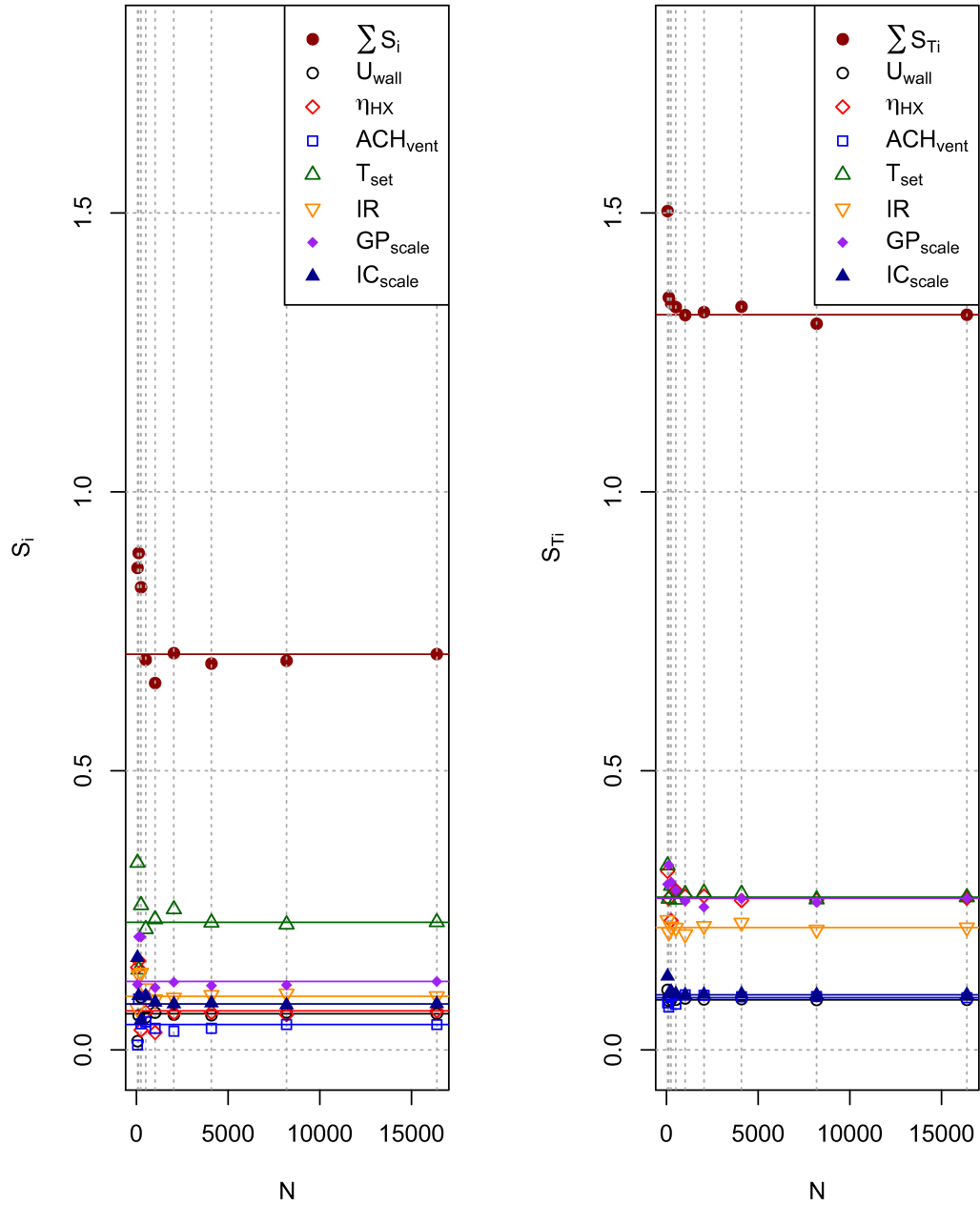


**Figure 5.14:** Convergence plot for the first-order ( $S_i$ ) and total ( $S_{Ti}$ ) sensitivity index estimates for the combined BPA and CBA.

**Table 5.16:** Convergence of  $S_i$  and  $S_{Ti}$  estimates for the combined BPA and CBA. Gray cells indicate estimates that have converged to the reference value  $\pm 5\%$ . The red cells indicate that the estimate falls within the target range but that convergence has not been reached.

$N$	<b>256</b>	<b>512</b>	<b>1,024</b>	<b>2,048</b>	<b>4,096</b>	<b>8,192</b>	<b>16,384</b>
	$S_i$						
$T_{\text{set}}$	0.259 +13.4%	0.216 -5.4%	0.234 +2.2%	0.252 +10.1%	0.228 -0.3%	0.225 -1.8%	0.229 0.0%
$GP_{\text{scale}}$	0.202 +65.1%	0.100 -18.0%	0.112 -8.9%	0.121 -1.0%	0.115 -6.2%	0.116 -5.1%	0.123 0.0%
$IR$	0.138 +43.8%	0.110 +14.7%	0.090 -5.9%	0.094 -2.4%	0.098 +2.3%	0.101 +4.9%	0.096 0.0%
$IC_{\text{scale}}$	0.053 -35.4%	0.096 +16.9%	0.085 +3.5%	0.082 -0.2%	0.084 +1.7%	0.080 -2.6%	0.082 0.0%
$\eta_{\text{HX}}$	0.035 -49.2%	0.068 -2.5%	0.031 -55.4%	0.066 -5.5%	0.067 -4.1%	0.063 -9.4%	0.070 0.0%
$U_{\text{wall}}$	0.094 +45.1%	0.058 -10.3%	0.067 +2.8%	0.063 -2.8%	0.062 -4.4%	0.067 +3.4%	0.065 0.0%
$ACH_{\text{vent}}$	0.047 +3.4%	0.050 +10.7%	0.039 -14.6%	0.033 -26.5%	0.039 -14.5%	0.045 +0.4%	0.045 0.0%
$\sum S_i$	0.829 +16.9%	0.699 -1.4%	0.657 -7.3%	0.711 -0.2%	0.692 -2.4%	0.697 -1.7%	0.709 0.0%
	$S_{Ti}$						
$T_{\text{set}}$	0.294 +7.4%	0.269 -1.6%	0.279 +2.1%	0.282 +3.0%	0.280 +2.2%	0.270 -1.4%	0.273 0.0%
$\eta_{\text{HX}}$	0.232 -14.7%	0.286 +5.2%	0.275 +1.3%	0.276 +1.5%	0.268 -1.5%	0.268 -1.2%	0.272 0.0%
$GP_{\text{scale}}$	0.300 +10.7%	0.286 +5.4%	0.266 -1.8%	0.256 -5.8%	0.271 -0.2%	0.265 -2.5%	0.271 0.0%
$IR$	0.221 +0.9%	0.219 -0.2%	0.207 -5.4%	0.222 +1.3%	0.228 +3.9%	0.215 -1.8%	0.219 0.0%
$IC_{\text{scale}}$	0.104 +5.8%	0.100 +1.4%	0.098 -0.3%	0.099 +0.5%	0.100 +1.3%	0.099 0.0%	0.099 0.0%
$ACH_{\text{vent}}$	0.096 +3.1%	0.082 -12.7%	0.099 +5.3%	0.098 +4.3%	0.095 +1.9%	0.095 +2.0%	0.094 0.0%
$U_{\text{wall}}$	0.090 +0.5%	0.090 +0.2%	0.092 +2.7%	0.090 +0.8%	0.091 +1.4%	0.089 -0.2%	0.090 0.0%
$\sum S_{Ti}$	1.338 +1.6%	1.331 +1.0%	1.317 0.0%	1.322 +0.4%	1.332 +1.1%	1.301 -1.2%	1.317 0.0%

Table 5.17 presents the ranking obtained by the VB method. The interactions between the investigated parameters lead to different rankings for  $S_i$  and  $S_{Ti}$ .  $GP_{\text{scale}}$ ,  $IR$  and  $\eta_{\text{HX}}$  have the most interactions with other parameters.  $1 - \sum S_i = 1 - 0.709 = 0.291$  indicates the detected interactions.

**Table 5.17:** Ranking of the seven most influential parameters and variables according to their influence on the  $NPV$  based on the VB method ( $N = 16,384$ ).

Ranking	Parameter	$S_i$	Parameter	$S_{Ti}$
1	$T_{\text{set}}$	0.229	$T_{\text{set}}$	0.273
2	$GP_{\text{scale}}$	0.123	$\eta_{\text{HX}}$	0.272
3	$IR$	0.096	$GP_{\text{scale}}$	0.271
4	$IC_{\text{scale}}$	0.082	$IR$	0.219
5	$\eta_{\text{HX}}$	0.070	$IC_{\text{scale}}$	0.099
6	$U_{\text{wall}}$	0.065	$ACH_{\text{vent}}$	0.094
7	$ACH_{\text{vent}}$	0.045	$U_{\text{wall}}$	0.090
	$\Sigma$	0.709	$\Sigma$	1.317

### Monte Carlo Filtering

For the separation into the behavioral and the non-behavioral bins, the threshold value for the  $NPV$  is defined to be 0 EUR, as a  $NPV \geq 0$  EUR indicates a cost-effective design. The underlying MC sample size is  $N = 16,384$  and the results produced for the VB method are used. The behavioral subset contains 663 results and the non-behavioral subset contains 15,721 results. Figure 5.15 shows the MCF plot and reveals that  $T_{\text{set}}$ ,  $IR$  and  $GP_{\text{scale}}$  have the greatest influence on whether  $NPV$  is greater than or equal to 0 EUR.

By investigating the figure, it becomes obvious that the design parameters (i.e.,  $U_{\text{wall}}$  and  $\eta_{\text{HX}}$ ) do not influence the  $NPV$  significantly, whereas the economic boundary conditions have a great influence.  $T_{\text{set}}$  is also influential. The findings are: low interest rates ( $IR$ ) lead to a positive  $NPV$  and for high gas prices ( $GP_{\text{scale}}$ ), a positive  $NPV$  is more likely. Both the interest rate and the gas price are very influential parameters in the analysis. The probability of an interest rate below 6% in the behavioral subset is higher than 90%, whereas the same probability in the non-behavioral subset is approx. 50%. In the case of the gas price, it is unlikely that a value for  $GP_{\text{scale}} < 0.2$  leads to a positive  $NPV$ . The investment costs have a visible influence on the  $NPV$  even though the influence is less than that for the gas price or the interest rates. As expected, it is evident that low values for  $T_{\text{set}}$  and  $ACH_{\text{vent}}$  lead to a positive  $NPV$ . Although  $\eta_{\text{HX}}$  has little influence on a positive  $NPV$ , it

can be seen that an increased heat exchanger efficiency increases the probability for a cost-effective design.

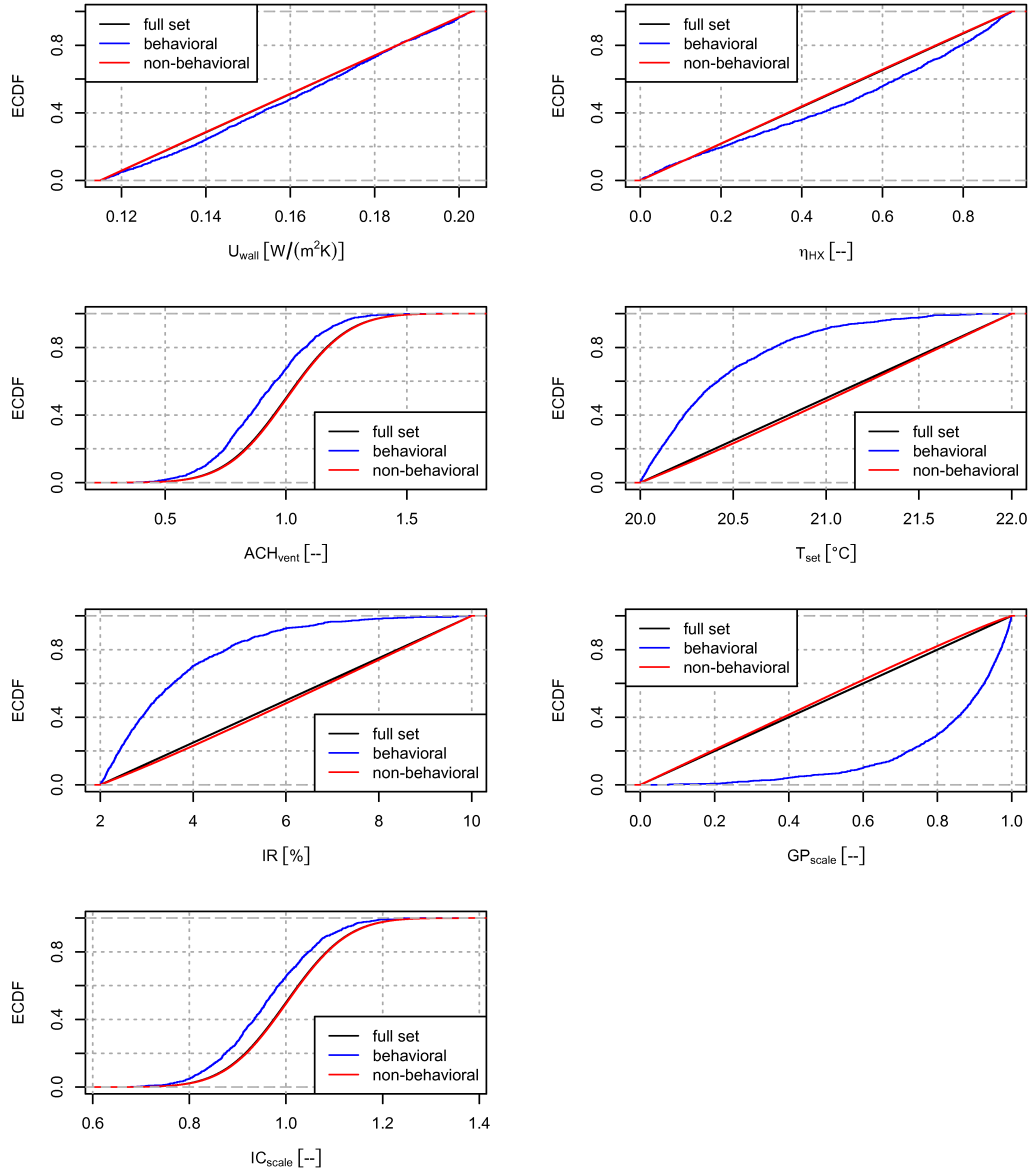


**Figure 5.15:** Monte Carlo filtering plot for the combined BPA and CBA ( $N = 16,384$ ).

Furthermore, a Kolmogorov-Smirnov test is conducted to compute the maximum distance between the behavioral and the non-behavioral ECDFs. Table 5.18 shows the results of the test and confirms the findings based on the visual inspection of Figure 5.15. The  $p$ -values reveal that, given a significance level of 0.05, the null hypothesis (i.e., the results for the behavioral and the non-behavioral subset come from the same distribution) can be rejected for all parameters (i.e., all  $p$ -values are below this threshold, which means that the two distributions are significantly different and the analyzed simulation input has a significant influence on the result) except  $U_{\text{wall}}$ . Also for this example, the ranking produced with the Kolmogorov-Smirnov test is different to the ranking based on the VB method. This is due to the fact that the ranking is based on the influence of the parameters on leading to values for  $NPV \geq 0$  EUR and not on the overall influence on the  $NPV$ .

**Table 5.18:** Results of the Kolmogorov-Smirnov test for the combined BPA and CBA ( $N = 16,384$ ).

Ranking	Parameter	$D$	$p$ -value
1	$GP_{\text{scale}}$	0.5560	$< 2.2\text{e-}16$
2	$IR$	0.4909	$< 2.2\text{e-}16$
3	$T_{\text{set}}$	0.4634	$< 2.2\text{e-}16$
4	$ACH_{\text{vent}}$	0.2028	1.016e-6
5	$IC_{\text{scale}}$	0.1757	$< 2.2\text{e-}16$
6	$\eta_{\text{HX}}$	0.1067	1.016e-6
7	$U_{\text{wall}}$	0.0508	0.07474

## 5.3 Summary

The methodology to conduct UA and SA for a building performance analysis and a combined building performance analysis and cost-benefit analysis was illustrated.

### 5.3.1 Building Performance Analysis

Given the varied design parameters and the assumed uncertainties in the boundary conditions for the BPA, the specific annual heating energy demand varies from 19.6 to 74.0 kWh/(m<sup>2</sup>a). Only approximately 28% of the model evaluations led to  $q_{\text{heat}} \leq 35$  kWh/(m<sup>2</sup>a).

The SA methodology was applied to analyze twelve parameters. The scatter plot provided a visual impression of the model structure and the influence of the investigated model inputs. This instrument could also be used for model validation (i.e., *Do all model parameters have the expected influence on the result?*). It was

also revealed that the ranking of the parameters included some unexpected results (i.e., strong influence of  $U_{\text{door}}$  even though the door represents a minor fraction of the overall envelope area).

The *EE* method was used for factor fixing and to gain a first impression of interactions between parameters or nonlinearities. On this basis,  $ACH_{\text{vent}}$  and  $\eta_{\text{HX}}$  were identified to interact. This is in accordance with prior knowledge based on the model. For these two steps of the methodology,  $256 + 104 = 360$  model evaluations would have been required if the model evaluations that were conducted for illustration reasons were not taken into account. Given modern computers and parallelization, this is affordable for most BPS models.

The six most influential parameters were further analyzed using the VB method. This revealed that the model is non-additive. However, only limited interactions between the parameters exist. Beside a reliable ranking according to the influence of the parameters on the result variance for factor prioritization and factor fixing, the VB method allows variance cutting. This is valuable if the aim is to reduce the result variance. Furthermore, it is possible to determine the sources of the variance (e.g., *Which fraction of the variance can be attributed to the uncertain boundary conditions and which fraction can be attributed to the variation of the design parameters?*). This allows a combined analysis without losing the power of analyzing separate effects.

In practice, a common question is: *Which design leads to energy efficiency or compliance with a certain standard (e.g., LEED or the Passivhaus standard)?* This application was illustrated with MCF. The question was: *Which parameter values lead to  $q_{\text{heat}} \leq 35 \text{ kWh}/(\text{m}^2 \text{ a})$ ?* It was revealed that an air handling unit with heat recovery is essential to reach the design goal. Furthermore, low U-values are important for a low energy demand, at which for the analyzed building,  $U_{\text{wall}}$  and  $\Delta U_{\text{TB}}$  are more important than  $U_{\text{floor}}$ .

### 5.3.2 Combined Building Performance and Cost-Benefit Analysis

A UA was conducted for the combined BPA and CBA. Three different types of parameters were investigated: uncertain economic boundary conditions, uncertain building analysis boundary conditions and design parameters. The *NPV* varies between -23,540 and +23,210 EUR. It was revealed that given the uncertain boundary conditions, a cost-effective design has only 3% probability when the building specification is improved toward a *Passivhaus* design. This would indicate that given the uncertainties and the economic boundary conditions in this case<sup>8</sup>, an energy-efficient design is not likely to be cost-effective. 3% probability will not be satisfactory in cases where the decisions are made purely on the basis of monetary values rather than for environmental reasons. This case study provides a good example of how

---

<sup>8</sup>Note that these statements are case-specific. However, similarities to many other newly built residential buildings exist.

UA and SA supplement each other because it demonstrates the analysis of why energy-efficient design is not cost-effective and how this situation can be improved.

For the SA of the combined BPA and CBA, all 16 parameters were analyzed. The scatter plot revealed that three uncertain economic boundary conditions have a strong influence on the result (i.e.,  $GP_{\text{scale}}$ ,  $IR$  and  $IC_{\text{scale}}$ ). Furthermore, the user behavior can improve the cost-effectiveness (i.e.,  $T_{\text{set}}$ ,  $ACH_{\text{vent}}$  and  $occ$ ). For the design parameters, the mean values in the slices (represented by the red points) reveal that the  $NPV$  decreases when the design specification becomes more advanced. This is due to the cost associated with improved design.

As for the separate BPA, the  $EE$  method was used for factor fixing and to gain a first impression on interactions between parameters or nonlinearities. It was revealed that in this case, the model contains more interactions and/or nonlinearities than the separate BPA. For these two steps of the methodology,  $1,024 + 136 = 1,160$  model evaluations would have been required if the model evaluations that were conducted for illustration reasons and for the convergence analysis were not taken into account.

For this example, the seven most influential parameters were further analyzed using the VB method. This revealed that the model is non-additive. The method provides a reliable ranking according to the influence of the parameters on the result variance for factor prioritization ( $S_i$ ) and factor fixing ( $S_{T_i}$ ) as well as information on variance cutting ( $S_{T_i}$ ). Furthermore, it is possible to determine the sources of the variance (e.g., *Which fraction of the variance can be attributed to the uncertain boundary conditions for the BPA and the CBA and which fraction can be attributed to the variation of the design parameters?*). The non-additivity leads to the fact that the ranking is different for the first-order sensitivity indices ( $S_i$ ) and the total sensitivity indices ( $S_{T_i}$ ). This example revealed that a convergence analysis is important as the required sample size required for convergence is not known *a priori*. 147,456 model evaluations were required for this analysis. This requires computationally cheap models and/or powerful computers.

MCF was used to further analyze the MC simulation results. In the example, it was revealed that the design parameters have much less influence on a positive  $NPV$  than the economic parameters and the occupant behavior (i.e.,  $T_{\text{set}}$ ). The future gas price ( $GP_{\text{scale}}$ ), the expected interest rate ( $IR$ ) and the room temperature set point ( $T_{\text{set}}$ ) are the most influential parameters. Also a significant reduction of the investment cost ( $IC_{\text{scale}}$ ) can lead to positive  $NPVs$ . However, compared to the other economic parameters, the investment cost is less influential than expected. This is due to the compound interest effect of the other parameters (gas price and interest rate). This information could lead to the conclusion that policy makers who want to promote energy-efficient buildings should provide low-interest loans instead of subsidies for the systems. The results also reveal that energy-efficient design is most effectively promoted by high prices for conventional energy sources.



# 6 Conclusions

## 6.1 Summary of Most Important Results

A review of the literature revealed that a holistic methodology and a toolchain for uncertainty and sensitivity analysis as outlined in this thesis did not exist. Hence, different methods were combined to define an overall methodology and a toolchain was developed.

The statistical foundations required for Monte Carlo based uncertainty and sensitivity analysis were introduced. Besides measures of location (e.g., arithmetic mean) and measures of spread (i.e., variance and standard deviation), quantiles to separate data into different subsets and the minimal and maximal values were identified as the most important descriptive statistics. Different distributions were introduced and advice was given on how they can be applied in a building performance simulation context. When the case studies were analyzed, quantifying the input uncertainty proved to be an important and difficult step within the analysis. The input uncertainty quantification influences the results of a subsequent uncertainty and sensitivity analysis. It is important to communicate and explain the assumptions to the decision makers involved in the analysis. Once the toolchain for uncertainty and sensitivity analysis as developed in this thesis is set up, an update of the input uncertainty quantification assumptions is straightforward and only requires more simulations for alternative results.

It was demonstrated that the chosen Monte Carlo based approach is applicable to different building performance simulation programs and models and that the computations can be parallelized. Different sampling techniques were analyzed with respect to their convergence speed and robustness. Sampling based on Sobol' sequences was identified to be the best sampling technique. This technique belongs to the family of quasi-random techniques that are rarely applied in the building performance simulation context<sup>1</sup>. The detailed comparison of sampling based on Sobol' sequences with other sampling techniques (i.e., random sampling, stratified sampling and Latin hypercube sampling) was novel in building performance simulation related research. It was revealed that the application of sampling based on Sobol' sequences reduces the required sample size and hence the number of necessary simulations, which improves the applicability of Monte Carlo techniques in practice.

---

<sup>1</sup>An exception is the recent research of Eisenhower et al. that was conducted in parallel to this thesis (e.g., Eisenhower et al. (2011, 2012a,b)).

The sample size for which a Monte Carlo simulation converges cannot be determined *a priori* so an empirical convergence test should be part of every Monte Carlo analysis. Therefore, guidelines on how to test for convergence were given. For most building performance simulation problems, convergence can be defined to be reached when the estimator falls within the range of the reference results  $\pm 5\%$ . A practicable Monte Carlo termination rule is when the estimator is within this range for the last three sample sizes where the largest sample size is used as the reference result. For this termination rule, the evaluated sample size is increased with  $N = 2^j$  where  $j \in \mathbb{N}^+$ . The practice of empirical convergence testing is based on the results of the case studies and contradicts the statements of Lomas and Eppel (1992) and Macdonald (2002), who state that Monte Carlo simulations usually converge at sample sizes of 60-80. In this thesis, it was shown that the model structure and the type of the estimator determines the required sample size. Visualization techniques were identified to be important to analyze Monte Carlo simulation results. Histograms, probability density functions and empirical cumulative distribution functions were used for a comprehensive analysis of stochastic output. A box plot, and a contour plot that indicates the probability density of time series data, were employed for analyzing stochastic time series output.

Three case studies were presented to illustrate different aspects of the methodology and its application. In the case study that investigated a residential building with a solar thermal collector (Section 3.2.5), the Monte Carlo simulation with sampling based on Sobol' sequences converged at a sample size of 128 for the variance estimate. Random sampling required a sample size of 1,024 until convergence. Hence, in this example, sampling based on Sobol' sequences allows a reduction of the computational cost of 87.5%.

Four methods for global sensitivity analysis that were identified as particularly useful in the context of building performance simulation were combined to a scalable methodology. This methodology covers all of the different sensitivity analysis applications (i.e., factor prioritization, factor fixing, variance cutting and factor mapping). The selected SA methods can be considered to be best practice and are based on recent research. The scatter plot method is used for a first visual inspection and ranking of the analyzed parameters. If many parameters are analyzed, the elementary effects method is used for identifying the most influential ones for further investigation (i.e., factor fixing). Furthermore, the  $\mu^*$ - $\sigma$  plot provides insights into the model structure (i.e., nonlinearities and interactions between parameters can be identified). As a subsequent step, the variance-based method is applied for detailed quantitative analysis with the computation of first-order and total sensitivity indices for the set of the most influential parameters. Finally, Monte Carlo filtering can be applied to determine the regions of the model inputs (e.g., design specifications and boundary conditions) that lead to the desired model output (e.g., an energy demand below a certain threshold).

The sensitivity analysis methodology was illustrated for implementing operational improvements of a large non-residential building and for the case study dealing with typical residential building design. For the application to residential building design (Chapter 5), sensitivity analysis was used to identify the most influential parameters. The efficiency of the heat recovery unit in the air handling unit was identified to be essential for the energy performance of the residential building (i.e., 65% of the variance in the results could be attributed to the variation of the efficiency and its interactions with the other parameters). The combination of all analyzed sensitivity analysis methods to a general methodology was novel to building research. Furthermore, Monte Carlo filtering was applied in a building performance simulation context for the first time, to the author's knowledge.

Furthermore, an approach for combining building performance simulation and cost-benefit analysis was proposed. With this approach, it is possible to perform an uncertainty analysis and a sensitivity analysis for this combination. This allows a direct comparison of the influence of the economic input (e.g., energy prices, interest rates) with building performance simulation input (e.g., insulation thickness, system efficiency). With this combination, it is possible to assess the cost-effectiveness of design options under consideration of uncertainties (decision support instrument). The proposed analysis can supplement the typical design process and offers insights into important aspects of the design and the role of the economic boundary conditions. The holistic approach to uncertainty analysis and sensitivity analysis for a combined building performance simulation and cost-benefit analysis was novel.

A combined building performance analysis and cost-benefit analysis was conducted for two case studies. The case studies revealed large variations of the net present value given the considered uncertainties. For the case study presented in Chapter 5, a sensitivity analysis was performed according to the proposed overall methodology. It revealed quantitatively that the design parameters had less influence on the cost-effectiveness than the economic parameters and the uncertainties introduced by occupant behavior.

Given the large variance of the results in the case studies, uncertainty analysis increased the transparency and helped to prevent a false sense of accuracy and engineering rigor. Hence, taking uncertainties into account can lead to robust design solutions or help to develop robust control strategies. Sensitivity analysis provided insights on the driving model parameters and variables. Furthermore, an analysis of the model structure was possible (e.g., analyzing linearity and additivity). However, the benefits come at the cost that the analysis may take longer than a classic building performance simulation and the computational cost increases. The methodology and the developed toolchain aims to reduce the additional effort. Furthermore, the links between uncertainty analysis and sensitivity analysis were illustrated. This holistic approach was introduced to building performance simulation within the framework of the research conducted for this thesis.

The investigated case studies are diverse and aim to illustrate different applications. They guide practitioners who want to apply the proposed uncertainty and sensitivity analysis methodology. R scripts for all steps of the methodology were developed (e.g., generating samples, performing statistical computations and arithmetic calculations, managing parallel simulations on different processor cores, processing simulation input and output and result visualization). Especially the parallelization improves the applicability and makes the full performance of modern multi-core processors accessible. This toolchain is now available for different operating systems (e.g., Windows, Linux, Mac OS X) and for different (building performance) simulation programs (e.g., Dymola, IDA ICE, ESP-r).

## 6.2 Guidelines for Applying the Developed Methodology

The application of the methodology can range from building design or operation to model development. The individual application defines the requirements. An important question is whether the main focus is uncertainty analysis or sensitivity analysis or both.

Figure 6.1 is a flow chart for conducting uncertainty analysis and sensitivity analysis for building performance simulation. The start of a sensitivity analysis is the definition of the outcome and the requirements for the analysis. This can be based on an agreement between the modeler and the client. The input uncertainty quantification is part of every analysis. In Section 2.2.4, a flow chart for this step was presented. If only an uncertainty analysis is the focus, the reader is referred to Chapter 3 and the case study within this chapter (Section 3.2.5). For guidelines on sensitivity analysis, more information can be found in Chapter 4 (a flow chart for sensitivity analysis in Section 4.2.5 and the case study in Section 4.2.6). For details on a combined uncertainty and sensitivity analysis, the reader is referred to Chapter 5. Depending on individual requirements, modifications of the methodology might be necessary.

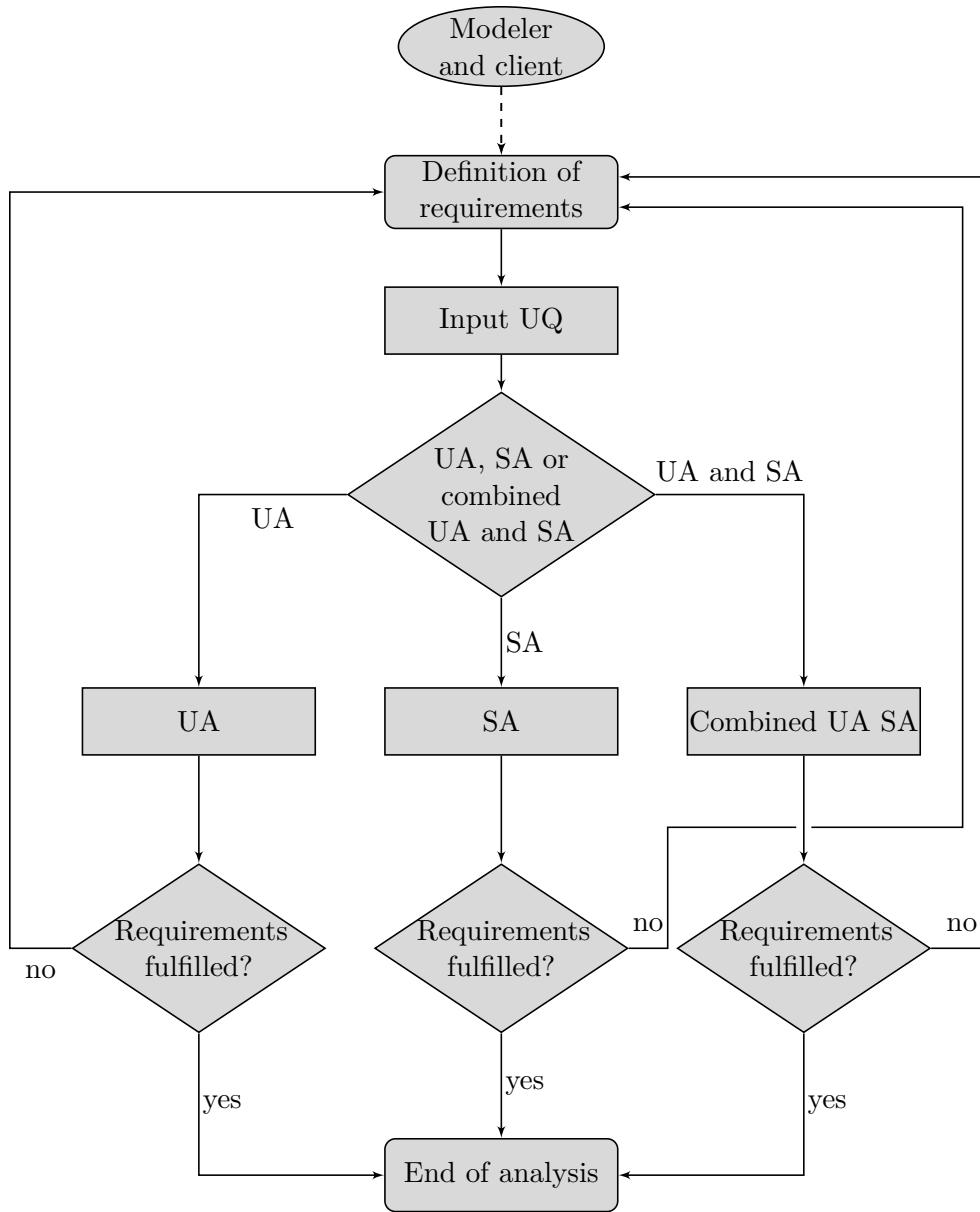


**Figure 6.1:** Flow chart for the overall uncertainty analysis and sensitivity analysis methodology (UQ = uncertainty quantification, UA = uncertainty analysis, SA = sensitivity analysis).

### 6.3 Potential of the Results and Expected Impact

The importance of uncertainty analysis and sensitivity analysis was also identified by the initiators of an Annex of the International Energy Agency, under the implementing agreement on Energy Conservation in Buildings and Community Systems (ECBCS). Annex 55 has the title, "Reliability of Energy Efficient Building Retrofitting - Probability Assessment of Performance & Cost (RAP-RETRO)". The author was invited to two Annex meetings to present some results of this thesis. This generated significant interest and a fruitful exchange of ideas.

Within the building performance simulation community, the interest in uncertainty and sensitivity analysis has increased in recent years. The outcome of this were special sessions on this topic at conferences organized by the International Building Performance Simulation Association (IBPSA). The author presented some of the results of this thesis at these conferences (e.g., Burhenne et al. (2010b, 2011)).

Several colleagues from the Fraunhofer Institute for Solar Energy Systems that were not involved in this work became interested to apply the proposed methodology for their ongoing projects. One example for this application was an analysis of thermo-active building systems (TABS). Uncertainty and sensitivity analyses were performed for a typical room equipped with TABS. It was analyzed how uncertainties influence the heating and cooling energy demand of the TABS system as well as the thermal comfort for the winter and summer case. This application demonstrated the applicability of the methodology and provided valuable results for research projects.

The sensitivity analysis methodology for the combined building performance and cost-benefit analysis can potentially be applied for supporting policy makers in promoting renewable and/or energy-efficient energy systems (i.e., *Which measures are most effective to improve energy efficiency at acceptable cost? or Which political boundary conditions promote renewable energy systems?*).

### 6.4 Outlook and Future Work

The quantification of input uncertainties proved to be a time-consuming and difficult part of the analysis. If uncertainty analysis and sensitivity analysis became common practice in building performance simulation, experience on the uncertainty quantification for different cases and requirements could be shared among researchers and practitioners. This is an iterative process, as uncertainty and sensitivity analyses commonly identify those parameters that have a great influence on the results. These parameters and variables have to be analyzed with special care, as correct uncertainty quantification is essential for influential model input. A database of typical cases and corresponding uncertainties could be established. Activities like the ECBCS Annex 55 mentioned above initiate exchange between researchers and

practitioners. This exchange is required for establishing a database on uncertainties that are common for building performance simulation input and advancing uncertainty and sensitivity analysis methods for building performance simulation.

Potentially, the methodology can be applied for more purposes than those illustrated in this thesis. This includes model development (e.g., analysis of parameter importance for model reduction, insights on model behavior under changing conditions, stress testing of new models and programs, generation of surrogate data with a white-box model to construct a black-box model), optimization (e.g., optimization in the face of uncertainty, identifying the influential parameters that are varied by the optimization algorithm) and in the development of methods for fault detection of HVAC systems (e.g., identification of fault-free scenarios taking uncertainties into account). Especially optimization in the face of uncertainty is a promising research topic. Jacob (2012), Hu and Augenbroe (2012) and Tanner and Henze (2013) aim to find control strategies for HVAC systems that take uncertainties into account. The methodology developed in this thesis is flexible and can be applied to all the mentioned cases and beyond. However, adaptations and changes might be necessary in order to fulfill certain requirements. Hence, an iterative application and improvement could advance the developed methodology.

The uncertainty and sensitivity analysis toolchain is based on various R scripts and interfaces between R and simulation programs (e.g., Dymola). The application requires knowledge of the R syntax and application. Adaptations in models and scripts (e.g., placing tokens in the simulation input text files, changing the investigated results and their post-processing) are prone to error. In the context of a single PhD thesis, improving the user friendliness beyond its current state is hardly possible. Furthermore, the transformation from a research tool into a user-friendly program with a graphical user interface is an iterative and time-consuming task. However, the R scripts proved to be reliable and can be used as a basis for future developments. Only the user front end and the interfaces to different building performance simulation programs have to be developed and improved.

The cost-benefit analysis aspects and the ARIMA predictions of future time series data were implemented from the viewpoint of a building performance simulation analyst. People working in the field of econometrics might be able to improve the details of the analysis.

As the reader may have observed, the application of uncertainty and sensitivity analysis to building performance simulation requires a basic understanding of statistical fundamentals. This is beyond the scope of many practitioners and the additional effort has to be justified by benefits of the analysis. This thesis aimed to illustrate the fundamentals and practical applications. However, it might take a while until uncertainty and sensitivity analysis is commonly part of building performance simulation in practice.

Potentially, the methodology can be applied for building performance simulation

applications that have not yet been mentioned. It is now up to other modelers to apply and adapt this methodology according to their needs, use cases or research questions. The same is true for many other disciplines beyond building performance simulation, wherever uncertainty and sensitivity analysis provide a better basis for decision-making.

# A Appendix

## A.1 Probability Distributions

### Discrete Uniform Distribution

A discrete uniform distribution describes the probability of  $n_e$  outcomes of an experiment where each outcome has the same probability (Evans et al., 2000, pp. 155-160). The PMF of the discrete uniform distribution is (Montgomery and Runger, 2003, p. 70)

$$p(x_i) = \frac{1}{n_e}. \quad (\text{A.1})$$

The expected value of a discrete uniform random variable  $X$  is

$$E(X) = \frac{b+a}{2} \quad (\text{A.2})$$

and the variance of this variable is

$$\text{Var}(X) = \frac{(b-a+1)^2 - 1}{12} \quad (\text{A.3})$$

where  $a, a+1, a+2, \dots, b$  are consecutive integers ( $a \leq b$ ) (Montgomery and Runger, 2003, p. 70).

Figure A.1 shows the PMF and the CDF of a discrete uniform distribution. In BPS this distribution can be used to select models. An example for this case is the distribution of the sky radiation where several empirical models can be applied (Macdonald, 2002, pp. 89-90). Since it is not possible to mix two models, the discrete distribution is the most applicable distribution in this case. The model selection is done on the basis of a categorical variable<sup>1</sup>. Another application could be the sampling of the number of occupants in a building. This is an example for a discrete quantitative variable.

### Uniform Distribution

The uniform distribution is a bounded continuous distribution where all possible values have the same probability (Evans et al., 2000, pp. 170-174). The PDF of the

---

<sup>1</sup>A categorical variable has a limited number of possible values. An example is gender with male and female as categories.

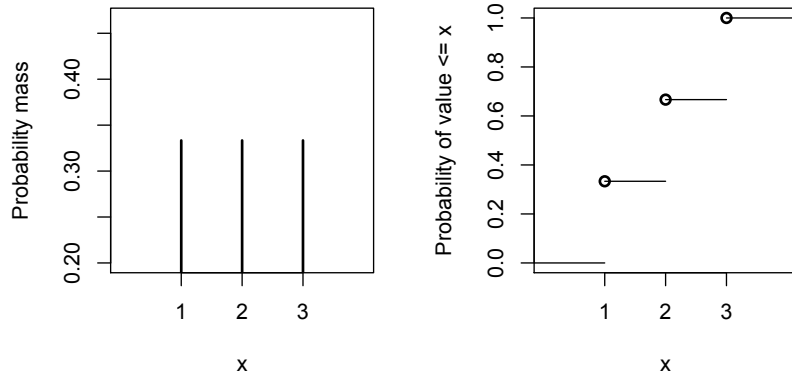


**Figure A.1:** PMF and CDF of a discrete uniform distribution.

uniform distribution is

$$p(x) = \frac{1}{b - a} \tag{A.4}$$

where  $a$  is the minimal and  $b$  is the maximal value.

The expected value of a continuous uniform random variable  $X$  over  $a \leq x \leq b$  is (Montgomery and Runger, 2003, p. 107)

$$E(X) = \frac{a + b}{2} \tag{A.5}$$

and the variance of this variable is

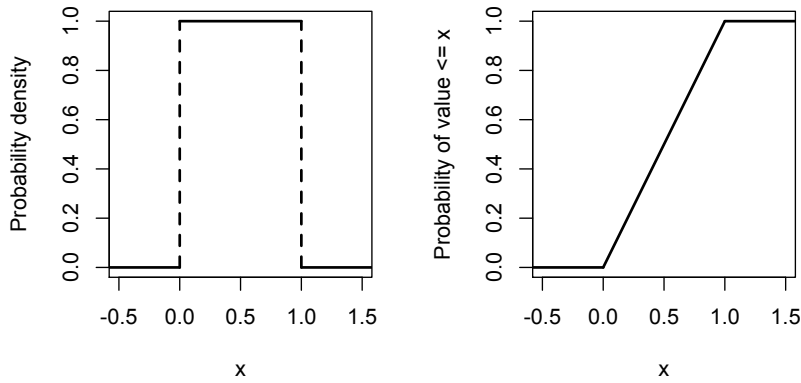
$$\text{Var}(X) = \frac{(b - a)^2}{12}. \tag{A.6}$$

Figure A.2 shows the PDF and the CDF of a uniform distribution. The uniform distribution might be the best guess when a parameter is poorly defined. However, this can lead to an overestimation of the uncertainty. Furthermore, the distribution is widely used for random number generation (Evans et al., 2000, pp. 170-174).

### Normal Distribution

The normal distribution is an unbounded distribution. Its expected value ( $\mu$ ) and its standard deviation ( $\sigma$ ) fully describe the distribution (Evans et al., 2000, pp. 145-150). The PDF is

$$p(x) = \frac{1}{\sigma\sqrt{2\pi}} \exp\left(-\frac{1}{2}\left(\frac{x - \mu}{\sigma}\right)^2\right). \tag{A.7}$$



**Figure A.2:** PDF and CDF of a uniform distribution  $U(0, 1)$ .

The expected value of a normal distributed random variable is

$$E(X) = \mu \quad (\text{A.8})$$

and the variance of this variable is

$$\text{Var}(X) = \sigma^2. \quad (\text{A.9})$$

Figure A.3 shows the PDF and the CDF of a discrete uniform distribution. The normal distribution is a widely used distribution. This can be explained with the central limit theorem. It describes the fact that under most conditions the distribution of a linear function of errors will tend to be normally distributed if the number of its components becomes large (Box et al., 2005, pp. 28-29). It is the most suitable distribution for measured physical data (Macdonald, 2002, pp. 91-92). Therefore it is a very useful distribution in the field of BPS where temperatures and lengths are often measured. It is symmetrical and unbounded (i.e., values can be negative). The latter can be a problem (e.g., a length can not be negative). A solution to this problem is to truncate the distribution. More details on this will be introduced in the course of this appendix.

### Log-normal Distribution

The log-normal distribution is non-symmetrical and unbounded towards positive infinity (Evans et al., 2000, pp. 129-133). The parameters of a log-normal distribution are  $\theta$  and  $\omega^2$ . These would be the mean and variance in the case of a normal

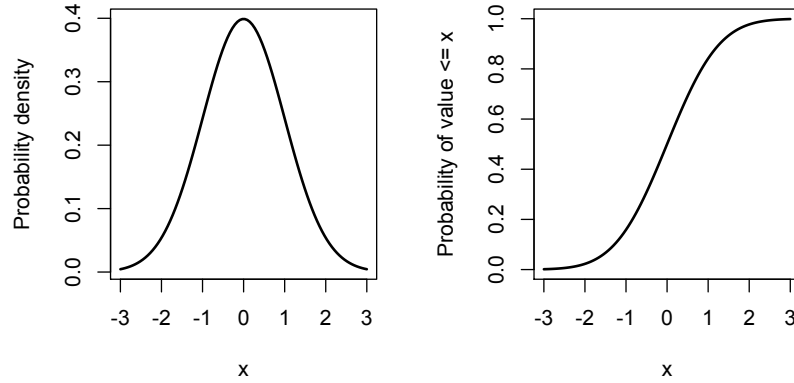


**Figure A.3:** PDF and CDF of a normal distribution  $\mathbf{N}(0,1)$ .

distribution which is not the case for the log-normal distribution<sup>2</sup>. In the case of the log-normal distribution the mean and variance are functions of  $\theta$  and  $\omega^2$  (see Equation A.11 and A.12). The PDF of  $X$  is (Montgomery and Runger, 2003, pp. 135-136)

$$p(x) = \begin{cases} \frac{1}{x\sigma\sqrt{2\pi}} \exp\left(-\frac{(\ln x - \theta)^2}{2\omega^2}\right) & x > 0 \\ 0 & x \leq 0 \end{cases}. \quad (\text{A.10})$$

The expected value of a log-normal random variable is (Montgomery and Runger, 2003, pp. 135-136)

$$E(X) = \exp\left(\theta + \frac{\omega^2}{2}\right) \quad (\text{A.11})$$

and the variance of this variable is

$$\text{Var}(X) = \exp\left(2\theta + \omega^2\right) \left(\exp\left(\omega^2\right) - 1\right). \quad (\text{A.12})$$

Figure A.4 shows the PDF and the CDF of a log-normal distribution. This distribution is suitable for describing parameters that cannot be negative. Examples are the metabolic rate of occupants or the air change rate of a building or zone (Macdonald, 2002, pp. 93-94).

---

<sup>2</sup>This fact can be confusing in the interpretation of the log-normal distribution.

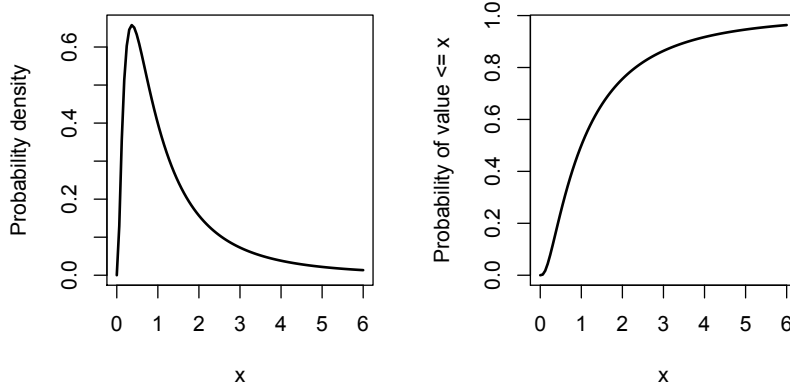


**Figure A.4:** PDF and CDF of a log-normal distribution  $\mathbf{L}(0, 1)$ .

### Triangular Distribution

The triangular distribution is a bounded distribution and can be described with a minimum ( $a$ ), a maximum ( $b$ ) and a most likely value ( $c$ ) (Evans et al., 2000, pp. 187-188). The PDF of the triangular distribution is

$$p(x) = \begin{cases} \frac{2(x-a)}{(b-a)(c-a)} & a \leq x \leq c \\ \frac{2(b-x)}{(b-a)(b-c)} & c \leq x \leq b \end{cases} \quad (\text{A.13})$$

The expected value of a triangular distributed random variable is

$$E(X) = \frac{a + b + c}{3} \quad (\text{A.14})$$

and the variance of this variable is

$$\text{Var}(X) = \frac{a^2 + b^2 + c^2 - ab - ac - bc}{18}. \quad (\text{A.15})$$

Figure A.5 shows the PDF and the CDF of a triangular distribution. The triangular distribution is an intermediate step between uniform distribution and normal distribution (Macdonald, 2002, pp. 94-95).

### Truncated Distributions

In BPS it might be necessary to restrict the domain of a distribution for uncertain simulation input (e.g., a normally distributed variable that can not be negative). A

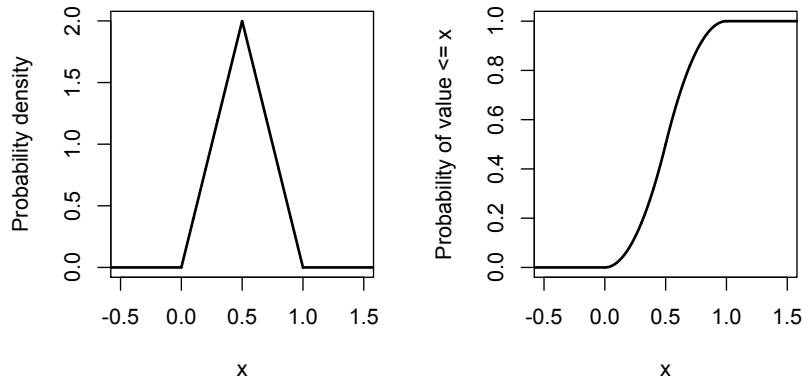


**Figure A.5:** PDF and CDF of a triangular distribution with  $a = 0$ ,  $b = 1$ ,  $c = 0.5$ .

truncated distribution is a conditional distribution of another probability distribution. It is important to truncate a distribution in a way that Equation 2.10 holds for the truncated distribution (i.e., normalizing the distribution that the total probability equals one). Therefore it is not possible to cut the domain without scaling the distribution up. The truncated distribution is

$$p(x) = \begin{cases} \frac{g(x)}{G(b)-G(a)} & a \leq x \leq b \\ 0 & \text{otherwise} \end{cases} \quad (\text{A.16})$$

where  $g(x)$  is the distribution that should be truncated and  $G(a)$  and  $G(b)$  are the values of the cumulative distribution function at  $a$  and  $b$  (Nadarajah and Kotz, 2006). An alternative is to cut a distribution at the borders of the domain ( $a, b$ ) and attribute the cut values to the borders. However, this overemphasizes these borders.

### Other Distributions

Many more distributions exist. The most relevant ones for BPS were introduced and further distributions are for example: Bernoulli distribution, binomial distribution, Poisson distribution, geometric distribution, categorical distribution and beta distribution. Readers interested in these and even more distributions are referred to Evans et al. (2000) or Montgomery and Runger (2003).

## A.2 Data Analysis for Identifying Dependence

In the literature, correlations are often employed to describe the dependence between different variables (e.g., Saltelli and Tarantola 2002; de Wit, 2003, p. 36; Herkel et al. 2008). Correlations have to be analyzed carefully to avoid incorrect interpretation of relationships between variables. A variable  $X$  can be correlated with a variable  $Y$ , solely because  $X$  and  $Y$  are each dependent on another variable  $Z$  (Good and Hardin, 2003, p. 134). Correlations can be quantified with Equation 2.5 and 2.6. The correlation coefficient is a measure of linear relationship between two random variables and can vary between  $-1$  and  $+1$ . If  $r_{XY} \neq 0$ , the analyzed variables are correlated. When  $|r_{XY}| = 1$ , the points of a scatter plot fall on a straight line. A positive  $r_{XY}$  indicates a positive gradient and a negative  $r_{XY}$  indicates a negative gradient of this line (Montgomery and Runger, 2003, pp. 174-177). If two variables are independent, it can be inferred that the variables are not correlated. However,  $r_{XY} = 0$  does not imply that the variables are independent (Montgomery and Runger, 2003, pp. 176-177). Therefore, the correlation coefficient is not suitable to test data for dependence among variables.

Tree diagrams can be used to analyze dependence (Montgomery and Runger, 2003, pp. 21-25). In tree diagrams, nodes represent events or certain outcomes of random variables. The path to a node indicates the probability for the event.

A test procedure involving tree diagrams consist of the following steps:

- (I) Plotting a scatter plot matrix of all variables and visually inspecting of the shape of the variables plotted against each other.
- (II) Discretization of the variables into appropriate intervals to obtain categorical variables.
- (III) Drawing a tree diagram with all categorical variables and the assumed (e.g. expert knowledge) dependence structure.
- (IV) Testing whether Equation 2.13 holds.

### A.3 Cost Functions

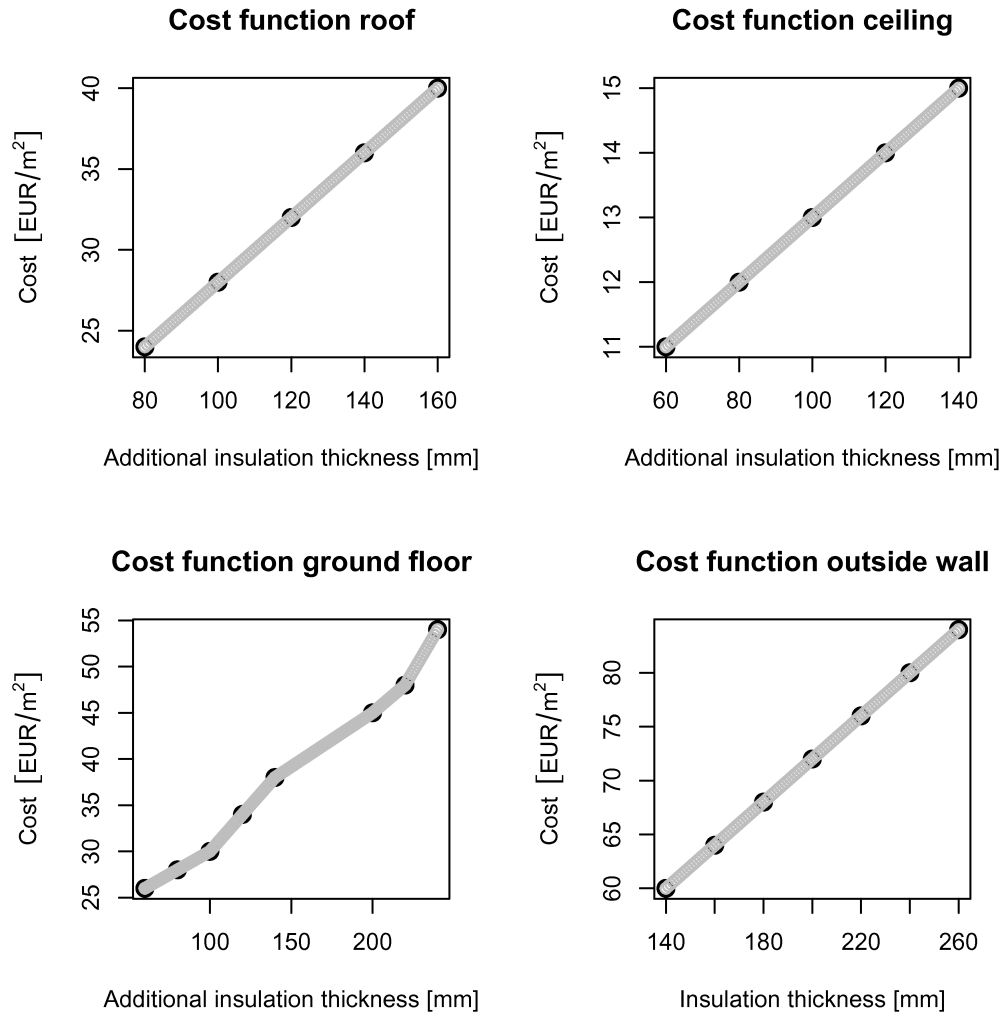


**Figure A.6:** Cost functions dependent on the additional insulation thickness of the building envelope elements.

## A.4 Nomenclature

### Abbreviations

AHU	Air handling unit
ANOVA	Analysis of variance
AR	Autoregressive
ARIMA	Autoregressive integrated moving average
ARMA	Autoregressive moving average
BPA	Building performance analysis
BPS	Building performance simulation
CBA	Cost-benefit analysis
CDF	Cumulative distribution function
COP	Coefficient of performance
CPU	Central processing unit
DAE	Differential algebraic equation
DHW	Domestic hot water
ECBCS	Energy Conservation in Buildings and Community Systems
ECDF	Empirical cumulative distribution function
EnEV	<i>Energieeinsparverordnung</i>
FF	Factor fixing
FM	Factor mapping
FP	Factor prioritization
GNU	General Public License
HVAC	Heating, ventilation and air conditioning
IBPSA	International Building Performance Simulation Association
IEA	International Energy Agency
LHS	Latin hypercube sampling
MA	Moving average
MC	Monte Carlo
MCF	Monte Carlo filtering
MSL	Modelica Standard Library
OAT	One-at-a-time
PDF	Probability density function
PHPP	<i>Passivhaus Projektierungspaket</i>
PMF	Probability mass function
Q-Q plot	Quantile-Quantile plots
R1-C1	One-resistor/one-capacitor
SA	Sensitivity analysis
SARIMA	Seasonal autoregressive integrated moving average

### Abbreviations *continued*

SHM	Simple hourly method
TABS	Thermo-active building systems
TMY	Typical meteorological year
UA	Uncertainty analysis
UQ	Uncertainty quantification
VB	Variance-based
VC	Variance cutting

### Notation

$a$	Coefficient of an autoregressive part of ARIMA model
$a$	Minimal value of a uniform or a triangular distribution
$A_{\text{ceiling}}$	Ceiling area
$A_{\text{floor}}$	Floor area
$A_{\text{NFA}}$	Net floor area
$A_{\text{roof}}$	Roof area
$A_{\text{wall}}$	Area of the outside walls
$A_{\text{win}}$	Window area
$ACH$	Air change rate
$ACH_{\text{AHU}}$	Air change rate provided by an air handling unit
$ACH_{\text{inf}}$	Infiltration air change rate
$ACH_{\text{nat}}$	Natural air change rate
$ACH_{\text{vent}}$	Scaling factor for the air change rate
$ACH_{50}$	Infiltration rate at 50 Pa pressure difference
$AIC$	Akaike information criterion
$\mathbf{A}$	Matrix used for the experimental design of the <i>EE</i> method and the VB method
$a_{ji}$	Element of matrix $\mathbf{A}$ ( $j$ indicates the row number and $i$ the column number)
$\mathbf{A}_B^{(i)}$	Matrix (all columns from matrix $\mathbf{A}$ except column $i$ that is from matrix $\mathbf{B}$ )
$A/V$	Envelope area to volume ratio
$b$	Coefficient of the MA part of an ARIMA model
$b$	Maximal value of a uniform or a triangular distribution
$B$	Behavioral subset of the simulation output
$\bar{B}$	Non-behavioral subset of the simulation output
$\mathbf{B}$	Matrix used for the experimental design of the <i>EE</i> method and the VB method

Notation *continued*

$b_{ji}$	Element of matrix $\mathbf{B}$ ( $j$ indicates the row number and $i$ the column number)
$c$	Mean value of a triangular distribution
$C$	Heat capacity
$c_p$	Specific heat capacity
$Ctrl_{\text{pump}}$	Control signal for a pump
$CF$	Future cash flow
$CF_t$	Future cash flow at time $t$
$c()$	Cost function
$\text{Cov}(\mathbf{X}, \mathbf{Y})$	Covariance of $\mathbf{X}$ and $\mathbf{Y}$
$d$	Order of differencing for an ARIMA model
$D$	Order of differencing for a seasonal ARIMA model
$D$	Kolmogorov-Smirnov test statistic (maximum distance between two CDFs)
$d_i$	Point sample density in an arbitrary hyper-parallelepiped
$d_t$	Theoretical sample density
$E(X)$	Expected value of a random variable $X$
$EE_i(\mathbf{X})$	Elementary effect for parameter $X_i$
$E_{\mathbf{X}_{\sim i}}(\cdot)$	Mean of argument $(\cdot)$ taken over all factors except $X_i$
$E_{\mathbf{X}_{\sim i}}(\text{Var}_{X_i}(Y \mathbf{X}_{\sim i}))$	Expected variance that would remain if all parameters apart from $X_i$ were treated as single-value estimates
$F(X   B)$	ECDF of the behavioral subset
$F(X   \bar{B})$	ECDF of the non-behavioral subset
$f()$	Generic function with its parameters in the bracket
$GP_{\text{scale}}$	Value to determine the gas price scenario
$g(x)$	Distribution to be truncated
$G(a)$	Value of the cumulative distribution function at $a$
$G(b)$	Value of the cumulative distribution function at $b$
$H_{\text{tr}}$	Heat transfer coefficient
$H'_T$	Specific heat transfer coefficient (EnEV)
$i$	Arbitrary index
$I_{\text{shad}}$	Irradiance threshold for control
$IC$	Investment cost
$IC_{\text{scale}}$	Scaling factor for the investment cost
$Infl_{\text{scale}}$	Value to determine the inflation rate scenario
$\overline{Infl}_t$	Average inflation rate from year 1 until year $t$
$Infl_z$	Inflation rate for year $z$ in the period from year 1 till year $t$
$IR$	Nominal interest rate
$j$	Arbitrary index

**Notation *continued***

$k$	Number of analyzed parameters
$l$	Number of levels for factorial design
$L$	Value of the likelihood function
$\ln(L)$	Log likelihood
$\mathbf{L}(\theta, \omega^2)$	Log-normal distribution with its parameters $\theta$ and $\omega^2$
$\dot{m}_{\text{DHW}}$	Mass flow rate of the domestic hot water
$\mathbf{M}_{\text{in}}$	Input matrix
$\mathbf{M}_{\text{out}}$	Output matrix
$ME_i$	Main effect of a factorial design
$N$	Sample size
$n$	Life cycle in years
$n_e$	Number of outcomes of an experiment
$n_{\text{ECDF}}$	Number of ECDFs
$n_i$	Number of sample points in an arbitrary interval
$n_{\text{SolFrac} \leq 20\%}$	Number of the MC simulation results for which the solar fraction is $\leq 20\%$
$n_{\text{sub}}$	Number of subsets
$NPV$	Net present value
$\mathbf{N}(\mu, \sigma)$	Normal distribution with its parameters $\mu$ and $\sigma$
$\mathbf{N}^+$	Set of positive natural numbers
$occ$	Number of occupants or the offset value for occupancy
$p$	Order of the AR part of an ARIMA model
$P$	Order of the seasonal AR part of an ARIMA model
$P_i$	Arbitrary hyper-parallelepiped
$\mathbf{p}$	Vector of parameters and/or constants
$PDV$	Present discounted value
$PDV_{\text{benefits}}$	Present discounted value of the benefits
$PDV_{\text{costs}}$	Present discounted value of the costs
$p(x)$	Probability mass function or probability density function
$P(\text{SolFrac} \leq 20\%)$	Probability that the solar fraction is $> 20\%$
$q$	Order of the MA part of an ARIMA model
$Q$	Order of the seasonal MA part of an ARIMA model
$q_{\text{prim}}$	Specific annual primary energy demand
$q_{\text{heat}}$	Specific annual heating energy demand
$q_{\text{heat,standard}}$	Specific annual heating energy demand for the standard configuration
$Q_{\text{collector}}$	Energy supplied by a solar collector
$Q_{\text{heat}}$	Heating energy
$\dot{Q}_{\text{heat}}$	Heating power
$\dot{Q}_{\text{int}}$	Internal heat gain

Notation *continued*

$Q_{\text{saving}}$	Potential energy saving
$Q_{\text{sol}}$	Solar heat gain
$Q_{\text{total}}$	Energy demand for space heating and DHW
$r$	Number of trajectories or blocks for the elementary effects method
$r_{XY}$	Pearson correlation coefficient
$s$	Number of strata for stratified sampling or LHS
$SE$	Standard error
$SolFrac$	Solar fraction
$StdDev(\mathbf{X})$	Standard deviation of a sample $\mathbf{X}$
$S_i$	First-order sensitivity index
$S_{Ti}$	Total sensitivity index
$t$	Time (and year at which cash flow takes place)
$T_e$	External temperature
$T_i$	Internal temperature
$T_{OAT}$	Outside air temperature
$T_{\text{set}}$	Set point temperature
$T_{\text{sup}}$	supply temperature in a heating circuit
$\bar{U}$	Mean U-value
$\mathbf{u}(t)$	Vector of input variables
$\mathbf{U}(a, b)$	Uniform distribution with its parameters $a$ and $b$
$U_{\text{ceiling}}$	U-value of the ceiling
$U_{\text{door}}$	U-value of the door
$U_{\text{floor}}$	U-value of the ground floor
$U_{\text{roof}}$	U-value of the roof
$U_{\text{wall}}$	U-value of the outside wall
$U_{\text{window}}$	U-value of the windows
$V_e$	Gross volume
$\dot{V}_{\text{ve}}$	Ventilation flow rate
$\text{Var}(\mathbf{X})$	Variance of a sample $\mathbf{X}$
$\text{Var}(X)$	Variance value of a random variable $X$
$\text{Var}_{X_i}(\cdot)$	Variance of argument $(\cdot)$ taken over the parameter $X_i$
$\text{Var}_{X_i}(\mathbb{E}_{\mathbf{X}_{\sim i}}(Y X_i))$	Expected reduction of the variance if $X_i$ were treated as a single-value estimate
$X$	Generic variable
$\bar{X}$	Arithmetic mean of a sample $\mathbf{X}$
$x_i$	Element of a sample $\mathbf{X}$
$\dot{\mathbf{x}}(t)$	Vector of differentiated state variables
$\mathbf{x}(t)$	Vector of state variables

**Notation *continued***

$X_i$	Generic variable or simulation input
$(X B)$	Subset of the simulation inputs that results in $B$
$(X \bar{B})$	Subset of the simulation inputs that results in $\bar{B}$
$\mathbf{X}_{\sim i}$	Matrix of all factors except $X_i$
$Y_i$	Generic model output
$Y(X_i)$	Result of a function evaluated at $X_i$
$y_t$	Output of ARIMA model
$\mathbf{y}(t)$	Vector of algebraic variables
$y^{(X_i)}$	Output of a OAT experiment for which parameter $X_i$ was perturbed
$\bar{Y}^-$	Average result of all simulation runs for which $X_i$ was at its low level (factorial design)
$\bar{Y}^+$	Average result of all simulation runs for which $X_i$ was at its high level (factorial design)
$z$	Year indicator
$\alpha$	Significance level
$\Delta$	Difference
$\Delta_i$	Difference (step size) in the domain of an input parameter analyzed with the <i>EE</i> method
$\Delta k_{\text{pump}}$	Hours of pump operation
$\Delta T$	Temperature difference
$\Delta T_{\text{set}}$	Offset value for the temperature set point
$\Delta U_{\text{TB}}$	U-value correction to account for thermal bridges
$\varepsilon$	Noise term
$\eta_{\text{HX}}$	Efficiency of the heat recovery unit of an AHU
$\mu$	Mean value as parameter for the normal distribution
$\mu_i$	Mean value for the elementary effects of one parameter
$\mu_i^*$	Mean value for the absolute values of the elementary effects of one parameter
$\rho_{\text{air}}$	Density of the air
$\sigma$	Standard deviation as parameter for the normal distribution
$\sigma_i$	Standard deviation for the elementary effects of one parameter
$\Omega$	Unit hypercube

# List of Figures

1.1	Energy flow paths in a building. . . . .	2
1.2	Classic building simulation approach versus building simulation approach with uncertainty analysis. . . . .	3
1.3	ANSI/ASHRAE Standard 140 reference case 600. . . . .	6
1.4	ANSI/ASHRAE Standard 140 reference results. . . . .	6
2.1	PDF and ECDF of a sample. . . . .	21
2.2	Q-Q plot. . . . .	22
2.3	Example of statistically independent inputs for a simulation model represented as a Bayesian network. . . . .	23
2.4	Example of dependent inputs for a simulation model represented as a Bayesian network. . . . .	24
2.5	Variation of set point values in a schedule. . . . .	26
2.6	Flow chart of the UQ process for simulation input. . . . .	31
3.1	Input and output of an MC simulation. . . . .	35
3.2	Two examples of sampling with a pseudo-random number generator. . . . .	38
3.3	Three-dimensional plot of the pseudo-randomly sampled points. . . . .	39
3.4	Three sampled parameters plotted against each other in pairs, for sample sets obtained by different sampling techniques. . . . .	40
3.5	Two examples of stratified sampling. . . . .	41
3.6	Scatter plot of a two-dimensional sample set obtained by stratified sampling. . . . .	42
3.7	Scatter plot of an LHS: $X_1$ vs. $X_2$ . . . . .	43
3.8	File system tree for the parallelization of an MC simulation. . . . .	46
3.9	Overview of the MC simulation with consecutively conducted BPS and CBA. . . . .	49
3.10	Contour plot of the simple mathematical model for $f(x_1, x_2)$ according to Equation 3.7. . . . .	51
3.11	3D-view of the building. . . . .	52
3.12	Variation of schedule values for air change rate ( $ACH$ ) and occupancy using scaling factors and offsets. . . . .	55
3.13	Time series for the inflation rate in Germany. . . . .	56

3.14	Box plot of the sampled values for the inflation rate used in the MC simulation. . . . .	58
3.15	Time series for the consumer gas price in Germany. . . . .	59
3.16	Box plot of the sampled values for the gas price used in the MC simulation. . . . .	60
3.17	Comparison of the mean and variance estimates, obtained by different sampling techniques applied to the evaluation of the simple mathematical model. . . . .	62
3.18	Comparison of ECDFs for the simple mathematical model with 100 repetitions, for four different sampling techniques. . . . .	64
3.19	PDF and ECDF for the simple mathematical model ( $N = 512$ ). . . . .	65
3.20	Comparison of the mean and variance estimates of the solar fraction, obtained by different sampling techniques applied to the evaluation of the BPS model. . . . .	67
3.21	Comparison of ECDFs for the four sampling techniques for the BPS model with 100 repetitions, for four different sampling techniques. . . . .	69
3.22	PDF and ECDF for the solar fraction ( $N = 256$ ). . . . .	71
3.23	Q-Q plot for the MC simulation result. . . . .	71
3.24	Convergence plot for the mean and variance estimates of the $NPV$ . . . . .	73
3.25	PDF and ECDF for the $NPV$ ( $N = 1,024$ ). . . . .	74
3.26	Time series for the heating power demand on January 13. . . . .	75
3.27	Box plot for the heating power demand on January 13. . . . .	76
3.28	Contour plot indicating the probability density for the heating power demand on January 13. . . . .	77
4.1	OAT design in a three-dimensional parameter space. . . . .	84
4.2	Full factorial design in a three-dimensional parameter space. . . . .	85
4.3	Example of a trajectory in a three-dimensional parameter space. . . . .	88
4.4	Mapping of input and output subsets. . . . .	90
4.5	Example of a radial sample in a three-dimensional parameter space. . . . .	95
4.6	Radial design for the elementary effects method. . . . .	96
4.7	Experimental design for the variance-based method. . . . .	100
4.8	Flow chart of the SA methodology. . . . .	102
4.9	SA methodology employed to improve building operation. . . . .	104
4.10	Floor plan of the building. . . . .	105
4.11	Schedules for the air change rates. . . . .	106
4.12	Convergence plot for the mean and variance estimates of the heating energy demand. . . . .	108
4.13	Scatter plots of heating energy demand of the building versus the analyzed parameters. . . . .	110
4.14	Convergence plot for the $\mu^*$ and $\sigma$ estimates. . . . .	112

---

4.15	$\mu^*$ and $\sigma$ estimates plotted against each other ( $r = 8$ ).	114
4.16	Convergence plot for the first-order ( $S_i$ ) and total ( $S_{Ti}$ ) sensitivity index estimates.	115
4.17	Monte Carlo filtering plot for the heating energy demand ( $N = 8,192$ ).	119
4.18	PDFs of $Q_{\text{heat}}$ for two operation strategies ( $N = 512$ ).	120
4.19	PDF and ECDF for the heating energy saving ( $N = 512$ ).	121
4.20	Carpet plot of the measured data in the building.	122
5.1	Analyzed residential building.	126
5.2	Cost functions dependent on the U-value of the building envelope elements and other building characteristics.	131
5.3	Convergence plot for the mean and variance estimates of $q_{\text{heat}}$ .	133
5.4	PDF and ECDF for the annual heating energy demand per square meter ( $N = 256$ ).	134
5.5	PDF and ECDF for the annual heating energy demand per square meter ( $N = 8,192$ ).	135
5.6	Scatter plots of the specific annual heating energy demand of the building versus the analyzed parameters.	137
5.7	$\mu^*$ and $\sigma$ estimates plotted against each other (analyzed result: $q_{\text{heat}}$ ; $r = 8$ ).	139
5.8	Convergence plot for the first-order ( $S_i$ ) and total ( $S_{Ti}$ ) sensitivity index estimates for the BPA.	140
5.9	Monte Carlo filtering plot for the BPA ( $N = 2,048$ ).	143
5.10	Convergence plot for the mean and variance estimates of the $NPV$ .	145
5.11	PDF and ECDF for the net present value ( $N = 1,024$ ).	146
5.12	Scatter plots of the net present value versus the analyzed parameters.	148
5.13	$\mu^*$ and $\sigma$ estimates plotted against each other (analyzed result: $NPV$ ; $r = 8$ ).	150
5.14	Convergence plot for the first-order ( $S_i$ ) and total ( $S_{Ti}$ ) sensitivity index estimates for the combined BPA and CBA.	151
5.15	Monte Carlo filtering plot for the combined BPA and CBA ( $N = 16,384$ ).	154
6.1	Flow chart for the overall uncertainty analysis and sensitivity analysis methodology.	163
A.1	PMF and CDF of a discrete uniform distribution.	168
A.2	PDF and CDF of a uniform distribution $\mathbf{U}(0, 1)$ .	169
A.3	PDF and CDF of a normal distribution $\mathbf{N}(0, 1)$ .	170
A.4	PDF and CDF of a log-normal distribution $\mathbf{L}(0, 1)$ .	171
A.5	PDF and CDF of a triangular distribution with $a = 0$ , $b = 1$ , $c = 0.5$ .	172

A.6 Cost functions dependent on the additional insulation thickness of the building envelope elements. . . . .	174
--	-----

# List of Tables

2.1	Probability distributions and possible application in BPS context. . .	20
3.1	Comparison of computers. . . . .	34
3.2	Building parameters. . . . .	52
3.3	Parameters selected for variation and their distributions for the BPS.	54
3.4	ARIMA model parameters for the inflation rate. . . . .	57
3.5	ARIMA model parameters for the gas price. . . . .	59
3.6	Parameters selected for variation and their distributions for the CBA.	61
3.7	Convergence of mean and variance estimates for the simple mathematical model to the analytically determined values. . . . .	63
3.8	Kolmogorov-Smirnov test results for the simple mathematical model.	65
3.9	Statistical summary of the result for the simple mathematical model ( $N = 512$ ). . . . .	66
3.10	Convergence of mean and variance estimates for the BPS model. . .	68
3.11	Kolmogorov-Smirnov test results for the BPS model. . . . .	68
3.12	Distribution parameters for the MC simulation result. . . . .	72
3.13	Statistical summary of the BPS result ( $N = 256$ ). . . . .	72
3.14	Convergence of mean and variance estimates for the combined BPS and CBA. . . . .	73
3.15	Statistical summary of the result for the combined BPS and CBA ( $N = 1,024$ ). . . . .	75
4.1	Overview SA methods. . . . .	93
4.2	Building parameters. . . . .	103
4.3	Building zones and their HVAC equipment. . . . .	105
4.4	Parameters selected for variation and their distributions. . . . .	107
4.5	Convergence of mean and variance estimates for the SA MC simulation.	109
4.6	Ranking of the parameters and variables according to their influence on the BPS result based on the scatter plot method ( $N = 128$ ). . . .	111
4.7	Convergence of $\mu^*$ and $\sigma$ estimates. . . . .	113
4.8	Ranking of the parameters and variables according to their influence on the BPS result based on the <i>EE</i> method ( $r = 8$ ). . . . .	114
4.9	Convergence of $S_i$ and $S_{Ti}$ estimates. . . . .	116
4.10	Results of the variance-based method ( $N = 8,192$ ). . . . .	117

4.11	Results of the Kolmogorov-Smirnov test ( $N = 8,192$ ). . . . .	118
5.1	Building parameters. . . . .	125
5.2	Key requirements for the <i>Energieeinsparverordnung</i> from 2009 and the <i>Passivhaus</i> standard. . . . .	127
5.3	Specification of the building components selected for variation and their distributions. . . . .	129
5.4	Uncertain boundary conditions selected for variation and their distributions. . . . .	130
5.5	Convergence of mean and variance estimates for $q_{\text{heat}}$ . . . . .	133
5.6	Statistical summary of the BPA result. . . . .	135
5.7	Ranking of the parameters and variables according to their influence on the BPA result based on the scatter plot method ( $N = 256$ ). . . . .	136
5.8	Ranking of the parameters and variables according to their influence on the BPA result based on the <i>EE</i> method ( $r = 8$ ). . . . .	138
5.9	Convergence of $S_i$ and $S_{T_i}$ estimates for the BPA. . . . .	141
5.10	Ranking of the six most influential parameters and variables according to their influence on $q_{\text{heat}}$ based on the VB method ( $N = 2,048$ ). . . . .	142
5.11	Results of the Kolmogorov-Smirnov test for the BPA ( $N = 2,048$ ). . . . .	144
5.12	Convergence of mean and variance estimates for <i>NPV</i> . . . . .	144
5.13	Statistical summary for the combined BPA and CBA result. . . . .	146
5.14	Ranking of the parameters and variables according to their influence on the combined BPA and CBA result based on the scatter plot method ( $N = 1,024$ ). . . . .	147
5.15	Ranking of the parameters and variables according to their influence on the <i>NPV</i> based on the <i>EE</i> method ( $r = 8$ ). . . . .	149
5.16	Convergence of $S_i$ and $S_{T_i}$ estimates for the combined BPA and CBA. . . . .	152
5.17	Ranking of the seven most influential parameters and variables according to their influence on the <i>NPV</i> based on the VB method ( $N = 16,384$ ). . . . .	153
5.18	Results of the Kolmogorov-Smirnov test for the combined BPA and CBA ( $N = 16,384$ ). . . . .	155

# Bibliography

- AG Energiebilanzen e.V. 2012. Auswertungstabellen zur Energiebilanz für die Bundesrepublik Deutschland 1990 bis 2011. Berechnungen auf Basis des Wirkungsgradansatzes. Stand: September 2012.
- ANSI/ASHRAE Standard 140 2011. Standard Method of Test for the Evaluation of Building Energy Analysis Computer Programs.
- Antretter, F., Sauer, F., Schöpfer, T., and Holm, A. 2011. Validation of a Hygrothermal Whole Building Simulation Software. In *Proceedings of Building Simulation 2011: 12th Conference of International Building Performance Simulation Association*, pages 1694–1701, Sydney.
- BMWi 2011. Forschung für eine umweltschonende, zuverlässige und bezahlbare Energieversorgung. Das 6. Energieforschungsprogramm der Bundesregierung. Technical report, Bundesministerium für Wirtschaft und Technologie.
- BMWi 2012. Entwicklung von Energiepreisen und Preisindizes. Web page. <http://www.bmwi.de/BMWi/Navigation/Energie/Statistik-und-Prognosen/Energiedaten/energiepreise-energiekosten.html>. Date accessed: 19.03.2012.
- Booth, A. T., Choudhary, R., and Spiegelhalter, D. J. 2011. Handling uncertainty in housing stock models. *Building and Environment*, 48:35–47.
- Box, G. E., Hunter, J. S., and Hunter, W. G. 2005. *Statistics for Experimenters. Design, Innovation, and Discovery*. Wiley & Sons, Inc., Hoboken.
- Box, G. E., Jenkins, G. M., and Reinsel, G. C. 2008. *Time Series Analysis: Forecasting and Control*. John Wiley & Sons, Inc., New Jersey, 4 edition.
- Brohus, H., Heiselberg, P., Simonsen, A., Sørensen, K. C., and Engineering, C. 2009. Uncertainty of Energy Consumption Assessment of Domestic Buildings. In *Proceedings of Building Simulation 2009: 11th Conference of International Building Performance Simulation Association*, pages 1022–1029.

- Burhenne, S., Elci, M., Jacob, D., Neumann, C., and Herkel, S. 2010a. Sensitivity analysis with building simulations to support the commissioning process. In *Proceedings of ICEBO 2010, 10th International Conference for Enhanced Building Operations*, Kuwait City.
- Burhenne, S. and Jacob, D. 2008. Simulation models to optimize the energy consumption of buildings. In *Proceedings of ICEBO 2008, 8th International Conference for Enhanced Building Operations*, Berlin.
- Burhenne, S., Jacob, D., and Henze, G. P. 2010b. Uncertainty analysis in building simulation with Monte Carlo techniques. In *Proceedings of SimBuild 2010, 4th National Conference of IBPSA-USA*, New York City.
- Burhenne, S., Jacob, D., and Henze, G. P. 2011. Sampling based on Sobol' sequences for Monte Carlo techniques applied to building simulations. In *Proceedings of Building Simulation 2011: 12th Conference of International Building Performance Simulation Association*, pages 1816–1823, Sydney.
- Burhenne, S., Tsvetkova, O., Jacob, D., Henze, G. P., and Wagner, A. 2013a. Uncertainty quantification for combined building performance and cost-benefit analyses. *Building and Environment*, 62:143–154.
- Burhenne, S., Wystrcil, D., Elci, M., Narmsara, S., and Herkel, S. 2013b. Building performance simulation using Modelica: Analysis of the current state and application areas. In *Proceedings of Building Simulation 2013: 13th Conference of International Building Performance Simulation Association*, pages 3259–3266, Chambéry.
- Campolongo, F., Saltelli, A., and Cariboni, J. 2011. From screening to quantitative sensitivity analysis. A unified approach. *Computer Physics Communications*, 182(4):978–988.
- Campolongo, F., Saltelli, A., Sørensen, T., and Tarantola, S. 2000. Hitchhiker's Guide to Sensitivity Analysis. In Saltelli, A., Chan, K., and Scott, E. M., editors, *Sensitivity Analysis*, chapter 2, pages 15–47. Wiley.
- Carnell, R. 2007. An Example of Augmenting a Latin Hypercube. Web page. <http://cran.r-project.org/web/packages/lhs/>. Date accessed: 04.03.2011.
- Choi Granade, H., Creyts, J., Derkach, A., Farese, P., Nyquist, S., and Ostrowski, K. 2009. Unlocking Energy Efficiency in the U.S. Economy. Technical report, McKinsey&Company.
- Clarke, J. A. 2001. *Energy Simulation in Building Design*. Butterworth-Heinemann, second edition.

- Cooke, R. M. and Goossens, L. J. H. 2000. Procedures guide for structured expert judgment. Technical report, Delft University of Technology for the European Commission.
- Corrado, V. and Mechri, H. E. 2009. Uncertainty and Sensitivity Analysis for Building Energy Rating. *Journal of Building Physics*, 33(2):125–156.
- Cox, D. C. and Baybutt, P. 1981. Methods for Uncertainty Analysis: A Comparative Survey. *Risk Analysis*, 1(4):251–258.
- Dassault Systèmes AB 2011. Dymola. Dynamic Modeling Laboratory. Dymola Release notes.
- de Wit, S. 2003. Uncertainty in building simulation. In Malkawi, A. M. and Augenbroe, G., editors, *Advanced Building Simulation*, pages 25–59. Taylor & Francis, Abingdon, UK.
- de Wit, S. and Augenbroe, G. 2002. Analysis of uncertainty in building design evaluations and its implications. *Energy and Buildings*, 34:951–958.
- DIN EN 15459 2008. Energieeffizienz von Gebäuden – Wirtschaftlichkeitsberechnungen für Energieanlagen in Gebäuden (German version of EN 15459:2007 Energy performance of buildings – Economic evaluation procedure for energy systems in buildings).
- Dodier, R. H. 1999. *Unified Prediction and Diagnosis in Engineering Systems by Means of Distributed Belief Networks*. PhD thesis, University of Colorado.
- Dutang, C. 2009. *randtoolbox: Generating and Testing Random Numbers*. R package.
- Eisenhower, B., Fonoberov, V., and Mezić, I. 2012a. Uncertainty-weighted Meta-model Optimization in Building Energy Models. In *Proceedings of Simulation and Optimization Conference 2012: 1st Conference of International Building Performance Simulation Association-England (BSO2012)*, pages 95–101, Loughborough, UK.
- Eisenhower, B., O’Neill, Z., Fonoberov, V. A., and Mezić, I. 2011. Uncertainty and sensitivity decomposition of building energy models. *Journal of Building Performance Simulation*, pages 1–14.
- Eisenhower, B., O’Neill, Z., Narayanan, S., Fonoberov, V. A., and Mezić, I. 2012b. A methodology for meta-model based optimization in building energy models. *Energy and Buildings*, 47:292–301.
- Elci, M. A. 2010. *Sensitivitätsanalysen mit Gebäudesimulationsmodellen*. Bachelor thesis, Biberach University of Applied Sciences.

- EnEV 2009. Verordnung über energiesparenden Wärmeschutz und energiesparende Anlagentechnik bei Gebäuden (Energieeinsparverordnung - EnEV).
- Equa Simulation AB 2010. Validation of IDA Indoor Climate and Energy 4.0 build 4 with respect to ANSI / ASHRAE Standard 140-2004. Technical report, Equa Simulation AB, Solna.
- European Commission 2011. Energy Efficiency Plan 2011. Technical report, European Commission, Brussels.
- European Commission Eurostat 2012. HICP - inflation rate. Annual average rate of change (%). Web page. [epp.eurostat.ec.europa.eu/tgm/table.do?tab=table&language=en&pcode=tsieb060&tableSelection=1&footnotes=yes&labeling=labels&plugin=1](http://epp.eurostat.ec.europa.eu/tgm/table.do?tab=table&language=en&pcode=tsieb060&tableSelection=1&footnotes=yes&labeling=labels&plugin=1). Date accessed: 19.03.2012.
- Evans, M., Hastings, N., and Peacock, B. 2000. *Statistical Distributions*. Wiley, New York, 3rd edition.
- Feist, W., Pfluger, R., Kaufmann, B., Schnieders, J., and Kah, O. 2007. Passivhaus Projektierungs Paket 2007. Anforderungen an qualitätsgeprüfte Passivhäuser.
- Fürbringer, J.-M. and Roulet, C. A. 1995. Comparison and Combination of Factorial and Monte-Carlo Design in Sensitivity Analysis. *Building and Environment*, 30(4):505–519.
- Good, P. I. and Hardin, J. W. 2003. *Common Errors in Statistics (and How to Avoid Them)*. John Wiley & Sons, Inc., Hoboken.
- Haldi, F. and Robinson, D. 2011. The impact of occupants' behaviour on building energy demand. *Journal of Building Performance Simulation*, 4(4):323–338.
- Helton, J. and Davies, F. 2003. Latin hypercube sampling and the propagation of uncertainty in analyses of complex systems. *Reliability Engineering & System Safety*, 81(1):23–69.
- Henninger, R. H. and Witte, M. J. 2012. EnergyPlus Testing with Building Thermal Envelope and Fabric Load Tests from ANSI / ASHRAE Standard 140-2011. Technical report, GARD Analytics for the U.S. Department of Energy, Arlington Heights.
- Henze, G. P. 1995. *Evaluation of Optimal Control for Ice Storage Systems*. PhD thesis, University of Colorado, Boulder.

- Henze, G. P., Felsmann, C., and Knabe, G. 2004. Evaluation of optimal control for active and passive building thermal storage. *International Journal of Thermal Sciences*, 43(2):173–183.
- Heo, Y. 2011. *Bayesian calibration of building energy models for energy retrofit decision-making under uncertainty*. PhD thesis, Georgia Institute of Technology.
- Herkel, S., Knapp, U., and Pfafferott, J. 2008. Towards a model of user behaviour regarding the manual control of windows in office buildings. *Building and Environment*, 43(4):588–600.
- Hirsch, R. L., Bezdek, R., and Wendling, R. 2005. Peaking of World Oil Production: Impacts, Mitigation, & Risk Management. Technical Report February, DOE - National Energy Technology Laboratory.
- Hoel, P. G. 1966. *Introduction to Mathematical Statistics*. John Wiley & Sons, Inc., Los Angeles, 3rd edition.
- Homma, T. and Saltelli, A. 1996. Importance measures in global sensitivity analysis of nonlinear models. *Reliability Engineering & System Safety*, 52(1):1–17.
- Hopfe, C. J. 2009. *Uncertainty and sensitivity analysis in building performance simulation for decision support and design optimization*. PhD thesis, Eindhoven University of Technology.
- Hopfe, C. J. and Hensen, J. L. M. 2011. Uncertainty analysis in building performance simulation for design support. *Energy and Buildings*, 43:2798–2805.
- Hu, H. and Augenbroe, G. 2012. A stochastic model based energy management system for off-grid solar houses. *Building and Environment*, 50:90–103.
- Hubbard, D. W. 2010. *How to Measure Anything. Finding the Value of "Intangibles" in Business*. John Wiley & Sons, Inc., New Jersey, 2nd edition.
- IPCC 2007. Climate Change 2007: Synthesis Report. An Assessment of the Intergovernmental Panel on Climate Change. Technical Report November, Intergovernmental Panel on Climate Change (IPCC).
- Isakson, P. and Eriksson, L. O. 1994. MFC 1.0 $\beta$ . Matched Flow Collector Model for simulation and testing. User's manual. Technical report, IEA SH&CP Task 14. Royal Institute of Technology (KTH), Stockholm.
- ISO 13790 2008. Energy performance of buildings - Calculation of energy use for space heating and cooling.

- Jacob, D. 2012. *Gebäudebetrieboptimierung. Verbesserungen von Optimierungsmethoden und Optimierung unter unsicheren Randbedingungen*. PhD thesis, Karlsruher Institut für Technologie (KIT).
- Jacob, D., Burhenne, S., Herkel, S., Wagner, A., Dodier, R. H., and Henze, G. P. 2011. Comparing two methods of stochastic modeling for buildings. In *Proceedings of Building Simulation 2011: 12th Conference of International Building Performance Simulation Association*, pages 1784 – 1791, Sydney.
- Jenkins, D., Liu, Y., and Peacock, A. 2008. Climatic and internal factors affecting future UK office heating and cooling energy consumptions. *Energy and Buildings*, 40(5):874–881.
- Jézéquel, F. and Chesneaux, J.-M. 2008. CADNA: a library for estimating round-off error propagation. *Computer Physics Communications*, 178(12):933–955.
- Jordan, U. and Vajen, K. 2003. Handbuch. DHWcalc. Werkzeug zur Generierung von Trinkwasser-Zapfprofilen auf statistischer Basis. Version 1.10 (2003). Technical report, Technical University of Denmark / Universität Kassel, Lyngby / Kassel.
- Kennedy, M. C. and O’Hagan, A. 2001. <http://www.jstor.org/stable/2680584>. *Journal of the Royal Statistical Society. Series B (Statistical Methodology)*, 63(3):425–464.
- KfW 2013. Energieeffizient bauen: Das KfW-Effizienzhaus. Web page. <https://www.kfw.de/inlandsfoerderung/Privatpersonen/Neubau/Das-KfW-Effizienzhaus/index.html>. Date accessed 21.04.2013.
- Lam, J. C. and Hui, S. C. 1996. Sensitivity analysis of energy performance of office buildings. *Building and Environment*, 31(1):27–39.
- Langner, M. R., Henze, G. P., Corbin, C. D., and Brandemuehl, M. J. 2011. An investigation of design parameters that affect commercial high-rise office building energy consumption and demand. *Journal of Building Performance Simulation*, 5(5):313–328.
- Ljung, L. 1987. *System Identification: Theory for the User*. Prentice-Hall, New Jersey.
- Lomas, K. and Eppel, H. 1992. Sensitivity analysis techniques for building thermal simulation programs. *Energy and Buildings*, 19(1):21–44.
- Macdonald, I. and Clarke, J. 2007. Applying uncertainty considerations to energy conservation equations. *Energy and Buildings*, 39(9):1019–1026.

- Macdonald, I. and Strachan, P. 2001. Practical application of uncertainty analysis. *Energy and Buildings*, 33(3):219–227.
- Macdonald, I. A. 2002. *Quantifying the Effects of Uncertainty in Building Simulation*. PhD thesis, University of Strathclyde.
- Mara, T. and Tarantola, S. 2008. Application of global sensitivity analysis of model output to building thermal simulations. *Building Simulation*, 1(4):290–302.
- Maurice, B., Frischknecht, R., Coelho-Schwartz, V., and Hungerbühler, K. 2000. Uncertainty analysis in life cycle inventory. Application to the production of electricity with French coal power plants. *Journal of Cleaner Production*, 8(2):95–108.
- Miller, R. 2005. Grundlagen Facility Management - Planung, Erstellung, und Nutzung. In Recknagel, H., Sprenger, E., and Schramek, E.-R., editors, *Taschenbuch für Heizung + Klimatechnik*, chapter 1.11, pages 417–445. Oldenbourg Industrieverlag, München, 72nd edition.
- Modelica Association 2012. Modelica® - A Unified Object-Oriented Language for Systems Modeling. Language Specification. Version 3.3. Technical report, Modelica Association.
- Montgomery, D. C. and Runger, G. C. 2003. *Applied Statistics and Probability for Engineers*. John Wiley & Sons, Inc., New York, third edition.
- Morris, M. D. 1991. Factorial Sampling Plans for Preliminary Computational Experiments. *Technometrics*, 33(2):161–174.
- Nadarajah, S. and Kotz, S. 2006. Journal of Statistical Software. *Journal Of Statistical Software*, 16:1–8.
- Nas, T. F. 1996. *Cost-Benefit Analysis: Theory and Application*. Sage Publications, Inc.
- Neumann, C. and Jacob, D. 2010. Results of the project Building EQ. Tools and methods for linking EPBD and continuous commissioning. Technical report, Fraunhofer Institute for Solar Energy Systems, Freiburg.
- Neumann, C., Jacob, D., Burhenne, S., Florita, A., Burger, E., and Schmidt, F. 2011. Modellbasierte Methoden für die Fehlererkennung und Optimierung im Gebäudebetrieb. Endbericht. Technical report, Fraunhofer-Institut für Solare Energiesysteme, Freiburg.
- Nilsen, T. and Aven, T. 2003. Models and model uncertainty in the context of risk analysis. *Reliability Engineering & System Safety*, 79(3):309–317.

- Nouidui, T. S., Phalak, K., Zuo, W., and Wetter, M. 2012. Validation and Application of the Room Model of the Modelica Buildings Library. In *Proceedings of the 9th International Modelica Conference, September 3 - 5*, pages 727–736, Munich.
- Page, J., Robinson, D., Morel, N., and Scartezzini, J.-L. 2008. A generalised stochastic model for the simulation of occupant presence. *Energy and Buildings*, 40(2):83–98.
- Pfafferoth, J. and Herkel, S. 2008. Abschlussbericht für das BBR - Forschungsvorhaben: Richtlinie zur Durchführung einer dynamisch thermischen Simulationsrechnung für den Sommerlastfall in Gebäuden. Technical report, Fraunhofer Institute for Solar Energy Systems ISE.
- Pietrzyk, K. and Hagendoft, C.-E. 2008. Reliability analysis in building physics design. *Building and Environment*, 43(4):558–568.
- Pindyck, R. S. and Rubinfeld, D. L. 2005. *Mikroökonomie*. Pearson Studium, Munich, 6th edition.
- R Core Team 2012. *R: A Language and Environment for Statistical Computing*. R Foundation for Statistical Computing, Vienna, Austria.
- Rahni, N., Ramdani, N., Candau, Y., and Dalicieux, P. 1997. Application of group screening to dynamic building energy simulation models. *Journal of Statistical Computation and Simulation*, 57:285–304.
- Rao, J. and Haghghat, F. 1993. A procedure for sensitivity analysis of airflow in multi-zone buildings. *Building and Environment*, 28(1):53–62.
- Reckhow, K. H. 1994. Water quality simulation modeling and uncertainty analysis for risk assessment and decision making. *Ecological Modelling*, 72(1-2):1–20.
- Rysanek, A. and Choudhary, R. 2011. Multi-period optimization of building refurbishment decisions: Assessing options and risk under economic uncertainty. In *Proceedings of Building Simulation 2011: 12th Conference of International Building Performance Simulation Association*, pages 2447–2454, Sydney.
- Sahlin, P. 1996. NMF Handbook. An Introduction to the Neutral Model Format. NMF version 3.02. Technical report, Royal Institute of Technology (KTH).
- Sahlin, P., Eriksson, L., Grozman, P., Johnsson, H., Shapovalov, A., and Vuolle, M. 2004. Whole-building simulation with symbolic DAE equations and general purpose solvers. *Building and Environment*, 39(8):949–958.
- Saltelli, A. and Annoni, P. 2010. How to avoid a perfunctory sensitivity analysis. *Environmental Modelling & Software*, 25(12):1508–1517.

- 
- Saltelli, A., Annoni, P., Azzini, I., Campolongo, F., Ratto, M., and Tarantola, S. 2010. Variance based sensitivity analysis of model output. Design and estimator for the total sensitivity index. *Computer Physics Communications*, 181(2):259–270.
- Saltelli, A., Ratto, M., Andres, T., Campolongo, F., Cariboni, J., Gatelli, D., Saisana, M., and Tarantola, S. 2008. *Global Sensitivity Analysis. The Primer*. John Wiley & Sons, Ltd.
- Saltelli, A. and Tarantola, S. 2002. On the Relative Importance of Input Factors in Mathematical Models: Safety Assessment for Nuclear Waste Disposal. *Journal of the American Statistical Association*, 97(459):702–709.
- Sartori, I., Napolitano, A., and Voss, K. 2012. Net zero energy buildings: A consistent definition framework. *Energy and Buildings*, 48:220–232.
- Sobol', I. M. and Levitan, Y. L. 1999. A pseudo-random number generator for personal computers. *Computers & Mathematics with Applications*, 37(4-5):33–40.
- Spitler, J. D., Fisher, D. E., and Zietlow, D. C. 1989. A Primer on the Use of Influence Coefficients in Building Simulation. In *Proceedings of Building Simulation 1989: 2nd Conference of International Building Performance Simulation Association*, pages 299–304, Vancouver.
- Tanner, R. A. and Henze, G. P. 2013. Quantifying the impact of occupant behavior in mixed mode buildings. In *Proceedings of the 2013 ASCE Architectural Engineering Conference*, State College.
- Tarantola, S. 2010. Variance based Sensitivity Analysis. Presentation at the Sixth SAMO Summer School, Fiesole.
- Thompson, K. M., Burmaster, D. E., and Crouch, E. A. C. 1992. Monte Carlo techniques for quantitative uncertainty analysis in public health risk assessments. *Risk analysis : an official publication of the Society for Risk Analysis*, 12(1):53–63.
- Tsvetkova, O. 2011. *Uncertainty and sensitivity analysis for decision support in building design*. Master thesis, University of Freiburg.
- Tuominen, P., Klobut, K., Tolman, A., Adjei, A., and de Best-Waldhober, M. 2012. Energy savings potential in buildings and overcoming market barriers in member states of the European Union. *Energy and Buildings*, 51:48–55.
- VDI 6007 Part 1 2007. Calculation of transient thermal response of rooms and buildings. Modelling of rooms.

- VDI 6020 Part 1 2001. Requirements on methods of calculation to thermal and energy simulation of buildings and plants. Buildings.
- Voss, K. and Musall, E. 2011. *Nullenergiegebäude: Klimaneutrales Wohnen und Arbeiten im internationalen Vergleich*. DETAIL - Institut für internationale Architektur-Dokumentation.
- Webster, M., Forest, C., Reilly, J., Babiker, M., Kicklighter, D., Mayer, M., Prinn, R., Sarofim, M., Sokolov, A., Stone, P., and Wang, C. 2003. Uncertainty Analysis of Climate Change and Policy Response. *Climatic Change*, 61(3):295–320.
- Wetter, M. 2008. GenOpt Generic Optimization Program. User Manual Version 2.1.0. Technical report, Lawrence Berkeley National Laboratory, Berkeley.
- Wong, J., Li, H., and Wang, S. 2005. Intelligent building research: a review. *Automation in Construction*, 14(1):143–159.
- Zoonekynd, V. 2007. Time series. Web page. [http://zoonek2.free.fr/UNIX/48\\_R/15.html](http://zoonek2.free.fr/UNIX/48_R/15.html). Date accessed: 22.02.2012.